LEABHARLANN CHOLÁISTE NA TRÍONÓIDE, BAILE ÁTHA CLIATH | TRINITY COLLEGE LIBRARY DUBLIN
Ollscoil Átha Cliath | The University of Dublin

Terms and Conditions of Use of Digitised Theses from Trinity College Library Dublin

Copyright statement

All material supplied by Trinity College Library is protected by copyright (under the Copyright and Related Rights Act, 2000 as amended) and other relevant Intellectual Property Rights. By accessing and using a Digitised Thesis from Trinity College Library you acknowledge that all Intellectual Property Rights in any Works supplied are the sole and exclusive property of the copyright and/or other IPR holder. Specific copyright holders may not be explicitly identified. Use of materials from other sources within a thesis should not be construed as a claim over them.

A non-exclusive, non-transferable licence is hereby granted to those using or reproducing, in whole or in part, the material for valid purposes, providing the copyright owners are acknowledged using the normal conventions. Where specific permission to use material is required, this is identified and such permission must be sought from the copyright holder or agency cited.

Liability statement

By using a Digitised Thesis, I accept that Trinity College Dublin bears no legal responsibility for the accuracy, legality or comprehensiveness of materials contained within the thesis, and that Trinity College Dublin accepts no liability for indirect, consequential, or incidental, damages or losses arising from use of the thesis for whatever reason. Information located in a thesis may be subject to specific use constraints, details of which may not be explicitly described. It is the responsibility of potential and actual users to be aware of such constraints and to abide by them. By making use of material from a digitised thesis, you accept these copyright and disclaimer provisions. Where it is brought to the attention of Trinity College Library that there may be a breach of copyright or other restraint, it is the policy to withdraw or take down access to a thesis while the issue is being resolved.

Access Agreement

By using a Digitised Thesis from Trinity College Library you are bound by the following Terms & Conditions. Please read them carefully.

I have read and I understand the following statement: All material supplied via a Digitised Thesis from Trinity College Library is protected by copyright and other intellectual property rights, and duplication or sale of all or part of any of a thesis is not permitted, except that material may be duplicated by you for your research use or for educational purposes in electronic or print form providing the copyright owners are acknowledged using the normal conventions. You must obtain permission for any other use. Electronic or print copies may not be offered, whether for sale or otherwise to anyone. This copy has been supplied on the understanding that it is copyright material and that no quotation from the thesis may be published without proper acknowledgement.

Molecular Gene and Regulatory Profiles in Thyroid Cancer

By

Karen Denning, B.Sc. (Hons), M.Sc., Ph.D

Trinity College

University of Dublin, 2009

Supervisor:

Professor Orla Sheils, MA (Dubl), MA (Lond), PhD, FAMLS

Declaration

I declare that, except where otherwise acknowledged, this thesis is entirely my own work, and has not been submitted previously for a Ph.D. degree at this or any other university. I agree that the library may lend or copy this thesis on request.

Karen Denning

TRINITY COLLEGE
10 AUG 2009
LIBRARY DUBLIN
THESIS
8827

For my parents, Bridie and Michael

Contents

Acknowledgements		i
List of abbreviations		iii
Publications		ix
Summary		xi

Chapter One

General Introduction ***1***

1.1	The thyroid gland: a brief history	2
1.2	Thyroid embryology and development	7
1.3	Anatomy of the thyroid gland	9
1.4	Thyroid hormones	11
1.5	Thyroid disease states	13
1.5.1	Goitre	13
1.5.2	Hyperplasia	13
1.5.3	Hyperthyroidism	14
1.5.4	Hypothyroidism	14
1.5.5	Thyroiditis	16
1.5.5.1	Hashimoto thyroiditis	16
1.5.5.2	Non-specific lymphocytic thyroiditis	18
1.5.5.3	Granulomatous thyroiditis/DeQuervain thyroiditis	19
1.5.6	Neoplasms of the thyroid	20
1.5.6.1	Adenoma	20
1.5.6.2	Papillary thyroid carcinoma	22
1.5.6.3	Follicular thyroid carcinoma	29
1.5.6.4	Hurthle cell carcinoma	31
1.5.6.5	Insular/Poorly differentiated carcinoma	32
1.5.6.6	Anaplastic thyroid carcinoma	33
1.5.6.7	Medullary thyroid carcinoma	34
1.6	Epidemiology of thyroid cancer	35

1.7	Aetiology of thyroid cancer	37
1.7.1	Iodine	37
1.7.2	External radiation	37
1.7.3	Other risk factors	39
1.8	Molecular pathology of thyroid cancer	40
1.8.1	RET	43
1.8.1.1	ret/PTC oncogenes and thyroid cancer	44
1.8.2	NTRK	46
1.8.3	RAS	47
1.8.4	BRAF	48
1.8.5	MET	49
1.8.6	PTEN	49
1.8.7	p53	50
1.8.8	PPARG-PAX8	50
1.9	Aims and objectives	51
1.10	References	52

Chapter Two

Materials and Methods ***59***

2.1	Introduction	60
2.2	Cell culture of thyroid cell lines	60
2.2.1	Cell lines	60
2.2.2	Formulation of cell culture media and other solutions	61
2.2.3	Thawing cells from stock	61
2.2.4	Splitting confluent flasks	61
2.2.5	Cryopreservation	62
2.3	Mycoplasma testing	63
2.3.1	Background	63
2.3.2	Mycoplasma detection protocol	63
2.4	Lymphocyte isolation	66
2.4.1	Background	66

2.4.2	Phlebotomy	66
2.4.3	Lymphocyte extraction, counting and activation	67
2.4.4	Co-culture procedure	70
2.5	Extraction of RNA from cell lines	71
2.5.1	Preparation of reagents	71
2.5.2	Protocol	71
2.6	Laser capture microdissection	75
2.7	Extraction of RNA from FFPE material	79
2.7.1	Preparation of reagents	79
2.7.2	Protocol	80
2.8	Nano-Drop® 1000 spectrophotometer	82
2.8.1	Loading of samples	82
2.8.2	Blank measurement	83
2.8.3	Sample measurement	83
2.9	cDNA synthesis	85
2.10	TaqMan® PCR	87
2.10.1	Real time quantitative TaqMan® PCR	90
2.10.2	Relative gene expression	91
2.10.3	TaqMan® low density arrays	92
2.10.3.1	Background	92
2.10.3.2	Loading the TILDA	93
2.10.3.3	Centrifuging the TILDA	93
2.10.3.4	Sealing the TILDA and running the gene expression reaction	94
2.10.4	Pre-amplification	95
2.10.4.1	Background	95
2.10.4.2	Pooling the assays	95
2.10.4.3	Preparing cDNA from RNA	95
2.10.4.4	Running the pre-amplification reaction	96
2.10.4.5	Running the gene expression reaction	97
2.11	Tissue microarray construction	98
2.11.1	Background	98
2.11.2	TMA construction	98
2.12	Immunohistochemistry	100
2.12.1	Background	100

2.12.2	ABC method	101
2.13	*In situ* hybridisation analysis of microRNAs	104
2.13.1	Background	104
2.13.2	Protocol	105
2.14	References	108

Chapter Three

ret/PTC-1 alters the immunoprofile of thyroid follicular cells ***109***

3.1	Summary	110
3.2	Introduction	112
3.2.1	Autoimmune thyroid disease and Hashimoto thyroiditis	112
3.2.2	ret/PTC-1 oncogene	113
3.2.3	ret/PTC-1 and Hashimoto thyroiditis	114
3.2.4	TaqMan® immune profiling low density arrays	115
3.3	Aims	117
3.4	Materials and methods	118
3.4.1	Samples	118
3.4.2	Cell culture	118
3.4.3	Lymphocyte extraction and co-culture	118
3.4.4	RNA extraction and cDNA archiving	120
3.4.5	TaqMan® LDAs	120
3.4.6	TLDA analysis	120
3.5	Results	121
3.5.1	Nthy-ori co-culture gene expression patterns	121
3.5.2	TPC-1 co-culture gene expression patterns	126
3.6	Discussion	130
3.6.1	Nthy-ori gene expression patterns	131
3.6.2	TPC-1 gene expression patterns	133
3.7	Conclusions	135
3.8	References	136

Chapter Four

Expression profiles in archival thyroid carcinoma lesions using pre-amplification Q-RT-PCR ***139***

4.1	Summary	140
4.2	Introduction	141
4.2.1	The follicular aspect	141
4.2.2	Patient management	142
4.2.3	Fine needle aspiration	143
4.2.4	Laser capture microdissection and pre-amplification	144
4.3	Aims	145
4.4	Materials and methods	146
4.4.1	Samples	146
4.4.2	Laser capture microdissection	163
4.4.3	RNA extraction and quantification	163
4.4.4	cDNA archiving and pre-amplification synthesis	164
4.4.5	TaqMan® gene expression reaction	164
4.4.6	Analysis of relative gene expression data using the comparative C_T method	166
4.4.7	Statistical analysis	166
4.5	Results	167
4.5.1	Boxplots	169
4.5.1.1	RAB23	169
4.5.1.2	MT1K	172
4.5.1.3	MT1X	173
4.5.1.4	CSNK1G2	175
4.5.1.5	TGFB1	177
4.5.1.6	IRF3	178
4.5.1.7	CD74	179
4.5.1.8	HLA-DMA	180
4.5.1.9	HLA-DQB1	181
4.6	Discussion	182
4.6.1	Pre-amplification and endogenous control	182
4.6.2	Expression patterns	183

4.6.1	Possible translational applications	188
4.7	Conclusions	189
4.8	References	190

Chapter Five

A molecular expression signature distinguishing thyroid carcinoma lesions using pre-amplification Q-RT-PCR and immunohistochemistry ***196***

5.1	Summary	197
5.2	Introduction	198
5.2.1	Tissue microarrays	198
5.3	Aims	200
5.4	Materials and methods	201
5.4.1	Samples	201
5.4.2	Laser capture microdissection	218
5.4.3	RNA extraction and quantification	218
5.4.4	cDNA archiving and pre-amplification synthesis	218
5.4.5	TaqMan® gene expression reaction	219
5.4.6	TMA construction and sectioning	220
5.4.7	Immunohistochemistry	221
5.4.8	Analysis of relative gene expression data using the comparative C_T method	222
5.4.9	Analysis of immunohistochemical scores	222
5.4.10	Statistical analysis	222
5.5	Results	223
5.5.1	Gene expression	226
5.5.1.1	Boxplots representing gene expression	227
5.5.1.1.1	APOE	227
5.5.1.1.2	TOP2A	229
5.5.1.1.2	LYN	230
5.5.2	Protein expression	231
5.5.2.1	Immunohistochemical images	233

5.5.2.1.1	MMP11	233
5.5.2.1.2	BAX	234
5.5.2.1.3	APOE	235
5.5.2.1.4	TOP2A	236
5.5.2.1.5	LYN	237
5.5.2.2	Boxplots representing protein expression	238
5.5.2.2.1	TOP2A	238
5.5.2.2.2	LYN	239
5.5.3	Corresponding gene and protein expression	240
5.5.3.1	Boxplots representing corresponding gene and protein expression	241
5.5.3.1.1	MMP11	241
5.5.3.1.2	BAX	243
5.5.3.1.3	APOE	244
5.5.3.1.4	TOP2A	246
5.6	Discussion	247
5.6.1	Pre-amplification and endogenous control	247
5.6.2	Expression patterns	247
5.7	Conclusions	254
5.8	References	255

Chapter Six

MicroRNA let-7a is down-regulated in thyroid malignancy ***261***

6.1	Summary	262
6.2	Introduction	263
6.2.1	MiRNA discovery	264
6.2.2	MiRNA location	264
6.2.3	MiRNA biogenesis	265
6.2.4	MiRNA roles and functions	268
6.2.5	MiRNA registry and target databases/prediction	270
6.2.6	ISH analysis of miRNA expression using LNA probes	273
6.3	Aims	274

6.4	Materials and methods	275
6.4.1	Samples	275
6.4.2	TMA construction and sectioning	284
6.4.3	MiRNA expression analysis using ISH	285
6.4.4	Analysis of *in situ* hybridisation scores	286
6.4.5	Statistical analysis	286
6.5	Results	287
6.5.1	*In situ* hybridisation images	289
6.5.2	Let-7a boxplots	292
6.6	Discussion	295
6.6.1	MiRNA analysis using ISH in archival samples	295
6.6.2	MiRNAs and cancer	296
6.6.3	MiRNAs as tumour suppressor genes and oncogenes	296
6.6.4	Let-7a expression in archival thyroid malignancy	299
6.7	Conclusions	302
6.8	References	304

Chapter Seven

General discussion, future work and conclusions ***310***

7.1	Background	311
7.2	Review of results	311
7.3	Conclusions	320
7.4	References	321

List of Figures

Figure 1.1	Oil on canvas painting by Edvard Munch	2
Figure 1.2	Low power photomicrograph of Hashimoto thyroiditis	17
Figure 1.3	Granulomatous thyroiditis	19
Figure 1.4	Follicular adenoma of the thyroid	21
Figure 1.5	Gross papillary thyroid carcinoma	22
Figure 1.6	Classic papillary thyroid carcinoma	23
Figure 1.7	Follicular variant papillary thyroid carcinoma	25
Figure 1.8	Tall cell (left) and columnar cell (right) variant papillary thyroid carcinoma	27
Figure 1.9	Encapsulated follicular thyroid carcinoma	30
Figure 1.10	Poorly differentiated carcinoma of the thyroid	32
Figure 1.11	Age standardised incidence rates for thyroid cancer throughout the world for 2002	36
Figure 1.12	Genetic signals in cancer development	40
Figure 1.13	Schematic representation of MAPK signalling	42
Figure 1.14	The role of RET in thyroid carcinogenesis	45
Figure 2.1	The band of lymphocytes that are formed at the sample/medium interface during lymphocyte extraction	68
Figure 2.2	Haemocytometer	69
Figure 2.3	The laser capture microdissection process	78
Figure 2.4	NanoDrop® spectrophotometer sample pedestal	82
Figure 2.5	The forklike structure dependent polymerisation associated 5′-3′ nuclease activity of AmpliTaq® gold DNA polymerase during PCR	88
Figure 2.6	Increased fluorescence activity due to cleaved probe	89
Figure 2.7	Example of an amplification plot	90
Figure 2.8	A TaqMan® LDA and its features	93
Figure 2.9	The tissue microarray process	99
Figure 2.10	The ABC method	100
Figure 3.1	The gene expression reagents that were factory loaded onto the TaqMan® immune profiling LDA	116
Figure 3.2	Heat map of Nthy-ori co-culture	122

Figure 3.3	Nthy-ori 6 hour co-culture	123
Figure 3.4	Expression levels for FASL, CD28 and G-CSF	125
Figure 3.5	Heat map of TPC-1 co-culture	127
Figure 3.6	TPC-1 6 hour co-culture	128
Figure 4.1	RAB23 boxplot: non-neoplastic (no hyperplasia, no thyroiditis) vs. malignant	170
Figure 4.2	RAB23 boxplot: benign vs. malignant	170
Figure 4.3	RAB23 boxplot: FA vs. PTC (all variants)	171
Figure 4.4	RAB23 boxplot: FA vs. FVPTC	171
Figure 4.5	MT1K boxplot: non-neoplastic (no hyperplasia, no thyroiditis) vs. malignant	172
Figure 4.6	MT1K boxplot: non-malignant (all benign, all non-neoplastic) vs. malignant	172
Figure 4.7	MT1X boxplot: non-neoplastic (no hyperplasia, no thyroiditis) vs. malignant	173
Figure 4.8	MT1X boxplot: benign vs. malignant	173
Figure 4.9	MT1X boxplot: FA vs. PTC (all variants)	174
Figure 4.10	MT1X boxplot: FA vs. FVPTC	174
Figure 4.11	CSNK1G2 boxplot: benign vs. malignant	175
Figure 4.12	CSNK1G2 boxplot: FA vs. PTC (all variants)	176
Figure 4.13	TGFB1 boxplot: thyroiditis vs. PTC (all variants)	177
Figure 4.14	IRF3 boxplot: HT vs. PTC (all variants)	178
Figure 4.15	CD74 boxplot: non-neoplastic (no hyperplasia, no thyroiditis) vs. malignant	179
Figure 4.16	CD74 boxplot: hyperplasia vs. malignant	179
Figure 4.17	HLA-DMA boxplot: non-neoplastic (no hyperplasia, no thyroiditis) vs. malignant	180
Figure 4.18	HLA-DMA boxplot: FA vs. FVPTC	180
Figure 4.19	HLA-DQB1 boxplot: non-neoplastic (no hyperplasia, no thyroiditis) vs. malignant	181
Figure 4.20	HLA-DQB1 boxplot: FA vs. FVPTC	181
Figure 5.1	APOE gene expression boxplot: FA vs. FVPTC	227
Figure 5.2	APOE gene expression boxplot: FA vs. FTC	228
Figure 5.3	TOP2A gene expression boxplot: FA vs. PTC (all variants)	229

Figure 5.4	LYN gene expression boxplot: non-neoplastic (no hyperplasia, no thyroiditis) vs. malignant	230
Figure 5.5	LYN gene expression boxplot: hyperplasia vs. malignant	230
Figure 5.6	MMP11 immunohistochemical staining, control tissue (positive)	233
Figure 5.7	MMP11 immunohistochemical staining, control tissue (negative)	233
Figure 5.8	MMP11 immunohistochemical staining, goitre	233
Figure 5.9	MMP11 immunohistochemical staining, PTC	233
Figure 5.10	BAX immunohistochemical staining, control tissue (positive)	234
Figure 5.11	BAX immunohistochemical staining, control tissue (negative)	234
Figure 5.12	BAX immunohistochemical staining, goitre	234
Figure 5.13	BAX immunohistochemical staining, PTC	234
Figure 5.14	APOE immunohistochemical staining, control tissue (positive)	235
Figure 5.15	APOE immunohistochemical staining, control tissue (negative)	235
Figure 5.16	APOE immunohistochemical staining, hyperplasia	235
Figure 5.17	APOE immunohistochemical staining, PTC	235
Figure 5.18	TOP2A immunohistochemical staining, control tissue (positive)	236
Figure 5.19	TOP2A immunohistochemical staining, control tissue (negative)	236
Figure 5.20	TOP2A immunohistochemical staining, hyperplasia	236
Figure 5.21	TOP2A immunohistochemical staining, FTC	236
Figure 5.22	LYN immunohistochemical staining, control tissue (positive)	237
Figure 5.23	LYN immunohistochemical staining, control tissue (negative)	237
Figure 5.24	LYN immunohistochemical staining, goitre	237
Figure 5.25	LYN immunohistochemical staining, FTC	237
Figure 5.26	TOP2A protein expression boxplot: FA vs. FTC	238
Figure 5.27	LYN protein expression boxplot: FA vs. FTC	239
Figure 5.28	MMP11 corresponding gene and protein expression boxplot: non-neoplastic (no hyperplasia, no thyroiditis) vs. malignant	241
Figure 5.29	MMP11 corresponding gene and protein expression boxplot: non-malignant (all benign, all non-neoplastic) vs. malignant	242
Figure 5.30	BAX corresponding gene and protein expression boxplot: non-neoplastic (no hyperplasia, no thyroiditis) vs. malignant	243
Figure 5.31	APOE corresponding gene and protein expression boxplot: FA vs. FVPTC	244

Figure 5.32	APOE corresponding gene and protein expression boxplot: non-neoplastic (no hyperplasia, no thyroiditis) vs. malignant	245
Figure 5.33	TOP2A corresponding gene and protein expression boxplot: non-neoplastic (no hyperplasia, no thyroiditis) vs. malignant	246
Figure 6.1	The microRNA biogenesis pathway and mechanism in mammals	267
Figure 6.2	Global overview of a TMA slide stained for let-7a expression	284
Figure 6.3	U6 ISH staining, thyroid follicular cells	289
Figure 6.4	U6 ISH staining, breast tissue	289
Figure 6.5	Let-7a ISH staining, breast tissue	289
Figure 6.6	Scrambled probe ISH staining, thyroid follicular cells	289
Figure 6.7	Let-7a ISH staining, follicular adenoma	290
Figure 6.7.1	Let-7a ISH staining, follicular adenoma	290
Figure 6.8	Let-7a ISH staining, FTC	290
Figure 6.9	Let-7a ISH staining, goitre	291
Figure 6.10	Let-7a ISH staining, PTC	291
Figure 6.11	Let-7a ISH staining, PTC	291
Figure 6.12	Let-7a boxplot: FA vs. FTC	292
Figure 6.13	Let-7a boxplot: benign vs. malignant	293
Figure 6.14	Let-7a boxplot: non-neoplastic (no hyperplasia) vs. malignant	293
Figure 6.15	Let-7a boxplot: benign vs. neoplastic	294
Figure 6.16	How microRNAs can function as tumour suppressor genes and oncogenes	297

List of Tables

Table 2.1	Recommended volumes and tube sizes for lymphocyte extraction	67
Table 2.2	Typical LCM laser parameters	76
Table 2.3	cDNA reaction preparation	85
Table 2.4	Pre-amplification reaction preparation	96
Table 2.5	Gene expression reaction preparation	97
Table 2.6	Primary antibodies	101
Table 3.1	Time-points at which RNA was extracted from thyrocytes and the various co-culture combinations	119
Table 4.1	Non-neoplastic (no hyperplasia, no thyroiditis) samples	147
Table 4.2	Non-neoplasia (no hyperplasia) samples	148
Table 4.3	Non-neoplastic (incl. hyperplasia and thyroiditis) samples	149
Table 4.4	Thyroiditis samples	151
Table 4.5	Hashimoto thyroiditis samples	151
Table 4.6	Hyperplasia samples	152
Table 4.7	Follicular adenoma samples	153
Table 4.8	Benign samples	153
Table 4.9	Non-malignant (all benign, all non-neoplastic)	164
Table 4.10	Hurthle cell carcinoma samples	156
Table 4.11	Follicular thyroid carcinoma samples	156
Table 4.12	Papillary thyroid carcinoma (not otherwise specified) samples	157
Table 4.13	Papillary thyroid carcinoma, follicular variant samples	157
Table 4.14	Papillary thyroid carcinoma (all variants) samples	158
Table 4.15	Anaplastic thyroid carcinoma sample	159
Table 4.16	Medullary thyroid carcinoma sample	159
Table 4.17	Neoplastic samples	159
Table 4.18	Malignant samples	161
Table 4.19	Panel of assays	165
Table 4.20	Analysis cohorts	167
Table 4.21	Significant p values for RAB23, MT1K, MT1X, CSNK1G2, TGFB1, IRF3, CD74, HLA-DMA and HLA-DQB1 gene expression	168

Table 5.1	Non-neoplastic (no hyperplasia, no thyroiditis) samples	202
Table 5.2	Non-neoplasia (no hyperplasia) samples	203
Table 5.3	Non-neoplastic (incl. hyperplasia and thyroiditis) samples	204
Table 5.4	Thyroiditis samples	206
Table 5.5	Hashimoto thyroiditis samples	206
Table 5.6	Hyperplasia samples	207
Table 5.7	Follicular adenoma samples	208
Table 5.8	Benign samples	208
Table 5.9	Non-malignant (all benign, all non-neoplastic)	209
Table 5.10	Hurthle cell carcinoma samples	211
Table 5.11	Follicular thyroid carcinoma samples	211
Table 5.12	Papillary thyroid carcinoma (not otherwise specified) samples	212
Table 5.13	Papillary thyroid carcinoma, follicular variant samples	212
Table 5.14	Papillary thyroid carcinoma (all variants) samples	213
Table 5.15	Anaplastic thyroid carcinoma sample	214
Table 5.16	Medullary thyroid carcinoma sample	214
Table 5.17	Neoplastic samples	214
Table 5.18	Malignant samples	216
Table 5.19	Panel of assays	219
Table 5.20	Primary antibodies	221
Table 5.21	MMP11 analysis cohorts	223
Table 5.22	BAX analysis cohorts	224
Table 5.23	APOE analysis cohorts	224
Table 5.24	TOP2A analysis cohorts	225
Table 5.25	LYN analysis cohorts	225
Table 5.26	Significant p values for MMP11, BAX, APOE, TOP2A and LYN gene expression	226
Table 5.27	Significant p values for MMP11, BAX, APOE, TOP2A and LYN protein expression	232
Table 5.28	Significant p values for gene and protein expression of MMP11, BAX, APOE, TOP2A and LYN in parallel samples	240

Table 6.1	Non-neoplastic (no hyperplasia) samples	276
Table 6.2	Non-neoplastic (incl. hyperplasia) samples	277
Table 6.3	Hyperplasia samples	278
Table 6.4	Follicular adenoma samples	279
Table 6.5	Benign samples	279
Table 6.6	Non-malignant (all benign, all non-neoplastic)	279
Table 6.7	Follicular thyroid carcinoma samples	281
Table 6.8	Papillary thyroid carcinoma (not otherwise specified) samples	281
Table 6.9	Anaplastic thyroid carcinoma sample	281
Table 6.10	Medullary thyroid carcinoma sample	281
Table 6.11	Neoplastic samples	282
Table 6.12	Malignant samples	283
Table 6.13	Sequence and melting temperatures of the miRNA probes	285
Table 6.14	Analysis cohorts	287
Table 6.14	Significant p values for let-7a expression	288

Acknowledgments

Firstly I would like to thank my supervisor Professor Orla Sheils for giving me the opportunity to do this Ph.D. You were always there when I needed your help with anything. You have encouraged me so much over the years and have been a kind and generous friend as well as a great supervisor. Also thanks to Professor John O' Leary our head of department for his support and encouragement over the years. I would also like to acknowledge the funding that I received from the Trinity Studentship Fund, the Irish Cancer Society Oncology Scholars Travel Award and the Trinity Travel Award.

A big thank you has to go to Paul Smyth, what would I have done without you? You have helped me at every step Paul. I have asked you some amount of (ridiculous) questions over the years and you have always had the time to help and explain things to me, I will always be grateful for everything you have taught me.

Thanks also to Richie Flavin, my own personal pathologist, you have looked at more immunos and in situ hybridisation slides for me than any man should ever have to. Thanks for being there to help me with all my pathological needs, and for answering the phone once or twice! Thanks also to Stephen Finn and Ciara Barrett for scoring slides. Sue Cahill, gone but not forgotten, you really helped me to settle in and get started when I first joined the lab, I was devastated when you left. Jinghuan thanks for all the help (especially with dilutions!) you have given me.

To my girls Sinead and Therese, I am going to miss you two so much. What will I do without the brown scones, coffees and chats?? I was so happy when you joined our lab Sinead, and Therese you may as well be in our lab! Thanks for always being there for me and making me laugh so much!!!! I'm really lucky that I have gotten some friends for life out of the past three years.....as well as a Ph.D!

A special shout out has to go to the Lab Rats, consecutive C league winning tag rugby champions, one of our finer ideas girls!!

Thanks to everyone in the diagnostic histopathology lab, St. James Hospital especially Susan Russell who helped me to no end with immunos and Eilish Conlon for her TMA making skills.

Thank you to all of my family especially my parents Bridie and Michael and my sister Laura. Mam and Dad thank you for always helping and supporting me, you have both always been there for me over the years, and have given me everything that I have ever wanted. Thank you for everything you have done for me, I couldn't have done it without you. Laura you have been the best sister in the world, I'm sorry for tormenting you about being quiet so I could study over the years, you never gave out. I promise you will never hear the chair scrapping on the floor again!! I don't say it enough but I love you all so much. David you're lucky you didn't have to adhere to my strict no noise policy! Thanks to all my relatives, Nana Markey and Nana Denning (thanks for all the nice dinners), thanks also to all of the Woods family.

To my girls at home, the best gang of friends a girl could have-I won't be a poverty stricken student anymore!!!

Colin thank you for putting up with me through the last eight years of college! Since day one in Maynooth you have encouraged and supported everything that I have done and you have always been there for me. Thank you for being so happy and proud of everything that I have done. I'm sorry it's taken so long for me to finally finish college, but we've done it-now let's get out of here!!!!!!!!!

List of Abbreviations

a	Adenine
ABC method	Avidin/biotinylated complex method
AI	Autoimmune
AITD	Autoimmune thyroid disease
AKT	v-akt murine thyoma viral oncogene homolog 1
AMO	Anti-microRNA oligonucleotides
AP	Alkaline phosphatase
APAF-1	Apoptotic protease activating factor 1
APC	Antigen presenting cell
APC gene	Adenomatous polyposis coli gene
APOE	Apolipoprotein E
ATC	Anaplastic thyroid carcinoma
β-ME	Beta mercaptoethanol
BAX	BCL-2 associated X protein
bp	Base pair
BRAF	v-raf murine sarcoma viral oncogene homolog B1
BSA	Bovine serum albumin
c	Cytosine
CB	Ciara Barrett
CCL5	Chemokine ligand 5
CD	Cluster of differentiation
CDC25a	Cell division cycle 25 homolog a
CDKN1B	Cyclin dependent kinase inhibitor 1B
CDK6	Cyclin dependent kinase 6
cDNA	Complementary DNA
CLIP	Class II associated invariant chain peptide
CLL	Chronic lymphocytic leukaemia
cm	Centimetre
CO_2	Carbon dioxide
CSNK1G2	Casein kinase 1 gamma 2
C_T	Threshold cycle
C terminus	Carboxyl terminus

DAB	Diaminobenzidene
DGCR8	DiGeorge syndrome critical region 8
DIG	Digoxigenin
DIG-POD	Digoxigenin coupled to horseradish peroxidase
DIT	Diiodotyrosine
DMSO	Dimethyl sulfoxide
DNA	Deoxyribonucleic acid
dNTP	Deoxynucleotide triphosphate
dsRNA	Double stranded RNA
dU	Deoxyuridine
dUTP	2′ Deoxyuridine 5′-triphosphate
ECACC	European collection of cell cultures
EDTA	Ethylenediaminetetraacetic acid
EGF receptor	Epidermal growth factor receptor
ELISA	Enzyme-linked immunosorbent assay
ERK	Extracellular signal regulated kinase
FA	Follicular adenoma
FADD	Fas associated protein with death domain
FAM	6 carboxyfluorescein
FCS	Fetal calf serum
FFPE	Formalin fixed paraffin embedded
FMTC	Familial medullary thyroid carcinoma
FNA	Fine needle aspiration
FTC	Follicular thyroid carcinoma
FVPTC	Follicular variant papillary thyroid carcinoma
GAPDH	Glyceraldehyde 3 phosphate dehydrogenase
G-CSF	Granulocyte colony stimulating factor
GDP	Guanosine diphosphate
GM-CSF	Granulocyte macrophage colony stimulating factor
GNDF	Glial cell line derived neurotrophic factor
G protein	Guanine nucleotide binding protein
GRB2	Growth factor receptor bound protein 2
GTP	Guanosine 5′ triphosphate
g	Guanine

gy	Gray
GZMB	Granzyme B
HCl	Hydrogen chloride
H&E	Haematoxylin and eosin
HER-2	Human epidermal growth factor receptor 2
HGF/SF	Hepatocyte growth factor/scatter factor
HLA	Human leukocyte antigen
HT	Hashimoto Thyroiditis
HUVEC	Human umbilical vein endothelial cell
IHS	Immunohistochemistry score
Ii	Invariant chain
IgG	Immunoglobulin G
IL-2	Interleukin 2
IQR	Inter quartile range
IRF3	Interferon regulatory factor 3
ISH	In situ hybridisation
JOE	6 carboxy 4,5-dichloro 2,7-dimethoxyfluorescein
JNK	c-Jun N terminal kinase
kDa	Kilodalton
LCM	Laser capture microdissection
LDA	Low density array
LDL	Low density lipoprotein
Let-7	Lethal 7
LNA	Locked nucleic acid
LOH	Loss of heterozygosity
LYN	v-yes- 1 yamaguchi sarcoma viral related oncogene homolog
MIT	Monoiodotyrosine
MTC	Medullary thyroid carcinoma
MEN	Multiple endocrine neoplasia
MAPK	Mitogen activated protein kinase
MEK	MAPK/ERK kinase
mL	Millilitre
mV	Millivolt
mW	Milliwatt

ms	Millisecond
mRNA	Messenger RNA
miRNA	MicroRNA
MHC	Major histocompatibility complex
MT	Metallothionein
miRISC	MicroRNA containing RNA induced silencing complex
NACl	Sodium chloride
NAOH	Sodium hydroxide
NBT/BCIP	Nitro blue tetrazolium chloride/5-bromo 4-chloro 3-indolyl phosphate, toluidine salt
ng	Nanogram
NGF	Nerve growth factor
NIH	National institutes of health
NOS	Not otherwise specified
nt	Nucleotide
NTRK	Neurotrophic tyrosine kinase receptor
OCT4	Octamer 4
PAX8	Paired box 8
P bodies	Processing bodies
PBMC	Peripheral blood mononuclear cells
PBS	Phosphate buffered saline
PBST	Phosphate buffered saline tween
PCR	Polymerase chain reaction
PDGFR	Platelet derived growth factor receptor
PFA	Paraformaldehyde
PI3K	Phosphatidylinositol 3 kinase
PK	Proteinase K
PMA	Phorbol 12 myristate
PPARG	Peroxisome proliferator activated receptor
Pri-miRNA	Primary microRNA
PTC	Papillary thyroid carcinoma
PTEN	Phosphate and tensin homolog
PTK	Protein tyrosine kinase
Q-RT-PCR	Quantitative real time polymerase chain reaction

RA	Rheumatoid arthritis
RAF	v-raf 1 murine leukaemia viral oncogene homolog 1
Ran-GTP	RAS related nuclear protein guanosine triphosphate
RANTES	Regulated on activation normal T expressed and secreted
RAS	Retrovirus associated sequence
RET	Rearranged during transformation
RF	Richard Flavin
RNA	Ribonucleic acid
rpm	Revolutions per minute
RPMI	Roswell park memorial institute
RQ	Relative quantitation
rRNA	Ribosomal RNA
RT	Reverse transcription
RT-PCR	Real time polymerase chain reaction
SCN	Solid cell nest
SDS	Sequence detection system
SF	Stephen Finn
SHH	Sonic hedgehog
siRNA	Small interfering RNA
SSC	Sodium chloride sodium citrate
SOX2	SRY box 2
STAT	Signal transducer and activator of transcription
SV40	Simian virus 40
t	Thymine
T_3	Triiodothyronine
T_4	Thyroxine
T_m	Melting temperature
TAMRA	6 carboxy-N,N,N′,N′ tetramethylrhodamine
TBG	Thyroxine binding globulin
TBS	Tris buffered saline
TCR	T cell receptor
TE	Tris ethylenediaminetetraacetic acid
TET	6 carboxy-4,7,2′,7′ tetrachlorofluroscein
TOP	Topoisomerase

TSH	Thyroid stimulating hormone
TBG	Thyroid hormone binding globulin
TGFB	Transforming growth factor beta
TK	Tyrosine kinase
TLDA	TaqMan® low density array
TMA	Tissue microarray
TMB	3,5,3′5′ tetramethylbenzidine
TNS	Trypsin neutralising solution
TPO	Thyroid peroxidase
TRBP	TAR RNA binding protein
TRH	Thyrotropin releasing hormone
u	Uracil
UNG	Uracil DNA glycosylase
UTR	Untranslated region
WHO	World health organisation
x g	G force
3′	3 prime
µL	Microlitre
µg	Microgram
µm	Micrometre
µs	Microsecond

Publications

Denning, K., Smyth, P., Cahill, S., Li, J., Flavin, R., Aherne, S., O' Leary, J.J. & Sheils, O. (2008) ret/PTC-1 expression alters the immunoprofile of thyroid follicular cells. *Mol Cancer,* 7**,** 44.

Li, J., Smyth, P., Cahill, S., Denning, K., Flavin, R., Aherne, S., Pirotta, M., Guenther, S. M., O'Leary, J. J. & Sheils, O. (2008) Improved RNA quality and TaqMan Pre-amplification method (PreAmp) to enhance expression analysis from formalin fixed paraffin embedded (FFPE) materials. *BMC Biotechnol,* 8**,** 10.

Flavin, R. J., Smyth, P. C., Finn, S. P., Laios, A., O'Toole, S. A., Barrett, C., Ring, M., Denning, K. M., Li, J., Aherne, S. T., Aziz, N. A., Alhadi, A., Sheppard, B. L., Loda, M., Martin, C., Sheils, O. M. & O'Leary, J. J. (2008) Altered eIF6 and Dicer expression is associated with clinicopathological features in ovarian serous carcinoma patients. *Mod Pathol,* 21**,** 676-84.

Flavin, R. J., Smyth, P. C., Laios, A., O'Toole, S. A., Barrett, C., Finn, S. P., Russell, S., Ring, M., Denning, K. M., Li, J., Aherne, S. T., Sammarae, D. A., Aziz, N. A., Alhadi, A., Sheppard, B. L., Lao, K., Sheils, O. M. & O'Leary, J. J. (2008) Potentially important microRNA cluster on chromosome 17p13.1 in primary peritoneal carcinoma. *Mod Pathol.*

Denning, K. M., Smyth, P. C., Cahill, S. F., Finn, S. P., Conlon, E., Li, J., Flavin, R. J., Aherne, S. T., Guenther, S. M., Ferlinz, A., O'Leary, J. J. & Sheils, O. M. (2007) A molecular expression signature distinguishing follicular lesions in thyroid carcinoma using preamplification RT-PCR in archival samples. *Mod Pathol,* 20**,** 1095-102.

Li, J., Smyth, P., Flavin, R., Cahill, S., Denning, K., Aherne, S., Guenther, S. M., O'Leary, J. J. & Sheils, O. (2007) Comparison of miRNA expression patterns using total RNA extracted from matched samples of formalin-fixed paraffin-embedded (FFPE) cells and snap frozen cells. *BMC Biotechnol,* 7**,** 36.

Flavin, R., Smyth, P., Crotty, P., Finn, S., Cahill, S., Denning, K., Jinghuan, L., O'Regan, E., O'Leary, J. & Sheils, O. (2007) BRAF T1799A mutation occurring in a case of malignant struma ovarii. *Int J Surg Pathol,* 15**,** 116-20.

Cahill, S., Smyth, P., Denning, K., Flavin, R., Li, J., Potratz, A., Guenther, S. M., Henfrey, R., O'Leary, J. J. & Sheils, O. (2007) Effect of BRAFV600E mutation on transcription and post-transcriptional regulation in a papillary thyroid carcinoma model. *Mol Cancer,* 6**,** 21.

Cahill, S., Smyth, P., Finn, S. P., Denning, K., Flavin, R., O'Regan, E. M., Li, J., Potratz, A., Guenther, S. M., Henfrey, R., O'Leary, J. J. & Sheils, O. (2006) Effect of ret/PTC 1 rearrangement on transcription and post-transcriptional regulation in a papillary thyroid carcinoma model. *Mol Cancer,* 5**,** 70.

Summary

Thyroid carcinoma is the most common endocrine malignancy, with an incidence of approximately eighty cases per year in Ireland and thirty seven thousand cases per year in the United States. While thyroid cancer may be considered a relatively infrequent cancer, accounting for one percent of all cancers, world wide thyroid cancer incidences rates are increasing year after year. Furthermore thyroid nodules are a common occurrence and distinguishing benign specimens from malignant can be problematic. It is estimated that five to ten percent of individuals will develop a clinically significant thyroid nodule during their lifetime. The development of robust molecular biomarkers would significantly aid in the diagnosis of thyroid malignancy. The purpose of this thesis was to examine gene and regulatory profiles in thyroid neoplastic and inflammatory disease to evaluate their potential as molecular markers of thyroid disease. The assessment was carried out using TaqMan® RT-PCR for gene expression analysis, immunohistochemistry for protein analysis and *in situ* hybridisation for microRNA expression analysis.

Hashimoto Thyroiditis (H.T.) is a destructive autoimmune condition. ret/PTC-1 is an oncogene previously thought to be specific to papillary thyroid carcinoma (PTC), but has since been found in benign conditions such as H.T. Activated H.T. and control lymphocytic supernatants were co-cultured with a normal thyroid cell line and a thyroid carcinoma cell line that expresses the oncogene ret/PTC-1 at 0, 6 and 18 hour time points. Immunoprofiling TaqMan® low density arrays were used to evaluate the immunogenic effect exposure to the lymphocytic supernatants would have on the cell line models. Global up-regulation of targets was found when H.T. supernatant was exposed to the normal cell line model, in particular a subset of five targets associated with apoptosis and T cell signalling which could be involved in H.T. pathogenesis. When the ret/PTC-1 expressing cell line was co-cultured with H.T. lymphocytic supernatant, down-regulation of the same five targets was seen. Consequently, it was hypothesised that ret/PTC-1 activation may dampen immunogenic response in the thyroid, which could facilitate development of PTC.

Using microarray analysis previously carried out by the group, a panel of ten markers were chosen to examine their utility as adjunctive markers in the diagnosis of thyroid

malignancy on a cohort of one hundred and ninety five archival thyroid tissues. Laser capture microdissection (LCM) and a novel pre-amplification technique were used to facilitate TaqMan® gene expression analysis of the panel of ten targets, which previously had not been possible using archival material and LCM due to RNA quantity restraints. Nine out of the ten targets analysed were able to significantly discriminate a range of benign from malignant categories of thyroid disease. This panel of markers could significantly aid in the diagnosis of thyroid malignancy.

After ascertaining in the previous project that unbiased pre-amplification of laser capture microdissected archival material could successfully be used in gene expression analysis, it was decided to again use this technique on another panel of five targets chosen via microarray technology and to expand the analysis of these targets to include protein expression using immunohistochemisty. The cohort of approximately two hundred archival samples used in the previous project was analysed and a tissue microarray (TMA) containing this cohort was constructed. All five targets significantly discriminated a range of benign from malignant disease states at mRNA and protein expression levels. Four out of the five targets were also shown to significantly discriminate corresponding groups of matched samples. This robust panel of markers may also prove valuable in assisting the classification and diagnosis of thyroid malignancy.

MicroRNAs are a recently discovered class of small (22 nucleotides) RNAs that negatively regulate their target mRNA, and are believed to be involved in cancer development. Of the five targets analysed in the previous project, two targets MMP11 and APOE, which were over-expressed in malignant tissues, were found to be targets of miRNA let-7a using miRNA target prediction databases. Analysis of let-7a expression was carried out in one hundred and four archival thyroid samples using a novel *in situ* hybridisation method for miRNA analysis on paraffin embedded material. Expression of let-7a was significantly down-regulated in all malignant groups versus benign. Not only has let-7a been proven capable of discriminating benign from malignant thyroid disease but its expression profile also lends further support to its role as a tumour suppressor miRNA, potentially by negatively regulating MMP11 and APOE.

Chapter One

General Introduction

1.1 The thyroid gland: a brief history

Little was known about the thyroid for most of early medical history. Only with the development of goitre (enlarged thyroid) was the gland more so appreciated. Dioscorides and other early Roman medical authorities believed goitre represented an anterior herniation of the bronchus or "bronchocoele" (Dioscroidis, 1829). Hippocrates felt that these prominences were deformities of the cervical glands that developed as a result of drinking snow water (Hippocratis, 1825-1827).

In 1600 BC the Chinese used burnt sponge and seaweed for the treatment of goitres. The word goitre itself is derived from the Latin term "guttur", which means throat. Goitre was known to mainly affect women, and was thought to round out and beautify the neck, and thus far became a symbol of beauty as reflected in the art of the Middle Ages.

Figure 1.1 Oil on canvas painting by Edvard Munch: The seducer II 1913 depicts a female with an enlarged neck, most probably the result of a goitreous thyroid gland (Giddings, 1998)

In the 16th century, the thyroid would first be identified as a discrete gland. The Renaissance artist Leonardo Da Vinci made the first drawing of the organ in 1511 as part of a series of anatomical studies he performed at the hospital of Santa Maria Nuova in Florence. Da Vinci, who at the time was unaware of the function of the thyroid, wrote in the margin: "These glands are made to fill the interval where the muscles are lacking and hold the trachea away from the forcula (sternal notch)" (O' Malley, 1952). Thomas Wharton coined the term "glandular thyroideae" when he published his monograph on glands of the human body in 1656. The name originated from the glands proximity to the nearby thyroid cartilage in the neck, which resembled a shield, or "thyreos" in Greek (DuBose et al., 2004).

The 19th Century brought with it a deeper understanding of thyroid physiology and disease. Until this point it was thought that an imbalance of the four humors: blood, phlegm, green bile and black bile, caused sickness in an individual. It was also believed that goitre was caused by an excess of phlegm. Treatment was quite empiric and several remedies were proposed, usually comprising of mixtures of seaweed and marine sponge (probably due to their high iodine content). These "treatments" were quite familiar to medieval Europeans, who were thought to have learned of them from the Chinese (via traders) who had been using such substances to treat goitre for over a thousand years (Braverman, 2005).

Iodine was discovered in 1812 in the residue of burnt seaweed by Courtois. Eight years later a Scottish trained physician named Coindet, who worked among goitrous people in Geneva, considered iodine to be the active ingredient in the therapies for goitre. He gave iodine to his patients (mostly as potassium salt) and after which their goitres shrank remarkably (Coindet, 1820). He also observed toxic effects in some patients who took too much of the remedy. This observation was in fact the earliest description of iodine-induced thyrotoxicosis (production of excessive thyroid hormone). As a consequence of these toxic effects the method of treatment soon fell out of favour. During this time few accepted that disease could be caused by a deficiency in something. Seen as toxic, the use of iodine replacement never became widespread. The usefulness of iodine as a prophylactic agent has still, to this day, not been implemented universally. At present, an international consortium (the

International Council for the Control of Iodine Deficient Disorders) attempts to ensure that everyone receives adequate amounts of iodine worldwide (Braverman, 2005).

In 1786 Caleb Hillier Parry first noted the association between an enlarged thyroid gland and the characteristic clinical features of hyperthyroidism in his descriptive account entitled "Enlargement of the Thyroid Gland in Connection with Enlargement or Palpitation of the Heart" published posthumously (Parry, 1825). In his published Meath Hospital lectures (Graves, 1835), Dublin doctor Robert Graves and his colleague Stokes described a group of women with goitre, palpitations and exophthalmos. Both believed the illness to be cardiac in origin. The descriptions were not well known on the European continent, so when Carl Adolf von Basedow described similar patients in 1840 (von Basedow, 1840), he was thought to be the first to describe the illness. Graves' and Basedow's disease subsequently became synonymously known as the former. At the time though, the disease was not thought to be connected to the thyroid.

Early attempts to treat thyroid enlargement and over-activity were associated with a very high mortality and morbidity due to haemorrhage, asphyxia, hospital gangrene and air embolism (Giddings, 1998). The first successful typical partial thyroidectomy was performed by French surgeon, Pierre Joesph Desault in 1791 (DuBose et al., 2004). Despite this initial success, the chance of surviving a thyroidectomy was a mere forty percent. Before the 1850s, thyroidectomy was considered "breathtaking heroics fraught with danger to the patient and almost certain bereavement for the family" (Becker, 1977). A quote from Samuel D. Gross gives a colourful explanation: "Can the thyroid gland when in the state of enlargement be removed with a reasonable hope of saving the patient? Experience emphatically answers "No"!!!....If a surgeon should be so foolhardy as to undertake it....every step he takes will be environed with difficulty, every stroke of his knife will be followed by a torrent of blood, and lucky will it be for him if his victim lives long enough to enable him to finish his horrid butcher. No honest and sensible surgeon would ever engage in it" (Becker, 1977).

By the mid 1800s surgeons were able to remove goitres from patients successfully. The most notable of these was Emil Theodore Kocher, who is considered the father of

thyroid surgery. He was awarded the Nobel Prize for Medicine in 1909 for "his work in physiology, pathology and surgery on the thyroid gland". Kocher performed five thousand thyroid excisions by 1912 with impressively reduced mortality (from 18 percent to less than 0.5 percent) (DuBose et al., 2004). Around the same time, in the United States, Charles Horace Mayo (co-founder, with his brother, of the Mayo clinic) became the leading authority on thyroid surgery, performing his first goitre operation in 1889, and his 5000th in 1918 (DuBose et al., 2004).

By 1900 the concept of an excess amount of thyroid hormone came into existence as the cause of thyroid disease. This became known as hyperthyroidism. Hypothyroidism (deficiency of thyroid hormone) as a clinical syndrome was recognised even later than hyperthyroidism and its cause was as equally obscure. It was first called myxoedema by Willian Ord in 1877 (Vellar, 1974), because of the swollen skin (oedema) and its excess content of mucin (myx). It was then considered a neurologic or skin disease for which there was no cure. Language barriers at the time prevented physicians from collaborating and reading each other's work (Ahmed and Ahmed, 2005). However this changed when Semon, a practicing laryngologist in London, presented to The Clinical Society of London that a number of Swiss patients who had undergone total thyroidectomy seemed similar to English ones with myxoedema. They set up a committee to investigate this and found that congenital hypothyroidism and myxoedema were the result of the loss of function of the thyroid. This was a major step in the journey of understanding thyroid disease (Cranefield, 1962).

Despite the increased level of understanding, a treatment proved elusive. At the time, Brown-Sequard was working on the subject of organotherapy - the use of tissue extracts for the treatment of diseases. Although his work with testicular extracts proved promising, most of the treatments failed. Until that is, George Murray began to inject sheep thyroid extract into myxoedema patients in 1891 (Murray, 1981), resulting in an unlikely cure. A year subsequently, the injections were disposed of and patients merely had to ingest ground or fried sheep thyroid, or tablets of dried thyroid tissue.

The active ingredient in thyroid extracts remained a mystery, even though Baumann discovered iodine in the thyroid gland in 1895. It was another twenty years before Professor Edward Kendall and his associate Osterberg of the Mayo Clinic isolated bioactive crystalline material from thyroid extract on Christmas Day, 1914, which they subsequently named thyroxin (Kendall, 1915). However, Kendall was mistaken about the molecule's structure and never actually succeeded in synthesising the active molecule. However, he did patent and release the isolated crystalline form. In 1926, Sir Charles Harington assumed the correct structure and a year later synthesised the molecule, renaming it thyroxine (Harrington, 1926, Harrington, 1927). However neither product was successful, either being ineffective (no one knew that thyroxine as the free acid is not well absorbed) or too expensive. In 1949 the successful synthesis of thyroxine in the form of sodium L-thyroxine, which is well absorbed from the gut, made therapy economically viable. It is now used in almost all treatment with thyroid hormone. An associate of Harington, Pitt-Rivers, along with her colleague Gross at the National Institute for Medical Research, Mill Hill, then discovered and synthesised triiodothyronine, (Gross and Pitt-Rivers, 1952) which was found to be the second thyroid hormone. A Parisian group almost simultaneously corroborated this finding (Roche et al., 1952).

1.2 Thyroid embryology and development

The thyroid gland is the first of the body's endocrine glands to develop, at twenty four to twenty eight days gestation. The gland originates as a proliferation of endodermal epithelial cells on the median surface of the developing pharyngeal floor. Development of the gland arises from three pharyngeal bodies: the median anlage and two lateral anlagen (Santisteban and Bernal, 2005).

The median anlage of the thyroid arises as a bilobated structure at the foramen cecum of the tongue; it is attached to the tongue by the thyroglossal duct. It is located between the first and second brachial arches and is adjacent to the newly differentiating myocardium. The initial descent of the rudimentary thyroid occurs anterior to the pharyngeal gut. At this point, the thyroid is still connected to the tongue via the thyroglossal duct. As the thyroid descends, it forms its mature shape, with a median isthmus connecting two lateral lobes. The thyroid completes its decent in the seventh gestational week, coming to rest in its final location immediately anterior to the trachea. The thyroglossal duct later solidifies and subsequently obliterates entirely (during gestational weeks seven to ten). Nonetheless, in some individuals, remnants of this duct may still persist. Ectopic thyroid tissue can occur anywhere along this course of development (Troncone, 1994).

Ultimobranchial bodies form the lateral anlage and they arise from the fourth or fifth branchial pouches. They migrate downwards, on each side of the neck together with the parathyroid IV primordial. Reaching their final position, they separate from the proximal parathyroids and fuse with the dorsolateral aspects of the median thyroid anlage and become incorporated into the developing lateral lobes. The connection from the lateral lobes to the pharynx is lost and cells from the differentiating medial anlage surround tissue derived from the lateral anlage. The merging of the anlage is usually complete by eight to nine weeks of gestation at which time the thyroid has assumed its definitive form. The ultimobranchial bodies give rise to the parafollicular or C cells. These cells are a special subset of cells within the thyroid gland that secrete calcitonin, a hormone necessary for the regulation of calcium. Since the

ultimobranchial bodies fuse with the medial anlage in its upper lateral aspects, the C cells are found in this area in the adult human thyroid (Wheeler, 1994).

The histological differentiation of the human fetal thyroid can be divided into three stages: from weeks seven to thirteen, the precolloid stage; weeks thirteen to fourteen, beginning colloid formation; and finally, after week fourteen, the follicular phase (LiVolsi, 1990). Thyroglobulin is detectable from a relatively early stage – even prior to colloid formation. Its synthesis seems independent of thyroid-stimulating hormone (TSH), as this is not detectable in the pituitary gland until week twelve. Thyroxine-binding globulin (TBG) is detectable by week ten and increases to term.

1.3 Anatomy of the thyroid gland

Macroscopic appearance

The normal adult thyroid consists of two lobes connected by an isthmus. The individual lobes have a pointed superior pole and a blunt inferior pole. Each lobe measures approximately two to two point five centimetres wide by four centimetres. long. The gland is loosely attached to the anterior trachea by loose connective tissue. The lobes lie along the lower halves of the lateral margins of the thyroid cartilage. Laterally lie the carotid sheaths and the sternocleidomastoid muscles; the recurrent laryngeal nerves lie between the posterior aspect of each lobe. Among normal variants discrepancies may be found in the sizes of the lobes, or the presence of a pyramidal lobe (LiVolsi, 1990).

Normal weights of the adult gland have been estimated to range from sixteen to twenty five grams and depend upon functional state, sex, hormonal status and size of the individual, as well as appropriate iodine intake. Thyroid tissue is light brown in colour, firm in consistency and often glistening on its cut surface. The normal gland is loosely attached to neighbouring structures, but fascial planes are distinct. Nodules are not uncommon in the adult gland and can be found grossly in about ten percent of the endocrinologically normal population (Ljungberg, 1992).

Blood supply is from the superior thyroid arteries, arising from the external carotid artery and from the inferior thyroid arteries, which arise as branches of the thyrocervical trunk extending from the brachiocephalic artery. Venous drainage includes the brachiocephalic, internal jugular and occasionally the anterior jugular veins. Lymphatic drainage is to upper and lower deep cervical nodes. The nerves are nonmedullated postganglionic fibres originating from superior and middle cervical sympathetic ganglia. These nerve fibres are vasomotor and influence thyroid secretion indirectly by their action on blood vessels (Thompson, 2006).

Light microscopic appearance

Microscopically, the thyroid is divided into lobules composed of about twenty to forty follicles. It is estimated that approximately three million follicles are present in the

thyroid of an adult man. The follicles are the functional unit of the thyroid and consist of a closed sac with an average diameter of two hundred nanometres, which are lined by a single layer of epithelium. The height of the follicular epithelial cells varies from low cuboidal to high columnar according to the functional activity of the gland. The lumen of the follicle contains a viscous material known as colloid, containing concentrated eosinophilic staining thyroglobulin. Follicular cells have a definite polarity, with their apices directed toward the lumen of the follicle and their bases toward the basement membrane (Thompson, 2006).

In the interfollicular stroma, and occasionally abutting between the follicular epithelial cells, are individual or small groups of parafollicular or C cells. These calcitonin-producing neuroendocrine C cells make up only 0.1% of the total thyroid cellular mass.

Solid irregular masses of epithelial cells about one millimetre in diameter are seen in up to sixty percent of thyroids and occur most commonly in the middle of the lateral lobes and may be single or multiple, unilateral or bilateral. They are called solid cell nests (SCN) and are said to represents remnants of the ultimobranchial body (Janzer et al., 1979). They have calcitonin immunoreactivity. SCN may communicate with follicles. Cells lining the walls of the cystic spaces of SCN may show thyroglobulin immunopositivity. The thyroid gland also has significant numbers of mast cells. Dendritic antigen presenting cells (APC) are present in the stroma and T-lymphocytes are found close to the follicular cells.

1.4 Thyroid hormones

The formation and regulated secretion of thyroid hormones is necessary for the normal metabolic homeostasis of each cell in the body. A major function of the thyroid gland is, therefore, to scavenge iodide, convert it to thyroid hormones, and then secrete them into the bloodstream in a regulated manner (Heymann, 2008).

The thyroid gland is composed of multiple functional units called follicles. Follicles consist of an outer layer of follicular cells surrounding a central mass of colloid. The follicular cells are critical for the production and secretion of thyroid hormones. Individual follicles differ in their morphological appearance and, presumably, their state of function at a given time. Presumably this is one means of achieving normal homeostasis, i.e., asynchronous function of individual follicles can minimise the extreme swings of a synchronous population (Wu, 1991).

Secretion of thyroid hormone is controlled by the interaction of stimulatory and inhibitory factors. However all steps of thyroid hormone formation and release are controlled by thyroid stimulating hormone (TSH) which is released from the anterior pituitary gland. Synthesis of thyroid hormone is dependent on an adequate supply of iodine. The normal European daily dietary intake of iodine is about 150 μg, of which 125 μg is taken up by the thyroid gland and used for hormone synthesis. Iodine ingested in the diet is reduced to iodide and iodide in the serum is actively transported into the follicular cell by an active mechanism situated at the base of the cell. The transport system concentrates the iodide within the cell, creating a fifty-fold or greater concentration gradient, and the iodide is, within a few minutes, transported through the cell, and secreted across the apical membrane facing the follicular lumen, where it is trapped by a process known as organification. Organification involves two separate cell proteins, both of which are "induced" by thyroid stimulating hormone (TSH), thyroglobulin and thyroid peroxidase (TPO) (Kohn, 1993).

Thyroglobulin is vectorially transported to the apical membrane of the cell and deposited into the follicular lumen. The TPO, which is synthesised in the same region of the cell, also moves to the apical membrane, but stays in the apical membrane as an

integral protein, rather than being secreted into the follicular lumen like thyroglobulin. At the apical membrane, the meeting of thyroglobulin, TPO, iodide and a hydrogen peroxide-generating system result in the organification process, i.e. the linking of iodide to tyrosine residues on the protein thyroglobulin. One iodine atom combining with tyrosine produces monoiodotyrosine (MIT) and two atoms combining produces diiodotyrosine (DIT). MIT and DIT residues on thyroglobulin couple and rearrange to form triiodothyronine (T_3) and thyroxine (T_4), the thyroid hormones (McDougall, 1992).

These macromolecular precursor forms of the thyroid hormones are stored in the follicular lumen until TSH-induced macropinocytosis causes pseudopod-like arms to emerge from the apical membrane and engulf material stored in the follicular lumen. Encapsulated in vesicles, the macromolecular thyroid hormone precursor molecules are moved to lysosomes where the vesicles and lysosomes fuse and the thyroglobulin is degraded to release free thyroid hormones (Braverman, 2005).

The thyroid hormones are transported to the basal membrane of the cell and secreted into the blood stream, where they are carried to cells complexed with proteins: thyroid hormone binding globulin (TBG), prealbumin and albumin. T_4 is converted peripherally to T_3, the active hormone, by tissue deiodinases 1 and 2. Most of the actions of thyroid hormone are affected by T_3 via binding to nuclear receptors encoded by two genes related to c-erb-A viral oncogene. They are members of a receptor superfamily which includes steroids, retinoic acid receptors and vitamin D. Binding alters the transcription of genes encoding proteins with wide ranging effects on metabolic processes including general carbohydrate, lipid and protein metabolism. They also interact with the sympathetic nervous system and regulate a variety of cellular and physiologic processes such as growth, development and metabolism. Thyroid hormone has prominent effects during gestation and early childhood. Thyroid hormones have an effect on many different pathways and organs, and the clinical manifestations and metabolic effects of hypothyroidism and hyperthyroidism highlight this (Wu, 1991).

1.5 Thyroid disease states

This thesis has employed a cohort of approximately two hundred archival thyroid samples. This cohort encompasses representatives from the majority of thyroid disease states. These and other disease states which affect the thyroid gland will now be discussed individually.

1.5.1 Goitre

Goitre is a diffuse or nodular enlargement of the thyroid gland, usually resulting from a benign process or a process of unknown origin. The incidence of goitre is very much dependent on the status of iodine intake of the population. Iodine deficiency can lead to insufficient thyroid hormone production, which, if the hypothalamic pituitary axis is intact, increases production of thyroid-stimulating hormone (TSH), which results initially in increased activity of thyroid follicular cells. The thyroid gland will respond with epithelial hyperplasia with tall epithelial cells and small amounts of colloid. This is the so called parenchymatous goitre, which later may develop follicular atrophy with extensive accumulation of colloid, causing further enlargement (diffuse colloid goitre) and as time passes progressive nodularity of the goitre (multinodular goitre) (Ljungberg, 1992). Nodular goitres typically result from over-distension of some involuted follicles, and persistence of regions of epithelial hyperplasia.

1.5.2 Hyperplasia

Hyperplasia represents the response of the thyroid to TSH, other growth factors, or circulatory stimulatory antibodies. The epithelial is tall and columnar; the follicles are collapsed and contain only scanty colloid. When the hyperplastic stage is extreme, hyperplasia may be confused with carcinoma because of the degree of cellularity and the presence of enlarged cells. The nuclei are enlarged and hyperchromatic because of follicular collapse, epithelial hyperplasia and hypertrophy is present; papillary changes can also be seen (Studer and Derwahl, 1995). Recognition of the benign nature of the process is possible because all of the glandular tissue is abnormal, unlike

carcinoma, where the neoplastic masses constitute one of more localized groups of abnormal cells with a background of non-neoplastic parenchyma.

1.5.3 Hyperthyroidism

Hyperthyroidism refers to over activity of the thyroid gland leading to excessive synthesis of thyroid hormones and accelerated metabolism in the peripheral tissues. Patients with hyperthyroidism are thyrotoxic; thyrotoxicosis being a pathophysiological condition resulting from action of excess T_4 and T_3. Graves' disease, an autoimmune condition, is the most common cause of hyperthyroidism, accounting for ~80% of cases. It affects predominantly young women who manifest diffuse thyroid enlargement, ophthalmopathy and hyperthyroid symptoms and signs (weight loss, fatigue, palpitations, heat intolerance) (Heymann, 2008). The central pathological features are increased height of the epithelium from cuboidal to columnar; and redundancy of the follicular wall, giving on section the picture of papillary infoldings, cytologic evidence of increased activity, hypertrophy of the Golgi apparatus, increased number of mitochondria, and increased vacuolization of colloid. There is also a characteristic lymphocyte and plasma cell infiltrate. This infiltrate may be mild and diffuse throughout the gland, but more typically occurs as aggregates of mononuclear cells and even lymphoid germinal centers, referred to as focal thyroiditis. Toxic multinodular goitre and toxic adenoma are additional common causes of hyperthyroidism. Rarer causes include TSH-secreting pituitary adenomas and iodine-induced hyperthyroidism.

1.5.4 Hypothyroidism

Hypothyroidism is the most common clinical disorder of thyroid function. It is most often caused by a disorder of the thyroid gland that leads to a decrease in thyroidal production and secretion of thyroxine (T_4) and triiodthyronine (T_3), this is referred to as primary hypothyroidism. Primary hypothyroidism is invariably accompanied by increased thyroid stimulating hormone (TSH) secretion. This form of hypothyroidism can be caused by many instances such as destruction of thyroid tissue due to surgical and or radiotherapeutic (radioiodine) ablation, usually for hyperthyroidism.

Infiltrative diseases of the thyroid are another cause. In areas where iodine intake is adequate, the most common cause of hypothyroidism is chronic autoimmune thyroiditis (Hashimoto Thyroiditis) which is discussed in section 1.5.5.1. Heritable biosynthetic defects, severe dietary iodine deficiency and antithyroidal drug therapy can also result in hypothyroidism (Wheeler, 1994).

Secondary hypothyroidism is less common and is caused by decreased thyroidal stimulation by TSH. Secondary hypothyroidism may be caused by pituitary or hypothalamic disease, the latter causing deficiency of thyrotropin-releasing hormone (TRH). Inadequate functioning of the pituitary may result from pituitary replacement by tumour, infarction or surgical extirpation

The development of hypothyroidism in infancy or early childhood is referred to as congenital hypothyroidism. Previously, this illness was fairly common in areas such as the Himalayas and certain parts of Africa where iodine dietary deficiency was endemic. However, with the recent iodine supplementation of food it has become less common. The infant may appear normal at birth, but soon develops signs of mental retardation and neuromuscular abnormalities. The severity of mental retardation in the child is influenced by the time at which thyroid deficiency occurs in utero.

The clinical manifestations of hypothyroidism are largely independent of its cause. It affects persons of all ages and both sexes, although the majority of patients are female. The underlying problem in hypothyroidism is slowing of many physiological processes, and the clinical manifestations reflect that slowing. Symptoms such as fatigue, sleepiness, mental impairment, cold intolerance, dry skin, weight gain are often seen (Heymann, 2008).

1.5.5 Thyroiditis

The term thyroiditis, or inflammation of the thyroid gland, is given to a diverse group of disorders that are all characterised by some degree of thyroid inflammation. Some of the more common and clinically significant types of thyroiditis will now be discussed.

1.5.5.1 Hashimoto Thyroiditis

Hashimoto Thyroiditis (H.T.) is the most common cause of hypothyroidism in iodine sufficient areas. It is most commonly seen in women; fewer than 5% of cases occur in males. The peak incidence is between forty to sixty years. The disease is characterised by gradual loss of thyroid function due to autoimmune destruction of the thyroid gland. Thyrocyte destruction in H.T. has classically been associated with thyroid specific B cell immune responses where B cells secrete autoantibodies against a variety of thyroid antigens such as thyroglobulin, thyroid peroxidase, TSH receptor and iodine transporter. Cytotoxic T cell responses are also proving to be an important causative effect of thyrocyte depletion in H.T. (this topic is discussed further in chapter three, section 3.6).

In Hashimoto Thyroiditis the gland is firm and symmetrically enlarged weighing twenty five to two hundred and fifty grams. Normal thyroid lobulation is accentuated by interlobular fibrosis. The thyroid has a tan yellow appearance attributed to the abundant lymphoid tissue. The thyroid follicles are small and atrophic. Colloid appears dense or may be absent. Follicular cells are metaplastic and include oncocytic (Hurthle cell), clear cell and squamous types. In stroma and in atrophic follicles, a lymphoplasmacytic infiltrate with well developed germinal centres is found. The nuclei of the follicular epithelial cells often have nuclear clearing, enlargement, and overlap akin to the nuclear changes seen in papillary thyroid carcinoma (discussed in section 1.5.6.2). Care must be taken not to over diagnose the nuclear changes seen in Hashimoto Thyroiditis for multifocal papillary thyroid carcinoma (Braverman, 2005). There is a less common fibrous variant (~10%) with associated severe hypothyroidism, marked fibrosis and extensive loss of thyroid tissue. The fibrous

variant is more common in men than the classic variety, which occurs more often in women.

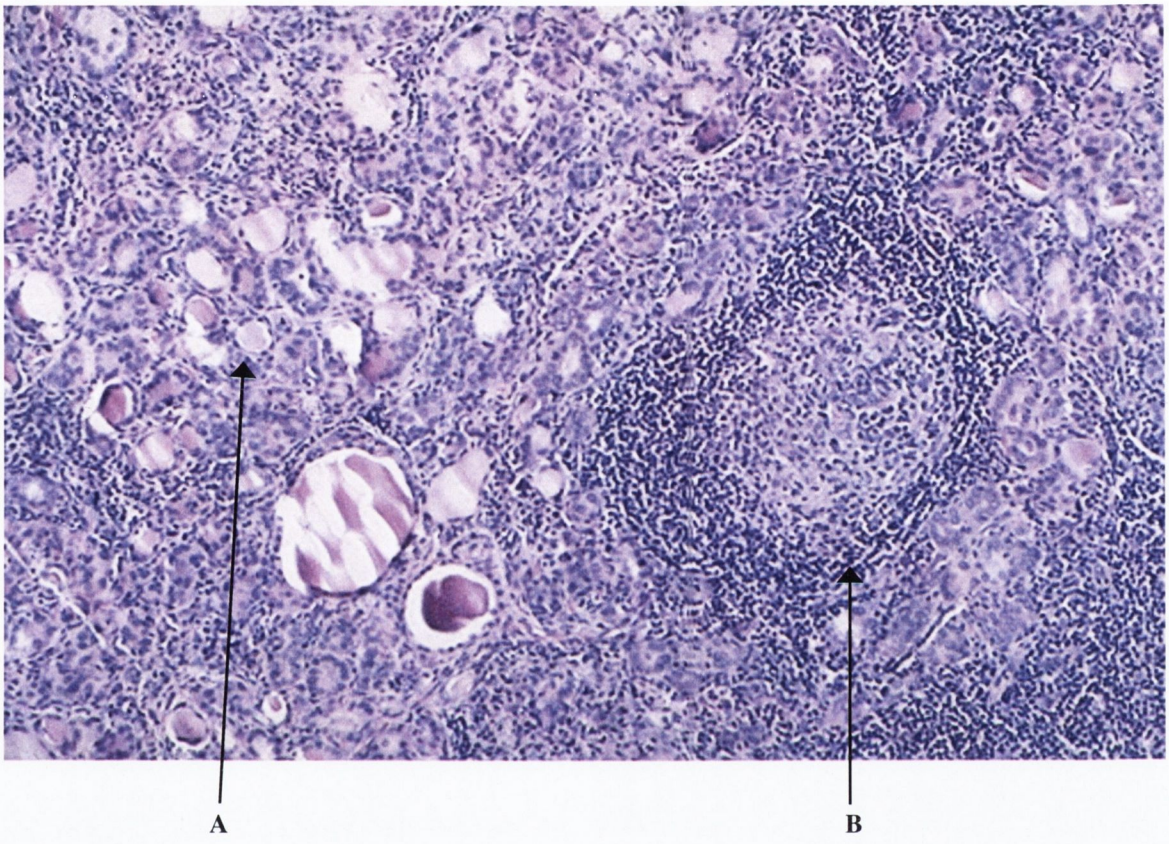

Figure 1.2 Low-power photomicrograph of Hashimoto Thyroiditis indicating Hurthle cells (A) and lymphoid follicle with germinal centre (B)

1.5.5.2 Non-specific lymphocytic thyroiditis

This is the most common type of thyroiditis in general hospital pathological material, although of less clinical interest than other forms of chronic thyroiditis. The lesion is usually an incidental finding in thyroid tissue surgically removed because of a mass in the gland. The microscopic picture is quite different from that seen in Hashimoto Thyroiditis. There are multifocal collections of lymphocytes, sometimes with admixture of plasma cells, but germinal centres are rare and oxyphil change is usually absent. The infiltrate tends to spare the follicles and is mainly located in the fibrous septa. This form of thyroiditis is probably not a nosological entity but represents a heterogeneous group of conditions with different aetiology. It probably includes reactions to various insults to the thyroid gland. A proportion of these non-specific thyroiditises may represent low grade autoimmune thyroiditis.

1.5.5.3 Granulomatous thyroiditis/ DeQuervain thyroiditis

Granulomatous subacute thyroiditis, also referred to as nonsuppurative or DeQuervain's disease, is a rare entity that usually presents in women. Patients present with a painful thyroid enlargement, general fever and malaise, and many will have a recent history of an upper respiratory infection. It is suggested that a viral infection leads to a corresponding viral antigen being presented by macrophages in the context of HLA-B35. This leads to the formation of cytotoxic T cells that damage the thyroid follicular cells. Because the immune response is not self-perpetuating, the process is limited and most patients become euthyroid after a few months. Occurrence is seasonal and tends to peak during summer months.

Microscopically, the inflammatory response, which is composed initially of polymorphonuclear leukocytes and even microabsecesses, progresses until lymphocytes, plasma cells and histiocytes become major inflammatory cells. The follicular epithelium is replaced by a rim of histiocytes and giant cells. A central fibrotic reaction occurs. Recovery is associated with regeneration of follicles from the viable edges of the involved areas.

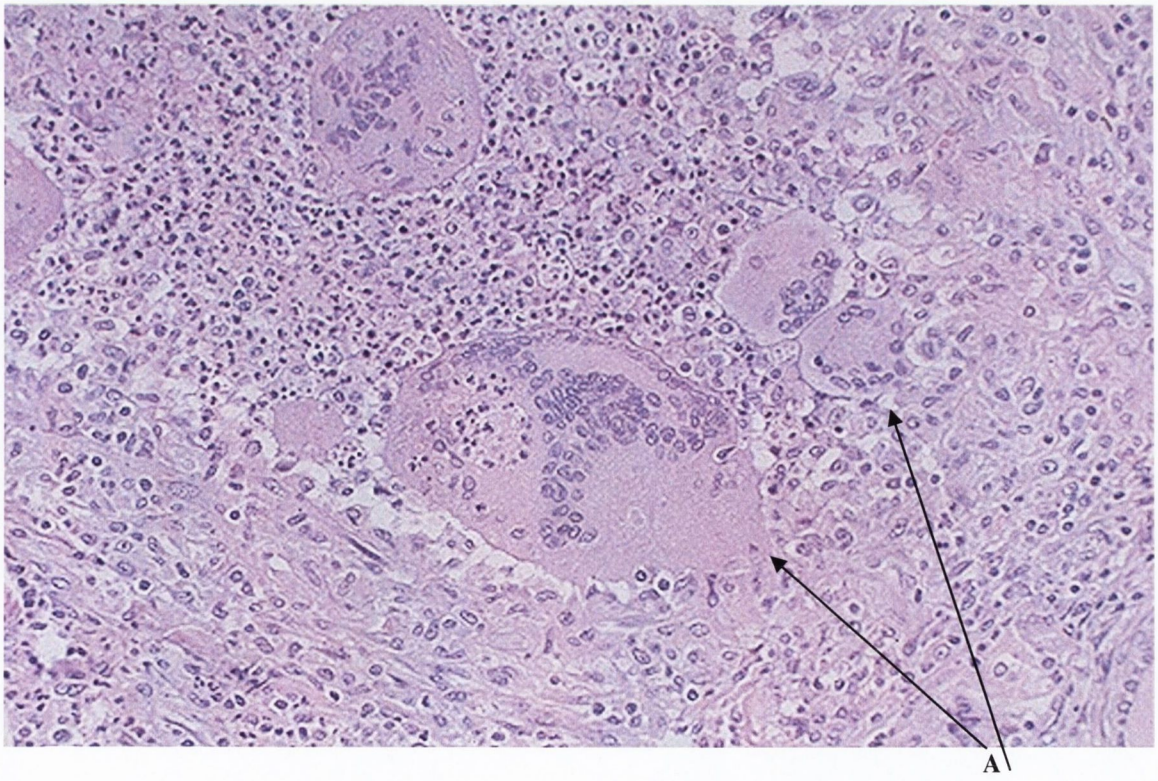

Figure 1.3 Granulomatous thyroiditis with its associated multinucleated giant cells (A)

1.5.6 Neoplasms of the thyroid

Thyroid cancers account for a small proportion of all thyroid masses and account for less than 0.5% of all cancer deaths. However, thyroid nodules occur frequently, with their incidence being about two to four percent in iodine sufficient populations. Nodules are four times more frequent in females and their incidence increases with age. The possibility of cancer in patients with thyroid nodules is therefore an important issue. Fortunately, the vast majority of nodules prove to be benign lesions such as nodular hyperplasia's and simple cysts. When nodules prove to be neoplastic, the majority of these (>90%) turn out to be adenomas. Less than one percent of solid thyroid nodules reveal a diagnosis of carcinoma. Of those that do, most are indolent with a ninety percent survival rate (the percentage of people living at least X amount of years after being diagnosed) even at twenty years. The following sections detail the major thyroid neoplasm's, both adenoma and carcinoma, in their various forms and variants.

1.5.6.1 Adenomas

Follicular adenoma (FA) is a benign encapsulated neoplasm composed of a collection of follicular epithelium that usually shows uniform architecture. These tumours are the most common of all thyroid neoplasms. Adenomas grow slowly, may remain dormant for years and typically are asymptomatic. Grossly the follicular adenoma typically ranges from one to three centimetres, is well demarcated and has a fibrous capsule that is intact. The cut surface is bulging and has a soft, greyish tan or brownish appearance. Tumours with little colloid appear dry and brittle whereas colloid rich lesions are shining, sometimes gelatinous in character. The tumour tends to compress the neighbouring thyroid parenchyma. Microscopically follicular adenomas show a variety of patterns (trabecular, microfollicular, macrofollicular and normofollicular) (Troncone, 1994). The lesions have a thin capsule, which contrasts with the thick capsules often seen in association with carcinomas. In the absence of previous diagnostic intervention (Fine Needle Aspiration FNA), mitotic activity is low. Variation in nuclear size may be evident and occasionally bizarre atypical cells may be seen. Degenerative features may be present and include myxoid degeneration, cystic degeneration, recent or older haemorrhage, calcification and ossification. The

most important aspect of histological evaluation remains the elimination of malignant potential. For this reason the capsule must be carefully examined for evidence of invasion and for the presence of vascular invasion.

Thyroid follicular lesions can be problematic to diagnose histologically in the lab. This could potentially lead to the misdiagnosis of follicular adenomas as follicular thyroid carcinomas or follicular variant papillary thyroid carcinomas, or more worryingly the misdiagnosis of malignant follicular lesions as benign ones (this topic is discussed further in chapter four, section 4.2.1).

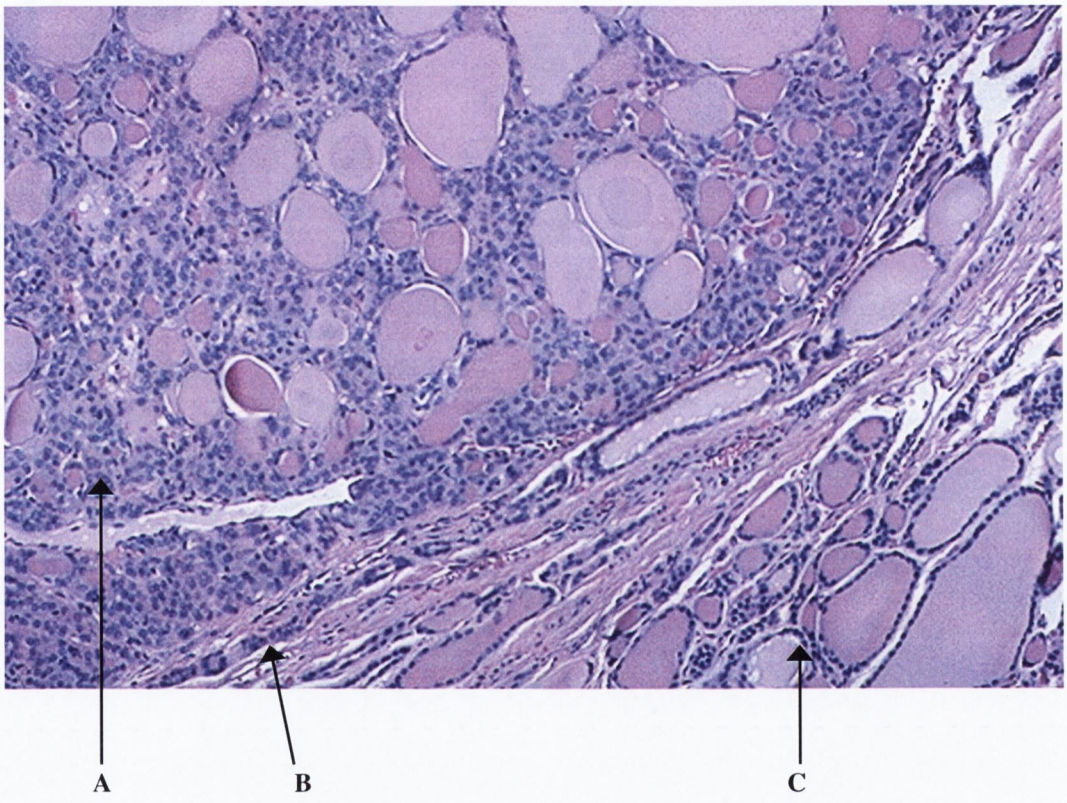

Figure 1.4 Follicular adenoma of the thyroid (A) surrounded by a capsule (B) and showing a background of normal thyroid (C)

1.5.6.2 Papillary thyroid carcinoma

Papillary carcinoma of the thyroid is the most common malignant tumour of the gland in countries having sufficient iodine in their diets and composes approximately eighty percent of thyroid malignancies (LiVolsi, 1999). Papillary thyroid carcinoma (PTC) affects females more frequently than males, with a ratio of 3:1 and can be present in any age group, the mean age at the time of initial diagnosis being approximately forty years. The association of radiation, in particular during childhood, with the development of PTC is well documented. The prognosis for patients with PTC is more favourable than that of follicular thyroid carcinoma (FTC) but worsens with increasing age at diagnosis (Fonseca et al., 2006).

The tumours can invade lymphatic's leading to multifocal lesions and to regional node metastases. Venous invasion rarely occurs and metastases outside the neck are unusual (five to seven percent of cases).

The gross appearance of PTC is quite variable. The lesion may appear anywhere in the gland. Typically PTC's are >1.0 to 1.5 cm, often averaging 2-3 cm, although lesions may be quite large. Lesions are firm and usually white in colour with an invasive appearance. Lesional calcification and cyst formation may be observed.

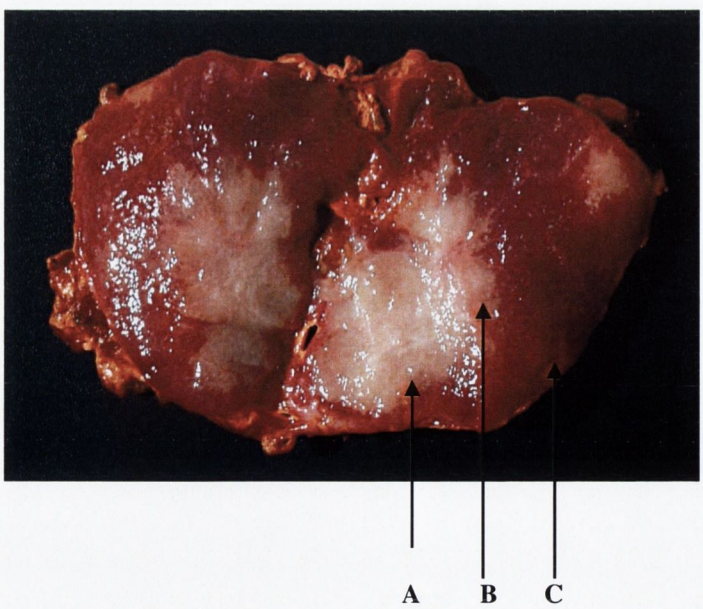

Figure 1.5 Gross PTC indicating the grey/white lesion (A) with irregular edges (B) and a background of normal thyroid (C)

Microscopically, the most diagnostic single feature in papillary carcinoma is the epithelial cell, which is usually cuboidal to low columnar, and contains a distinctive nucleus. As their name implies, papillary carcinomas contain papillae. The neoplastic papilla contains a central core or fibrovascular (occasionally just fibrous) tissue lined by one or occasionally several layers of cells with crowed oval nuclei. Psammoma bodies (also known as "ghosts of dead papillae") are formed by focal areas of infarction of the tips of papillae attracting calcium that is deposited upon the dying cell (Fonseca et al., 2006). They are usually present within the cores of papillae or in the tumour stroma. The cells of PTC have classic nuclear features. Currently the diagnosis of PTC is dependent on their presence rather than the papillary architecture. These nuclear features consist of enlarged overlapping and irregular nuclei with finely dispersed optically clear chromatin (so called ground-glass or Orphan-Annie nuclei), eosinophilic intranuclear inclusions (representing cytoplasmic invaginations) and longitudinal nuclear grooves (representing folds of redundant nuclear membrane). Mitotic figures may occur and over half of cases show extensive fibrosis

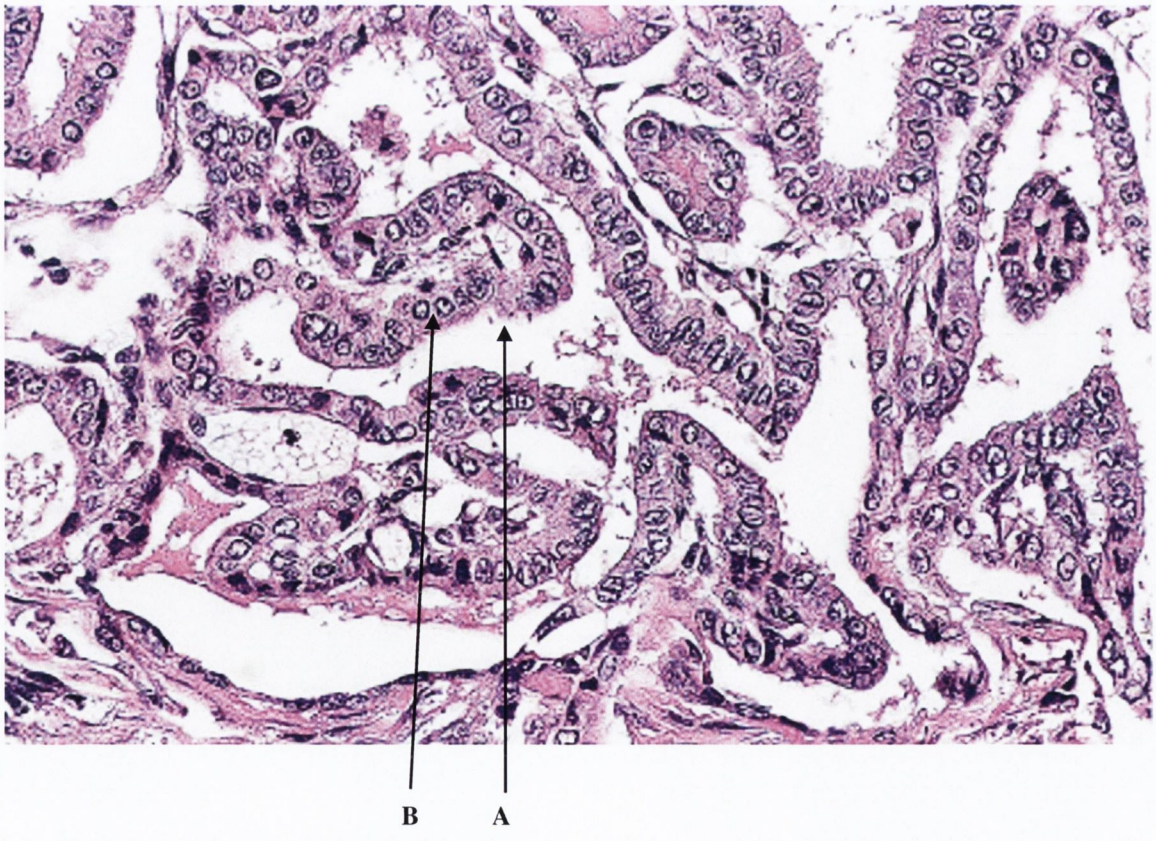

Figure 1.6 Classic PTC illustrating branching papillae (A) and nuclear features of PTC such as classic clear "Orphan Annie" nuclei (B)

There are several variants of papillary thyroid carcinoma which will now be discussed.

Papillary microcarcinoma

The papillary microcarcinoma (or occult papillary carcinoma) is defined as a papillary carcinoma one centimetre or less in diameter. These lesions are quite common as incidental findings at autopsy or in thyroidectomy. Unlike other thyroid carcinomas it is more common in men than women. The microcarcinoma is a non-encapsulated sclerotic, white to tan nodule often located subcapsularly. Histologically, the tumours may be totally follicular or show papillary areas also. Sceloris may be a prominent feature with the lesions infiltrate the surrounding thyroid.

Encapsulated variant

The encapsulated variant presents grossly as an adenoma and composes eight to thirteen percent of papillary cancers. This variant is thought to have a better prognosis than usual papillary cancers, although metastasis to lymph nodes may occur. The frequency of nodal metastasis is approximately twenty five percent, whereas usual PTC has a node metastasis rate of fifty percent. Microscopically, such lesions usually show total encapsulation; however there are cytological features of papillary cancer including nuclear changes and psammoma bodies. Some of these lesions show focal invasion into the capsule.

Follicular variant

Lindsay (Lindsay, 1970, Lindsay, 1969) originally thought that the follicular variant of papillary thyroid carcinoma (FVPTC) was a subtype of follicular carcinoma, although he later classified it among the papillary carcinomas. In 1977 Chen and Rosai (Chen and Rosai, 1977) gave a detailed clinicopathological description of this tumour and confirmed it as a variant of papillary carcinoma with similar biological behavior. The incidence of this variant is hard to determine as in the past some of these lesions have been described as follicular carcinomas or adenomas. Despite the almost total follicular pattern in the primary site, features that suggest a tumour is a follicular variant of papillary cancer include clear nuclei, psammoma bodies, and

desmoplastic response at invasive areas (Salajegheh et al., 2008). In this variant the follicles that compose the tumour often contain colloid with peripheral scalloping, mimicking the appearance of a hyperplastic gland. Also, clearing of the cytoplasm in addition to nuclear clearing can be seen. The prognosis for FVPTC is similar to PTC, although there may be a greater risk for this variant to metastasize outside the neck and for vascular invasion.

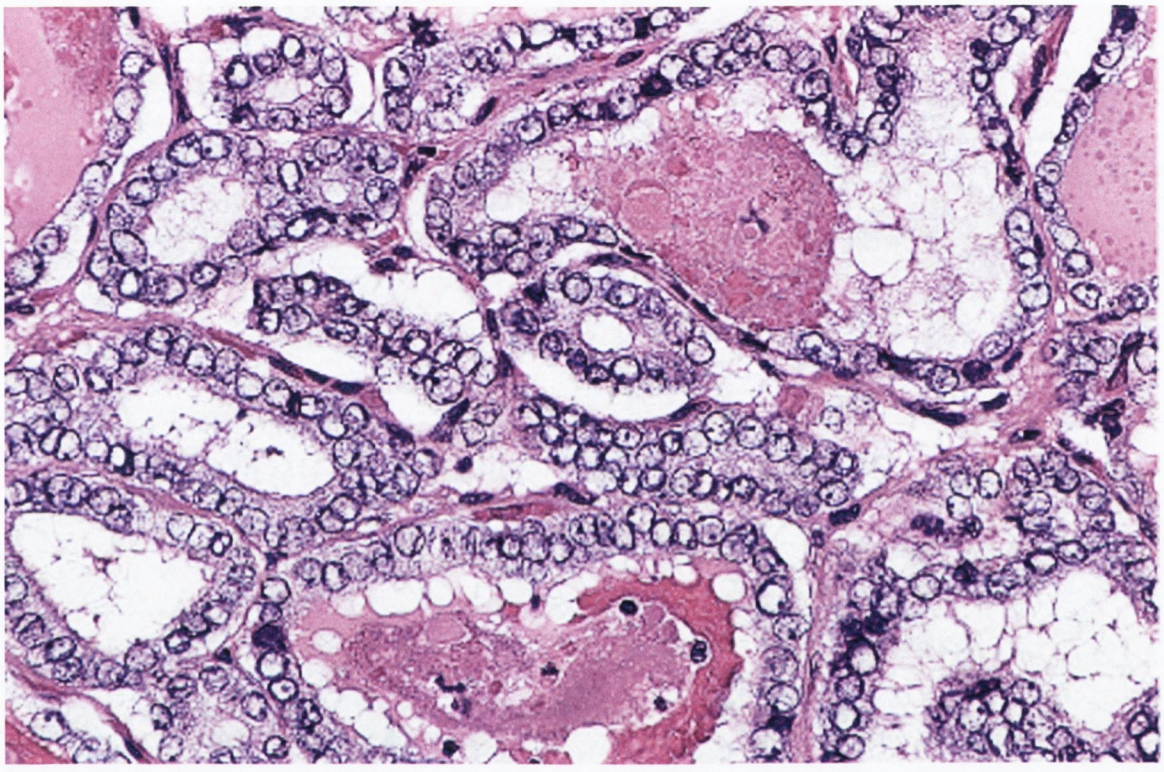

Figure 1.7 Follicular variant of PTC exhibiting classical nuclear features

The follicular variant has two further subtypes depending on the nature of the tumour boundaries.

Diffuse follicular variant: the gland is diffusely replaced by tumour. Lymph node and distant metastases are common. Prognosis appears to be poor in these patients, although only a handful of cases have been described (Sobrinho-Simoes, 1990).
Encapsulated follicular variant: refers to the follicular variant which is characterized by the presence of a capsule around the lesion.

Solid variant

A solid growth pattern is noted in many papillary carcinomas. When the solid growth represents greater than fifty percent of the tumour mass, a diagnosis of solid variant of papillary carcinoma may be made. These lesions are more common in children and although usually rare, have been reported in up to thirty percent of PTC resulting from the nuclear accident at Chernobyl (Furmanchuk et al., 1992). The nuclear features are of papillary carcinoma. Its prognosis is unclear with contradictions in the literature but is generally thought to be less favourable than classic PTC, especially in children.

Diffuse sclerosing variant

Diffuse sclerosis variant is rare, representing approximately three percent of all papillary carcinomas. The tumour, which most often affects children and young adults, may present as bilateral goitre. Features of this tumour include dense sclerosis, frequent psammoma bodies, extensive solid foci, squamous metaplasia and prominent lymphocytic infiltration. Nodal, lung and brain metastases are common.

Tall cell variant

Tall cell variant papillary carcinoma is characterised by tall columnar cells, their height being twice their breath and their cytoplasm is often eosinophilic. Tall cells should represent more than thirty percent of the papillary carcinoma cells to make the diagnosis of tall cell variant (LiVolsi, 1999). The tumour is large (>6 cm), extends extrathyroidally, and shows mitotic activity and vascular invasion more often than usual papillary cancer. The tumour tends to occur in elderly patients.

Columnar cell variant

The columnar cell variant is extremely rare. Grossly the tumours often measure less than six centimetres. Microscopically the tumour is characterised by papillary growth. There is prominent nuclear stratification and the cytoplasm is clear as opposed to acidophilic. Distant metastases are common.

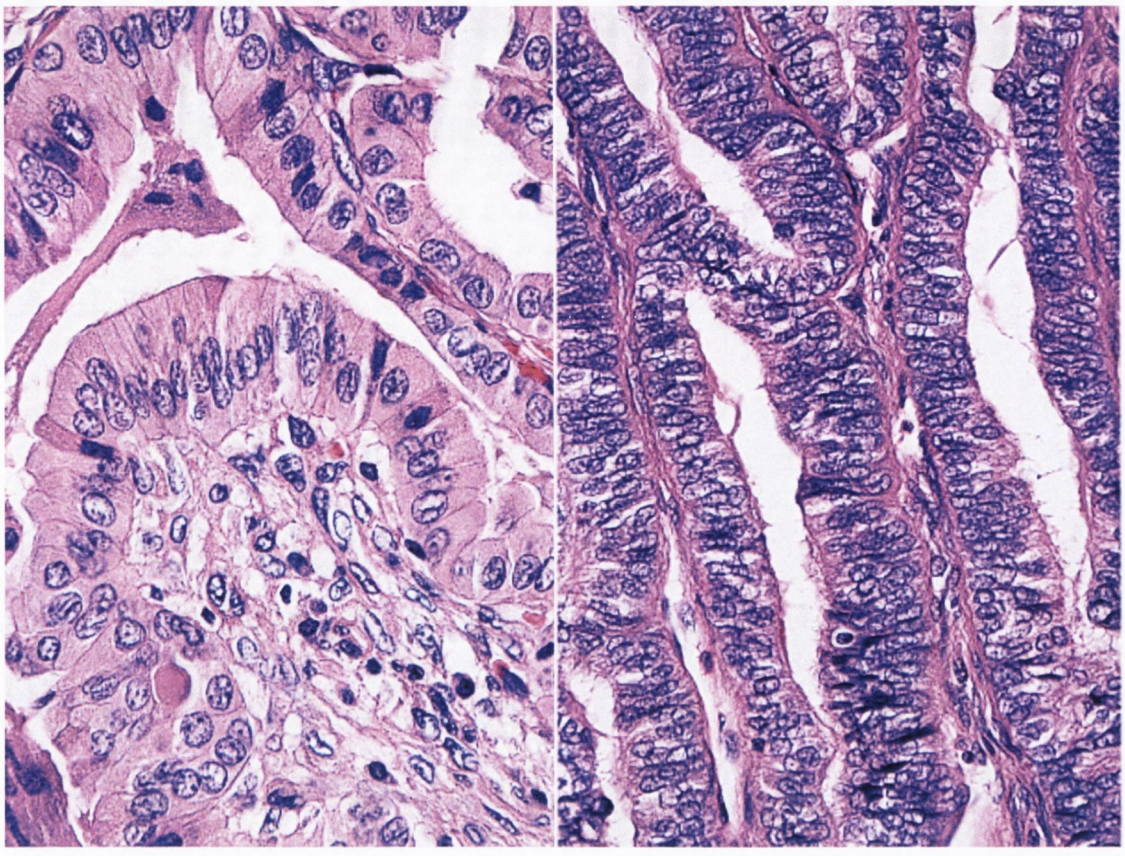

Figure 1.8 On the left, tall cell variant of PTC exhibiting abundant oxyphilic cytoplasm and on the right columnar cell variant of PTC

Cribriform-morular variant

This variant is associated with mutations of the APC gene and is therefore generally syndromic, although somatic cases can occur. It is usually found in young women (aged sixteen to thirty). The variant is characterized by the presence of a cribriform pattern of growth, follicles without colloid and papillary formations of tall cells with abundant eosinophilic cytoplasm and pseudostratification.

Oncocytic/oxyphilic variant

Papillary cancer composed of Hurthle cells (oxyphilic cells) can occur but is unusual. These must be differentiated from papillary zones in otherwise classic follicular carcinomas of Hurthle cell types (discussed section 1.5.6.4). The tumour may be encapsulated or invasive.

Warthin-like variant

This rare variant, again usually affecting women, resembles the salivary gland tumour. It is circumscribed, papillary, often centrally cystic, has papillary nuclear features with oncocytic cytoplasm, with a brisk lymphoplasmacytic infiltrate in papillary stalks. Prognosis is very good.

Nodular fasciitis like stroma

This is a rare form where exuberant stroma obscures classic tumour features.

1.5.6.3 Follicular thyroid carcinoma

Follicular thyroid carcinoma (FTC) can be defined as a malignant thyroid tumour showing evidence of follicular cell differentiation but lacking the diagnostic features of papillary carcinoma. Follicular carcinoma composes about fifteen percent of thyroid cancers; however in iodine-deficient areas, prevalence rises to twenty five to forty percent. True incidence of follicular carcinoma is difficult to determine due to the diagnostic difficulties that lie in diagnosing follicular lesions such as FTC, FVPTC and FA (discussed further in chapter four, section 4.2.1). Risk factors include iodine deficiency, older age, female gender and radiation exposure. Clinically, follicular carcinoma usually presents as a solitary mass in the thyroid.

Follicular carcinoma has a marked propensity for vascular invasion (not through lymphatics), it disseminates hematogenously and metastasizes to bone, lungs, brain and liver (Ruegemer et al., 1988). A complication that may occur in patients with follicular carcinoma is transformation into anaplastic cancer; this may occur de novo in an untreated follicular lesion, or in metastatic foci.

Grossly FTC usually presents as a grey-tan-pink fleshy, solid, encapsulated mass, sometimes with focal fibrosis or calcification. Histologically, most FTCs resemble normal thyroid with uniform cells forming small follicles containing colloid. The nuclear features of papillary carcinoma must be absent. Its appearance is variable, and well-formed follicles, cribriform areas, or trabecular formations may be present. Focal or extensive cytoplasmic clear changes can occur. Psammoma bodies are absent and metaplasia is rare (Widder et al., 2008).

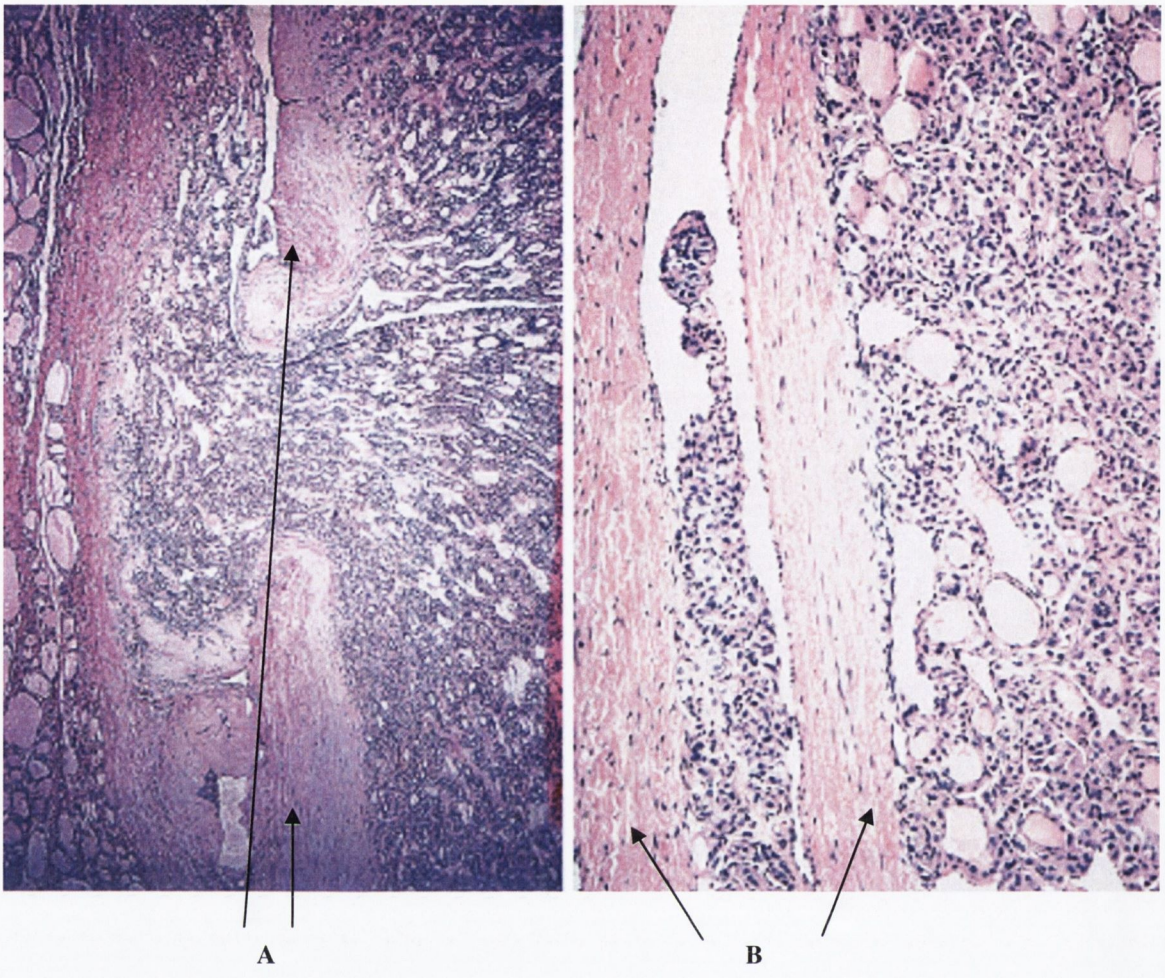

Figure 1.9 Encapsulated FTC demonstrating capsular invasion on the left (A) and vascular invasion on the right (B)

There are two variants of follicular thyroid carcinoma

Minimally invasive follicular carcinoma

Grossly it resembles a follicular adenoma; the lesion is encapsulated with a prominent and thick capsule. Microscopically the tumour demonstrates a microfollicular pattern with regular, small round follicles. Patients have a prolonged survival rate (>80% at ten years).

Widely invasive follicular carcinoma

Widely invasive follicular carcinomas are usually only partly encapsulated or totally devoid of a capsule and show marked invasiveness into surrounding tissues and or blood vessels. Patients who have follicular carcinoma that is widely invasive fare poorly. The mortality rate is twenty to fifty percent (Rosai, 1993).

1.5.6.4 Hurthle cell lesions

Hurthle cells are derived from follicular epithelium and are characterised morphologically by large size, distinct cell borders, voluminous granular cytoplasm, large nucleus and prominent nucleolus. There has been much debate and confusion regarding Hurthle cell lesions and how they should be diagnosed. However since Hurthle cell neoplasms are follicular in pattern, the criterion for distinguishing benign from malignant is the same as for follicular neoplasms i.e. the identification of capsular and or vascular invasion. Hurthle cell neoplasms are brown to mahogany solitary mass lesions with complete or partial encapsulation. Unlike follicular carcinomas Hurthle cell lesions show invasion more often and can also metastasize to regional lymph nodes.

1.5.6.5 Insular/Poorly differentiated carcinoma

Insular carcinoma is a follicular-derived carcinoma with a prognosis between well-differentiated thyroid carcinomas (papillary or follicular) and anaplastic thyroid carcinoma. The term insular is used to describe the lesion's histologic growth pattern which is somewhat "carcinoid-like". Their incidence varies with geographic location (Papotti et al., 1993). Patients are usually older than those with well-differentiated lesions.

The lesions are often large, grey-white in colour, infiltrative and show extensive necrosis. The tumour is composes of solid nests (insulae) of cells that have a neuroendocrine growth pattern. Necrosis (in a peritheliomatous pattern), vascular invasion and mitoses are prominent features.

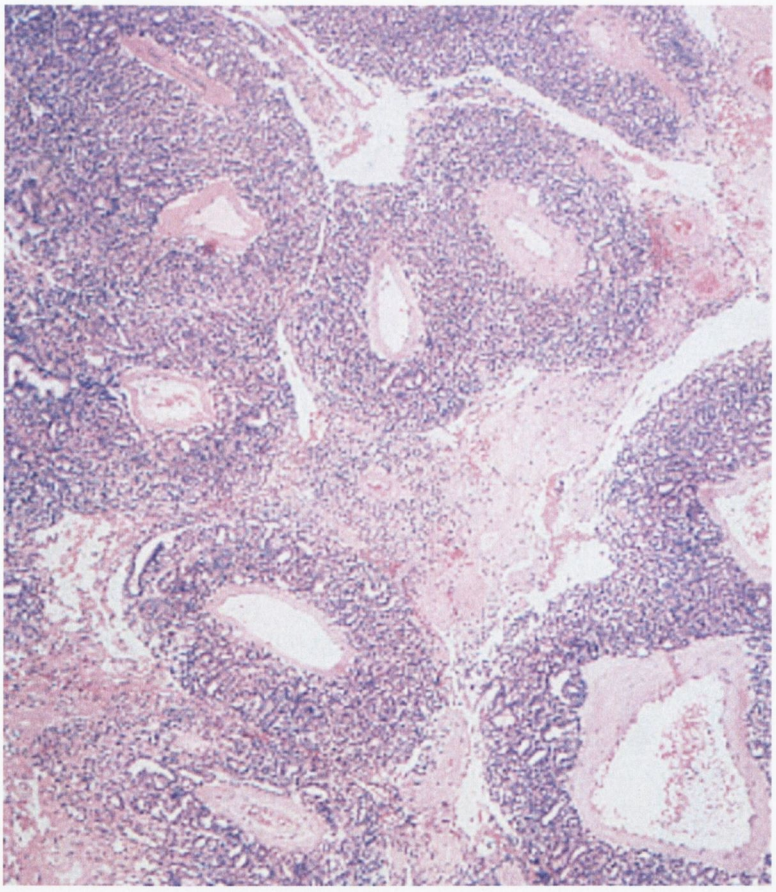

Figure 1.10 Poorly differentiated carcinoma of the thyroid exhibiting sheaths of malignant follicular epithelial cells

1.5.6.6 Anaplastic / Undifferentiated carcinoma

Anaplastic thyroid carcinomas (ATC) are a group of high grade, rare thyroid carcinomas that are usually undifferentiated histologically. They mainly present in the elderly, with a slight female preponderance. They carry an extremely poor prognosis, with many patients surviving less than six months following diagnosis. Risk factors are largely unknown but may include history of radiation and iodine deficiency (Getaz et al., 1979).

Anaplastic carcinoma typically presents as a rapidly growing, firm or hard mass in the region of the thyroid gland. Typical local symptoms include hoarseness, dysphagia and dyspnoea. These tumours invade the cervical soft tissue and involve the regional lymph nodes, often by direct extension.

Grossly, the tumour is usually ill-defined and replaces large parts of the gland. Necrosis, vascular invasion and mitoses are quite prominent. Histologically, a variety of patterns have been described. Most tumours are composed of giant cells and spindle cells, although "squamoid" differentiation is seen in about one-third of cases. Pathological examination of anaplastic carcinomas often demonstrate a high (50-70%) incidence of remnants of well differentiated follicular or papillary carcinoma or adenoma or adenomatous nodules, leading to the assumption that ATC is a progression of well-differentiated carcinoma.

1.5.6.7 Medullary carcinoma

Medullary thyroid carcinoma (MTC) is a thyroid malignancy originating from the calcitonin secreting C-cells (also known as parafollicular cells) of the thyroid gland. It is a rare, aggressive tumour and composes less than 10% of all thyroid malignancies.

The majority of medullary carcinomas are sporadic, however about ten to twenty percent are familial. Familial cases are associated with syndromes such as Multiple Endocrine Neoplasia (MEN) types 2A and 2B, familial medullary thyroid carcinoma syndrome, Von Hippel-Lindau syndrome or neurofibromatosis. The clinical features are similar in both sporadic and familial cases that are symptomatic.

Most patients with MTC present with a thyroid nodule that is painless but firm. In up to 50% of cases, obvious nodal metastases are present at the time of diagnosis.

On gross examination, most MTCs are firm, white or yellow and infiltrative. Histologically, MTCs are composed of polygonal to spindle shaped cells, which can form nests, trabeculae and even follicles. Nuclei have a "salt and pepper" chromatin pattern and there are often differences in nuclear size.

1.6 Epidemiology of thyroid cancer.

The thyroid is the largest of the endocrine glands and by far the most common site of all primary endocrine cancers. However, thyroid carcinoma is relatively rare, accounting for only one percent of all cancers. There is an impressive geographical variation between countries and even within larger countries (Davies and Welch, 2006).

Females are three times more likely than males to be affected by thyroid carcinoma. It is among the most curable neoplasms, however 5% to 20% of survivors develop local or regional recurrences, and <5% to 10% distant metastases, generally in the first years of follow-up, but sometimes after many years (Schlumberger, 1999).

Although thyroid cancer can occur in any age group, it is most common in those over 30 years old, with a median age at diagnosis of 47 years. The median age at diagnosis is much younger for familial medullary cancers and much older for anaplastic cancers (Dawson and Punwani, 2007).

World wide thyroid cancer incidences are increasing year after year. It remains to be seen whether this trend is a true increase in the incidence of disease or if it is due to greater rate of detection through more common use of diagnostic imaging studies and fine needle aspiration (FNA) biopsy. The American Cancer Society estimated 33,550 new cases of thyroid cancer in 2007, 25,480 occurring in women and 8,070 in men. Thyroid cancer is in the top twenty most common cancers for UK females (number 18), with 1,196 new cases diagnosed in 2004, compared to 445 cases in males (cancer research UK website: http://info.cancerresearchuk.org/cancerstats/types/thyroid/incidence/). The highest rates for thyroid cancer in the world occur in Northern America, where the female age-standardised rate is 8.1 per 100,000 females, compared with 1.4 per 100,000 females in Western Africa. Incidence is low in all parts of Africa, as seen in figure 1.11.

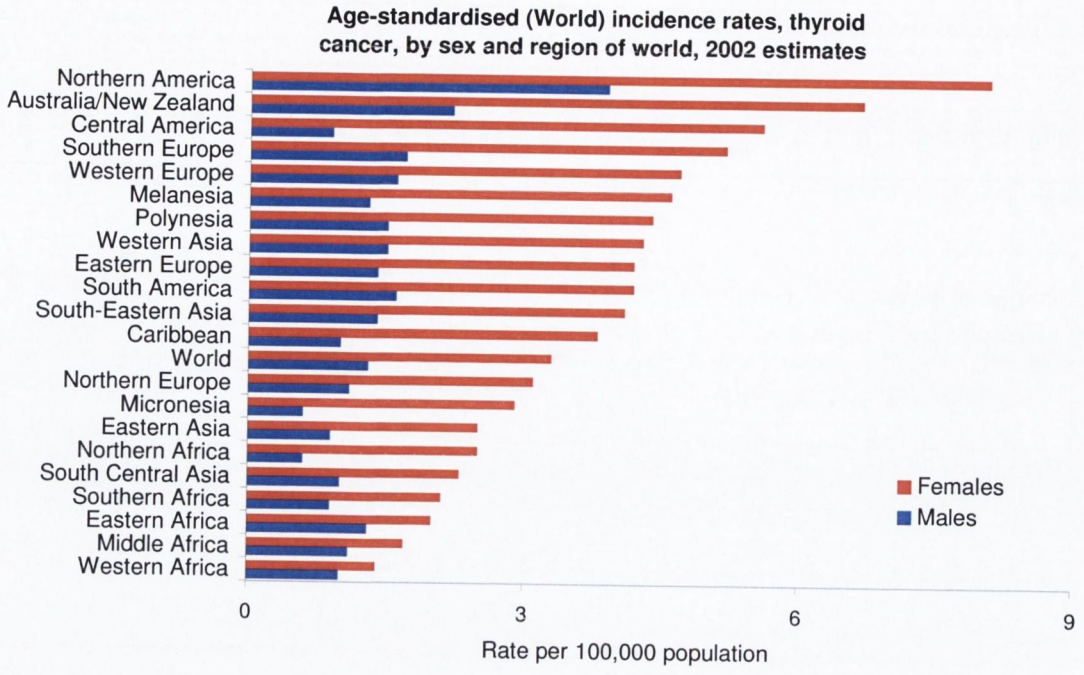

Figure 1.11 Illustrates the age-standardised incidence rates for thyroid cancer throughout the world for 2002. Adapted from the cancer research UK website: http://info.cancerresearchuk.org/cancerstats/types/thyroid/incidence/

In Ireland the annual average number of new thyroid cancer cases between 1998-2002 was fifty three in females and nineteen in males. Taking into consideration both demographic change and the change in cancer rates (and using the years 1998-2002 as a baseline) the Irish national cancer registry estimates 109 ± 27 annual female cases of thyroid cancer by the year 2020 and 45 ± 19 annual male cases. This equates to a 106% female and 137% male overall percentage change between 1998-2002 and 2020 (95% prediction intervals). This demonstrates that the overall trend in incidence of thyroid carcinoma is predicted to increase in both sexes in Ireland in the next decade. The National Cancer Registry attribute this to an increase in population ageing (demographic factors) but also as a result of increase in underlying incidence rates for most cancers (National Cancer Registry, 2006).

1.7 Aetiology of thyroid carcinoma

The aetiology of thyroid carcinoma is not fully understood however there are several risk factors thought to predispose to neoplasia. Some of those risk factors are outlined below.

1.7.1 Iodine

The dietary iodine requirement of adult humans is estimated to be 150 µg/day. The distribution of histological subtypes of thyroid cancer seems to be related to the intake of iodine, with fewer of the more aggressive follicular and anaplastic carcinomas and more papillary carcinomas in iodine rich areas. Populations starting iodine prophylaxis demonstrate an increase in the ratio of papillary to follicular carcinoma (Feldt-Rasmussen, 2001).

1.7.2 External Radiation

Exposure to radiation especially exposure occurring during childhood is a well-known risk factor for papillary thyroid carcinoma.

Radiation can be broken down into two categories: ionizing radiation and non-ionizing radiation. Non-ionizing radiation is a low energy radiation, examples of which include microwaves, visible light and infrared light. Injury is usually related to local heat production and is generally less severe.

Ionizing radiation is the focus of radiation-induced injury. Ionizing radiation refers to either high energy particles or electromagnetic waves that have the ability to deposit enough energy to break chemical bonds and produce an ion pair. Ionization occurs when the process of energy transfer liberates an orbital electron from an atom or molecule producing this ion pair. If living cells receive this energy, cellular function becomes compromised by DNA damage and mutation (Grubbs et al., 2008).

Ionizing radiation can initiate carcinogenesis via breakage of DNA strands (direct action) or from production of hydroxyl or peroxide radicals that cause oxidative damage to DNA (indirect action). Both mechanisms ultimately lead to DNA strand breaks, which can lead to chromosomal rearrangements. This can result in malignant transformation through altered gene expression, formation of chimeric genes, or loss of tumour suppressor gene function.

There have been many radiation exposing incidents over the past century, some through human error some through technical fault.

The atomic bombs deployed on Hiroshima and Nagasaki on the 6th and 9th of August 1945 respectively represent one of the first and largest population exposures to radiation. The exposure of this population was almost entirely to whole body radiation from gamma rays and neutrons. Exposure to more than 5 gray (Gy- SI unit of absorbed radiation) led to death. About 80,000 people with known radiation doses are still being followed, and new consequences of radiation exposure recorded (Williams, 2006).

Other exposure over the years include nuclear tests carried out on the Marshal Islands in the western Pacific Ocean in 1954, atmospheric tests carried out at the Nevada test site (USA) between 1951 and 1962 and the accident at the Three Mile Island Unit 2 nuclear power plant in Pennsylvania (USA) in 1979.

However it is the explosion at the Chernobyl nuclear power plant on the 26th of April, 1986 that is considered the world's worst civilian nuclear disaster and the one that has resulted in the largest number of characterised cases of thyroid carcinoma. The power plant at Chernobyl in the far north of Ukraine, (at the time a part of the USSR), contained four reactors. These reactors lacked an additional outer shell found in modern Western reactors. Reactor four was due for a periodic shutdown, and was to be the subject of a test of the ability of the inertia in the moving components of the system to maintain water circulation without the emergency auxiliary pumps. Through a series of human and mechanical errors, the combination of inadequate water circulation and rapidly increasing reactor power led to a rapid rise in temperature, a

steam explosion which blew the massive lid off the reactor, a runaway reaction which could not be controlled and, a fire in the graphite core. This led to the release of huge amounts of radioactive isotopes (Grubbs et al., 2008). Concentrated areas of radiation contamination were spread in a spotty pattern over Ukraine, Belarus, Russia and into Europe. The most heavily contaminated areas, in which measurements of 137-caesium exceeded 37 $kBqm^2$, were in Belarus, the Russian Federation and Ukraine. Heavy rains exacerbated the radionuclide fallout, resulting in contamination of groundwater and soil. The first evidence of an increase in thyroid cancer came in 1990, when physicians in Minsk and Kiev noticed increased numbers of thyroid cancer in children, only 4 years after the accident (Williams, 2006). Their reports led to a WHO organised visit to Minsk in 1992, followed by 2 letters to Nature (Kazakov et al., 1992, Baverstock et al., 1992). In 2000 about 2,000 cases of thyroid carcinoma had been reported in those exposed as children in the former Soviet Union, and in 2005, the number was estimated at 4,000 (WHO data). The latest estimates for the year 2056 ranges from 3400 to 72,000 (Cardis et al., 2006). The association between Chernobyl related ionizing radiation exposure and thyroid cancer in adults is less clear. Longer follow-up periods are needed for increased rates to become apparent, as the adult gland is less sensitive to radiation.

1.7.3 Other risk factors

As mentioned the complete aetiology of thyroid cancer remains to be discovered. While ionizing radiation has been established as a definite risk factor, some other factors that may be associated with thyroid cancer development are autoimmune thyroid disease (this topic is discussed further in chapter three, section 3.6) and familial syndromes such as multiple endocrine neoplasia (MEN) types 2A and 2B, familial medullary thyroid carcinoma (FMTC), Werner's syndrome, familial adenomatous polyposis, and Cowden syndrome. Hormonal factors have also been implicated with disease development due to the dramatic differences in thyroid cancer incidence between men and women in virtually all settings, and the high incidence of the disease in women of reproductive to middle age. Although the role of hormone related factors has been suspected, it has not yet been elucidated, with inconsistent results being produced (Akslen et al., 1992, Mack et al., 1999, Negri et al., 1999).

1.8 Molecular pathology of thyroid cancer

Carcinogenesis results from the subversion of the processes that control the normal growth, location and mortality of cells. This loss of normal control mechanisms arises from the acquisition of mutations in three broad categories of genes:

1. Proto-oncogenes, the normal products of which are components of signalling pathways that regulate proliferation and which, in their mutated form, become dominant oncogenes
2. Tumour suppressor genes, which generally exhibit recessive behaviour, the loss of function of which in cancer leads to deregulated control of cell cycle progression, cellular adhesion, etc. and
3. DNA repair enzymes, mutations in which promote genetic instability (figure 1.12).

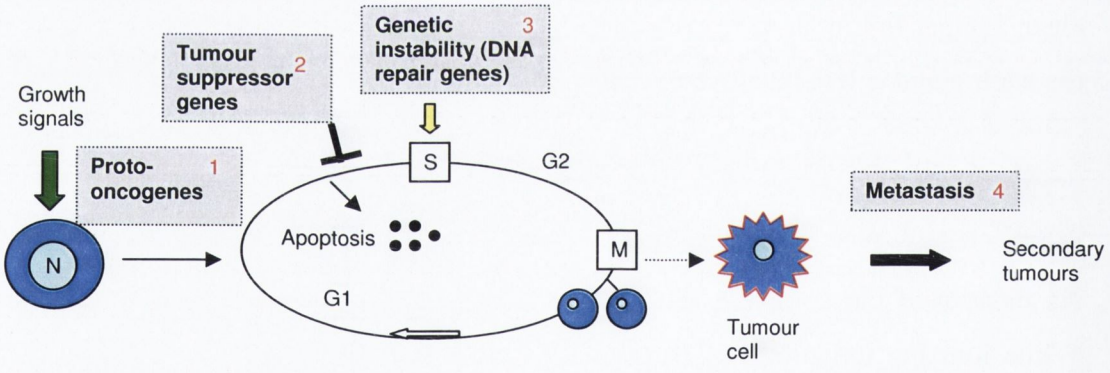

Figure 1.12 Genetic signals in cancer development. Three broad functional categories may be distinguished within which mutations may arise: (1) and (2) pathways driving cell proliferation and controlling cell cycle progression and apoptosis (proto-oncogenes and tumour suppressor genes), (3) in the promotion of genetic instability through mutations in DNA repair genes, and (4) effects associated with metastases. Adapted from The oncogene and tumour suppressor genes factsbook (Hesketh, 1997)

According to the model of multi-step carcinogenesis which is the prevailing theory of cancer pathogenesis nowadays, tumours develop as a result of the sequential accumulation of alterations in the genes involved in the control of cell proliferation, differentiation or death. Therefore, a sequence of somatic mutational events leads to

the clonal expansion of genetically modified cells that progressively show a selective growth advantage over normal non-transformed cells and acquire an invasive and metastatic potential, thus resulting in malignant transformation of cells and tumour progression. It is well known that multiple genetic events are usually necessary to create a cancer. The incidence of human cancers suggests that typically six to seven events are required over a span of twenty to forty years to induce a growth (Petro, 1997).

Thyroid cancers accumulate a number of alterations at the genomic level. The majority of mutations in thyroid tumours are somatic; however germline mutations do exist for example in familial cancer syndromes such as MEN II. Abnormal synthesis of growth factors that stimulate cellular proliferation, or constitutive activation of related receptors and signal transduction pathways, have been implicated in thyroid tumour formation. The formation of fusion oncoproteins also represents a pathogenic mechanism that has been observed consistently in leukaemias/lymphomas and sarcomas, but not in carcinomas, making thyroid carcinogenesis unique among other epithelial malignant neoplasms. Many of the genetic alterations in thyroid cancer exert their oncogenic actions at least partially through the activation of the RET/PTC → RAS → RAF → mitogen-activated protein kinase (MAP kinase) /extracellular-signal-regulated kinase (ERK) kinase (MEK) → MAP kinase/ERK pathway (MAP kinase pathway).

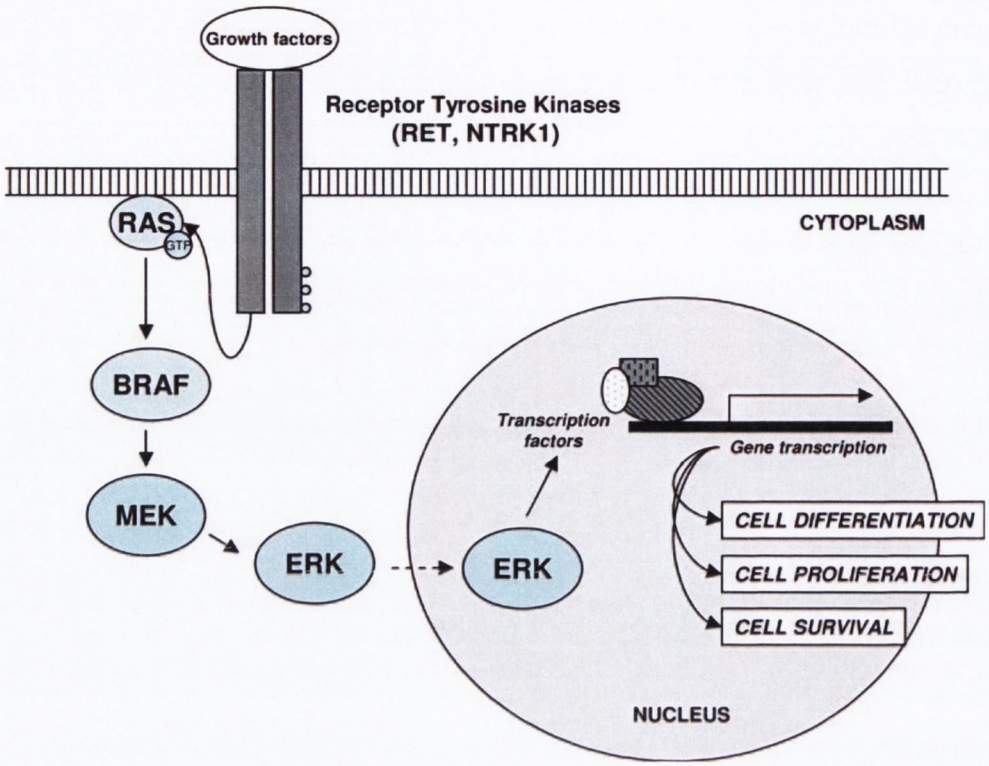

Figure 1.13 Schematic representation of MAPK signalling pathway. Physiologically, binding of growth factor to receptor tyrosine kinases (TKs) such as RET and NTRK1, results in receptor dimerization and activation via autophosphorylation of tyrosine residues in the intracellular domain. The activated receptor, through a series of adaptor proteins, leads to activation of RAS located at the inner face of the plasma membrane by substitution of GDP with GTP. The GTP-bound form of RAS binds to and recruits RAF proteins, mainly BRAF in thyroid follicular cells, to the plasma membrane. Activated BRAF is now able to phosphorylate and activate the MEK, which in turn phosphorylates and activates the ERK. Once activated, ERK phosphorylates cytoplasmic proteins and translocates into the nucleus, in which it regulates transcription of the genes involved in cell differentiation, proliferation, and survival. Alterations of this pathway in thyroid cancer can occur at different levels as a result of point mutations or rearrangements involving the RET, RAS and BRAF genes (Ciampi and Nikiforov, 2007)

Some of the genes that are involved in thyroid tumourigenesis are described below.

1.8.1 RET

The RET oncogene was identified by Takahashi and colleagues in 1985 (Takahashi et al., 1985) who reported a novel gene rearrangement with transforming activity in NIH 3T3 cells transfected with human lymphoma DNA. The name RET stems from "*re*arranged during *t*ransfection". The human RET gene lies on the chromosome band 10q11.2 and comprises 21 exons.

RET encodes a transmembrane receptor tyrosine kinase (TK) with a cadherin-related motif and a cysteine-rich domain that binds TGFβ-related neurotrophic factors, including the glial cell line derived neurotrophic factor (GDNF) family. Binding of the ligand causes receptor dimerization, autophosphorylation of tyrosine residues within the intracellular domain, and activation of the signalling cascade.

RET protein is composed of three domains; an extracellular ligand-binding domain with four cadherin-like repeats and a cysteine-rich region, a hydrophobic transmembrane domain, and a cytoplasmic portion with the TK domain split by an insertion of 27 amino acids (Arighi et al., 2005). Three isoforms of RET are generated by alternative 3' splicing. The long, intermediate and short RET isoforms, which differ by 51, 43 and 9 amino acids in the C terminus, are referred to as RET51, RET43 and RET9 respectively.

RET is normally expressed in cells of neural crest origin such as neural and ganglion cells. Tumours of neural crest origin such as neuroblastoma, phaeochromocytoma and medullary thyroid carcinoma also express RET. It is clear that RET plays a significant role during embryogenesis, particularly with development of the neural and excretory systems (Sheils, 2005). In 1996, glial cell line-derived neurotrophic factor (GDNF) was identified as a long sought after RET ligand by several groups (Durbec et al., 1996, Jing et al., 1996, Treanor et al., 1996, Trupp et al., 1996). Mutations (both germline and somatic) in the RET proto-oncogene are associated with several diseases including multiple endocrine neoplasia, types IIA and IIB (MEN2A and MEN2B),

Hirschsprung disease, and medullary thyroid carcinoma. Like most receptor tyrosine kinases, RET has the ability to activate a variety of signalling pathways, including RAS/RAF/MEK/ERK, phosphatidylinositol 3-kinase (PI3K)/AKT, p38 MAPK and c-Jun N-terminal kinase (JNK) pathways.

1.8.1.1 ret/PTC oncogenes and thyroid carcinoma

In 1987 the demonstration of an activating oncogene specific for papillary thyroid carcinoma was shown using NIH 3T3 transfection assays (Fusco et al., 1987). This oncogene was shown to be a rearranged form of RET called ret/PTC. To date, twelve rearranged forms of RET referred to as ret/PTC 1-9, PCM1-ret, ELKS-ret, and RFP-ret have been isolated from sporadic and radiation associated PTCs. In each case, the intracellular domain of RET is fused to different activating genes, namely H4 (for ret/PTC-1), RIα (ret/PTC2), RFG/ELE1/ARA70 (ret/PTC3 and ret/PTC4), RFG5 (ret/PTC5), hTIF (ret/PTC-6), RFG7/TF1γ (ret/PTC7), kinectin (ret/PTC8), RFG9 (ret/PTC9), PCM1 (PCM1-ret), ELKS (ELKS-ret), and RFP (RFP-ret). This results in ligand-independent dimerization and constitutive activation of these chimeric proteins (Arighi et al., 2005).

ret/PTC rearrangements activate the transforming potential of RET by multiple mechanisms. First, by substituting its transcriptional promoter with those of the fusion partners, they allow the expression of RET in the epithelial follicular thyroid cells, where it is normally transcriptionally silent. Secondly, the rearrangements generate constitutively active chimeric oncoproteins which are distributed in the cytosolic compartment of the cell. Finally, activation of the RET kinase is mediated by fusion to domains that are capable of dimerization.

The prevalence of ret/PTC rearrangements in thyroid cancer varies widely among studies, with rates between 3 and 85% being reported (Kondo et al., 2006, Nikiforov, 2002, Tallini and Asa, 2001). This wide variation probably reflects geographic location and detection methods used.

The different types of ret/PTC rearrangements are thought to reflect phenotypic differences in neoplastic thyroid cells. ret/PTC-3 rearrangements are more often associated with the solid/follicular variant of PTC,, whereas ret/PTC-1 are more common in the classic papillary type (Finn et al., 2003), Thomas et al., 1999). The role of RET in thyroid carcinoma is illustrated below.

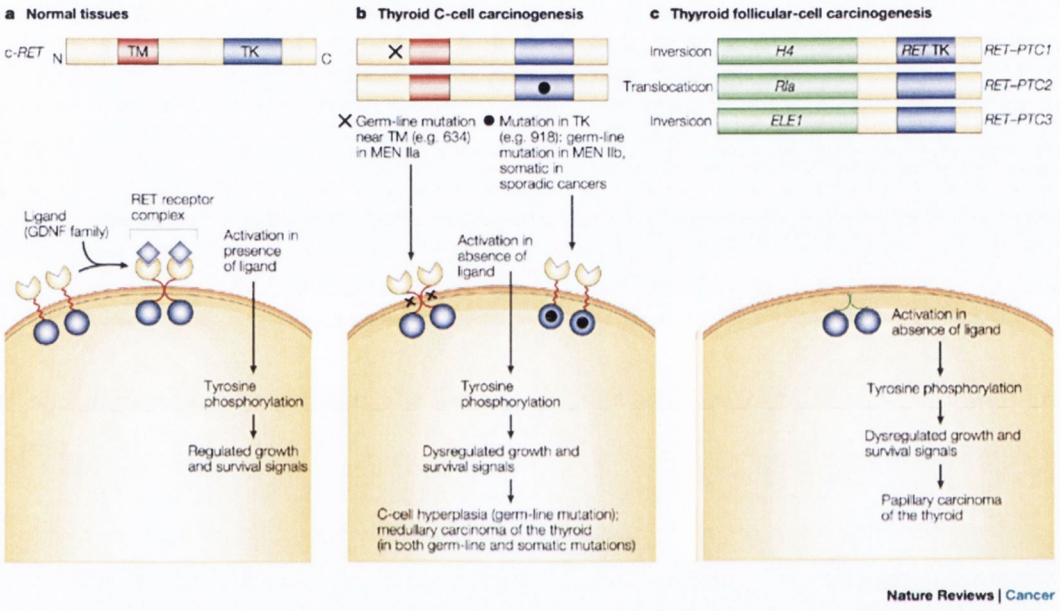

Figure 1.14 The role of RET in thyroid carcinogenesis

A) The receptor tyrosine kinase c-RET is normally expressed im the developing neural-crest-derived tissues, including thyroid C cells. It binds to members of the gliall-derived neurotrophic factor (GDNF) family of ligands, leading to dimerization of c-RET and activation of its tyrosine kinase activity. Downstream signalling events lead to growth and survival signals that are controlled by receptor occupancy, as well as crosstalk with other ligand–receptor interacttions.

B) Germ-line or somatic point mutations either close to the transmembrane (TM) or in the tyrosine kinase (TK) regions of c-RET contribute to thyroid C-cell carciinogenesis. These mutations cause c-RET to dimerize independently of ligands or have kinase activity that is independent of dimerization. Germ-line point mutations are a feature of multiple endocrine neoplasia type II syndrome (MEN II), which predisposes to phaeochromocytoma, in addition to thyroid carcinoma. The mutations are dominant; normal receptors are not shown.

C) By contrast, somatic rearrangements of c-RET contribute to thyroid follicular-cell carcinogenesis: inversions or translocations fuse the part of c-RET that encodes the tyrosine kinase domain with one of several genes that encode coiled-coil-domain-containing proteins. Fusion to H4 (a gene of unknown function), RI α (which encodes a regulatory subunit of protein kinase A) and ELE1 (a transcriptional co-activator of the androgen receptor) are the most commonly involved, giving rise to the ret/PTC-1, ret/PTC-2 and ret/PTC-3 oncogenes, respectively. H4 and ELE1 are also involved in rare rearrangements with differing breakpoints. The resulting coiled-coil-domain-containing fusion protein dimerizes, leading to a constitutively active c-RET tyrosine kinase. (Williams, 2002)

1.8.2 NTRK

The human neurotrophin tyrosine receptor kinase (NTRK or TRK) gene, located on chromosome 1q22, encodes a transmembrane tyrosine kinase receptor for the nerve growth factor (NGF). Similar to RET, NTRK may become activated in thyroid follicular cells by chromosomal rearrangements that fuse the 3'-end of the NTRK gene, including its TK domain, with the 5'-end and the promoter region of a ubiquitously expressed gene resulting in constitutively active TK activity. The rearrangements originate four chimeric genes: three are intrachromosomic rearrangements (TRK, TRK-T1 and TRK-T2) and one is an interchromosomic rearrangement (TRK-T3).

In the thyroid, the NTRK proto-oncogene has been found to be activated only in a minority of "spontaneous" and radiation associated papillary carcinomas (Bongarzone et al., 1996, Bongarzone et al., 1989, Said, 1994) with similar frequencies (12%). However TRK family receptors have also been implicated in the pathogenesis of medullary thyroid carcinoma (McGregor et al., 1999).

1.8.3 RAS

The RAS proto-oncogene codes for a G protein, p21, which plays a critical intermediate role in connecting the stimulatory signal from tyrosine kinases such as EGF receptor and via RAF-1 to a mitogenic cascade involving the MAP kinases. Final products act upon nuclear transcription factors such as c-FOS and c-JUN.

The three RAS proteins (H, K, and N-RAS), which are linked to the inner portion of the cytoplasmic membrane and exhibit guanosine triphosphate (GTPase) activity, exist in two states: an inactive form which is bound to guanosine diphosphate (GDP) and an active form, able to bind and hydrolize GTP. Their function is to convey signals originating from TK membrane receptors to a cascade of mitogen-activated phosphokinases (MAPK) which ultimately, activate the transcription of target genes, thus inducing mitotic activation.

Point mutations in codons 12, 13 and 61 have the effect of constitutive activation of RAS proteins, which in turn lead to genomic instability and additional mutations and malignant transformation.

RAS mutations are found in thirty percent of human cancers. Reports of RAS mutations in thyroid tumours vary widely in prevalence and are seen in a spectrum of tumour types (Ezzat et al., 1996, Lemoine et al., 1988, Suarez, 1998). However it is generally accepted that RAS mutations are more commonly found in FTC than PTC and that they are more prevalent in carcinomas than benign tumours (Ezzat et al., 1996). Besides activating point mutations, some thyroid tumours may also contain RAS gene amplifications or exhibit enhanced expression of RAS p21 proteins, strongly implicating RAS as an important player in tumourigenesis.

18.4 BRAF

BRAF belongs to the family of RAF proteins (ARAF, BRAF, CRAF), which are intracellular effectors of the MAP kinase (MAPK) signalling cascade. The discovery of activating mutations of the gene for BRAF has expanded the array of the known genetic alterations that activate the MAPK pathway and underscores the importance of this pathway in human cancer (Davies et al., 2002). Upon activation triggered by RAS binding and protein recruitment to the cell membrane, these serine-threonine kinases phosphorylate and activate MAPK/ERK kinase (MEK), which in turn activates ERK and consequently effectors of the MAPK cascade.

BRAF activating missense point mutations in the kinase domain are clustered in exons 11 and 15 of the gene and the T1799A transversion mutation accounts for more than 80% of all the BRAF mutations (Davies et al., 2002). The T1799A mutation results in a V600E amino acid substitution in the protein product and subsequent constitutive activation of the BRAF kinase.

BRAF mutations have been reported in numerous cancers, being most prevalent in melanomas and nevi (Davies et al., 2002, Pollock et al., 2003). BRAF mutation is the most common genetic event occurring in sporadic adult papillary carcinomas of the thyroid; it prevails in approximately 45% of all cases (Ciampi and Nikiforov, 2005, Xing, 2005). Virtually all mutations found in these tumours are V600E. BRAF mutations are highly prevalent in classical papillary carcinomas and the tall cell variant of PTC, but are rare in the follicular variant.

1.8.5 MET

c-MET is a two-subunit 190 kDa transmembrane tyrosine kinase receptor which acts as the ligand for hepatocyte growth factor/scatter factor (HGF/SF). HGF/SF is a potent epithelial cell mitogen and one of the most potent stimuli of thyrocyte proliferation. Oncogenic potential of MET may occur through gene amplification or over-expression, through a defect in post-translational processing, by fusion and aberrant dimerization, or through a variant in which the receptor is not cleaved into its alpha and beta subunits.

MET oncogene is seen in various human cancer types, including up to 70% of papillary thyroid carcinomas and 25% of follicular thyroid carcinomas, although it is not detected in MTC or in normal thyroid tissues (Di Renzo et al., 1991).

1.8.6 PTEN

Phosphate and tensin homolog (PTEN) is a protein tyrosine phosphatase, located on chromosome 10q23.3, thought to exert its tumour-suppressor effect by antagonising protein TK activity. PTEN was isolated from a region on chromosome 10 found to be deleted in thyroid, brain and prostate tumours. It encodes a dual specificity phosphatase, impacting on the PI3K and the AKT/protein kinase B pathways. The finding of loss of heterozygosity (LOH) at 10q in thyroid tumours generated interest in the role of PTEN.

Somatic PTEN mutations are rare in primary thyroid tumours, however hemizygous deletion has been found to occur in ten to twenty percent of adenomas and carcinomas. Hemizygous deletions can be detected in up to sixty percent of anaplastic thyroid carcinomas.

1.8.7 p53

The p53 gene maps to chromosome 17p13 and encodes a nuclear phosphoprotein that, as a tetramer, acts as a transcription factor. It is the archetypal checkpoint regulator, which has become known as the "guardian of the genome". The tumour suppressor gene has a dual action for the protection from cancer development: 1) cell cycle arrest allowing damaged DNA to undergo repair, and 2) allowing damaged cells to undergo apoptosis before they divide, thereby avoiding passage of DNA damage to the next cell generation.

Cells with impaired p53 function are more likely to permit the accumulation of genetic damage, thus providing a selective advantage for the clonal expansion of neoplastic cells exhibiting more malignant phenotypes.

p53 gene mutations have been shown to be almost exclusively detected in poorly differentiated and anaplastic tumours (22-83%) (Donghi et al., 1993, Ito et al., 1992, Nakamura et al., 1992). These data suggest that the inactivation of the p53 gene represents a late event, involved in the progression from differentiated to undifferentiated forms of thyroid cancer.

1.8.8 PPARγ-PAX8

PAX8 encodes a paired domain transcription factor, which is essential for the genesis of the thyroid follicular cell lineage and regulation of thyroid-specific gene expression. As with most differentiation markers, PAX8 is mainly expressed in benign rather than in malignant thyroid neoplasias and, among the latter, more abundantly in differentiated than in undifferentiated carcinomas (Puglisi et al., 2000).

PPARγ is a member of the nuclear hormone receptor superfamily that includes thyroid hormone, retinoic acid, and androgen and oestrogen receptors. Since PPARγ ligands may inhibit growth and promote differentiation of cancer cell lines (Demetri et al., 1999) and mutations of PPARγ have been associated with human colon cancer (Sarraf

et al., 1999), it has been hypothesised that abrogation of normal PPARγ function may be important in cancer development.

A specific t(2;3)(q13;p25) chromosomal translocation that causes an in-frame fusion of the DNA binding domain of PAX8 to domains A to F of the PPARγ1 has been found in follicular neoplasms (Kroll et al., 2000, Marques et al., 2002) and follicular variants of PTC (Castro et al., 2005).

1.9 Aims and objectives

The overall aim of this thesis was to search for prognostic markers in thyroid malignancy. Specific objectives were:

i. To evaluate the immune related gene expression profiles of ret/PTC-1 positive and negative cells lines after a time-course of co-culture with activated Hashimoto thyroiditis and control donor lymphocytic supernatant.
ii. To interrogate the gene and protein expression profiles of a panel of targets to assess their utility to aid in the diagnosis of thyroid malignancy
iii. To analyse expression of a microRNA in thyroid malignancy to determine its ability to act as a molecular marker of the disease.

1.10 References:

Ahmed, A. M. & Ahmed, N. H. (2005) History of disorders of thyroid dysfunction. *East Mediterr Health J,* 11, 459-69.

Akslen, L. A., Nilssen, S. & Kvale, G. (1992) Reproductive factors and risk of thyroid cancer. A prospective study of 63,090 women from Norway. *Br J Cancer,* 65, 772-4.

Arighi, E., Borrello, M. G. & Sariola, H. (2005) RET tyrosine kinase signaling in development and cancer. *Cytokine Growth Factor Rev,* 16, 441-67.

Baverstock, K., Egloff, B., Pinchera, A., Ruchti, C. & Williams, D. (1992) Thyroid cancer after Chernobyl. *Nature,* 359, 21-2.

Becker, W. F. (1977) Presidential address: Pioneers in thyroid surgery. *Ann Surg,* 185, 493-504.

Bongarzone, I., Fugazzola, L., Vigneri, P., Mariani, L., Mondellini, P., Pacini, F., Basolo, F., Pinchera, A., Pilotti, S. & Pierotti, M. A. (1996) Age-related activation of the tyrosine kinase receptor protooncogenes RET and NTRK1 in papillary thyroid carcinoma. *J Clin Endocrinol Metab,* 81, 2006-9.

Bongarzone, I., Pierotti, M. A., Monzini, N., Mondellini, P., Manenti, G., Donghi, R., Pilotti, S., Grieco, M., Santoro, M., Fusco, A. & Et Al. (1989) High frequency of activation of tyrosine kinase oncogenes in human papillary thyroid carcinoma. *Oncogene,* 4, 1457-62.

Braverman, L., Utiger, R (2005) *Werner and Ingbar's the thyroid: a fundamental and clinical text,* London, Lippincott Williams and Williams.

Cardis, E., Krewski, D., Boniol, M., Drozdovitch, V., Darby, S. C., Gilbert, E. S., Akiba, S., Benichou, J., Ferlay, J., Gandini, S., Hill, C., Howe, G., Kesminiene, A., Moser, M., Sanchez, M., Storm, H., Voisin, L. & Boyle, P. (2006) Estimates of the cancer burden in Europe from radioactive fallout from the Chernobyl accident. *Int J Cancer,* 119, 1224-35.

Castro, P., Roque, L., Magalhaes, J. & Sobrinho-Simoes, M. (2005) A subset of the follicular variant of papillary thyroid carcinoma harbors the PAX8-PPARgamma translocation. *Int J Surg Pathol,* 13, 235-8.

Chen, K. A. & Rosai, J. (1977) Follicular variant of thyroid papillary carcinoma: A clinicopathologic study of six cases. *Am J Surg Pathol,* 1, 123.

Ciampi, R. & Nikiforov, Y. E. (2005) Alterations of the BRAF gene in thyroid tumors. *Endocr Pathol,* 16, 163-72.

Ciampi, R. & Nikiforov, Y. E. (2007) RET/PTC rearrangements and BRAF mutations in thyroid tumorigenesis. *Endocrinology,* 148, 936-41.

Cranefield, P. F. (1962) The discovery of cretinism. *Bull Hist Med,* 36, 489-511.

Davies, H., Bignell, G. R., Cox, C., Stephens, P., Edkins, S., Clegg, S., Teague, J., Woffendin, H., Garnett, M. J., Bottomley, W., Davis, N., Dicks, E., Ewing, R., Floyd, Y., Gray, K., Hall, S., Hawes, R., Hughes, J., Kosmidou, V., Menzies, A., Mould, C., et al. (2002) Mutations of the BRAF gene in human cancer. *Nature,* 417, 949-54.

Davies, L. & Welch, H. G. (2006) Increasing incidence of thyroid cancer in the United States, 1973-2002. *Jama,* 295, 2164-7.

Dawson, P. & Punwani, S. (2007) The thyroid dose burden in medical imaging A re-examination. *Eur J Radiol.*

Demetri, G. D., Fletcher, C. D., Mueller, E., Sarraf, P., Naujoks, R., Campbell, N., Spiegelman, B. M. & Singer, S. (1999) Induction of solid tumor differentiation by the peroxisome proliferator-activated receptor-gamma ligand troglitazone in patients with liposarcoma. *Proc Natl Acad Sci U S A,* 96, 3951-6.

Di Renzo, M. F., Narsimhan, R. P., Olivero, M., Bretti, S., Giordano, S., Medico, E., Gaglia, P., Zara, P. & Comoglio, P. M. (1991) Expression of the Met/HGF receptor in normal and neoplastic human tissues. *Oncogene,* 6, 1997-2003.

Dioscroidis, P. (1829) Lipsiae, De materia medica. *Curtius Sprengel,* II, 175.

Donghi, R., Longoni, A., Pilotti, S., Michieli, P., Della Porta, G. & Pierotti, M. A. (1993) Gene p53 mutations are restricted to poorly differentiated and undifferentiated carcinomas of the thyroid gland. *J Clin Invest,* 91, 1753-60.

Dubose, J., Barnett, R. & Ragsdale, T. (2004) Honest and sensible surgeons: the history of thyroid surgery. *Curr Surg,* 61, 213-9.

Durbec, P., Marcos-Gutierrez, C. V., Kilkenny, C., Grigoriou, M., Wartiowaara, K., Suvanto, P., Smith, D., Ponder, B., Costantini, F., Saarma, M. & Et Al. (1996) GDNF signalling through the Ret receptor tyrosine kinase. *Nature,* 381, 789-93.

Ezzat, S., Zheng, L., Kolenda, J., Safarian, A., Freeman, J. L. & Asa, S. L. (1996) Prevalence of activating ras mutations in morphologically characterized thyroid nodules. *Thyroid,* 6, 409-16.

Feldt-Rasmussen, U. (2001) Iodine and cancer. *Thyroid,* 11, 483-6.

Finn, S. P., Smyth, P., O'leary, J., Sweeney, E. C. & Sheils, O. (2003) Ret/PTC chimeric transcripts in an Irish cohort of sporadic papillary thyroid carcinoma. *J Clin Endocrinol Metab,* 88, 938-41.

Fonseca, E., Soares, P., Cardoso-Oliveira, M. & Sobrinho-Simoes, M. (2006) Diagnostic criteria in well-differentiated thyroid carcinomas. *Endocr Pathol,* 17, 109-17.

Furmanchuk, A. W., Averkin, J. I., Egloff, B., Ruchti, C., Abelin, T., Schappi, W. & Korotkevich, E. A. (1992) Pathomorphological findings in thyroid cancers of

children from the Republic of Belarus: a study of 86 cases occurring between 1986 ('post-Chernobyl') and 1991. *Histopathology,* 21, 401-8.

Fusco, A., Grieco, M., Santoro, M., Berlingieri, M. T., Pilotti, S., Pierotti, M. A., Della Porta, G. & Vecchio, G. (1987) A new oncogene in human thyroid papillary carcinomas and their lymph-nodal metastases. *Nature,* 328, 170-2.

Getaz, E. P., Shimaoka, K. & Rao, U. (1979) Anaplastic carcinoma of the thyroid following external irradiation. *Cancer,* 43, 2248-53.

Giddings, A. E. (1998) The history of thyroidectomy. *J R Soc Med,* 91 Suppl 33, 3-6.

Graves, R. J. (1835) Clinical Lectures (part II). *Lond Med Surg,* 7, 516.

Gross, J. & Pitt-Rivers, R. (1952) The identification of 3:5:3'-L-triiodothyronine in human plasma. *Lancet,* 1, 439-41.

Grubbs, E. G., Rich, T. A., Li, G., Sturgis, E. M., Younes, M. N., Myers, J. N., Edeiken-Monroe, B., Fornage, B. D., Monroe, D. P., Staerkel, G. A., Williams, M. D., Waguespack, S. G., Hu, M. I., Cote, G., Gagel, R. F., Cohen, J., Weber, R. S., Anaya, D. A., Holsinger, F. C., Perrier, N. D., Clayman, G. L. & Evans, D. B. (2008) Recent advances in thyroid cancer. *Curr Probl Surg,* 45, 156-250.

Harrington, C. R. (1926) Chemistry of thyroxine. II. Constitution and synthesis of desiodo-thyroxine. *Biochem J,* 20, 300.

Harrington, C. R. (1927) Chemistry of thyroxine. III. Constitution and synthesis of thyroxine. *Biochem J,* 21, 169.

Hesketh, M. (1997) *Genetic events in cancer development, The oncogene and tumour suppressor genes factsbook.* Academic Press.

Heymann, W. (2008) *Thyroid disorders with cutaneous manifestations,* London, Springer.

Hippocratis, M. (1825-1827) Lipsiae, Opera Omnia. *Carulus Gottlob Kunh,* III, 658.

Ito, T., Seyama, T., Mizuno, T., Tsuyama, N., Hayashi, T., Hayashi, Y., Dohi, K., Nakamura, N. & Akiyama, M. (1992) Unique association of p53 mutations with undifferentiated but not with differentiated carcinomas of the thyroid gland. *Cancer Res,* 52, 1369-71.

Janzer, R. C., Weber, E. & Hedinger, C. (1979) The relation between solid cell nests and C cells of the thyroid gland: an immunohistochemical and morphometric investigation. *Cell Tissue Res,* 197, 295-312.

Jing, S., Wen, D., Yu, Y., Holst, P. L., Luo, Y., Fang, M., Tamir, R., Antonio, L., Hu, Z., Cupples, R., Louis, J. C., Hu, S., Altrock, B. W. & Fox, G. M. (1996) GDNF-induced activation of the ret protein tyrosine kinase is mediated by GDNFR-alpha, a novel receptor for GDNF. *Cell,* 85, 1113-24.

Kazakov, V. S., Demidchik, E. P. & Astakhova, L. N. (1992) Thyroid cancer after Chernobyl. *Nature,* 359, 21.

Kendall, E. C. (1915) The isolation in crystaline form of the compound which occurs in the thyroid: its chemical nature and physiologic activity. *JAMA,* 64, 2042.

Kohn, L., Saji, M., Kosugi, S., Ban, J., Giuliani, C., Hidaka, A., Shimura, H., Shimura, Y., Okajima F. (1993) *The synthesis and secretion of thyroid hormones: regulators by multiple hormones and signals which can be subverted by autoantibodies to the thyrotropin receptor, Thyroid Diseases Basic Science, pathology, clinical and laboratory diagnoses. TRONCONE, L.* London, CRC Press.

Kondo, T., Ezzat, S. & Asa, S. L. (2006) Pathogenetic mechanisms in thyroid follicular-cell neoplasia. *Nat Rev Cancer,* 6, 292-306.

Kroll, T. G., Sarraf, P., Pecciarini, L., Chen, C. J., Mueller, E., Spiegelman, B. M. & Fletcher, J. A. (2000) PAX8-PPARgamma1 fusion oncogene in human thyroid carcinoma [corrected]. *Science,* 289, 1357-60.

Lemoine, N. R., Mayall, E. S., Wyllie, F. S., Farr, C. J., Hughes, D., Padua, R. A., Thurston, V., Williams, E. D. & Wynford-Thomas, D. (1988) Activated ras oncogenes in human thyroid cancers. *Cancer Res,* 48, 4459-63.

Lindsay, S. (1969) *Papillary thyroid carcinoma revisited, Thyroid Cancer. HEDINGER, C.* Sprunger-Verlag, Heidelberg.

Lindsay, S. (1970) Microspectrophotometric measurements of deoxyribonucleic acid in human thyroid carcinomas. *Surg Gynecol Obstet,* 131, 905-13.

Livolsi, V. (1990) *Developmental biology and anatomy of the thyroid, including aberrant thyroid, Surgical Pathology of the Thyroid. BENNINGTON, J.* Philadelphia, W.B. Saunders Company.

Livolsi, V., Montone, K., Sack, M (1999) *Pathology of thyroid disease, Diagnostic Surgical Pathology. STERNBERG, S.* Philadelphia, Lippincott Williams & Williams.

Ljungberg, O. (1992) *Biopsy pathology of the thyroid and parathyroid,* Cambridge, Chapman and Hall Medical.

Mack, W. J., Preston-Martin, S., Bernstein, L., Qian, D. & Xiang, M. (1999) Reproductive and hormonal risk factors for thyroid cancer in Los Angeles County females. *Cancer Epidemiol Biomarkers Prev,* 8, 991-7.

Marques, A. R., Espadinha, C., Catarino, A. L., Moniz, S., Pereira, T., Sobrinho, L. G. & Leite, V. (2002) Expression of PAX8-PPAR gamma 1 rearrangements in both follicular thyroid carcinomas and adenomas. *J Clin Endocrinol Metab,* 87, 3947-52.

Mcdougall, I. (1992) *Thyroid physiology, Thyroid Disease in Clinical Practice.* London, Chapman & Hall Medical.

Mcgregor, L. M., Mccune, B. K., Graff, J. R., Mcdowell, P. R., Romans, K. E., Yancopoulos, G. D., Ball, D. W., Baylin, S. B. & Nelkin, B. D. (1999) Roles of trk family neurotrophin receptors in medullary thyroid carcinoma development and progression. *Proc Natl Acad Sci U S A,* 96, 4540-5.

Murray, G. R. (1981) Note on the treatment of myxoedema by hypodermic injections of an extract of the thyroid gland of a sheep. *British Medical Journal,* 2, 796.

Nakamura, T., Yana, I., Kobayashi, T., Shin, E., Karakawa, K., Fujita, S., Miya, A., Mori, T., Nishisho, I. & Takai, S. (1992) p53 gene mutations associated with anaplastic transformation of human thyroid carcinomas. *Jpn J Cancer Res,* 83, 1293-8.

Negri, E., Dal Maso, L., Ron, E., La Vecchia, C., Mark, S. D., Preston-Martin, S., Mctiernan, A., Kolonel, L., Yoshimoto, Y., Jin, F., Wingren, G., Rosaria Galanti, M., Hardell, L., Glattre, E., Lund, E., Levi, F., Linos, D., Braga, C. & Franceschi, S. (1999) A pooled analysis of case-control studies of thyroid cancer. II. Menstrual and reproductive factors. *Cancer Causes Control,* 10, 143-55.

Nikiforov, Y. E. (2002) RET/PTC rearrangement in thyroid tumors. *Endocr Pathol,* 13, 3-16.

O' Malley, C. (1952) *Leonardo on the Human Body,* New York, Dover.

Papotti, M., Botto Micca, F., Favero, A., Palestini, N. & Bussolati, G. (1993) Poorly differentiated thyroid carcinomas with primordial cell component. A group of aggressive lesions sharing insular, trabecular, and solid patterns. *Am J Surg Pathol,* 17, 291-301.

Parry, C. H. (1825) *Collections from the Unpublished Papers of the Late Caleb Hillier Parry,* London, Fleetstreet Press.

Petro, R. (1997) *Epidemiology multistage models, short term mutagenesis tests, Origins of Human Cancer. PETRO, R.* New York, Cold Spring Harbor Laboratoty Press.

Pollock, P. M., Harper, U. L., Hansen, K. S., Yudt, L. M., Stark, M., Robbins, C. M., Moses, T. Y., Hostetter, G., Wagner, U., Kakareka, J., Salem, G., Pohida, T., Heenan, P., Duray, P., Kallioniemi, O., Hayward, N. K., Trent, J. M. & Meltzer, P. S. (2003) High frequency of BRAF mutations in nevi. *Nat Genet,* 33, 19-20.

Puglisi, F., Cesselli, D., Damante, G., Pellizzari, L., Beltrami, C. A. & Di Loreto, C. (2000) Expression of Pax-8, p53 and bcl-2 in human benign and malignant thyroid diseases. *Anticancer Res,* 20, 311-6.

Roche, J., Lissitsky, S. & Michel, R. (1952) Sur la triiodothyronine, produit intermediaire de la transformation de la diiodothyronine en thyroxine. *Compt Rend Acad Sci,* 234, 997.

Rosai, J., Carcangiu, M., Delellis, R (1993) *Tumors of the thyroid gland, Atlas of tumor pathology. ROSAI, J. & SOBIN, L.* Washington DC, Armed Forces Institute of Pathology.

Ruegemer, J. J., Hay, I. D., Bergstralh, E. J., Ryan, J. J., Offord, K. P. & Gorman, C. A. (1988) Distant metastases in differentiated thyroid carcinoma: a multivariate analysis of prognostic variables. *J Clin Endocrinol Metab,* 67, 501-8.

Said, S., Schlumberger, M., Suarez, Hg. (1994) Oncogenes in human epithelial thyroid tumorigenesis. *J Endocrinol Invest,* 6, 53-56

Salajegheh, A., Petcu, E. B., Smith, R. A. & Lam, A. K. (2008) Follicular variant of papillary thyroid carcinoma: a diagnostic challenge for clinicians and pathologists. *Postgrad Med J,* 84, 78-82.

Santisteban, P. & Bernal, J. (2005) Thyroid development and effect on the nervous system. *Rev Endocr Metab Disord,* 6, 217-28.

Sarraf, P., Mueller, E., Smith, W. M., Wright, H. M., Kum, J. B., Aaltonen, L. A., De La Chapelle, A., Spiegelman, B. M. & Eng, C. (1999) Loss-of-function mutations in PPAR gamma associated with human colon cancer. *Mol Cell,* 3, 799-804.

Schlumberger, M. J. (1999) Diagnostic follow-up of well-differentiated thyroid carcinoma: historical perspective and current status. *J Endocrinol Invest,* 22, 3-7.

Sheils, O. (2005) Molecular classification and biomarker discovery in papillary thyroid carcinoma. *Expert Rev Mol Diagn,* 5, 927-46.

Sobrinho-Simoes, M., Soars, J., Carneiro, F, Et Al. (1990) Diffuse follicular variant of papillary carcinoma of the thyroid. *Surg Pathol,* 3, 189.

Studer, H. & Derwahl, M. (1995) Mechanisms of nonneoplastic endocrine hyperplasia--a changing concept: a review focused on the thyroid gland. *Endocr Rev,* 16, 411-26.

Suarez, H. G. (1998) Genetic alterations in human epithelial thyroid tumours. *Clin Endocrinol (Oxf),* 48, 531-46.

Takahashi, M., Ritz, J. & Cooper, G. M. (1985) Activation of a novel human transforming gene, ret, by DNA rearrangement. *Cell,* 42, 581-8.

Tallini, G. & Asa, S. L. (2001) RET oncogene activation in papillary thyroid carcinoma. *Adv Anat Pathol,* 8, 345-54.

Thomas, G. A., Bunnell, H., Cook, H. A., Williams, E. D., Nerovnya, A., Cherstvoy, E. D., Tronko, N. D., Bogdanova, T. I., Chiappetta, G., Viglietto, G., Pentimalli, F., Salvatore, G., Fusco, A., Santoro, M. & Vecchio, G. (1999) High prevalence of RET/PTC rearrangements in Ukrainian and Belarussian post-Chernobyl thyroid papillary carcinomas: a strong correlation between RET/PTC3 and the solid-follicular variant. *J Clin Endocrinol Metab,* 84, 4232-8.

Thompson, L. (2006) *Endocrine pathology, Foundations in diagnostic pathology.* Elsevier.

Treanor, J. J., Goodman, L., De Sauvage, F., Stone, D. M., Poulsen, K. T., Beck, C. D., Gray, C., Armanini, M. P., Pollock, R. A., Hefti, F., Phillips, H. S., Goddard, A., Moore, M. W., Buj-Bello, A., Davies, A. M., Asai, N., Takahashi, M., Vandlen, R., Henderson, C. E. & Rosenthal, A. (1996) Characterization of a multicomponent receptor for GDNF. *Nature,* 382, 80-3.

Troncone, L., Shapiro, B., Satta, M., Monaco, F (1994) *Thyroid diseases. Basic science, pathology, clinical and laboratory diagnosis,* Florida, CRC Press.

Trupp, M., Arenas, E., Fainzilber, M., Nilsson, A. S., Sieber, B. A., Grigoriou, M., Kilkenny, C., Salazar-Grueso, E., Pachnis, V. & Arumae, U. (1996) Functional receptor for GDNF encoded by the c-ret proto-oncogene. *Nature,* 381, 785-9.

Vellar, I. D. (1974) Thomas Peel Dunhill, The forgotten man of thyroid surgery. *Med History,* 18, 22-50.

Von Basedow, C. A. (1840) Exopthalmos durch Hypertropie des Zellgewebes in der Augenhohle. *Wchnschr ges Heilk,* 6, 197.

Wheeler, M. A. L., J (1994) *Diseases of the thyroid. Pathophysiology and management* Essex, Chapman and Hall Medical.

Widder, S., Guggisberg, K., Khalil, M. & Pasieka, J. L. (2008) A pathologic re-review of follicular thyroid neoplasms: the impact of changing the threshold for the diagnosis of the follicular variant of papillary thyroid carcinoma. *Surgery,* 144, 80-5.

Williams, D. (2002) Cancer after nuclear fallout: lessons from the Chernobyl accident. *Nat Rev Cancer,* 2, 543-9.

Williams, E. D. (2006) Chernobyl and thyroid cancer. *J Surg Oncol,* 94, 670-7.

Wu, S. (1991) *Thyroid hormone metabolism regulation and clinical implications,* Cambridge, Blackwell scientific publications.

Xing, M. (2005) BRAF mutation in thyroid cancer. *Endocr Relat Cancer,* 12, 245-62.

Chapter Two

Materials and Methods

2.1 Introduction

This chapter is a comprehensive account of all the methodologies employed in this thesis, accompanied by background information on some of the newer techniques. Several of the techniques are used in a number of chapters. Where this occurs, the full description of the technique is restricted to this chapter, with specifics appearing in their relevant chapters only.

2.2 Cell culture of thyroid cell lines

Two thyroid cell lines were utilised during this thesis, Nthy-ori and TPC-1. These cell lines were used for the purpose of a co-culture procedure with human T lymphocytes. The two cell lines are described as follows;

2.2.1 Cell lines

The human thyroid follicular epithelial cell line (Nthy-ori 3-1 ECACC number 90011609) is derived from normal thyroid tissue of an adult. The cells have been immortalized by transfection with a plasmid encoding for the Simian Virus 40 (SV40) large T antigen (Lemoine et al., 1989). Nthy-ori expresses specific features of thyroid epithelial function (iodide-trapping and thyroglobulin production). This cell line has been characterised in detail and was found to be growth factor-independent and capable of anchorage-independent growth at low frequency but is non-tumourigenic in nude mice.

TPC-1 is a cell line derived from a papillary thyroid carcinoma. This cell line expresses the ret/PTC-1 oncogene.

2.2.2 Formulation of cell culture media and other solutions

Culture media: RPMI, 10% Foetal Calf Serum (FCS), 2% Penicillin/ Streptomycin (5000 U/mL). Store at 4°C.

Trypsin Neutralising Solution (TNS): RPMI, 20% FCS. Store at -20°C.

Freezing Solution: RPMI, 20% FCS, 10% Dimethyl sulfoxide (DMSO). Store at - 20°C.

2.2.3 Thawing cells from stocks

- Pre-warm cell culture media for 30 minutes at 37°C. Add 15 mL cell culture media into two T75 flasks (Nunc™, NY, USA).
- Remove one cryovial of cells (1 mL in each) from liquid nitrogen and bring to room temperature.
- Add the thawed cells drop-wise to 8 mL of media in a 15 mL tube. Centrifuge for 4 minutes at 1000 rpm.
- Resuspend pellets in 1 mL media and add 500 µL to each T75 flask.
- Cells are grown to confluence in a humidified atmosphere containing 5% CO_2 at 37°C.
- Change medium initially after 3 days (cells adherent) and at 3-day intervals until confluent.

2.2.4 Splitting confluent flasks

Again all cell culture media and other solutions are pre-warmed for 45 minutes at 37°C.

- Remove old medium waste from each flask into a designated waste bottle.
- Wash cells with 5 mL phosphate buffered saline (PBS).
- Remove PBS and discard.
- Add 5 mL of 1X trypsin/EDTA to the flask and incubate at 37°C for 2-3 minutes.
- Examine flasks by phase microscopy to assess cell detachment.
- Lightly tap flasks to encourage the release of cells from the plastic surface.

- When > 90% of cells detach, add an equal volume 5 mL of trypsin neutralising solution (TNS).
- Remove cell suspension to a new 15 mL tube.
- Wash the flask with 5 mL PBS and remove to the same 15 mL tube.
- Pellet the cells (4 min @ 1000 rpm) and remove supernatant.
- Resuspend cell pellet in 2 mL RPMI (light tapping). Seed new flasks with 25% (500 µL, 1:4 split ratios) of the trypsinized cells.

2.2.5 Cryopreservation

- After pelleting by centrifugation resuspend the cells in 2 mL freezing solution in cryovials (1 mL in each cryovial).
- Place the vials on ice for 10 minutes, then at -20°C for 1 hour and overnight at -80°C. Transfer to a liquid nitrogen storage tank for long-term storage.

2.3 Mycoplasma testing

2.3.1 Background

First discovered as the aetiological agent of contagious bovine pleuropneumonia in 1898 and classified in the mid 1950s, mycoplasma was found to have a broad range of hosts - humans, animals, insects, and plants. Mycoplasma infection of cell cultures are persistent, tedious to detect, and difficult to remedy. Statistics prove that 30 to 60% of all cell cultures are contaminated with mycoplasmas, resulting in alterations of growth rates, morphology, and cell viability. Furthermore this may have an effect on experimental results and can lead to findings that do not reflect the true experimental variation.

2.3.2 Mycoplasma detection protocol (Roche, West Sussex, UK)

Stage 1: Enrichment of mycoplasma by centrifugation of the cell free supernatant, alkaline lysis (NaOH) and neutralization of the lysate

- Transfer 1 mL of culture supernatant into a centrifuge tube and pellet cells and/or cellular debris by centrifuging at 200 x *g* for 10 minutes at room temperature.
- Transfer the supernatant into a fresh sterile tube and centrifuge at 13,000 x *g* for 10 minutes at 2-8°C. This sediments the mycoplasma.
- Decant all of the supernatant. Leave the pellet and remove all medium.
- Add 10 µL of ultrapure water and 10 µL of lysis reagent to the pellet and allow to solubilise.
- Use 2 negative (10 µL of water and 10 µL of lysis reagent) and 1 positive controls (10 µL of positive control DNA and 10 µL of lysis reagent).
- Incubate at 37°C for one hour. Add 30 µL of neutralization reagent.

Stage 2: Mycoplasma PCR**:** Amplification of a conserved and mycoplasma-specific region of the DNA in the presence of digoxigenin-labelled dUTP (DIG-dUTP). The label is incorporated into the amplicon.

- Transfer 25 µL of PCR ready to go mix and 15 µL of sterile water into PCR tubes. Instead of water, UNG (Uracil-DNA glycosylase) may be used. UNG hydrolyses uracil-glycosidic bonds at dU-containing DNA sites and therefore destroys carry over products.
- To each PCR tube add 10 µL of sample, positive control or negative control.
- Transfer to a thermal cycler (PE 9600 GeneAmp PCR system Applied Biosystems, CA, USA) and cycle as follows:

  Cycle 1: 95°C for 5 minutes.

  Cycle 2-40: 94°C for 30 seconds, 62°C for 30 seconds, 72°C for 1 minute.

  Cycle 41: 72°C for 10 minutes.

  Hold at 8°C.

Stage 3: Hybridisation and ELISA procedure:

- Add 40 µL of denaturation reagent into a suitable reaction tube using a pipette with aerosol-preventive pipette tips.
- Transfer 10 µL of the amplification product per tube and incubate at 15-25°C for 10 minutes.
- Add 450 µL of hybridisation reagent per tube and mix thoroughly.
- Transfer 200 µL of the mixture per well of the microplate.
- Cover the wells with the self-adhesive cover foil.
- Incubate at 37°C on a shaker at 300 rpm for 3 hours. Remove hybridisation mixture by flicking and wash 3 times with 250 µL washing buffer (1X) per well. Remove the washing buffer by flicking.
- Add 200 µL of anti-DIG-POD working dilution per well. Cover the wells with the self-adhesive cover foil. Incubate at 15–25°C on a shaker (300 rpm) for 30 minutes.
- Remove anti-DIG-POD by flicking and wash five times with 250 µL washing buffer (1X) per well. Remove the washing buffer by flicking.
- Add 100 µL of TMB substrate solution, pre-warmed to 15-25°C, per well. Cover the wells with the self-adhesive cover foil. Incubate at 15–25°C on a shaker (300 rpm) for approx. 20 minutes.

- Add 100 µL of stop reagent per well and measure absorbance using a microplate (ELISA) reader at 450 nm (reference wavelength approx. 690 nm) within 1 hour after addition of the stop reagent.

Interpretation of results

Negative control: The absorbance of the negative control should be lower than 0.25 A450 nm – A690 nm units. If values are higher, the whole experiment (amplification included) should be repeated.

Positive control: The absorbance of the positive control should be higher than 1.2 A450 nm – A690 nm -units. If values are lower, the whole experiment (including amplification) should be repeated.

Samples: Subtract the mean of the absorbance readings of the negative controls from those of the samples. Samples are regarded as mycoplasma-contaminated if the difference in absorbance is higher than 0.2 A450 nm – A690 nm –units.

2.4 Lymphocyte isolation

2.4.1 Background

Human lymphocytes were extracted from whole blood for the purpose of co-culturing them with Nthy-ori and TPC-1 thyroid cell lines. Ethical approval was obtained from the Trinity College Faculty of Health Sciences Research Ethics Committee.

The RosetteSep® Human T cell enrichment cocktail is designed to enrich T cells from whole blood. The RosetteSep® antibody cocktail crosslinks unwanted cells in human whole blood to multiple red blood cells, forming immunorosettes. This increases the density of the unwanted (rosetted) cells, such that they pellet along with the free red blood cells when centrifuged over a buoyant density medium. Desired cells are never labelled with antibody and are easily collected as a highly enriched population at the interface between the plasma and the buoyant density medium.

2.4.2 Phlebotomy

- Whole blood is taken from donors by a physician trained in phlebotomy.
- An accessible vein is located and the puncture site is cleansed with an alcohol wipe; a tourniquet is applied to the arm.
- The vein is punctured using a winged infusion set or butterfly needle and blood is drawn into heparinised Vacuette® collection tubes (Greiner bio-one, Austria).

2.4.3 Lymphocyte extraction, counting and activation

- Blood taken in heparinised collection tubes is inverted gently to prevent coagulation of the blood.
- Blood is pipetted slowly and carefully into a 50 mL sterlin, taking care not to introduce any air bubbles into the blood.
- Add RosetteSep® Human T cell Enrichment Cocktail (StemCell Technologies, UK) at 50 µL/mL of whole blood.
- The solution is incubated at room temperature for 20 minutes with intermittent mixing.
- Dilute the sample with an equal volume of phoshate buffered saline (PBS) and 2% fetal calf serum (FCS) and mix gently and slowly.
- Layer the diluted sample in excess on top of the density medium (Lymphoprep ™, AXIS-SHIELD, Oslo, Norway). See table 2.1 for recommended volumes and tube sizes. Extreme care is needed when layering sample over density medium not to mix medium and sample.

Recommended Volumes and Tube Sizes			
Whole Blood	**PBS + 2% FCS**	**Density Medium**	**Tube Size**
1 mL	1 mL	1.5 mL	5 mL
2 mL	2 mL	3 mL	15 mL
3 mL	3 mL	3 mL	15 mL
4 mL	4 mL	4 mL	15 mL
5 mL	5 mL	15 mL	50 mL
10 mL	10 mL	15 mL	50 mL
15 mL	15 mL	15 mL	50 mL

Table 2.1 Recommended volumes and tube sizes for lymphocyte extraction

- Centrifuge for 20 minutes at 1400 rpm at 4°C with the brake off.

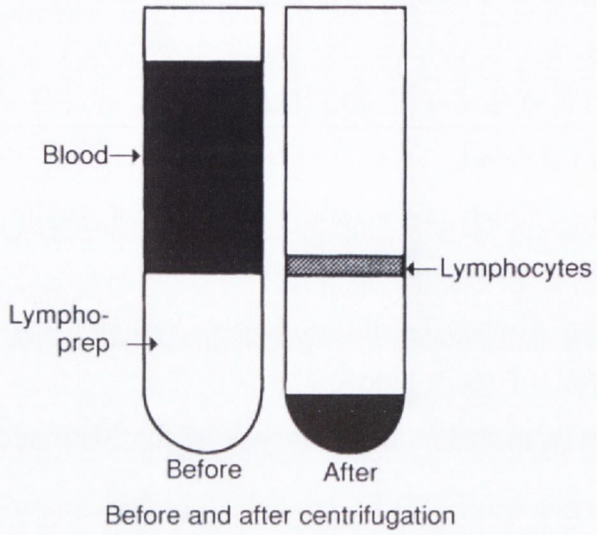

Figure 2.1 Illustrates the band of lymphocytes that are formed at the sample/medium interface during lymphocyte extraction

- After centrifugation, the T cells form a distinct band at the sample/medium interface, as shown in figure 2.1. The cells are removed from the interface using a sterile Pasteur pipette without removing the upper layer and placed in a tube.
- T cells are washed with PBS and 2% FCS and spun in a centrifuge at 1000 rpm for 8 minutes. If a large pellet of lymphocytes is achieved repeat this wash and centrifugation.
- Remove the supernatant and gently resuspend the pellet in 1 mL of RPMI.
- Cells are counted using a haemocytometer as follows:
- Clean the haemocytometer with detergent and ethanol.
- Place a coverslip over the haemocytometer.
- Add 9/10 μL of the well mixed resuspension by placing the pipette tip just above the coverslip, the haemocytometers chamber will fill due to capillary action.

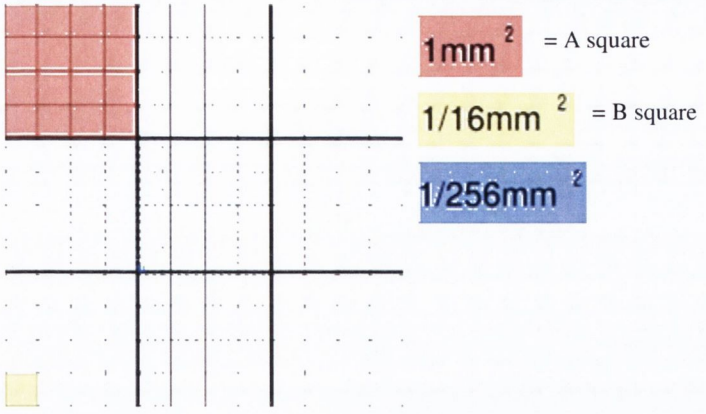

Figure 2.2 Haemocytometer illustrating the different squares within it that are used to count cells

- Cells are counted in the sixteen small B squares (yellow) within an A square (red) (figure 2.2).
- T cells are circular, yellow and shiny under the microscope.
- Count the cells within two A squares, average them and use the following formula to calculate the number of cells in the mixture from which the sample was taken, (number of cells counted and averaged) multiplied by (amount resuspended in) multiplied by 10^4 (volume of the haemocytometer).
- Approximately 1 x 10^6 cells are required for each well used in a 12 well plate. Additional RPMI is added as needed so that 1 x 10^6 cells in 1 mL of media are present in each well used.
- Phorbol 12-Myristate 13-Acetate (PMA) (Sigma, St. Louis, MO) (25 ng/mL) is added to lymphocytes to activate them.
- Lymphocytes not activated with PMA serve as controls.
- Lymphocytes are left to activate for 3 days in a humidified atmosphere containing 5% CO_2 at 37°C.
- After 3 days, control lymphocytes should not have changed in appearance whereas activated cells will clump together in large groups.

2.4.4 Co-culture procedure

- After splitting (section 2.2.4) and counting thyroid cells (same protocol used as for lymphocyte counting, section 2.4.3), 2.5 x 10^5 cells in 1 mL of media are plated in each well needed in a 12 well plate (Nunc™, NY, USA).
- After the 3 day lymphocyte activation (section 2.4.3), the T cells are scrapped with cell scrappers (Nunc™, NY, USA) and spun down at 1000 rpm for 6 minutes.
- The activated T cell supernatant is removed from the lymphocyte pellet (approximately 1 mL) and added to the 2.5 x 10^5 thyroid cells previously plated in a 12 well plate.
- Co-culture is carried out for 6 and 18 hour intervals. At the 6 and 18 hour intervals, thyroid cells are scrapped and spun down at 1000 rpm for 5 minutes and the activated lymphocyte supernatant is removed.
- The cell pellet is now ready for RNA extraction.

2.5 Extraction of RNA from cell lines

This was performed on thyroid cell lines before and after they had been co-cultured with lymphocyte supernatant using the RNeasy® Mini Kit (Qiagen Ltd., West Sussex, UK).

2.5.1 Preparation of reagents

Buffer RLT

- β-Mercaptoethanol (β-ME) must be added to buffer RLT before use. β-ME is toxic and should be dispensed in a fume hood while wearing appropriate protective clothing.
- Add 10 µL β-ME per 1 mL buffer RLT.
- Buffer RLT is stable for 1 month after addition of β- ME.

Buffer RPE

- Buffer RPE is supplied as a concentrate. Before using for the first time, add 4 volumes of ethanol (96–100%), as indicated on the bottle, to obtain a working solution.

2.5.2 Protocol

- Add 600 µL buffer RLT to each prepared sample to lyse. Vortex and centrifuge briefly to mix.
- After vortexing further homogenise the sample using a Qiagen Shredder column containing the appropriate lysis buffer (600 µL). After vortexing, the sample was further homogenised using a Qiagen Shredder column.

QIAshredders® (Qiagen Ltd., West Sussex, UK) are a commercially available spin column based shearing system. They can be used for further homogenisation of tissue initially homogenised by mortar and pestle and for cultured cells as the primary form of homogenisation.

- Lysates are pipetted directly onto a QIAshredder® spin column placed in a 2 mL collection tube, and centrifuged for 2 minutes at maximum speed. The flow through is used for subsequent RNA extraction.
- Add 1 volume of 70% ethanol to the cleared lysate, and mix immediately by pipetting. Do not centrifuge. A precipitate may form after the addition of ethanol, but this will not affect the RNeasy® procedure.
- Apply up to 700 µL of the sample, including any precipitate that may have formed, to an RNeasy® mini column placed in a 2 mL collection tube (supplied). Close the tube gently, and centrifuge for 15 seconds at >8000 x *g* (>10,000 rpm). Discard the flow through.
- Reuse the collection tube.
- If the volume exceeds 700 µL, load aliquots successively onto the RNeasy® column, and centrifuge as above. Discard the flow-through after each centrifugation step.

Protocol for on column DNase digestion

Although the RNeasy® silica-membrane technology efficiently removes most of the DNA without DNase treatment, further DNA removal may be necessary for certain RNA applications that are sensitive to very small amounts of DNA (e.g. TaqMan® RT-PCR analysis with a low-abundant target).

- Prepare DNase 1 stock solution before using the RNase-Free DNase set for the first time. Dissolve the solid DNase I (1500 Kunitz units) in 550 µL of the RNase-free water provided. Take care that no DNase 1 is lost when opening the vial. Mix gently by inverting the tube.
- DNase 1 is especially sensitive to physical denaturation and must not be vortexed. Mixing should only be carried out by gently inverting the tube. For long-term storage of DNase 1, remove the stock solution from the glass vial, divide it into single-use aliquots, and store at –20°C for up to 9 months. Thawed aliquots can be stored at 2–8°C for up to 6 weeks. Do not refreeze the aliquots after thawing.

- Pipette 350 µL buffer RW1 into the RNeasy® mini column, and centrifuge for 15 s at ≥8000 x *g* (≥10, 000 rpm) to wash. Discard the flow-through.
- Add 10 µL DNase I stock solution (see above) to 70 µL Buffer RDD. Mix by gently inverting the tube. Buffer RDD is supplied with the RNase-Free DNase set.
- Pipette the DNase 1 incubation mix (80 µL) directly onto the RNeasy® silica-gel membrane, and place on the bench top (20–30°C) for 15 minutes.

  Note: Make sure to pipette the DNase 1 incubation mix directly onto the RNeasy silica-gel membrane. DNase digestion will be incomplete if part of the mix sticks to the walls of the RNeasy column.
- Pipette 350 µL buffer RW1 into the RNeasy® mini column, and centrifuge for 15 s at ≥8000 x *g*. Discard the flow-through. Continue with the first Buffer RPE wash step.
- Transfer the RNeasy® column into a new 2 mL collection tube (supplied). Pipette 500 µL buffer RPE onto the RNeasy® column. Close the tube gently, and centrifuge for 15 seconds at >8000 x *g* (>10,000 rpm) to wash the column. Discard the flow-through. Reuse the collection tube in the next step.
- Add another 500 µL buffer RPE to the RNeasy® column. Close the tube gently, and centrifuge for 2 minutes at >8000 x *g* (>10,000 rpm) to dry the RNeasy® silica-gel membrane.
- It is important to dry the RNeasy® silica-gel membrane since residual ethanol may interfere with downstream reactions. This centrifugation ensures that no ethanol is carried over during elution.

  Note: Following the centrifugation, remove the RNeasy® mini column from the collection tube carefully so the column does not contact the flow-through as this will result in carryover of ethanol.
- Place the RNeasy® column in a new 2 mL collection tube and discard the old collection tube with the flow-through. Centrifuge in a microcentrifuge at full speed for 1 minute.
- To elute, transfer the RNeasy® column to a new 1.5 mL collection tube. Pipette 30–50 µL RNase-free water directly onto the RNeasy® silica-gel membrane. Close the tube gently, and centrifuge for 1 min at ≥8000 x *g* (≥10,000 rpm) to elute.

- If the expected RNA yield is >30 µg, repeat the elution step. Elute into the same collection tube. To obtain a higher total RNA concentration, this second elution step may be performed by using the first elute. The yield will be 15–30% less than a yield obtained using a second volume of RNase-free water, but the final concentration will be higher.

2.6 Laser capture microdissection

Laser capture microdissection (LCM) was carried out on formalin fixed paraffin embedded (FFPE) material using the PixCell®II LCM System (Arcturus Engineering, Inc., CA, USA). Briefly, 4-7 μm FFPE histological sections were cut and stained with a standard haematoxylin and eosin (H&E) stain. Upon drying they are placed on the PixCell®II microscopic stage and the following protocol is observed:

- Enable the laser via the keyswitch located on the front of the controller.
- Remove the CapSure® cassette module from the PixCell®II platform. It should slide out smoothly over the detents.
- Press down on the flanges of the cassette module. Press the end locking pins in to hold the plate down in the load position.
- Slide a CapSure® cartridge, which holds four film carriers, into the cassette module until it hits a stop. The cassette loads from one end only.
- If more than four caps are required, load a second cartridge in the same manner, making sure there is no space between the two loaded cartridges.
- Press down on the flanges of the loaded cassette. Retract the locking pins and gently raise the cassette to its loaded position.
- The cartridge is now ready to be loaded into the PixCell®II.
- Slide the loaded CapSure® cassette module to any detent position.
- After LCM, when the CapSure® cartridges are empty, press down on the plate and lock into position by pushing the locking pins in. Carefully slide out the spent cartridges and discard.
- Move the joystick to the vertical position. This centres the translation stage on the optical axis and ensures proper registration of the sample slide relative to the capture area. This also maximises the transfer area available for microdissection.
- Turn off the vacuum chuck via the switch located on the front of the controller.
- Place the slide on the translation stage, covering the vacuum chuckhole. Manually position it to locate the transfer area in the centre of the field of view.

- Choose the appropriate objective for the desired magnification. Turn on the vacuum chuck.
- Adjust illumination control.
- Adjust focus control.
- Rotate the CapSure® placement arm over the tissue sample.
- Insert the visualiser by pressing the silver plunger button located above the joystick.
- Adjust the microscope light source to obtain a good image on the monitor.
- To perform a microdissection, retract the visualiser by pressing the tab located below the plunger button, and re-adjust the microscope light source.
- Slide the CapSure® cassette module to a detent position, making sure there is a CapSure® cap at the load line.
- Rotate the placement arm to the cap pick-up position. The arm will automatically line up with the cap.
- Raise the placement arm vertically to remove the cap from the cassette module.
- Rotate the placement arm to transfer position over the slide. Release the placement arm. The cap will automatically lower onto the slide. Upon contact with the slide, the placement arm will seat the cap properly on the sample.

When the laser is enabled, an aiming beam is visible on the monitor.

- Select the laser spot size with the 'Spot Size Adjust' located on the left of the laser tower.
- Use the joystick or the XY controls to aim the laser beam on the capture region.

Use the front panel digital controls on the controller to adjust laser parameters. Typical values are:

Spot Size	Power	Duration
<7.5 μm	40 mW	450 μs
~15 μm	25 mW	1.5 ms
~30 μm	20 mW	5 ms

Table 2.2 Typical LCM laser parameters

- Fire the laser by pressing the remote thumb switch or the 'fire' button on the front of the controller.
- There is an audible beep when the laser fires. The activated portion of the transfer film will be visible as a ring of film fused to the tissue.
- Use the joystick to move to other areas in the tissue and capture other cells of interest.
- To remove the captured tissue, lift the placement arm in a smooth but swift motion.
- With the cap in place, lift and rotate the placement arm to the unload platform.
- Lower the placement arm onto the unload platform – dropping the cap into the extraction slot.
- Rotate the placement arm to the rest position. The cap will be extracted from the arm and suspended in the unload platform.
- Slide the cap insertion tool onto the unload platform. Make sure the open end of the insertion tool faces the suspended cap and the groove fits over the guide rail.
- Slide the insertion tool down the groove until the cap is engaged.
- Remove with cap attached.
- Insert cap into 0.5 mL reagent tube.
- Press down firmly to ensure an even seal.

Continue extraction according to appropriate protocol.

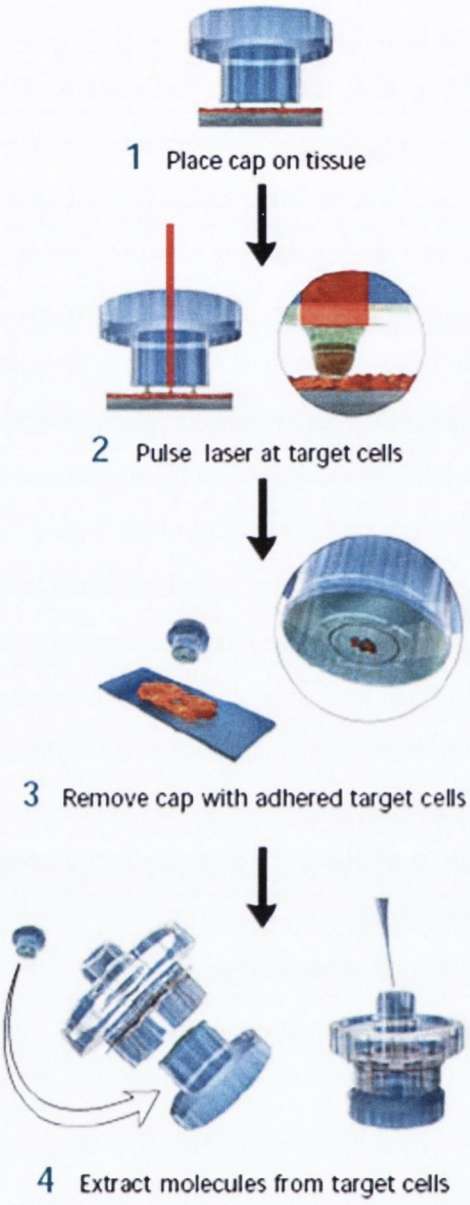

Figure 2.3 The laser capture microdissection process

2.7 Extraction of RNA from FFPE material

This was performed on samples following LCM. The Absolutely RNA® FFPE (formalin fixed paraffin embedded) Kit (Stratagene, CA, USA) was utilised for this function.

2.7.1 Preparation of reagents

RNase-free DNase I

- Reconstitute the lyophilized RNase-free DNase I by adding 290 µL of DNase reconstitution buffer to the vial.
- Mix thoroughly to ensure that all the powder goes into solution.
- Store at -20°C.

High salt wash buffer

- Prepare 1X high salt wash buffer by adding 16 mL of 100% ethanol to the bottle of 1.67X high salt wash buffer.
- Store at room temperature.

Low salt wash buffer

- Prepare 1X low salt wash buffer by adding 68 mL of 100% ethanol to the bottle of 5X low salt wash buffer.
- Store at room temperature.

Ethanol wash solution

- Prepare 90% and 70% ethanol solutions (1 mL of each wash solution per tissue sample) using DNase-, RNase-free H_2O.

2.7.2 Protocol

Cell lysis

- Perform microdissection and place cap in a 0.5 mL microfuge tube containing 110 µL of Proteinase K solution. Prepare a fresh working solution of Proteinase K before each use.
- Incubate overnight at 55°C with constant agitation (i.e. a rotary oven).

RNA isolation

- Transfer solution to a fresh 1.5 mL microcentrifuge tube and for each tissue sample; add 0.875 µL of β-mercaptoethanol (β-ME) to 125 µL of RNA binding buffer.
- Prepare a fresh mixture of RNA binding buffer and β-ME before each use.
- Add 125 µL of the RNA binding buffer- β-ME mixture to each sample and vortex or pipette the sample repeatedly until homogenized.
- Transfer each sample to a pre-filter spin cup. Place the spin cup in the 2 mL receptacle tube provided and spin in a microcentrifuge for 1 minute at maximum speed (14,000 rpm/16,000 x *g*). To each filtrate in the receptacle tubes, add 125 µL of 100% ethanol and mix thoroughly by vortexing for 5 seconds. It is important to vortex until the lysate and ethanol are thoroughly mixed.
- Transfer this mixture to a RNA-binding spin cup that has been seated within a 2 mL receptacle tube and snap the cap of the tube onto the top of the spin cup.
- Spin in a microcentrifuge for 30–60 seconds at 14,000 x *g* to load the RNA onto the spin cup matrix.
- Remove and retain the spin cup and discard the filtrate.
- *Note*: up to this point, the RNA has been protected from RNases by the presence of guanidine thiocyanate.
- Replace the spin cup in the receptacle tube, then add 600 µL of 1X low- salt wash buffer and cap the tube. Spin the sample in a microcentrifuge at 14,000 x *g* for 30–60 seconds.

- Remove and retain the spin cup and discard the filtrate. Replace the spin cup in the receptacle tube, cap the tube, and spin the sample in a microcentrifuge at 14,000 x *g* for 2 minutes to dry the fiber matrix.
- Prepare the DNase treatment solution by gently mixing 5 µL of reconstituted RNase-free DNase I with 25 µL of DNase digestion buffer. Gentle mixing is necessary because the DNase I is very sensitive to denaturation.
- Store the reconstituted DNase I at –20°C.
- Add the 30 mL of DNase treatment solution directly onto the fiber matrix inside the spin cup and cap the tube. Place the samples in a 37°C incubator for 15 minutes.
- Add 500 µL of 1X high-salt wash buffer to the spin cup, cap the tube, and spin the sample in a microcentrifuge at 14,000 x *g* for 30–60 seconds.
- Remove and retain the spin cup, discard the filtrate, and replace the spin cup in the receptacle tube. Add 600 µL of 1X low-salt wash buffer. Cap the tube and spin the sample in a microcentrifuge at 14,000 x *g* for 30–60 seconds.
- Remove and retain the spin cup, discard the filtrate, and replace the spin cup in the receptacle tube. Add 300 µL of 1X low-salt wash buffer. Cap the tube and spin the sample in a microcentrifuge at 14,000 x *g* for 30–60 seconds.
- Remove and retain the spin cup and discard the filtrate. Replace the spin cup in the receptacle tube, cap the tube, and spin the sample in a microcentrifuge at 14,000 x *g* for 2 minutes to dry the fiber matrix.
- Transfer the spin cup to a 1.5 mL collection tube.
- Pre-heat the elution buffer (30 µL per sample) to 75°C. Add 30 µL of elution buffer directly onto the fiber matrix inside the spin cup. Snap the cap of the collection tube onto the spin cup and incubate the sample at room temperature for 2 minutes.
- The elution buffer must be added directly onto the fiber matrix of the spin cup to ensure that the elution buffer permeates the entire fiber matrix.
- Spin the sample in a microcentrifuge at maximum speed for 1 minute.
- The purified RNA is in the elution buffer in the microcentrifuge tube. Cap the tube to store the RNA. The RNA can be stored at –20°C for up to one month or at –80°C for long-term storage.

- RNA quality and quantity are assessed using the NanoDrop® ND-1000 spectrophotometer.

2.8 Nano-Drop® 1000 spectrophotometer

Nucleic acid samples were checked for concentration and quality using the NanoDrop® ND-1000 spectrophotometer. To measure nucleic acid samples select the 'Nucleic Acid' application module. The NanoDrop® ND-1000 is a full-spectrum (220-750nm) spectrophotometer that measures 1 μL samples with high accuracy and reproducibility. It utilizes a patented sample retention technology that employs surface tension alone to hold the sample in place. In addition, the ND-1000 has the capability to measure highly concentrated samples without dilution (50X higher concentration than the samples measured by a standard curvette spectrophotometer).

2.8.1 Loading of samples (nucleic acid and water)

- With the sampling arm open, pipette the sample onto the lower measurement pedestal.
- Close the sampling arm and initiate a spectral measurement using the operating software on the PC. The sample column is automatically drawn between the upper and lower measurement pedestals and the spectral measurement made.

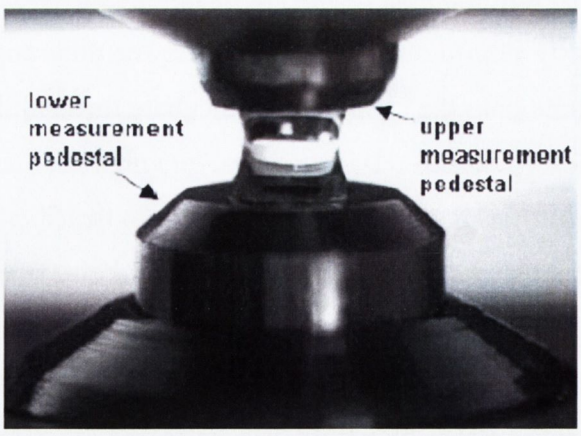

Figure 2.4 NanoDrop® spectrophotometer sample pedestal

- When the measurement is complete, open the sampling arm and wipe the sample from both the upper and lower pedestals using a soft laboratory wipe. Simple wiping prevents sample carryover in successive measurements for samples varying by more than 1000 fold in concentration.

2.8.2 Blank measurement

- Ensure measurement pedestal surfaces are clean. Load 1 µL water sample onto the lower measurement pedestal and then click 'OK'. After clicking OK, the message "*Initializing spectrometer- please wait*" will appear. When this message disappears, the instrument will be ready for use.
- Before making a sample measurement, a blank must be measured and stored. This will assure the user that the instrument is working well and that any non-specific fluorescence is not a concern.
- Load a blank sample (the buffer, solvent, or carrier liquid used with your samples) onto the lower measurement pedestal and lower the sampling arm into the 'down' position. Click on the 'Blank' button.
- Analyze an aliquot of the blanking solution as though it were a sample. This is done using the 'Measure' button. The result should be a spectrum with a relatively flat baseline. Wipe the blank from both measurement pedestal surfaces and repeat the process until the spectrum is flat.

2.8.3 Sample measurement

- 1 µL samples are sufficient to ensure accurate and reproducible results when measuring aqueous nucleic acid samples. After blank measurement load the sample as outlines above in section 2.8.1.
- *Results*

  A260**:** absorbance of the sample at 260 nm represented as if measured with a conventional 10 mm path. *Note*: This is 10X the absorbance

actually measured using the 1 mm path length and 50X the absorbance actually measured using the 0.2 mm path length.

A280**:** sample absorbance at 280 nm represented as if measured with a conventional 10 mm path. *Note*: This is 10X the absorbance actually measured using the 1 mm path length and 50X the absorbance actually measured using the 0.2 mm path length.

260/280**:** ratio of sample absorbance at 260 and 280 nm. The ratio of absorbance at 260 and 280 nm is used to assess the purity of DNA and RNA. A ratio of ~1.8 is generally accepted as "pure" for DNA; a ratio of ~2.0 is generally accepted as "pure" for RNA. If the ratio is appreciably lower in either case, it may indicate the presence of protein, phenol or other contaminants that absorb strongly at or near 280 nm.

260/230**:** ratio of sample absorbance at 260 and 230 nm. This is a secondary measure of nucleic acid purity. The 260/230 values for "pure" nucleic acid are often higher than the respective 260/280 values. They are commonly in the range of 1.8-2.2. If the ratio is appreciably lower, this may indicate the presence of co-purified contaminants.

Concentration (ng/μL): sample concentration in ng/uL based on absorbance at 260 nm and the selected analysis constant.

2.9 cDNA synthesis

The High Capacity cDNA Archive Kit (Applied Biosystems, CA, USA) was used to convert total RNA to single stranded cDNA. This kit uses the random primer scheme for initiating cDNA synthesis. Random primers ensure that the first strand synthesis occurs efficiently with all species of RNA molecules present including messenger RNA (mRNA) and ribosomal RNA (rRNA).

cDNA reaction preparation

A 2X reverse transcription (RT) master mix was prepared using the following reagents.

Components	Volume per reaction (µL)	Concentration in 2X mix
10X RT buffer	10	2X
25X dNTP mixture	4	2X
10X random primers	10	2X
Multiscribe RT (500U/µL)	5	5U/µL
RNase free water	21	-
Final Volume	50	

Table 2.3 cDNA reaction preparation

To avoid RNase contamination, RNase-free reagents and consumables were used. 50 µL 2X RT master mixes was used for each reaction. An equal volume of RNA sample was added per reaction and brought up to 50 µL with RNase free water; this amount differed in each experiment and is noted in each corresponding chapter. cDNA synthesis was performed (PE 9600 GeneAmp PCR system Applied Biosystems, CA, USA) using the following conditions: 25°C for 10 minutes, 37°C for 2 hours.

2.10 TaqMan® PCR

A TaqMan® PCR-based system was selected for mRNA quantitation in this study. The TaqMan® system was chosen for a number of reasons. Firstly TaqMan® PCR and Reverse-Transcriptase (RT) PCR requires only a few nanograms of target DNA/RNA. This is highly significant since the amount of DNA/RNA extractable from formalin fixed and paraffin embedded archival material is low. Secondly, TaqMan PCR and RT-PCR products are small (generally less than 200 base pairs) and thus can be used to amplify partially degraded or fragmented DNA/RNA such as that obtained from FFPE material.

TaqMan® PCR exploits the 5´ nuclease activity of AmpliTaq Gold® DNA Polymerase to cleave a TaqMan probe during PCR. The TaqMan probe contains a reporter dye at the 5´ end of the probe and a quencher dye at the 3´ end of the probe. During the reaction, cleavage of the probe separates the reporter dye and the quencher dye, resulting in increased fluorescence of the reporter. Accumulation of PCR products is detected directly by monitoring the increase in fluorescence of the reporter dye, shown in figure 2.5.

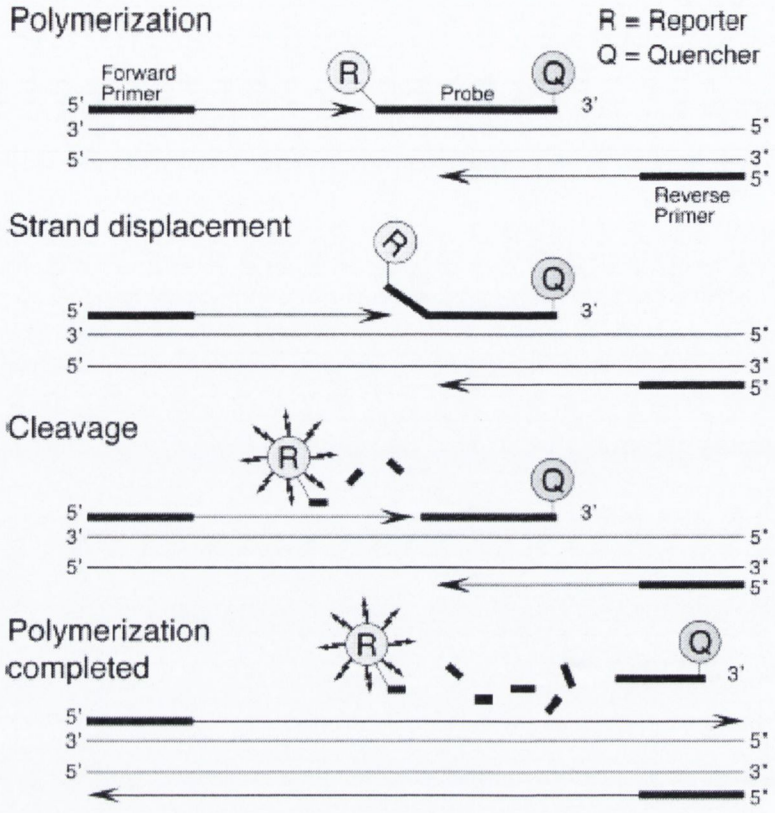

Figure 2.5 The forklike-structure-dependent, polymerisation-associated, 5´–3´ nuclease activity of AmpliTaq® Gold DNA Polymerase during PCR

When the probe is intact, the proximity of the reporter dye to the quencher dye results in suppression of the reporter fluorescence primarily by Förster-type energy transfer (Forster, 1948, Lakowicz, 1983). During PCR, if the target of interest is present, the probe specifically anneals between the forward and reverse primer sites.

The 5´-3´ nucleolytic activity of the AmpliTaq® Gold DNA Polymerase cleaves the probe between the reporter and the quencher only if the probe hybridises to the target. The probe fragments are then displaced from the target, and polymerisation of the strand continues. The 3´ end of the probe is blocked to prevent extension of the probe during PCR. This process occurs in every cycle and does not interfere with the exponential accumulation of product.

The probe consists of an oligonucleotide with a 5´-reporter dye and a 3´-quencher dye. A fluorescent reporter dye, such as FAM (6-carboxyfluorescein), is covalently linked to the 5´ end of the oligonucleotide. TET (6-carboxy-4,7,2´,7´-tetrachlorofluorescein), JOE (6-carboxy-4,5-dichloro-2,7-dimethoxyfluorescein), and VIC are also used as reporter dyes. In older TaqMan® probes each of the reporters is quenched by TAMRA (6-carboxy-N,N,N´,N´-tetramethylrhodamine) at the 3´ end.

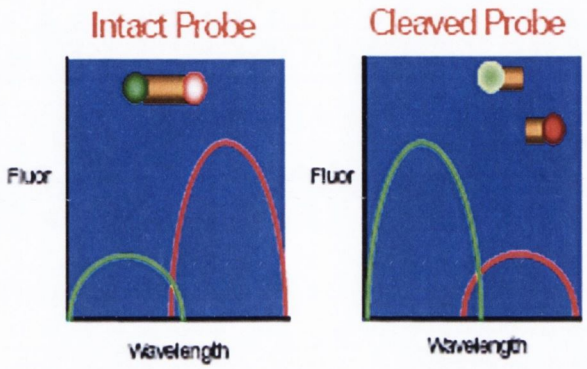

Figure 2.6 Increased fluorescence activity due to cleaved probe

2.10.1 Real-time quantitative TaqMan® RT-PCR

Real-time RT-PCR is the ability to monitor the progress of the PCR as it occurs (i.e., in real time). Data is therefore collected throughout the PCR process, rather than at the end of the PCR. This completely revolutionizes the way one approaches PCR-based quantitation of DNA and RNA. In real-time RT-PCR, reactions are characterized by the point in time during cycling when amplification of a target is first detected rather than the amount of target accumulated after a fixed number of cycles. The higher the starting copy number of the nucleic acid target, the sooner a significant increase in fluorescence is observed. In contrast, an endpoint assay (also called a "plate read assay") measures the amount of accumulated PCR product at the end of the PCR cycle. RT-PCR can be one-step or two-step in nature. All of the RT-PCR carried out in this thesis was two-step in nature.

In the initial cycles of PCR, there is little change in fluorescence signal. This defines the baseline for the amplification plot. An increase in fluorescence above the baseline indicates the detection of accumulated target. A fixed fluorescence threshold can be set above the baseline. The parameter C_T (threshold cycle) is defined as the fractional cycle number at which the fluorescence passes the fixed threshold (see figure 2.7).

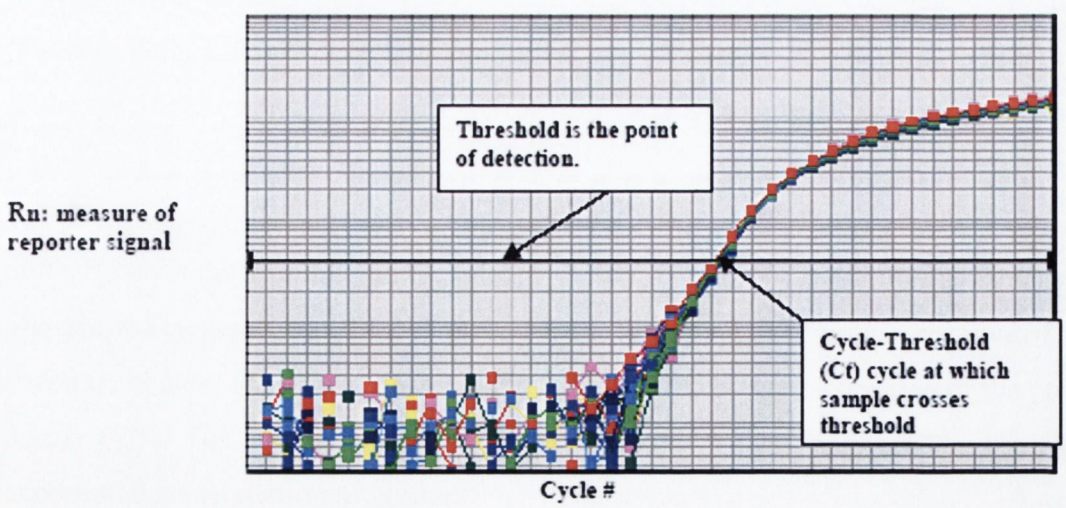

Figure 2.7 Example of an amplification plot

2.10.2 Relative gene expression

The ABI Prism® 7900HT Sequence Detection System supports real-time relative quantification of nucleic acids using the Comparative C_T method. Relative quantification describes the change in expression of the target gene relative to some reference group such as an untreated control or a sample at time zero in a time-course study. In the comparative C_T method, quantity is expressed relative to a calibrator sample that is used as the basis for comparative results. Therefore, the calibrator is the 1X sample and all other quantities are expressed as an n-fold difference relative to the calibrator. The Comparative C_T Method uses the following arithmetic formula to achieve results for relative quantification (Livak and Schmittgen, 2001).

$$2^{-\Delta\Delta C_T}$$

Where:

ΔC_T is achieved by subtracting the endogenous control C_T from your samples' C_T, therefore $\Delta C_T = C_T$ (sample) – C_T (endogenous control). To work out $\Delta\Delta C_T$ you must compare expression levels relative to a calibrator sample, thus $\Delta\Delta C_T = \Delta C_T$ (sample) - ΔC_T (calibrator).

Using the $2^{-\Delta\Delta C_T}$ method, the data are presented as the fold change in gene expression normalized to an endogenous reference gene and relative to the untreated control.

Relative quantification on the 7900HT instrument is accomplished through the use of the polymerase chain reaction and the fluorogenic 5′ nuclease assay. After selection of endogenous control, probe and primer sets are designed or chosen for both target and control sequences. Unknown samples containing master mix and assays targeting specific nucleic acid sequences are loaded onto the 7900HT. During the run, the instrument records the emission resulting from the cleavage of TaqMan® probes in the presence of the target sequence. After the run, the SDS software processes the raw fluorescence data to produce threshold cycle (C_T) values for each sample. The SDS software computes relative quantities from the C_T values of the calibrator sample and the data from the unknown samples within the gene expression profile.

Relative quantification values (gene fold changes) can be achieved manually by collecting C_T values and inputting them into the $2^{-\Delta\Delta C_T}$ formula or the SDS software can collect data and produce RQ values for you.

2.10.3 TaqMan® Low Density Arrays

2.10.3.1 Background

TaqMan® Low Density Arrays (TLDAs) are used for profiling gene expression using the comparative C_T method of relative quantification. The TLDAs evaluate from one to eight cDNA samples generated from human total RNA in a two step RT-PCR experiment.

The TLDAs function as an array of reaction vessels for the PCR detection step. Typically, the wells of the TLDA contain ABI fluorogenic 5′ nuclease assays that detect the real-time amplification of user-specified targets. Relative levels of gene expression are determined from the fluorescence data generated during PCR using the ABI Prism® 7900HT Sequence detection System. The TLDA acts as a vessel for RT-PCR.

Immune-profiling/inflammation LDAs (TILDAs) were used in this thesis, which comprise gene expression markers for ninety three immune related targets plus three endogenous controls. These TILDAs are preconfigured in 384 well formats. Each of the eight separate loading ports feeds into forty eight separate wells with four well replicates per assay (see figure 2.8). Each well contains dried ABI TaqMan® primers and probes for one mRNA target. TILDAs were used to analyse thyroid cell lines co-cultured with activated lymphocytic supernatant from Hashimoto Thyroiditis and normal subjects.

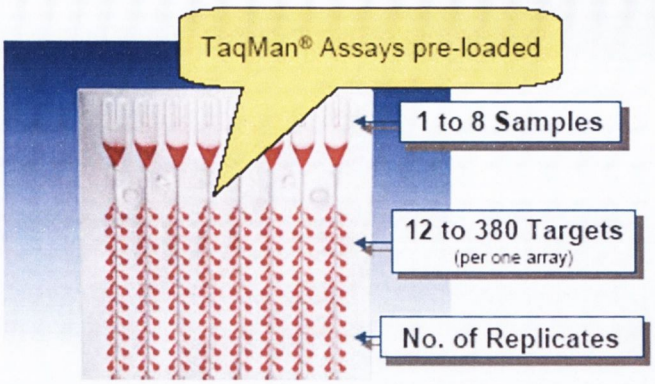

Figure 2.8 A TLDA and its features

2.10.3.2 Loading the TILDA

- Remove the TILDA from its packaging and place on a lab bench, foil side down.
- One sample is analysed per card.
- Each loading port is filled with a 100 µL volume containing 5 µL cDNA (20ng/µL), 45 µL of nuclease free water and 50 µL of TaqMan® universal PCR master mix (2X).
- Dispense the reaction mix so that it sweeps in and around the fill reservoir towards the vent port.

2.10.3.3 Centrifuging the TILDA

- Insert the TILDA into a Sorvall®/Heraeus® card holder and custom bucket (Applied Biosystems, CA, USA) and centrifuge in a Sorvall® Legend T EASYset centrifuge (Thermo Electron Corporation, Germany) for a total of 2 consecutive 1 minute spins at 1200 rpm to ensure complete distribution of the sample from the loading port into each well.
- Examine the TILDA to determine whether filling is complete. The amount of cDNA sample remaining in the fill reservoirs should be uniform and consistent from reservoir to reservoir.

2.10.3.4 Sealing the TILDA and running the gene expression reaction

- Place the sealers' carriage into the starting position.
- Insert the TILDA into the sealer so that it is seated securely in the insert plate.
- Push the carriage across the base of the sealer in the direction of the arrows in one firm, smooth motion until you reach the end of the sealer.
- Remove the TILDA and trim off the fill reservoirs from the TILDA using a scissors.
- The TILDA is ready to be run on the 7900HT with the following thermal cycling conditions: 2 minutes at 50°C, 10 minutes at 94.5°C, and for 40 cycles, 30 seconds at 97°C and 1 minute at 59.7°C.

2.10.4 Pre-amplification

2.10.4.1 Background

Gene expression analysis is often limited by the amount of RNA that can be extracted from the tissues or cells being studied. This is especially true when working with formalin fixed paraffin embedded (FFPE) material and using techniques such as laser capture microdissection (LCM). LCM achieves accurate, pure populations of cells for extraction however the yield produced is extremely low.

The TaqMan® Pre-Amp Master Mix Kit is intended for use with very small quantities of cDNA. The kit allows you to increase the quantity of your RNA for later use in gene expression studies. Starting material is increased prior to PCR and the resulting pre-amplification product is then used for PCR.

The Pre-Amp kit enables multiplex pre-amplification up to 100-plex and provides unbiased amplicons of specific regions of the starting cDNA.

2.10.4.2 Pooling the assays

In this procedure, a 0.2X pooled assay mix is prepared which will be used for running the pre-amplification reaction.

- In a microcentrifuge tube, combine equal volumes of each of the 20X gene expression assays being used, for example 10 µL of each of the 15 assays.
- Dilute the pooled assays using 1X Tris EDTA (TE) buffer so that each assay is at a final concentration of 0.2X, for the above example add 850 µL of 1X TE to the pooled assays for a total volume of 1 mL.

2.10.4.3 Preparing cDNA from RNA

See section 2.9.

2.10.4.4 Running the pre-amplification reaction

Use the following table (table 2.4) to prepare the reactions, and then add them to a 96-well plate (Applied Biosystems, CA, USA).

Component	Volume (µL/reaction)	Final concentration
TaqMan® Pre-Amp master mix (2X)	25	1X
Pooled assay mix (0.2X)	12.5	0.05X (each assay)
cDNA sample (2.5 ng/µL)	10	0.5 ng/µL
Nuclease free water	2.5	-
Total	50	-

Table 2.4 Pre-amplification reaction preparation

- Seal the 96-well plate with an ABI Prism® Optical Adhesive cover (Applied Biosystems, CA, USA).
- Centrifuge the plate briefly.
- The pre-amplification reaction is performed for 10 minutes at 95°C, and 10 cycles of 15 seconds at 95°C and 4 minutes at 60°C (PE 9600 GeneAmp PCR system Applied Biosystems, CA, USA).
- Upon completion, immediately remove the plate from the thermal cycler and place it on ice for immediate use or store at -20°C.

2.10.4.5 Running the gene expression reaction

- Dilute the TaqMan® gene expression assays (20X) 1:5 (to 4X) using 1X TE buffer.
- Make 1:5 dilutions of the pre-amplified products using 1X TE buffer.

Set up the gene expression reactions using the following table (table 2.5), and then load the plate.

Component	Volume (µL/reaction)
TaqMan® gene expression master mix w/UNG (2X)	10
Pre-amplification product, diluted	5
TaqMan® gene expression assay (4X)	5
Total	20

Table 2.5 Gene expression reaction preparation

- Seal the plate with an ABI Prism® Optical Adhesive Cover and centrifuge briefly.
- Perform the following thermal cycling specifications on the ABI Prism® 7900HT Sequence Detection System; (Applied Biosystems, CA, USA) 2 minutes at 50°C, 10 minutes at 95°C and 40 cycles each for 15 seconds at 95°C and 1 minute at 60°C.

2.11 Tissue microarray construction

2.11.1 Background

The tissue microarray (TMA) technique was described in its current form by Kononen and colleagues (Kononen et al., 1998) as late as 1998 and since then has become a well established method for high throughput of paraffin embedded tissue samples for immunohistochemistry and *in situ* techniques.

It is a mechanical technique, which can be done using a Beecher manual tissue arrayer (Beecher Instruments Inc., Wisconsin, USA). The process involves taking tissue core samples from multiple "donor" blocks with subsequent precise insertion (arraying) into an empty "recipient" block- the TMA block. The tissue cores are taken with a steel tube with a hollow core and inserted into empty holes in the TMA block. The TMA block is processed essentially as a regular wax block.

2.11.2 TMA construction

Note: Before construction begins, all blocks have been collected, and their corresponding H&E slide is examined by a pathologist and the area of interest is marked. An Excel sheet or map is constructed of the layout the TMA will take and the blocks are organised into this layout ready for construction in the microarrayer.

- Place the recipient block in the block holder, fitting it into the upper left hand corner of the holder and tighten the screws. *Note*: the recipient block is deeper than a normal block (9 mm). Align the punch needle (0.6 mm) (Beecher Instruments Inc., Wisconsin, USA) marked in red over the position where the first core is to be made. Punch a hole in the recipient block using the recipient punch (marked in red) by moving the turret downwards.
- The depth the punch enters will depend on the setting of the depth stop. Move the punch an angle of 90° and back to loosen the core and then allow the turret to move back up and out of the block. Discard the extracted core.

- Switch the turret and insert the stage to support the donor block. Using the donor punch (marked in blue) take a relevant core from the donor block in a similar fashion as above. The marked H&E slides are used at this stage to choose the correct area. Remove the stage and place the punch in the newly made hole of the recipient block by pushing the turret down.
- Using the micrometers on the arrayer, move the punches along a defined length. It is recommended that at least 1mm be left between cores of 0.6mm. Do not zero the digital precision devices as this can lead to error.
- Clean the punches with a small amount of xylene during the array process to help avoid wax build up. Do not remove the punches once the array process has begun as this may lead to cores not being aligned properly.
- When finished arraying remove the block and place cassette facing up on a glass slide in a 37°C oven overnight.
- Remove the block from the oven the following morning but do not attempt to remove the slide as this will distort the block. Instead place both on a cold plate for a few minutes to help harden the block. Then remove the slide from the block.

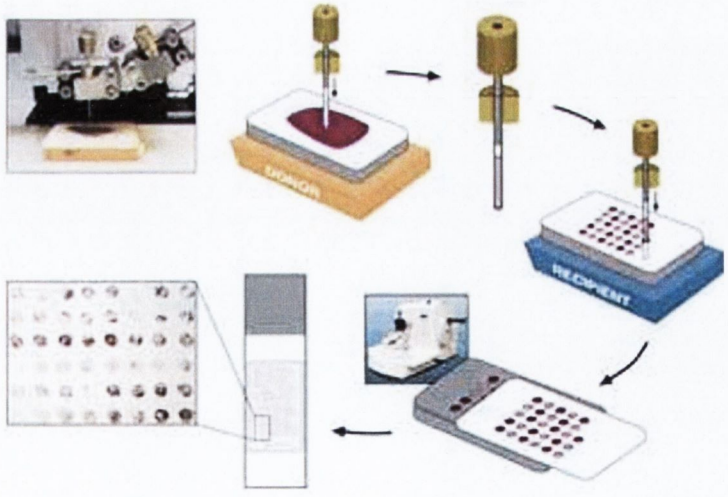

Figure 2.9 The TMA construction process

2.12 Immunohistochemisty

2.12.1 Background

Immunohistochemistry is a technique for identifying cellular or tissue constituents (antigens) by means of antigen-antibody interactions, the site of antibody binding being identified either by direct labelling of the antibody, or by use of a secondary labelling method. After a pressure cooker antigen retrieval step to unmask antigen sites, the ABC method was used (figure 2.10). The first step of the procedure is to incubate the section with primary antibody raised against the antigen of interest, such as mouse antibody to a tumour-associated antigen. Next, a biotin-labelled secondary antibody is added, for example biotinylated anti-mouse IgG. This introduces many biotins into the section at the location of the primary antibody. The avidin: biotinylated enzyme complex (ABC) is then added and binds to the biotinylated secondary antibody. In the last step of the procedure, the tissue antigen is localized by incubation with a substrate for the enzyme, in this case diaminobenzidene (DAB) which yields a crisp, insoluble, dark brown reaction end product.

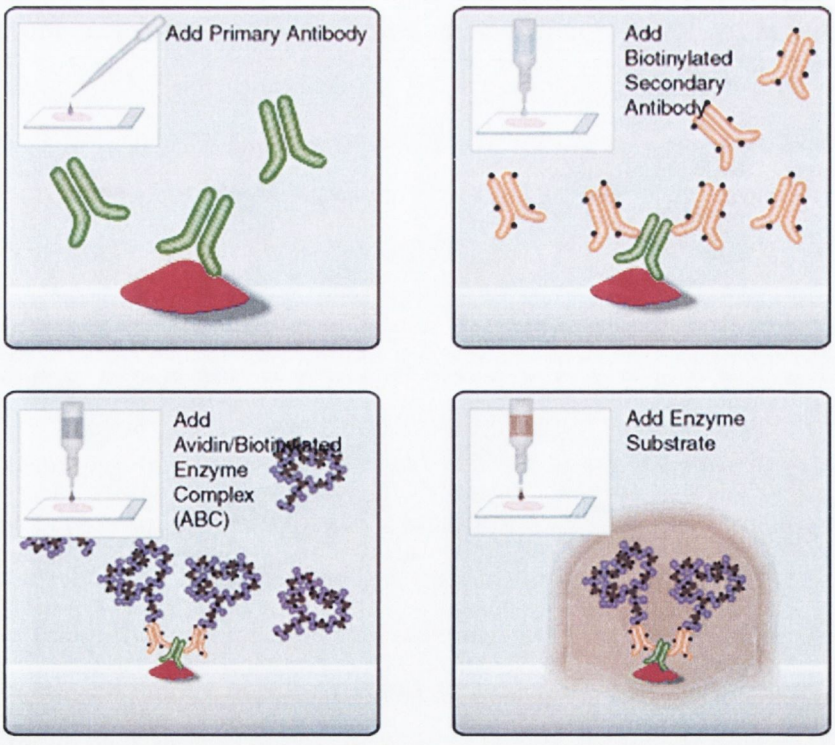

Figure 2.10 The ABC method

The following table (table 2.6) lists the antibodies that were used, their species, clonality, dilution (diluted in TBS) and the positive control that was used for each.

Primary Antibody	Species/Clonality	Dilution	Positive control
MMP11	Mouse/Monoclonal	Bought prediluted	Placenta
BAX	Mouse/Monoclonal	Bought prediluted	Breast
APOE	Mouse/Monoclonal	1 in 100	Brain
TOP2A	Mouse/Monoclonal	1 in 10	Tonsil
LYN	Mouse/Monoclonal	1 in 100	Tonsil

Table 2.6 Primary antibodies

2.12.2 ABC (*elite*) peroxidise method

- 4 µm sections of TMA blocks are cut using a microtome and placed on charged slides.
- Sections are dried overnight at 37°C or for 1 hour at 60°C.
- Sections are deparaffinised in xylene (Sigma-aldrich, St. Louis, MO) for 5 minutes, 4 minutes and 4 minutes.
- Sections are dehydrated in ethanol (Sigma-aldrich, St. Louis, MO) for 3, 2 and 1 minutes.
- Sections are brought to running water (6 minutes).
- Sections are incubated in 0.3% H_2O_2-methanol (Sigma-aldrich, St. Louis, MO) for 30 minutes to block endogenous peroxidises.
- Rinse sections in running water.

Antigen retrieval

- 15 mL of antigen unmasking solution (Vector Laboratories Inc. CA, USA) is added to 1600 mL of deionised water and placed in a pressure cooker (Medical Supply Company Ltd. Dublin, Ireland).

- Sections are added and antigen retrieval takes place on high pressure for approximately 10 minutes (length of antigen retrieval can vary depending on antibody).
- Rinse sections in running water.

Note: TOP2A does not require an antigen retrieval step.

Note: sections are now transferred to the Lab Vision Autostainer (Lab Vision Corporation, CA, USA) which automates the following steps.

- Sections are rinsed in Tris buffered saline (10X) (TBS) (Sigma-aldrich, St. Louis, MO) washed with TBS and left covered in TBS for 5 minutes.
- Sections are covered in 0.1% bovine serum albumen (BSA) (Vector Laboratories Inc. CA, USA) for 10 minutes.
- Sections are decanted and covered with diluted primary antibody for approximately 30-60 minutes (primary antibody concentration and incubation time is optimised for each antibody; primary antibody was omitted for the negative control).
- Sections are washed with TBS and left covered in TBS for 5 minutes.
- Sections are decanted, and incubated in secondary antibody for 30 minutes.
- Sections are washed with TBS and left covered in TBS for 5 minutes.
- Sections are decanted and incubated in ABC reagent (Vectastain ABC kit, Vector Laboratories Inc. CA, USA), for 30 minutes. ABC reagent must be made up 30 minutes before use by adding 2 drops of reagent A to 5 mL of TBS and then adding 2 mL of reagent B, mixing well and allowing to stand.
- Wash slides in TBS and leave covered for 5 minutes.
- Incubate sections in diaminobenzidine chromogen (DAB) (DakoCytomation, West Sussex, UK) solution for 7-10 minutes. DAB is made by adding 20 µL of liquid DAB to 1 mL of substrate buffer.
- Wash sections with TBS.

Note: sections are removed from the Autostainer and the following steps are carried out manually.

- Wash sections in running water for 2 minutes.
- Counterstain sections in haematoxylin (Vector Laboratories Inc. CA, USA) for 10 seconds.

- Differentiate sections in 1% acid alcohol (Sigma-aldrich, St. Louis, MO) for 10 seconds.
- Blue in lukewarm running water for 3-5 minutes, dehydrate and clear sections by going backwards through the ethanol and xylene baths
- Apply pertex (Medite, Burgdorf, Germany) and coverslip.

2.13 *In situ* hybridization analysis of microRNAs

2.13.1 Background

In situ hybridization (ISH) is a technique widely used in research and diagnostic laboratories to study gene expression. This technique is based on the hybridization of 300-1500 nucleotide (nt) long probes to their cognate sequences in target tissue sections or whole mounts. MicroRNAs (miRNAs) are a class of small (~22 nt) endogenous non-coding RNAs that regulate gene expression post-transcriptionally by binding to their target mRNAs. Increasing evidence suggests that miRNAs play important roles in cancer. As a result of their small size, detection of miRNAs using ISH methods has been technically challenging.

The recent introduction of locked nucleic acid (LNA) modified oligonucleotides allow probes as short as 20 nt to have high melting temperatures. LNA nucleosides are a class of nucleic acid analogues in which the ribose ring is "locked" by a methylene bridge connecting the 2′-0 atom with the 4′-C atom. LNA nucleosides contain the five common nucleobases (t, c, g, a, u) that appear in DNA and RNA and are able to form base pairs according to standard Watson-Crick base pairing rules. However, by "locking" the molecule with the methylene bridge the LNA is constrained in the ideal conformation for Watson-Crick binding. LNA therefore makes the pairing with a complementary nucleotide strand more rapid and increases the stability of the resulting duplex. This increases thermal stability provides the basis for the high stringency required for ISH.

2.13.2 Protocol

Sample Preparation

- 4 µm sections of TMA blocks are cut using a microtome and placed on charged slides.
- Sections are dried overnight at 37°C or for 1 hour at 60°C.

Deparaffinization

- Sections are deparaffinised in xylene (Sigma-aldrich, St. Louis, MO) in 3 slide mailers for 5 minutes, 4 minutes and 4 minutes.
- Sections are dehydrated in ethanol (Sigma-aldrich, St. Louis, MO) for 3, 2 and 1 minutes.
- Sections are placed in water for 2 minutes.

Deproteination

- Sections are placed in PBS (Sigma-aldrich, St. Louis, MO) twice for 5 minutes each.
- 12.5 µL of stock Proteinase K (14-22 mg/mL) (Roche, West Sussex, UK) is added to 25 mL of warm PK buffer (30m*M* Tris-HCl (pH 8)) (Sigma-aldrich, St. Louis, MO) (10µg/mL) in a mailer. Slides are added and incubated at 37 °C in an oven for 15 minutes.
- 5 µL of 100% glycine (Sigma-aldrich, St. Louis, MO) is added to 25 mL of PBS (0.2 % glycine in PBS) in a mailer and slides are washed for 30 seconds.
- Sections are washed in PBS twice for 5 minutes each.
- Sections are removed from mailer and excess liquid is removed with tissue.
- Sections are fixed by adding 200 µL of 4% PFA (Sigma-aldrich, St. Louis, MO) to each slide for 10 minutes.
- Sections are washed in PBS twice for 30 seconds each time.

Prehybridization

- Excess liquid is wiped from slides and a dako pen (DakoCytomation, CA, USA) is used to draw a delimiting circle around the TMA.

- Sections are placed in the humidified chamber with paper towels dampened with 50% formamide, 5X SSC (Sigma-aldrich, St. Louis, MO) at the bottom. 150 µL of hybridization buffer (50% formamide, 5X sodium chloride-sodium citrate (SSC) buffer, 500µg/µL yeast tRNA, 1X Denhardts solution, all reagents Sigma-aldrich, St. Louis, MO) is added to each slide, nescofilm cut to size is placed on top of each section and the lid of the humidified chamber is sealed with nescofilm. Prehybridisation takes place at the hybridization temperature (melting temperature (T_m) probe-20-25 °C) for 2 hours.

Hybridisation

- Diluted microRNA probes (Exiqon, Vedbaek, Denmark) are warmed to hybridisation temperature prior to application.
- Excess liquid is wiped from slides and they are placed in a new humidified chamber with paper towels dampened with 50% formamide, 5X SSC at the bottom.
- 150 µL of diluted probe is added to each slide, nescofilm cut to size is placed on top of each section and the lid of the humidified chamber is sealed with nescofilm.
- Hybridisation takes place at the hybridisation temperature overnight.

Stringency Wash

- Pre-warm 2X SSC to hybridisation temperature.
- Sections are washed in 2X SSC for 10 minutes with shaking at the hybridisation temperature in a slide mailer.

Immunological Detection

- Blocking buffer is prepared by adding 60 µL of sheep serum (Sigma-aldrich, St. Louis, MO) to 3 mL of 2mg/mL BSA/PBST (2% sheep serum, 2mg/mL BSA/PBST) (Sigma-aldrich, St. Louis, MO). Prepare fresh.
- 200 µL of blocking buffer is applied to sections at room temperature for 1 hour. Sections are covered with nescofilm cut to size.
- Anti-Digoxigenin-AP, Fab fragments (Roche, West Sussex, UK) is diluted 1:1000 in blocking buffer.

- Excess liquid is removed from slides and slides are placed in a new humidified chamber with paper towel dampened with water at the bottom.
- 200 µL of diluted anti-body is applied to each section, covered with nescofilm and the humidified chamber is sealed with nescofilm. Antibody incubation takes place overnight at 4°C.
- Sections are washed 5 times in PBST for 5 minutes each.
- Sections are washed 3 times in AP buffer for 5 minutes each.

Colour Reaction

- NBT/BCIP developer solution (Roche, West Sussex, UK): 3.4µL 100 mg/mL NBT 3.5 µL 50 mg/mL BCIP, 2.4 µL 24 mg/mL levamisole (Sigma-aldrich, St. Louis, MO), 5 µL 10% tween (Sigma-aldrich, St. Louis, MO) and 986 µL AP buffer (0.1 M Tris-HCl, pH 9.5 0.1 M NaCl) (Sigma-aldrich, St. Louis, MO). Prepare fresh.
- Remove excess liquid from slides and place slides in a new humidified chamber with paper towels dampened with water at the bottom.
- Add 200 µL of colour solution to each slide, cover with nescofilm and seal the lid of the humidified chamber with nescofilm.
- The colour reaction can take from 2 hours to 48 hours. The colour reaction can be stopped when a deep blue staining is seen in the sections.
- Wash slides in PBST 3 times for 5 minutes each.
- Liquefy glycerol (DakoCytomation, CA, USA) under hot (50°C) running water for 3 minutes.
- Remove excess liquid from slides, apply glycerol and coverslip.

2.14 References:

Forster, V. (1948) Zwischenmolekulare Engergiewanderung und Fluoreszenz. *Annal of Physics,* 2, 55-75.

Kononen, J., Bubendorf, L., Kallioniemi, A., Barlund, M., Schraml, P., Leighton, S., Torhorst, J., Mihatsch, M. J., Sauter, G. & Kallioniemi, O. P. (1998) Tissue microarrays for high-throughput molecular profiling of tumor specimens. *Nat Med,* 4, 844-7.

Lakowicz, J. (1983) *Principles of Fluoresence Spectroscopy,* New York, Plenum Press.

Lemoine, N. R., Mayall, E. S., Jones, T., Sheer, D., Mcdermid, S., Kendall-Taylor, P. & Wynford-Thomas, D. (1989) Characterisation of human thyroid epithelial cells immortalised in vitro by simian virus 40 DNA transfection. *Br J Cancer,* 60, 897-903.

Livak, K. J. & Schmittgen, T. D. (2001) Analysis of relative gene expression data using real-time quantitative PCR and the 2(-Delta Delta C(T)) Method. *Methods,* 25, 402-8.

Chapter Three

ret/PTC-1 expression alters the immunoprofile of thyroid follicular cells

3.1 Summary

Hashimoto Thyroiditis (H.T) is a destructive autoimmune thyroid condition whose precise molecular pathogenesis remains unclear. ret/PTC-1 is a chimeric transcript which has been described in autoimmune thyroid disease (AITD) and thyroid neoplasia. A common morphological feature in both AITD and thyroid neoplasia is the presence of a florid lymphocytic infiltrate. It is unclear if the presence of ret/PTC-1 facilitates cross-talk between the infiltrate and thyrocytes. Moreover the extent to which ret/PTC-1 may be involved with molecular pathobiology and disease progression remains to be seen. The purpose of this study was to observe the immunogenic effect exposure to H.T and control lymphocyte supernatant would have on normal (Nthy-ori) and ret/PTC-1 (TPC-1) expressing thyroid cell line models.

A 2x2 matrix comprising Nthy-ori and TPC-1 cell lines and H.T. and control lymphocyte supernatant was designed and utilised as follows; activated lymphocytic supernatant from a H.T and normal control were co-cultured with a cell line derived from normal thyroid (Nthy-ori) and also a cell line derived from a papillary thyroid carcinoma that endogenously expresses ret/PTC-1 (TPC-1). The co-cultures were harvested at 0, 6 and 18 hour time points. Gene expression analysis was performed on RNA extracted from thyrocytes using TaqMan® Immune profiling Low-Density Arrays (Applied Biosystems, CA, USA) comprising gene expression markers for ninety three immune related targets plus three endogenous controls.

Stimulation of the normal thyroid cell line model with activated T cell supernatant from the H.T. donor yielded global up-regulation of immune targets when compared with control supernatant stimulation. In particular, a cohort of targets (granzyme B, CD3, CD25, CD152, CD45) associated with cytotoxic cell death; T cell receptor (TCR) and T cell signaling were up-regulated in the normal cell line model. When the ret/PTC-1 expressing thyroid cell line was co-cultured with H.T. lymphocyte supernatant, in comparison to control supernatant stimulation, marginal down-regulation of the same subset of immune targets was seen.

Co-culturing H.T. lymphocyte supernatant with a normal thyroid cell line model leads to over-expression of a subset of targets which could contribute to the pathogenesis of H.T via cytotoxic cell death and TCR signalling. Stimulation of the ret/PTC-1 positive cell line with the same stimulus led to a down-regulated shift in the gene expression pattern of the cohort of immune targets. We hypothesize that ret/PTC-1 activation may dampen immunogenic responses in the thyroid, which could possibly facilitate papillary thyroid carcinoma development.

3.2 Introduction

3.2.1 Autoimmune thyroid disease and Hashimoto Thyroiditis

Autoimmune thyroid disease

Autoimmune thyroid disease (AITD) is a clinically heterogeneous disease including Hashimoto Thyroiditis (H.T.), Graves' disease and primary myxedema. AITD involves genetic and environmental factors and is associated with functional impairment of both the immune system and the target organ.

A prominent feature of AITD is infiltration of the thyroid with lymphocytes and monocytes/macrophages. These cells release an array of pro-inflammatory cytokines which have a pathophysiological role in the production of thyroid autoantibodies and cell mediated cytotoxicity directed towards the thyroid follicular epithelium (Gretzer et al., 2000), resulting in thyroid destruction.

Hashimoto Thyroiditis

In 1912 Dr Harkaru Hashimoto described four patients with a chronic disorder of the thyroid which he termed struma lymphomatosa. The thyroid glands of these patients were characterised by diffuse lymphocytic infiltration, fibrosis, parenchymal atrophy and an eosinophilic change in some of the acinae cells (Hashimoto, 1912). His initial findings are akin to those used today to describe the most common form of autoimmune thyroid disease (AITD). Hashimoto Thyroiditis (H.T.) is a disease characterised by inflammatory infiltrate and diffuse fibrosis which leads to progressive thyrocyte depletion. This loss of thyrocyte capacity results in impaired thyroid hormone production and clinical hypothyroidism.

H.T. is most commonly seen in females, with a peak incidence of forty to sixty years of age. While H.T. is most often diagnosed in a euthyroid patient on the basis of goitre and the presence of autoantibodies, over time this usually progresses to a deficit in thyroid hormone production and the symptoms of hypothyroidism (Bretz and Baker, 2001).

The factors that initiate the autoimmune destruction in H.T. remain to be elucidated as they occur long before the diagnosis is made. In addition, the destruction of thyroid cells occurs slowly, with cell death occurring over years.

Although the pathogenic mechanisms determining thyrocyte destruction in Hashimoto Thyroiditis have been extensively investigated, it is still unclear exactly how this destructive process occurs. While H.T. has classically been associated with thyroid specific B cell immune responses, as determined by antibodies to thyroid peroxidase and thyroglobulin (Arscott and Baker, 1998), thyrocyte-specific cytotoxic T cell responses are also extremely significant.

3.2.2 ret/PTC-1 oncogene

The ret/PTC oncogenes represent activated, rearranged forms of the RET proto-oncogene. RET is essential for the development of the sympathetic, parasympathetic and enteric nervous systems, the kidneys and the testes The RET proto-oncogene resides on chromosome 10q11.2 and codes for a cell membrane receptor tyrosine kinase. The oncogenes are formed as a result of chromosomal inversions within chromosome 10 resulting in the fusion of the tyrosine kinase domain of RET to another donor gene.

The first ret/PTC chimera, named ret/PTC-1, was identified in NIH 3T3 mouse fibroblasts transfected with DNA extracted from human thyroid papillary carcinomas (Fusco et al., 1987). To date, twelve rearranged forms of RET referred to as ret/PTC 1-9, PCM1-ret, ELKS-ret, and RFP-ret have been isolated from sporadic and radiation associated PTCs. The most commonly detected rearrangement is ret/PTC-1 (~ 70%), in which the tyrosine kinase moiety of c-RET is fused to the 5' end of the H4 gene (Grieco et al., 1990). ret/PTC-1 is an intrachromosomal paracentric inversion because both genes participating in the fusion are located on chromosome 10q (Minoletti et al., 1994). The membrane-anchoring and extracellular ligand-binding domains of RET are lost as a result of this fusion, while the 5' sequences that donate their promoters become juxtaposed to the RET tyrosine kinase domain. In their native form, each protein acting as a donor in the generation of a RET chimera, is ubiquitously

expressed. Thus, all ret/PTC oncogenes are i) ubiquitously expressed due to the inheritance of a new 5' promoter, ii) cytoplasmic due to the loss of their transmembrane domains and iii) constitutively activated due to oligomerisation of the oncoprotein and subsequent tyrosine phosphorylation leading to ligand-independent tyrosine kinase activity (Sheils, 2005).

3.2.3 ret/PTC-1 and Hashimoto Thyroiditis

It had previously been thought that ret/PTC-1 activation was exclusive to papillary thyroid carcinomas (PTC). However it has since been demonstrated by our group and others that ret/PTC-1 activation is present in benign conditions such as H.T. (Wirtschafter et al., 1997, Sheils et al., 2000). Wirtschafter and colleagues found mRNA expression for ret/PTC-1 and or ret/PTC-3 in 95% of patients categorized as having H.T. using RT-PCR. Our group (Sheils et al., 2000) analysed twenty seven cases of various forms of non-lymphomatous lymphoid infiltrate of the thyroid using TaqMan® RT-PCR. They found that twenty one cases (78%) were found to express ret/PTC-1, with 18 cases of H.T. being found positive (95%).

The observation that ret/PTC-1 was not restricted to PTC raised the possibility that a) H.T. might represent an early malignant state to which some patients are able to mount an immune response, or b) that ret/PTC-1 occurs in the absence of malignancy and is not specific for PTC.

3.2.4 TaqMan® immune profiling low density arrays

Gene expression analysis provides a view of transcriptional activity and regulation, which can consequently be extremely useful as an indicator of likely protein expression and potential function. Current approaches to measuring gene expression vary from technologies that involve parallel quantification of large numbers of mRNA transcripts in single samples (for example, using gene chip technologies) to very focussed approaches (such as quantitative real-time-PCR (QRT-PCR)) that look at the expression of single genes in multiple samples. Low density array (LDA) technology combines the ability to measure the expression of many genes in a single sample as with the chip array approach, while retaining the sensitivity and quantitative capacity offered by QRT-PCR (Goulter et al., 2006).

TaqMan® immune profiling/inflammation low density arrays (TILDAs) were utilised to analyse the expression of a panel of immune related gene expression markers in ret/PTC-1 positive and negative thyroid cell lines (Nthy-ori and TPC-1) over a time course of co-culture with activated T cell supernatant. The immune profiling low density arrays are preconfigured in 384 well formats, with each of the 8 separate loading ports feeding into 48 separate wells -with 4 well replicates per assay. Each well contains immune related gene expression assays (primers and probes) for one mRNA target. The assays are for profiling gene expression markers known to have implications in immune response. These markers include cytokines, chemokines, growth factors, immune regulators, apoptosis markers, ischemia markers, tissue specific markers, and many other markers, as well as three endogenous controls. Figure 3.1 illustrates and lists the immune profiling gene expression reagents that were preconfigured onto the TILDA.

IL-1a	IL-1a	IL-1b	IL-1b	IL-2	IL-2	IL-3	IL-3	IL-4	IL-4	IL-5	IL-5	IL-6	IL-6	IL-7	IL-7	IL-8	IL-8	IL-9	IL-9	IL-10	IL-10	IL-12p35	IL-12p35
IL-1a	IL-1a	IL-1b	IL-1b	IL-2	IL-2	IL-3	IL-3	IL-4	IL-4	IL-5	IL-5	IL-6	IL-6	IL-7	IL-7	IL-8	IL-8	IL-9	IL-9	IL-10	IL-10	IL-12p35	IL-12p35
IL-12p40	IL-12p40	IL-13	IL-13	IL-15	IL-15	IL-17	IL-17	IL-18	IL-18	Mip-1a	Mip-1a	Mip-3c	Mip-3c	MCP-1	MCP-1	Rantes	Rantes	CCR2	CCR2	CCR4	CCR4	CCR5	CCR5
IL-12p40	IL-12p40	IL-13	IL-13	IL-15	IL-15	IL-17	IL-17	IL-18	IL-18	Mip-1a	Mip-1a	Mip-3c	Mip-3c	MCP-1	MCP-1	Rantes	Rantes	CCR2	CCR2	CCR4	CCR4	CCR5	CCR5
CCR7	CCR7	CXCR3	CXCR3	IP10	IP10	TIA	TIA	CSF-1	CSF-1	CSF-2	CSF-2	CSF-3	CSF-3	Stat3	Stat3	NFKB2	NFKB2	IAB2	IAB2	CD3	CD3	CD4	CD4
CCR7	CCR7	CXCR3	CXCR3	IP10	IP10	TIA	TIA	CSF-1	CSF-1	CSF-2	CSF-2	CSF-3	CSF-3	Stat3	Stat3	NFKB2	NFKB2	IAB2	IAB2	CD3	CD3	CD4	CD4
CD8	CD8	CD19	CD19	CD25	CD25	CD28	CD28	CD38	CD38	CD40	CD40	CD45	CD45	CD68	CD68	CD80	CD80	CD86	CD86	CD152	CD152	CD154	CD154
CD8	CD8	CD19	CD19	CD25	CD25	CD28	CD28	CD38	CD38	CD40	CD40	CD45	CD45	CD68	CD68	CD80	CD80	CD86	CD86	CD152	CD152	CD154	CD154
CD8	CD8	CD19	CD19	CD25	CD25	CD28	CD28	ICOS	ICOS	iNos (Nos2A)	iNos (Nos2A)	BCL2	BCL2	BCL-XL	BCL-XL	BAX	BAX	CD54 (ICAM)	CD54 (ICAM)	CD62E (SELP)	CD62E (SELP)	CD62E (SELE)	CD62E (SELE)
HLA-DRA	HLA-DRA	HLA-DR	HLA-DR	T-bet (TBX21)	T-bet (TBX21)	GITR (TNFRSF18)	GITR (TNFRSF18)	ICOS	ICOS	iNos (Nos2A)	iNos (Nos2A)	BCL2	BCL2	BCL-XL	BCL-XL	BAX	BAX	CD54 (ICAM)	CD54 (ICAM)	CD62E (SELP)	CD62E (SELP)	CD62E (SELE)	CD62E (SELE)
HLA-DRA	HLA-DRA	HLA-DR	HLA-DR	T-bet (TBX21)	T-bet (TBX21)	GITR (TNFRSF18)	GITR (TNFRSF18)	ICOS	ICOS	iNos (Nos2A)	iNos (Nos2A)	BCL2	BCL2	BCL-XL	BCL-XL	BAX	BAX	CD54 (ICAM)	CD54 (ICAM)	CD62E (SELP)	CD62E (SELP)	CD62E (SELE)	CD62E (SELE)
HO-1	HO-1	CCR2	CCR2	REN/IN (REN)	REN/IN (REN)	MEGALIN	MEGALIN	MYH6	MYH6	RPL3L	RPL3L	CYP7A2	CYP7A2	CYP7A1	CYP7A1	IFN-g	IFN-g	PRF1	PRF1	GZMB	GZMB	GNLY	GNLY
HO-1	HO-1	CCR2	CCR2	REN/IN (REN)	REN/IN (REN)	MEGALIN	MEGALIN	MYH6	MYH6	RPL3L	RPL3L	CYP7A2	CYP7A2	CYP7A1	CYP7A1	IFN-g	IFN-g	PRF1	PRF1	GZMB	GZMB	GNLY	GNLY
Fas	Fas	Fasl	Fasl	TGF-b	TGF-b	MADH-3	MADH-3	MADH-7	MADH-7	SXI	SXI	FN	FN	Collagen IV (COL4A5)	Collagen IV (COL4A5)	C3	C3	TNF-a	TNF-a	TNF-b	TNF-b	ACE	ACE
Fas	Fas	Fasl	Fasl	TGF-b	TGF-b	MADH-3	MADH-3	MADH-7	MADH-7	SXI	SXI	FN precursor	FN precursor	Collagen IV (COL4A5)	Collagen IV (COL4A5)	C3	C3	TNF-a	TNF-a	TNF-b	TNF-b	ACE	ACE
Fas	Fas	Fasl	Fasl	TGF-b	TGF-b	MADH-3	MADH-3	MADH-7	MADH-7	SXI	SXI	FN precursor	FN precursor	Collagen IV (COL4A5)	Collagen IV (COL4A5)	C3	C3	TNF-a	TNF-a	TNF-b	TNF-b	ACE	ACE
VEGF A	VEGF A	CD34	CD34	AT1R (AGTR1)	AT1R (AGTR1)	AT2R (AGTR2)	AT2R (AGTR2)	Endothelin (EDN1)	Endothelin (EDN1)	EOE1	EOE1	18S	18S	GAPDH	GAPDH	Beta Actin (ACTB)	Beta Actin (ACTB)	CD71	CD71	GUSB	GUSB	PGK1	PGK1
VEGF A	VEGF A	CD34	CD34	AT1R (AGTR1)	AT1R (AGTR1)	AT2R (AGTR2)	AT2R (AGTR2)	Endothelin (EDN1)	Endothelin (EDN1)	EOE1	EOE1	18S	18S	GAPDH	GAPDH	Beta Actin (ACTB)	Beta Actin (ACTB)	CD71	CD71	GUSB	GUSB	PGK1	PGK1
VEGF A	VEGF A	CD34	CD34	AT1R (AGTR1)	AT1R (AGTR1)	AT2R (AGTR2)	AT2R (AGTR2)	Endothelin (EDN1)	Endothelin (EDN1)	EOE1	EOE1	18S	18S	GAPDH	GAPDH	Beta Actin (ACTB)	Beta Actin (ACTB)	CD71	CD71	GUSB	GUSB	PGK1	PGK1

Figure 3.1 The gene expression reagents that were factory loaded onto the TaqMan® immune profiling LDA

3.3 Aims

The aim of this study was to observe the immune response elicited by a normal thyroid cell line model upon exposure to lymphocytic supernatant derived from a H.T. and normal donor at varying time points using functional genomics. To further evaluate the role of the ret/PTC-1 oncogene in a similar setting, the immune response elicited by an endogenously expressing ret/PTC-1 thyroid cell line stimulated with H.T. and normal lymphocyte supernatant was also observed.

Immunoprofiling TaqMan® low density arrays were used to evaluate the expression profiles of ret/PTC-1 positive and negative thyrocytes over a time course of co-culture with activated T cell supernatant.

3.4 Materials and methods

3.4.1 Samples

Fresh whole blood was withdrawn by a trained phlebotomist (see section 2.4.2) from a donor with Hashimoto Thyroiditis and from a healthy control donor. The H.T. donor was a female who had tested positive for TPO and TMA antibodies, and who had raised TSH and decreased T_4 levels. The control donor was a male with no clinical history of thyroid disease. The same donors were utilised throughout the experiment and approximately 12 mL of blood was withdrawn and used for each co-culture time point analysed (6 and 18 hours). Ethics approval was obtained from the Trinity College Faculty of Health Sciences Research Ethics Committee.

3.4.2 Cell culture

The thyroid cell lines Nthy-ori and TPC-1 were used in this experiment for the purpose of a co-culture procedure with lymphocytic supernatant from the H.T. and normal subjects. Cell lines were grown in a humidified atmosphere containing 5% CO_2 at 37°C in the appropriate plating medium (see section 2.2.2). After passaging and counting cells (see section 2.2.4) from a T75 flask, 2.5 x 10^5 Nthy-ori and TPC-1 cells were plated in a 12 well plate ready for co-culture with activated lymphocytic supernatant from the H.T. and control donors.

3.4.3 Lymphocyte extraction and co-culture

Lymphocytes were isolated from whole blood and activated over three days (see section 2.4.3) in a humidified atmosphere containing 5% CO_2 at 37°C. Approximately 3 x 10^6 T cells were isolated from 12mls of whole blood. For each subject, a 24 well plate was plated with 1 x 10^6 T cells in three wells. In two of these wells, phorbol 12-myristate 13-acetate (PMA) (Sigma-Aldrich, MO, USA) (25ng/ml) was added to activate the T cells. The untreated well served as the control.

After 3 days, the activated T cells were spun down and supernatant collected was added to the wells plated with 2.5 x 10^5 Nthy-ori cells and 2.5 x 10^5 TPC-1 cells for the co-culture procedure. Table 3.1 shows the time points at which RNA was extracted from the thyrocytes and the various co-culture combinations.

0 Hour Time point	6 Hour Time point	18 Hour Time point
Nthy-ori cells	Nthy-ori cells	Nthy-ori
TPC-1 cells	TPC-1 cells	TPC-1
	Nthy-ori cells + H.T lymphocyte supernatant	Nthy-ori cells + H.T lymphocyte supernatant
	TPC-1 cells + H.T lymphocyte supernatant	TPC-1 cells + H.T lymphocyte supernatant
	Nthy-ori cells + control lymphocyte supernatant	Nthy-ori cells + control lymphocyte supernatant
	TPC-1 cells + control lymphocyte supernatant	TPC-1 + control lymphocyte supernatant

Table 3.1 Time points at which RNA was extracted from thyrocytes and the various co-culture combinations

Preliminary work (data not shown) co-culturing both thyroid cell lines with activated lymphocytes for time intervals of 6 and 18 hours resulted in strong aggregation of thyrocytes and lymphocytes impairing isolation of pure populations of thyrocytes for gene expression analysis. This phenomenon was most likely due to HLA incompatibility and/or contact inhibition. Hence, it was decided to extract supernatant from activated T cells for stimulation of thyrocytes to provide a uniform trigger across both ret/PTC-1 positive and negative cell types.

3.4.4 RNA extraction and cDNA archiving

At 0, 6 and 18 hour time points' cells were scrapped (Sigma-aldrich, MO, USA) and centrifuged to remove supernatant. RNA was extracted from the cell pellet using a RNeasy® mini kit (Qiagen Ltd., West Sussex, UK), see section 2.5. RNA quantity was assessed using a NanoDrop® ND-1000 Spectrophotometer (Wilmington, USA), see section 2.8. The RNA was reverse transcribed to single stranded cDNA using a High Capacity cDNA Archive Kit (Applied Biosystems, CA, USA) in 100 µL reactions, see section 2.9. 1.5 µg of RNA from each sample was used in each 100 µL reaction.

3.4.5 TaqMan® low density array (TLDA)

Gene expression analysis was performed using TaqMan® immune-profiling/inflammation Low Density Arrays (TLDAs). The panel of assays included in the TLDA format is designed to simultaneously assess gene expression patterns of multiple targets in a micro-fluidic system. Each Immune profiling TLDA contains lyophilised gene expression reagents (primers and probes [FAM labeled]) in a preconfigured 384 well format and spotted on a microfluidic card. Each of the 8 separate loading ports feeds into 48 separate wells and there are 4 well replicates per assay. One sample (i.e. one of the co-culture combinations and time-points, see table 3.1) was analysed per card. See section 2.10.3.2 for the TILDA loading protocol.

3.4.6 TaqMan® low density array analysis

TLDA cards were analyzed with relative quantification (RQ) documents and RQ manager software for automated data analysis (Applied Biosystems, CA, USA). For analysis purposes, the Nthy-ori time points and the TPC-1 time points were analysed as two separate RQ studies. Expression values were calculated using the comparative threshold cycle (C_T) method. Briefly, this technique uses the formula $2^{-\Delta\Delta C}{}_T$ (Livak and Schmittgen, 2001) to calculate the expression of target genes normalised to a calibrator (un-stimulated N-thy-ori or TPC-1 at 0 hours). Glyceraldehyde-3-phosphate dehydrogenase (GAPDH) was selected as the endogenous control.

The threshold cycle C_T indicates the cycle number by which the amount of amplified target reaches a fixed threshold. The C_T data for all inflammation target genes and GAPDH were used to create ΔC_T values [ΔC_T=C_T (target gene)-C_T(GAPDH)]. $\Delta\Delta C_T$ values were calculated by subtracting the calibrator (Nthy-ori at 0 hrs or TPC-1 at 0 hrs) from the ΔC_T value of each target. Relative quantification (RQ) values were calculated using the equation $2^{-\Delta\Delta C}{}_{T.}$

3.5 Results

TaqMan® low density array immunoprofiling data was analyzed using SDS 2.1 software (Applied Biosystems, CA, USA). Independent RQ studies were carried out for each cell line. In both cell lines (Nthy-ori and TPC-1), the 6 hour time point displayed peak expression differentials compared with T_0 and between different stimuli (Normal and H.T.).

3.5.1 Nthy-ori co-culture gene expression patterns

In the normal thyroid cell line model (Nthy-ori), exposure to H.T. lymphocyte supernatant led to global up-regulation of ninety two inflammation targets (with the exception of one, Heme oxygenase-1 where expression between each cohort was equivocal) in comparison to stimulation with normal control lymphocytes. The Nthy-ori co-culture heat map (figure 3.2) illustrates expression of the ninety three immune related targets assayed plus endogenous control at each co-culture combination and time point analysed. The heat map demonstrates increased expression levels of targets exposed to H.T. lymphocyte supernatant compared to control at the 6 hour time point. It also demonstrates a reduced level of gene expression in Nthy-ori cells that were not exposed to stimulus at the 18 and 6 hour time points.

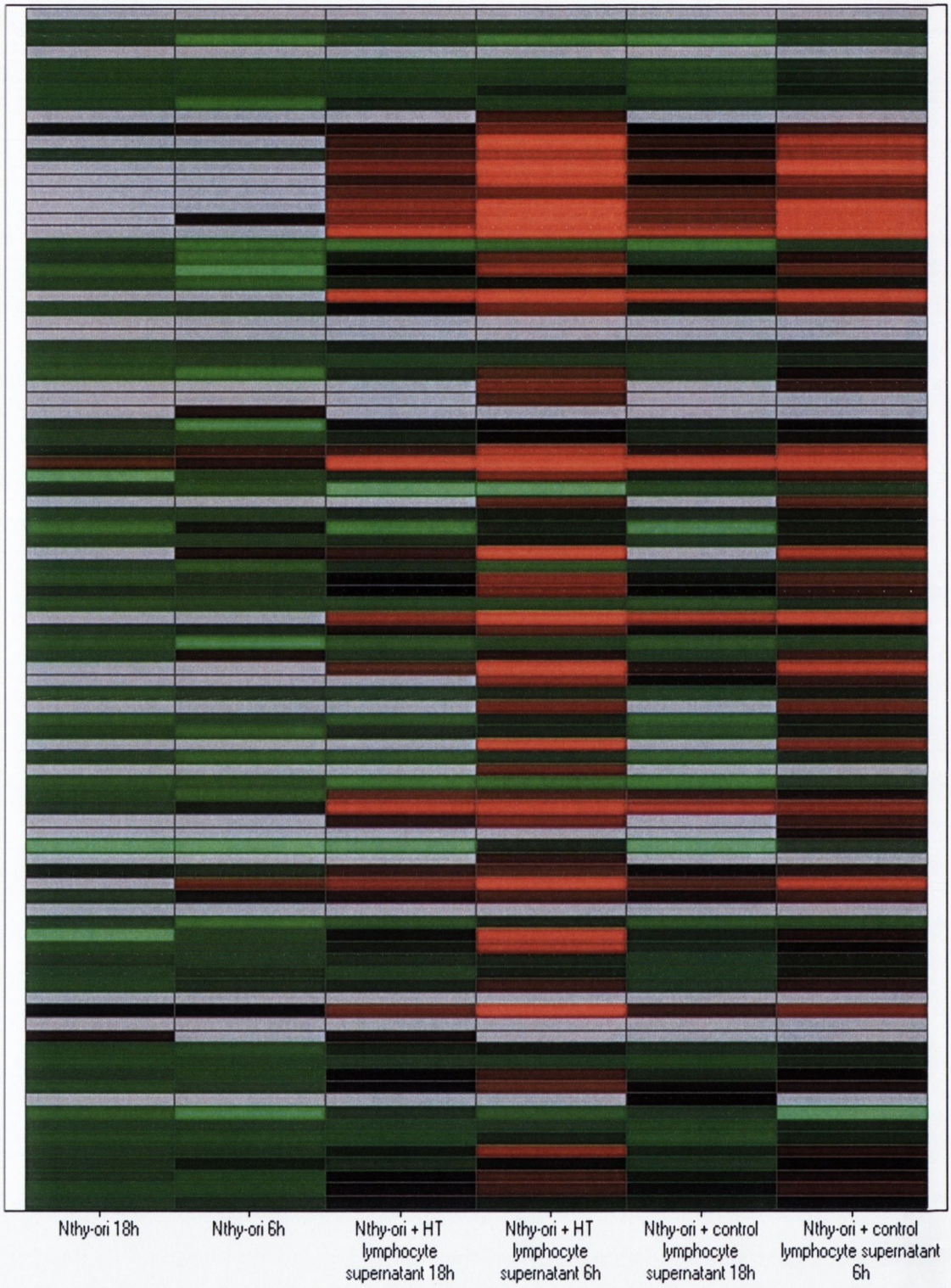

Figure 3.2 Heat map of Nthy-ori co-culture. This heat map represents all 93 immune targets assayed (plus endogenous control) at each time point/co-culture combination that RNA was extracted at. Relative quantification (RQ) values for each target were used to create the heat map. Red denotes genes with a relative increased expression while green denotes genes with relative decreased expression

Figure 3.3 displays a subset of targets which were over-expressed in the normal thyroid cell line model (Nthy-ori) when exposed to H.T. lymphocytic supernatant compared to control at the 6 hour time point. They included granzyme B (GZMB), a known effector in cytotoxic cell death, CD3, CD25, CD152 and CD45 all of which are involved with the T cell receptor (TCR) or signaling in the T cell.

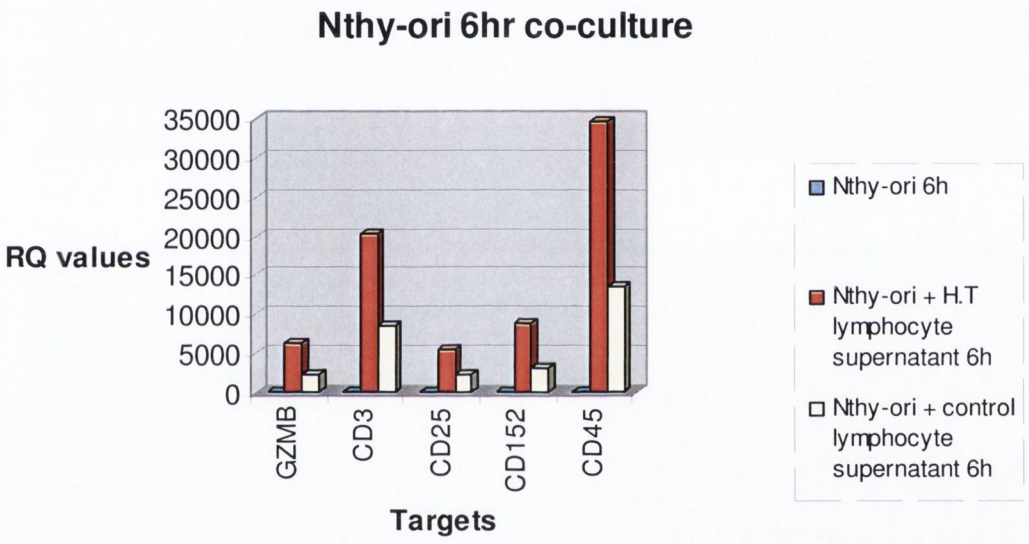

Figure 3.3 Nthy-ori 6 hour co-culture. Figure 3.3 displays targets that were up-regulated in ret/PTC-1 negative thyrocytes when co-cultured with Hashimoto Thyroiditis lymphocyte supernatant in comparison to exposure to control lymphocytic supernatant after a 6 hour interval

Figure 3.4 displays the gene expression level of Fas ligand (FasL) (3.4.1), CD28 (3.4.2) and granulocyte colony stimulating factor (G-CSF) (3.4.3) in the Nthy-ori co-culture. These targets also displayed increased expression levels in the normal thyroid cell line model which was exposed to H.T. lymphocyte supernatant when compared to exposure to control supernatant.

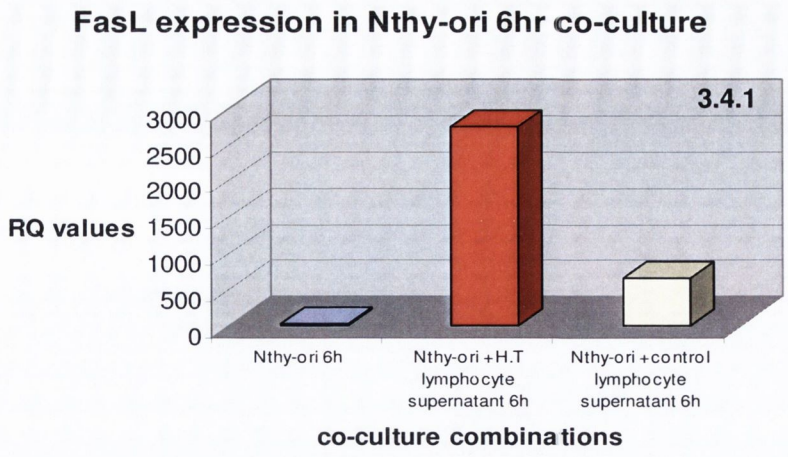

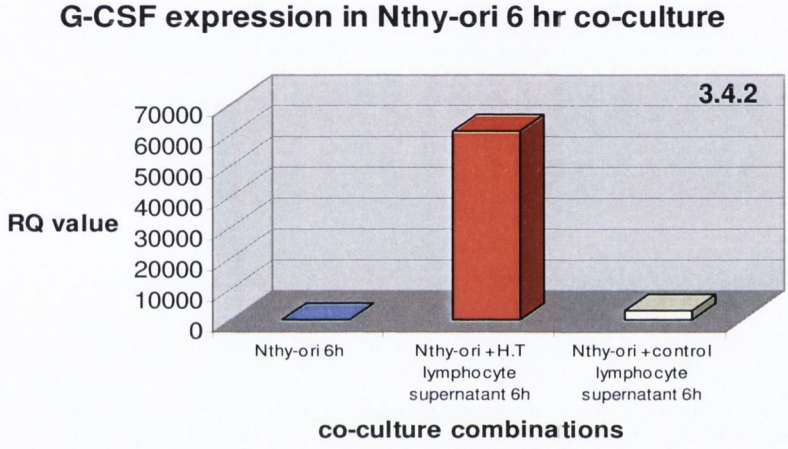

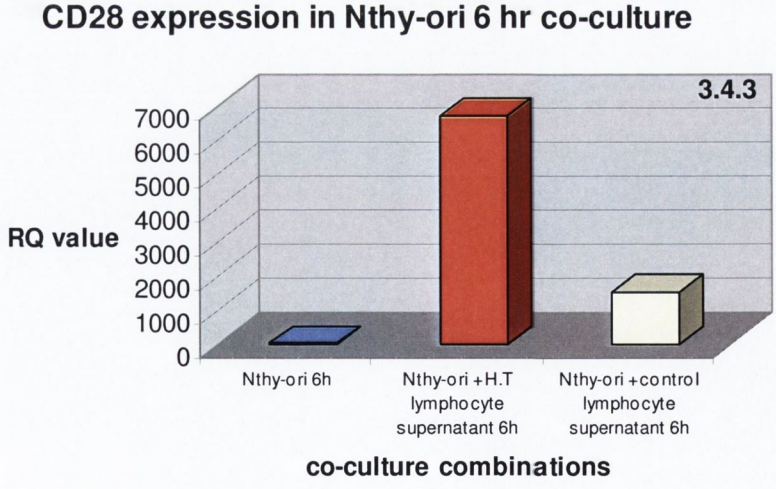

Figure 3.4 Expression levels for FasL, CD28 and G-CSF. Figure 3.4 displays gene expression levels for FasL (3.4.1), CD28 (3.4.2) and G-CSF (3.4.3) expression in the Nthy-ori 6 hour co-culture. Each target is over-expressed in the normal thyroid cell line when exposed to Hashimoto Thyroiditis lymphocyte supernatant in comparison to exposure to control lymphocyte supernatant

3.5.2 TPC-1 co-culture gene expression patterns

In the ret/PTC-1 harboring cell line, approximately forty percent of targets (with a relative quantification (RQ) value >100) were down-regulated when stimulated with H.T. lymphocyte supernatant in comparison to exposure with control supernatant. The TPC-1 co-culture heat map (figure 3.5) illustrates the reduction in gene expression at the TPC-1 18 and 6 hour time points where there is no exposure to supernatant.

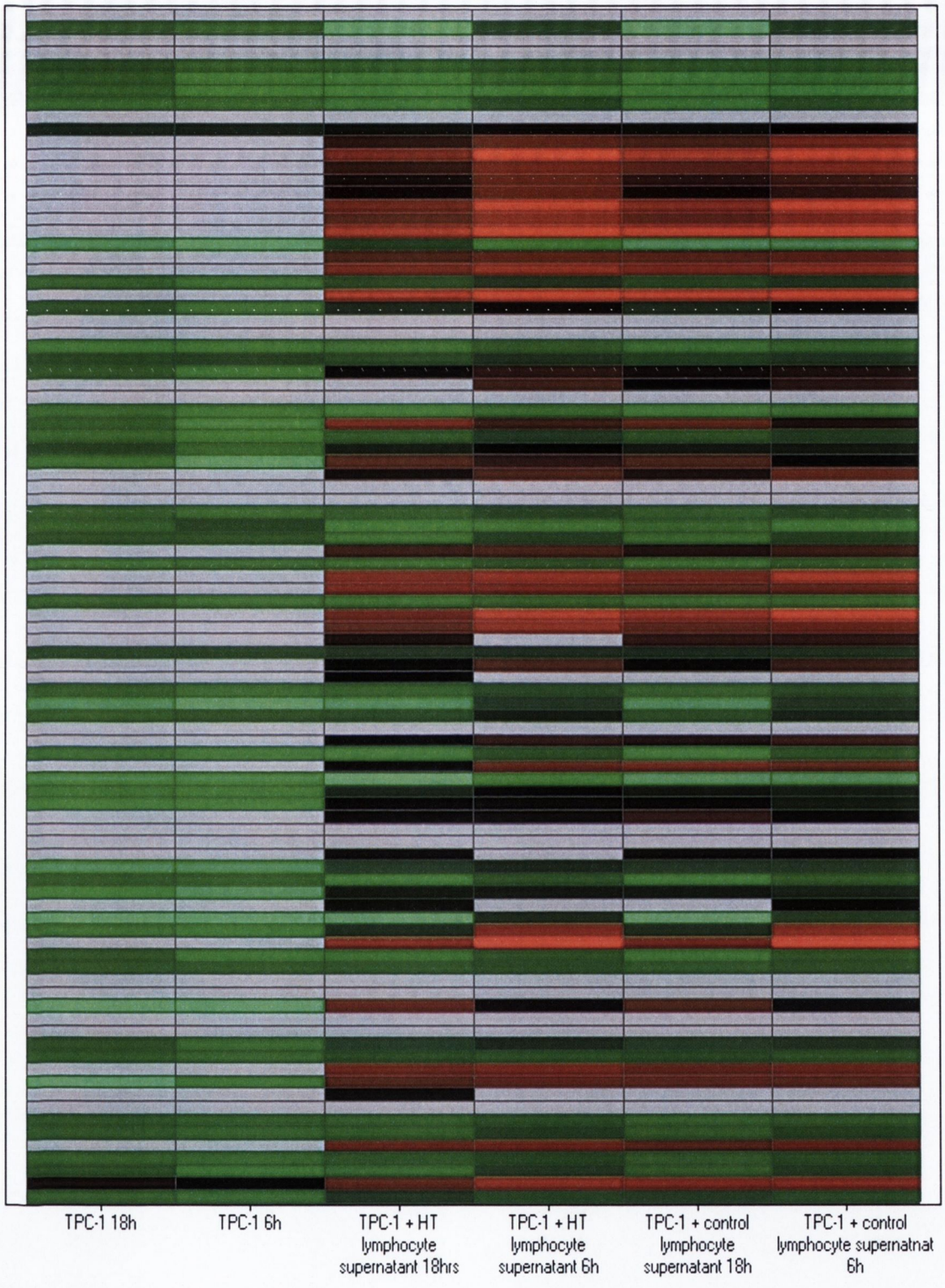

Figure 3.5 Heat map of TPC-1 co-culture. This heat map represents all 93 immune targets assayed (plus endogenous control) at each time point/co-culture combination that RNA was extracted at. Relative quantification (RQ) values for each target were used to create the heat map. Red denotes genes with a relative increased expression while green denotes genes with relative decreased expression

Figure 3.6 represents the gene expression pattern for granzyme B, CD3, CD25, CD152 and CD45 in the ret/PTC-1 positive cell line (TPC-1). As previously stated, figure 3.3 demonstrates the over-expression of these targets in the normal thyroid cell line model when exposed to H.T. lymphocyte supernatant in comparison to stimulation with control supernatant. However figure 3.6 illustrates that when a ret/PTC-1 positive thyroid cell line model is co-cultured with H.T. supernatant; in comparison to co-culture with control supernatant, this group of targets are marginally down-regulated. This illustrates an important gene expression pattern, one that demonstrates a shift in expression of the cohort of targets when ret/PTC-1 activation is introduced.

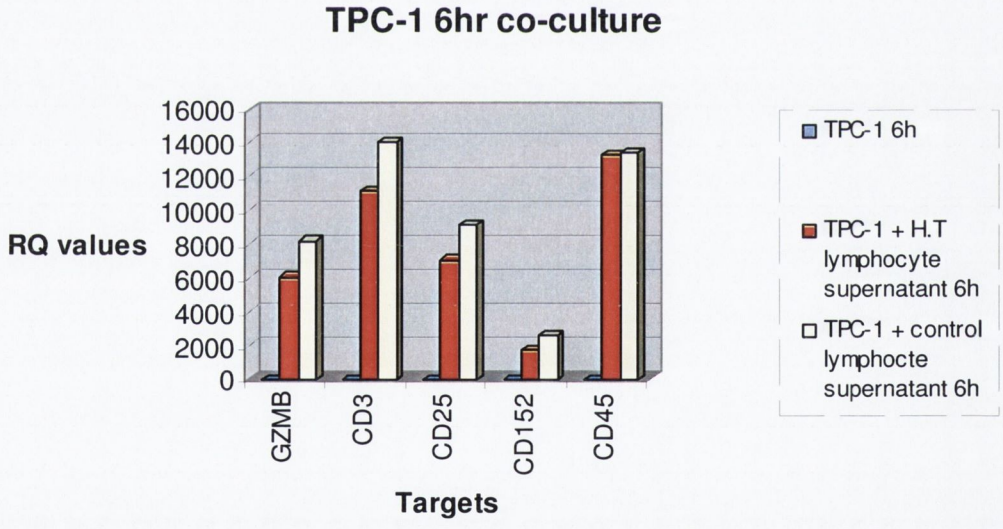

Figure 3.6 TPC-1 6 hour co-culture. Figure 3.6 displays how targets that were up-regulated in ret/PTC-1 negative thyrocytes (figure 3.3) are down-regulated in ret/PTC-1 positive thyrocytes when co-cultured with Hashimoto Thyroiditis lymphocyte supernatant in comparison to exposure to control lymphocytic supernatant after a 6 hour interval

It is noteworthy that, in figures 3.3 and 3.6, the cell line models that were not exposed to stimulus i.e. Nthy-ori at 6h and TPC-1 at 6h did not show any level of gene expression for the targets displayed. Relative quantification (RQ) values representing all co-culture combinations/timepoints for each assay have been normalized to a house keeping gene (Glyceraldehyde-3-phosphate dehydrogenase (GAPDH)) and then normalized to a calibrator sample (un-stimulated N-thy-ori or TPC-1 at 0 hours) according to the $2^{-\Delta\Delta C}{}_T$ comparative threshold cycle (C_T) method (Livak and Schmittgen, 2001). From this we can interpret that the gene expression patterns detected are a result of stimulation with H.T. or control lymphocytic supernatant and also the presence or absence of the ret/PTC-1 oncogene.

3.6 Discussion

Although the pathogenic mechanisms determining thyrocyte destruction in Hashimoto Thyroiditis have been extensively investigated, it is still unclear exactly how this destructive process occurs.

Among oncogenes studied in the setting of thyroid neoplasia, activated c-RET and ret/PTC-1 in particular have been found to associate with papillary thyroid carcinoma (PTC) and Hashimoto Thyroiditis (H.T.). Its presence has also been noted in lesions which have an affiliated inflammatory infiltrate. However, despite extensive studies into the prevalence and sequelae of the presence of activated ret/PTC-1 it remains unclear if ret/PTC-1 activation orchestrates, maintains or modulates the inflammatory response so often observed as a feature of ret/PTC-1 positive lesions.

The aim of this project was to observe the immune response elicited by a normal thyroid cell line model upon exposure to lymphocytic supernatant derived from a H.T. and normal donor at varying time points. To further evaluate the role of the ret/PTC-1 oncogene in a similar setting, we also observed the immune response elicited by an endogenously expressing ret/PTC-1 thyroid cell line stimulated with H.T. and normal lymphocyte supernatant. As this was a proof of principle experiment it was decided to analyse the gene expression of a large panel of immune related targets (93 in total), at different co-culture time-points on two subjects. The use of pooled lymphocytic supernatants was not employed as it was felt that pooled extracts may hide biological variance. An endogenously expressing ret/PTC-1 cell line was used in this experiment rather than transfecting a normal thyroid cell line with RET as it was felt that in the setting of this experiment, it was more biologically plausible to compare a normal thyroid cell line with a thyroid cancer cell line which natively expresses the oncogene. It was also decided to utilise supernatant from activated T lymphocytes in each group to stimulate the cell line models to ensure assessment of gene expression accurately reflected the repertoire of the epithelial cells alone.

3.6.1 Nthy-ori gene expression pattern

When thyroid cells from the Nthy-ori cell line model were exposed to Hashimoto Thyroiditis (H.T.) lymphocyte supernatant, a universal up-regulation of all immune targets was observed when compared to exposure to control lymphocyte supernatant (figure 3.2) (with the exception of Heme oxygenase-1 where expression between each cohort was equivocal).

However, within the global increased expression on stimulation by H.T. supernatant, some clusters of genes appeared to be particularly interesting. They included subsets of targets which may contribute to the pathogenesis of H.T. via cell mediated cytotoxic cell death and TCR signalling.

Thyrocyte specific CD8 cytotoxic T cell responses are a pivotal factor in the tissue specific destruction that is seen in H.T. Cell mediated cytotoxicity is initiated through two different mechanisms 1) effector cell expression of death ligands presented to target cells and 2) effector cell release of exocytic granules containing perforin and granzyme B (Bretz and Baker, 2001).

Over expression of both Fas ligand (FasL) and granzyme B were seen when the normal thyroid cell line model was stimulated with H.T. lymphocyte supernatant compared to control supernatant.

Granzyme B is a serine protease that plays an important role in inducing apoptotic changes in target cells during granule exocytosis-induced cytotoxicity (Casciola-Rosen et al., 1999) while FasL induces apoptosis by binding to and activating its receptors, which in turn bind to adaptor molecules that activate the caspase family. Interestingly, until recently it had been thought that Fas ligand (FasL) expression had been restricted, occurring only on activated T cells and a few other "immune privileged" tissues such as the cornea and testis (Arscott and Baker, 1998). However many groups have found FasL expression in thyrocytes (Stassi et al., 1999, Giordano et al., 1997, Kie et al., 2001, Chen et al., 2004, Mitsiades et al., 1998). Leading some to suggest that the thyroid may act as an immune privileged site.

Increased expression of these cytotoxic agents in the normal thyroid cell line model exposed to H.T. lymphocyte supernatant suggests that these targets are specifically involved in cytotoxic cell death in H.T. leading to apoptosis of thyroid follicular epithelial cells and the resultant destruction of thyroid tissue that is indicative of H.T.

Moreover, targets involved with the T cell receptor (TCR) and T cell signalling were also up-regulated which may be responsible for exacerbation of the destructive process seen in H.T. These targets included CD3, CD25, CD28, CD152 and CD45.

T cell activation requires not only the generation of an initial signal through interaction of the antigenic peptide with the TCR-CD3 complex but also a subsequent antigen non-specific co-stimulatory signal, provided primarily by the interaction of CD28 on T cells with B7 molecules (Simmonds and Gough, 2004). Whereas the binding of B7 to CD28 on T cells co-stimulates T cell activation, the presence of CD152, which has a higher affinity for B7, down-regulates T cell activation by competing for the binding of B7 to CD28 (Tomer and Davies, 2003). As CD152 – CD28 molecules control the rate of T cell activation and to a large extent the fate of the immune response, they are likely to play a major role in the development of autoimmune disease (Simmonds and Gough, 2004). CD45 is a receptor linked protein tyrosine phosphatase that is expressed on leucocytes, and plays a crucial role in the function of these cells (Altin and Sloan, 1997). It is well established that CD45 is a positive regulator of the Src family of protein tyrosine kinases (PTKs) that mediate TCR signalling. It seems that CD45 maintains PTKs in a dephosphorylated state ready to participate in signal transduction upon subsequent TCR ligation (Mustelin et al., 2004).

It is interesting to hypothesize that these over-expressed TCR and T cell signalling associated targets may be involved in the disease pathogenesis seen in H.T. via dysregulation of T cell signalling and control of T cell activation resulting in the over-activity of immune responses typically seen in autoimmune diseases such as H.T.

Finally, a large fold change difference (RQ value) was observed for granulocyte colony stimulating factor (G-CSF) when comparing thyrocytes exposed to H.T. and

control lymphocyte supernatant in the normal cell line model (figure 3.4.2). G-CSF is the major regulator of granulocyte production, however also exerts other effects including the activation of mature leukocytes and immune cell functions (Vial and Descotes, 1995). In 1996 de Luis and Romero (de Luis and Romero, 1996) reported a case of clinical hypothyroidism during treatment with G-CSF (filgrastim) in a breast cancer patient with previously normal thyroid function and no pre-existing thyroid antibodies. Similar results have been observed with administration of granulocyte-macrophage colony stimulating factor (GM-CSF), which is comparable to G-CSF. In a study of twenty five cancer patients with previously normal thyroid function receiving GM-CSF, two patients developed reversible hypothyroidism (Hoekman et al., 1991).

G-CSF elicits an effect on the immune system via its role in monocyte/macrophage activation, neutrophil stimulation and regulation of inflammatory cytokine/chemokine production. One cause of tissue damage in the thyroid is infiltration by lymphocytes and monocytes/macrophages. The over-expression of G-CSF in thyrocytes exposed to H.T. lymphocyte supernatant suggests that G-CSF may play a role in promoting the inflammatory aggravation and subsequent tissue destruction seen in autoimmune thyroid diseases such as H.T.

3.6.2 TPC-1 gene expression pattern

To further evaluate the expression and role of the ret/PTC-1 oncogene in a similar context, the co-culture conditions were reapplied to another thyroid cell line expressing this oncogene (TPC-1 cell line).

As previously stated, the Nthy-ori co-culture displayed up-regulation of a discrete subset of immune targets which may contribute to the disease pathogenesis seen in H.T. These targets included granzyme B, CD3, CD25, CD152 and CD45; targets which are involved in apoptosis, T cell signalling and T cell activation. In the ret/PTC-1 cell line model, these five targets showed a shift in gene expression pattern whereby they were down-regulated in ret/PTC-1 positive thyrocytes exposed to H.T. supernatant when compared to exposure to control supernatant. There has been much

speculation surrounding the role that ret/PTC-1 plays in the inflammatory response in RET positive lesions. In this study it has been shown that exposure to supernatant derived from H.T. peripheral blood mononuclear cells (PBMCs) results in the normal thyroid cell line model and the ret/PTC-1 positive thyroid cell line model producing different immunogenic patterns. Perhaps the expression of the ret/PTC-1 oncogene in the TPC-1 cell line acts to down-regulate apoptotic and T cell signalling targets, resulting in this change in gene expression pattern that we have seen. As a result of this expression pattern in the stimulated ret/PTC-1 expressing cell line, it is interesting to speculate that ret/PTC-1 activation in AITD may dampen the immune response and facilitate tumour growth and development.

ret/PTC has been shown to function in the MAPK (mitogen-activated protein kinase) signalling cascade by binding adaptor proteins such as growth receptor-bound protein 2 (GRB2), which in turn activate RAS. RAS activates AF kinases such as BRAF and its downstream signalling cascade including MEK (MAP kinase) and ERK (extracellular signal-regulated kinases or MAPK). Activated ERK1 and ERK2 translocate to the nucleus where they activate transcription factors such as ELK-1 and STAT3. Hwang and colleagues (Hwang et al., 2003) have demonstrated that ret/PTC associates with and activates STAT3, while microarray analysis has demonstrated up-regulation of STAT3 in ret/PTC-3 thyrocytes (Puxeddu et al., 2005). Furthermore STAT3 has been shown to contribute to malignancy by inactivating intrinsic and extrinsic apoptotic pathways (Barre et al., 2007). ret/PTC activation and the resultant STAT3 transcription factor activation via the MAPK signalling cascade may be involved in impeding apoptosis in thyrocytes by down-regulation of granzyme B. Although a link between STAT3 activation and dysregulation of apoptotic mechanisms via granzyme B down-regulation cannot be proven from this study alone it is interesting to speculate that STAT3 activation through ret/PTC MAPK signalling may contribute to malignancy in the setting of thyroid neoplasia.

3.7 Conclusions

This study has highlighted a set of immune related gene expression markers which were shown to be up-regulated in a normal thyroid cell line model upon exposure to H.T lymphocyte supernatant when compared to control. These targets included genes which could plausibly be in involved in exacerbating the disease pathogenesis seen in H.T. To further ascertain the extent to which the oncogene ret/PTC-1 is involved in immunogenic responses in AITD, a ret/PTC-1 positive thyroid cell line model employing the same co-culture methods was used. It was found that when this cell line was stimulated with H.T. supernatant, a shift in the immunogenic pattern was seen, whereby the same set of immune markers were down-regulated compared to control supernatant stimulation. One can hypothesise that ret/PTC-1 expression in the TPC-1 thyroid cell line may lead to down-regulation of these immune targets. Consequently one can speculate that ret/PTC-1 activation in the setting of AITD may lead to under-expression of these immune targets, resulting in tumour growth and development. Nonetheless, this study, utilising TaqMan® low density immune arrays, gives further insight into the molecular immunogenesis of H.T. and some of the targets that may be involved in exacerbating disease pathogenesis.

3.8 References:

Altin, J. G. & Sloan, E. K. (1997) The role of CD45 and CD45-associated molecules in T cell activation. *Immunol Cell Biol,* 75, 430-45.

Arscott, P. L. & Baker, J. R., Jr. (1998) Apoptosis and thyroiditis. *Clin Immunol Immunopathol,* 87, 207-17.

Barre, B., Vigneron, A., Perkins, N., Roninson, I. B., Gamelin, E. & Coqueret, O. (2007) The STAT3 oncogene as a predictive marker of drug resistance. *Trends Mol Med,* 13, 4-11.

Bretz, J. D. & Baker, J. R., Jr. (2001) Apoptosis and autoimmune thyroid disease: following a TRAIL to thyroid destruction? *Clin Endocrinol (Oxf),* 55, 1-11.

Casciola-Rosen, L., Andrade, F., Ulanet, D., Wong, W. B. & Rosen, A. (1999) Cleavage by granzyme B is strongly predictive of autoantigen status: implications for initiation of autoimmunity. *J Exp Med,* 190, 815-26.

Chen, S., Fazle Akbar, S. M., Zhen, Z., Luo, Y., Deng, L., Huang, H., Chen, L. & Li, W. (2004) Analysis of the expression of Fas, FasL and Bcl-2 in the pathogenesis of autoimmune thyroid disorders. *Cell Mol Immunol,* 1, 224-8.

De Luis, D. A. & Romero, E. (1996) Reversible thyroid dysfunction with filgrastim. *Lancet,* 348, 1595-6.

Fusco, A., Grieco, M., Santoro, M., Berlingieri, M. T., Pilotti, S., Pierotti, M. A., Della Porta, G. & Vecchio, G. (1987) A new oncogene in human thyroid papillary carcinomas and their lymph-nodal metastases. *Nature,* 328, 170-2.

Giordano, C., Stassi, G., De Maria, R., Todaro, M., Richiusa, P., Papoff, G., Ruberti, G., Bagnasco, M., Testi, R. & Galluzzo, A. (1997) Potential involvement of Fas and its ligand in the pathogenesis of Hashimoto's thyroiditis. *Science,* 275, 960-3.

Goulter, A. B., Harmer, D. W. & Clark, K. L. (2006) Evaluation of low density array technology for quantitative parallel measurement of multiple genes in human tissue. *BMC Genomics,* 7, 34.

Gretzer, C., Thomsen, P., Jansson, S. & Nilsson, M. (2000) Co-culture of human monocytes and thyrocytes in bicameral chamber: monocyte-derived IL-1alpha impairs the thyroid epithelial barrier. *Cytokine,* 12, 32-40.

Grieco, M., Santoro, M., Berlingieri, M. T., Melillo, R. M., Donghi, R., Bongarzone, I., Pierotti, M. A., Della Porta, G., Fusco, A. & Vecchio, G. (1990) PTC is a novel rearranged form of the ret proto-oncogene and is frequently detected in vivo in human thyroid papillary carcinomas. *Cell,* 60, 557-63.

Hashimoto, H. (1912) Zur kerrtriss der lymphomatosen veranderung der schilddruse. *Arch Klin Chir,* 97, 219.

Hoekman, K., Von Blomberg-Van Der Flier, B. M., Wagstaff, J., Drexhage, H. A. & Pinedo, H. M. (1991) Reversible thyroid dysfunction during treatment with GM-CSF. *Lancet,* 338, 541-2.

Hwang, J. H., Kim, D. W., Suh, J. M., Kim, H., Song, J. H., Hwang, E. S., Park, K. C., Chung, H. K., Kim, J. M., Lee, T. H., Yu, D. Y. & Shong, M. (2003) Activation of signal transducer and activator of transcription 3 by oncogenic RET/PTC (rearranged in transformation/papillary thyroid carcinoma) tyrosine kinase: roles in specific gene regulation and cellular transformation. *Mol Endocrinol,* 17, 1155-66.

Kie, J. H., Cho, M. S. & Yang, W. I. (2001) Expression of CD40 and apoptosis related molecules in autoimmune thyroid diseases. *Yonsei Med J,* 42, 488-96.

Livak, K. J. & Schmittgen, T. D. (2001) Analysis of relative gene expression data using real-time quantitative PCR and the 2(-Delta Delta C(T)) Method. *Methods,* 25, 402-8.

Minoletti, F., Butti, M. G., Coronelli, S., Miozzo, M., Sozzi, G., Pilotti, S., Tunnacliffe, A., Pierotti, M. A. & Bongarzone, I. (1994) The two genes generating RET/PTC3 are localized in chromosomal band 10q11.2. *Genes Chromosomes Cancer,* 11, 51-7.

Mitsiades, N., Poulaki, V., Kotoula, V., Mastorakos, G., Tseleni-Balafouta, S., Koutras, D. A. & Tsokos, M. (1998) Fas/Fas ligand up-regulation and Bcl-2 down-regulation may be significant in the pathogenesis of Hashimoto's thyroiditis. *J Clin Endocrinol Metab,* 83, 2199-203.

Mustelin, T., Alonso, A., Bottini, N., Huynh, H., Rahmouni, S., Nika, K., Louis-Dit-Sully, C., Tautz, L., Togo, S. H., Bruckner, S., Mena-Duran, A. V. & Al-Khouri, A. M. (2004) Protein tyrosine phosphatases in T cell physiology. *Mol Immunol,* 41, 687-700.

Puxeddu, E., Knauf, J. A., Sartor, M. A., Mitsutake, N., Smith, E. P., Medvedovic, M., Tomlinson, C. R., Moretti, S. & Fagin, J. A. (2005) RET/PTC-induced gene expression in thyroid PCCL3 cells reveals early activation of genes involved in regulation of the immune response. *Endocr Relat Cancer,* 12, 319-34.

Sheils, O. (2005) Molecular classification and biomarker discovery in papillary thyroid carcinoma. *Expert Rev Mol Diagn,* 5, 927-46.

Sheils, O. M., O'eary J, J., Uhlmann, V., Lattich, K. & Sweeney, E. C. (2000) ret/PTC-1 Activation in Hashimoto Thyroiditis. *Int J Surg Pathol,* 8, 185-189.

Simmonds, M. J. & Gough, S. C. (2004) Genetic insights into disease mechanisms of autoimmunity. *Br Med Bull,* 71, 93-113.

Stassi, G., Todaro, M., Bucchieri, F., Stoppacciaro, A., Farina, F., Zummo, G., Testi, R. & De Maria, R. (1999) Fas/Fas ligand-driven T cell apoptosis as a

consequence of ineffective thyroid immunoprivilege in Hashimoto's thyroiditis. *J Immunol,* 162, 263-7.

Tomer, Y. & Davies, T. F. (2003) Searching for the autoimmune thyroid disease susceptibility genes: from gene mapping to gene function. *Endocr Rev,* 24, 694-717.

Vial, T. & Descotes, J. (1995) Immune-mediated side-effects of cytokines in humans. *Toxicology,* 105, 31-57.

Wirtschafter, A., Schmidt, R., Rosen, D., Kundu, N., Santoro, M., Fusco, A., Multhaupt, H., Atkins, J. P., Rosen, M. R., Keane, W. M. & Rothstein, J. L. (1997) Expression of the RET/PTC fusion gene as a marker for papillary carcinoma in Hashimoto's thyroiditis. *Laryngoscope,* 107, 95-100.

Chapter Four

Expression profiles in archival thyroid carcinoma lesions using pre-amplification Q-RT-PCR

4.1 Summary

Thyroid carcinoma is the most frequently occurring endocrine malignancy, and although it may be considered a relatively rare cancer, world wide thyroid cancer incidence rates are increasing year after year. Thyroid nodules are a common entity and distinguishing benign thyroid specimens from malignant can be problematic. Follicular lesions in thyroid carcinoma can also frequently cause difficulties from a diagnostic perspective. Robust molecular markers would greatly aid in the diagnosis of malignant thyroid lesions.

The purpose of this study was to interrogate a cohort of archival thyroid lesions (n=195) using gene expression analysis of a panel of markers to assess their use as adjunctive markers in the diagnosis of thyroid malignancy. Laser capture microdissection (LCM) was used to procure pure cell populations for extraction. In addition a novel, multiplex pre-amplification technique was used to facilitate analysis of a panel of ten targets including RAB23, MT1K, MT1X, CSNK1G2, KRAS, TGFβ1, IRF3, CD74, HLA-DMA and HLA-DQB1 plus one endogenous control. Expression profiles for each target were generated using TaqMan® Real –Time PCR.

Nine out of the ten targets analysed were found to differentially discriminate (p value < 0.05) benign from malignant and between malignant phenotypes in thyroid disease. This panel of molecular markers may have utility for broader use in the setting of fine-needle aspiration (FNA) cytology and could improve the definitive diagnosis of certain categories of thyroid malignancy.

4.2 Introduction

Thyroid specimens, taken from partial or complete thyroidectomies are frequently encountered by the practicing pathologist, reflecting the fact that nodules of the thyroid gland are very common. It is estimated that as many as four to seven percent of the adult population has a palpable thyroid enlargement, and up to ten times this number of individuals have subclinical nodules that can be detected by ultrasound or at autopsy (Faquin, 2008).

The histological classification of thyroid epithelial tumours is the current standard to distinguish benign from malignant thyroid tumours and to assign specific tumours into histologic subtypes. The WHO classification has recently been revised (Chan, 2004) to distinguish thyroid tumour types. For many of these tumour types the histological criteria are subjective and thus difficult to implement (Eszlinger et al., 2008). The application of reliable molecular markers of thyroid malignancy, along with fine needle aspiration cytology could help to definitively define and diagnose malignant thyroid lesions.

4.2.1 The follicular aspect

Well differentiated thyroid tumours of follicular cell origin are sub-divided into follicular adenoma (FA), follicular thyroid carcinoma (FTC) and papillary thyroid carcinoma (PTC) (Liu et al., 2006). Approximately eighty percent of thyroid carcinomas are papillary carcinomas (Lote et al 1980). Papillary thyroid carcinoma is defined as a malignant tumour showing evidence of follicular differentiation and characterised by distinctive nuclear features (Chan, 2004). Because papillary structures may occasionally be found in follicular adenoma and follicular thyroid carcinoma, the diagnosis of papillary thyroid carcinoma ultimately depends on its nuclear features i.e. ground glass appearance, irregularity of nuclear contours, grooves and pseudo-inclusions (Schmid and Farid, 2006).The diagnosis of papillary thyroid carcinoma does not simply depend on the presence of these nuclear features but the extent to which they are present in "a significant proportion of the neoplasm" (Chan, 2004). The lack of appreciation of the diagnostic features of a papillary thyroid carcinoma, particularly in encapsulated tumours, may either lead to the misdiagnosis

of a follicular thyroid carcinoma or that of a benign follicular adenoma (Schmid and Farid, 2006).

The follicular variant of papillary thyroid carcinoma (FVPTC) is found in 9% to 22.5% of patients with a papillary thyroid carcinoma (Liu et al., 2006). Follicular variant of papillary thyroid carcinoma is composed predominantly by follicles, which are lined by cells that have the nuclear features of papillary thyroid carcinoma (Rosai, 1992). Follicular variant of papillary thyroid carcinoma may cause (if the nuclear features of papillary thyroid carcinoma are insufficiently appreciated) severe problems in discrimination from follicular thyroid carcinoma or follicular adenoma. Characteristically follicular adenoma is encapsulated, cellular and has a relatively uniform follicular pattern (Baloch, 2005). Follicular thyroid carcinoma is unifocal, encapsulated and metastasizes directly to distant organs (Liu et al., 2006). Microscopically follicular thyroid carcinoma most often has a microfollicular pattern and may resemble a cellular follicular adenoma (Baloch, 2005).

4.2.2 Patient management

Because cytology cannot always accurately discriminate between benign and malignant follicular thyroid tumours, patients displaying a follicular thyroid lesion are advised to undergo surgery, usually a hemithyroidectomy, to verify an accurate diagnosis and to decide additional treatment. Those who ultimately reveal a carcinoma are generally advised to undergo a second operation, a complete thyroidectomy (Barden et al., 2003). However, only ten to twenty percent of these undetermined nodules are malignant on histology (Baloch, 2005). Patient management would be greatly enhanced by additional diagnostic tests. Moreover, unnecessary surgeries, patient distress, post-operative complications and health care costs would be reduced. There is a role for accurate molecular markers that can further classify problematic groups in thyroid malignancy.

4.2.3 Fine needle aspiration (FNA)

As previously mentioned, thyroid nodules are extremely common, with a lifetime risk of developing a clinically significant nodule of ten percent or higher (Barden et al., 2003). Fine needle aspiration (FNA) biopsy is the most widely used test for initial thyroid nodule diagnosis. FNA of the thyroid gland was first introduced by Soderstrom in 1952 (Soderstrom, 1952) and became utilised worldwide in the 1970's and 80's. The main goal of this diagnostic procedure is to detect thyroid neoplasms for surgical resection and to identify non-neoplastic lesions that may be managed conservatively. Although FNA is currently the best available diagnostic test, with low costs and without complications, it has its inadequacies. McCall and colleagues (McCall et al., 1986) describe the cytodiagnosis of nodules by FNA as complex for the following reasons: a) overlap of cytological patterns between neoplastic and non-neoplastic lesions, b) overlap of cytological features between various neoplasms, and c) coexistence of non-neoplastic and neoplastic processes and multiple malignancies in the same gland.

Sangalli and colleagues (Sangalli et al., 2006) described FNAs inadequacies as three-fold, not only did they describe FNAs inability to give a differential diagnosis of benign and malignant follicular neoplasms, but they also described the high number of false negatives (1.3-17%) (Amrikachi et al., 2001, Hall et al., 1989) with a consequent failure to treat a malignant neoplasm and thirdly they mentioned FNA cases where it is impossible to formulate a diagnosis due to inadequate material (2-31%) (Hawkins et al., 1987, Ravetto et al., 2000), which results in a decrease in the accuracy of the method and an increased number of lobectomies performed. In their attempt to gauge the accuracy of classification of variants of papillary thyroid carcinoma on aspirates, Nair and colleagues (Nair et al., 2001) found their greatest difficulty to be correctly identifying follicular variant papillary thyroid carcinoma on FNA, with only 16% of histologically documented follicular variant papillary thyroid carcinoma being diagnosed on FNA smears, and only 50% of cases diagnosed as follicular variant papillary thyroid carcinoma on FNA being confirmed on histology. They found that unsatisfactory aspirates from follicular variant papillary thyroid carcinoma made up 31.8%.

4.2.4 Laser capture microdissection and pre-amplification

Molecular profiling of a pure cell population, which is reflective of the cell population's *in vivo* genomic and proteomic state, is essential for correlating molecular signatures in diseased and disease-free cells. Direct microscopic visualisation of the cells permits the selection of normal, pre-malignant and malignant cells, or disease and disease free cells, as distinct cell populations from the heterogeneous tissue. Therefore the use of laser capture microdissection enables researchers to isolate specific cells of interest, without contamination from surrounding cells (Espina et al., 2006). Consequently, LCM produces accurate yet low yields of RNA, the factors that may result in the low yields attained are quality of sample, time to preservation before microdissection, type of preservation, fixation method and efficiency of microdissection (Espina et al., 2006).

In this study a novel pre-amplification technique was applied to circumvent the low yields typically attained when utilising LCM. The aim of this chapter was to analyse the utility of a panel of markers in a cohort of archival thyroid samples. As previous gene expression studies have been limited to analysis of typically less than four targets (Kuramochi et al., 2006, Azuma et al., 2006, Chen and Ou, 2006, Vernooy et al., 2007), it was decided to employ a technique which would amplify the low amount of RNA achieved from using LCM. This technique facilitates multiplex pre-amplification up to 100-plex and produces unbiased amplicons of specific regions of the starting cDNA which will then be analysed using the panel of ten targets.

4.3 Aims

The aim of this chapter was to validate the utility of a panel of molecular markers, previously identified by microarray analysis (Finn et al., 2007) by its application to a larger series (n=195) of archival benign and malignant thyroid lesions.

As laser capture microdissection was used to obtain follicular epithelial cells, and this technique can result in a low yield of RNA, a novel pre-amplification technique was employed to allow interrogation of the panel of targets in the study cohort.

4.4 Materials and methods

4.4.1 Samples

One hundred and ninety five cases of formalin-fixed paraffin embedded thyroid samples were analysed. These cases were accessioned from archives dating from 2000 - 2005 at St. James Hospital, Dublin. The study had the approval of the St. James Hospital and Adelaide and Meath Hospital research ethics committee. Haematoxylin and eosin (H&E) sections were reviewed by a histopathologist (S.F) and classified according to a recognized system (Rosai, 1992). Corresponding paraffin blocks were then collected from the archives of St. James Hospital. The tables overleaf list the one hundred and ninety five samples grouped into their corresponding diagnostic categories. The majority of the categories have an overlap of the one hundred and ninety five samples. There are three non-neoplastic categories, the first being "non-neoplastic (no thyroiditis, no hyperplasia)", which is a representation of the typically normal samples such as goitre and no evidence of malignancy. The second is the typically normal samples plus the thyroiditis samples and is termed "non-neoplastic (no hyperplasia)". And thirdly the "non-neoplastic (incl. hyperplasia and thyroiditis)" group includes the typically normal samples plus thyroiditis and hyperplasic samples. The reason for these groupings is to assess whether the inclusion or exclusion of groups such as thyroiditis and hyperplasia, which are neither normal, benign or malignant, will have any influence on expression profiles. The non-malignant cohort encompasses the benign samples and all of the non-neoplastic samples. The non-neoplastic (incl. hyperplasia and thyroiditis) group (n=105) and the neoplastic group (n=90) constitute the overall cohort of one hundred and ninety five samples.

The following tables (tables 4.1- 4.18) represent the grouping of samples into analysis cohorts. All samples emanate from the cohort of one hundred and ninety five. Some samples are represented more than once in the different analysis groups.

Non-neoplastic (no thyroiditis, no hyperplasia) (n=47)
No evidence of malignancy
No evidence of malignancy
No evidence of malignancy
No evidence of malignancy
No evidence of malignancy
No evidence of malignancy
No evidence of malignancy
No evidence of malignancy
No evidence of malignancy
No evidence of malignancy
No evidence of malignancy
No evidence of malignancy
No evidence of malignancy
No evidence of malignancy
No evidence of malignancy
No evidence of malignancy
Goitre, colloid
Goitre, colloid
Goitre, colloid
Goitre, colloid
Goitre
Goitre, colloid
Goitre, colloid
Goitre, colloid
Goitre, colloid
Goitre, colloid
Goitre, colloid
Goitre, colloid
Goitre, colloid
Goitre, colloid
Goitre, colloid
Goitre, colloid
Goitre, colloid
Goitre, colloid
Goitre, colloid
Goitre
Goitre, colloid
Goitre
Goitre, adenomatous
Goitre
Goitre, adenomatous
Goitre, colloid
Goitre, colloid
Goitre, colloid
Goitre, colloid

Goitre, colloid
Goitre, adenomatous
Goitre, adenomatous

Table 4.1 Non-neoplastic (no hyperplasia, no thyroiditis) samples

Non-neoplastic (no hyperplasia) (n=54)
Hashimoto Thyroiditis
Hashimoto Thyroiditis
Hashimoto Thyroiditis
Hashimoto Thyroiditis
Hashimoto Thyroiditis
Inflammation, chronic
Lymphocytic thyroiditis
No evidence of malignancy
No evidence of malignancy
No evidence of malignancy
No evidence of malignancy
No evidence of malignancy
No evidence of malignancy
No evidence of malignancy
No evidence of malignancy
No evidence of malignancy
No evidence of malignancy
No evidence of malignancy
No evidence of malignancy
No evidence of malignancy
No evidence of malignancy
No evidence of malignancy
No evidence of malignancy
Goitre, colloid
Goitre, colloid
Goitre, colloid
Goitre, colloid
Goitre
Goitre, colloid
Goitre, colloid
Goitre, colloid
Goitre, colloid
Goitre, colloid
Goitre, colloid
Goitre, colloid
Goitre, colloid
Goitre, colloid
Goitre, colloid
Goitre, colloid
Goitre, colloid
Goitre, colloid
Goitre
Goitre, colloid
Goitre
Goitre, adenomatous
Goitre
Goitre, adenomatous
Goitre, colloid
Goitre, colloid
Goitre, colloid

Goitre, colloid
Goitre, colloid
Goitre, adenomatous
Goitre, adenomatous

Table 4.2 Non-neoplastic (no hyperplasia) samples

Non-neoplastic (incl. hyperplasia and thyroiditis) (n=105)
Hashimoto Thyroiditis
Hashimoto Thyroiditis
Hashimoto Thyroiditis
Hashimoto Thyroiditis
Hashimoto Thyroiditis
Inflammation, chronic
Lymphocytic thyroiditis
No evidence of malignancy
No evidence of malignancy
No evidence of malignancy
No evidence of malignancy
No evidence of malignancy
No evidence of malignancy
No evidence of malignancy
No evidence of malignancy
No evidence of malignancy
No evidence of malignancy
No evidence of malignancy
No evidence of malignancy
No evidence of malignancy
No evidence of malignancy
No evidence of malignancy
No evidence of malignancy
Goitre, colloid
Goitre, colloid
Goitre, colloid
Goitre, colloid
Goitre
Goitre, colloid
Goitre, colloid
Goitre, colloid
Goitre, colloid
Goitre, colloid
Goitre, colloid
Goitre, colloid
Goitre, colloid
Goitre, colloid
Goitre, colloid
Goitre, colloid
Goitre, colloid
Goitre, colloid
Goitre, colloid
Goitre, colloid
Goitre
Goitre, colloid
Goitre
Goitre, adenomatous

Goitre
Goitre, adenomatous
Goitre, colloid
Goitre, colloid
Goitre, colloid
Goitre, colloid
Goitre, colloid
Goitre, adenomatous
Goitre, adenomatous
Graves
Graves
Graves
Graves
Graves
Hyperthyroidism
Hyperplasia, nodular
Hyperplasia, nodular
Hyperplasia, nodular
Hyperplasia, nodular
Hyperplasia, nodular
Hyperplasia, nodular
Hyperplasia
Hyperplasia, nodular
Hyperplasia, nodular
Hyperplasia, nodular
Hyperplasia, nodular
Hyperplasia, nodular
Hyperplasia, nodular
Hyperplasia
Hyperplasia, nodular
Hyperplasia + lymphocytic thyroiditis
Hyperplasia + lymphocytic thyroiditis
Hyperplasia, nodular + lymphocytic thyroiditis
Hyperplasia + lymphocytic thyroiditis
Hyperplasia, nodular
Hyperplasia
Hyperplasia, nodular
Hyperplasia, nodular
Hyperplasia, nodular
Hyperplasia, nodular
Hyperplasia, nodular
Hyperplasia
Hyperplasia
Hyperplasia
Hyperplasia, nodular
Hyperplasia, nodular
Hyperplasia, nodular
Hyperplasia
Hyperplasia
Hyperplasia
Hyperplasia
Hyperplasia, adenomatous
Hyperplasia, adenomatous
Hyperplasia, nodular
Hyperplasia

Hyperplasia, nodular
Hyperplasia, nodular
Hyperplasia, nodular
Hyperplasia, nodular
Hyperplasia, nodular

Table 4.3 Non-neoplastic (incl. hyperplasia and thyroiditis) samples

Thyroiditis (n=7)
Hashimoto Thyroiditis
Hashimoto Thyroiditis
Hashimoto Thyroiditis
Hashimoto Thyroiditis
Hashimoto Thyroiditis
Inflammation, chronic
Lymphocytic thyroiditis

Table 4.4 Thyroiditis samples

Hashimoto Thyroiditis (n=5)
Hashimoto Thyroiditis
Hashimoto Thyroiditis
Hashimoto Thyroiditis
Hashimoto Thyroiditis
Hashimoto Thyroiditis

Table 4.5 Hashimoto Thyroiditis samples

Hyperplasia (n=51)
Graves
Graves
Graves
Graves
Graves
Hyperthyroidism
Hyperplasia, nodular
Hyperplasia, nodular
Hyperplasia, nodular
Hyperplasia, nodular
Hyperplasia, nodular
Hyperplasia, nodular
Hyperplasia
Hyperplasia, nodular
Hyperplasia, nodular
Hyperplasia, nodular
Hyperplasia, nodular
Hyperplasia, nodular
Hyperplasia, nodular
Hyperplasia
Hyperplasia, nodular
Hyperplasia + lymphocytic thyroiditis
Hyperplasia + lymphocytic thyroiditis
Hyperplasia, nodular + lymphocytic thyroiditis
Hyperplasia + lymphocytic thyroiditis
Hyperplasia, nodular
Hyperplasia
Hyperplasia, nodular
Hyperplasia, nodular
Hyperplasia, nodular
Hyperplasia, nodular
Hyperplasia, nodular
Hyperplasia
Hyperplasia
Hyperplasia
Hyperplasia, nodular
Hyperplasia, nodular
Hyperplasia, nodular
Hyperplasia
Hyperplasia
Hyperplasia
Hyperplasia
Hyperplasia, adenomatous
Hyperplasia, adenomatous
Hyperplasia, nodular
Hyperplasia
Hyperplasia, nodular
Hyperplasia, nodular
Hyperplasia, nodular
Hyperplasia, nodular
Hyperplasia, nodular

Table 4.6 Hyperplasia samples

Follicular adenoma (n=19)
Follicular adenoma
Follicular adenoma
Follicular adenoma
Follicular adenoma
Follicular adenoma
Follicular adenoma
Follicular adenoma
Follicular adenoma
Follicular adenoma
Follicular adenoma
Follicular adenoma
Follicular adenoma
Follicular adenoma
Follicular adenoma
Follicular adenoma
Follicular adenoma
Follicular adenoma
Follicular adenoma
Follicular adenoma
Follicular adenoma

Table 4.7 Follicular adenoma samples

Benign (n=27)
Adenoma
Adenoma
Adenoma
Adenoma, mixed cell
Adenoma
Hurthle cell adenoma
Hurthle cell adenoma
Hurthle cell adenoma
Follicular adenoma
Follicular adenoma
Follicular adenoma
Follicular adenoma
Follicular adenoma
Follicular adenoma
Follicular adenoma
Follicular adenoma
Follicular adenoma
Follicular adenoma
Follicular adenoma
Follicular adenoma
Follicular adenoma
Follicular adenoma
Follicular adenoma
Follicular adenoma
Follicular adenoma
Follicular adenoma
Follicular adenoma
Follicular adenoma
Follicular adenoma
Follicular adenoma

Table 4.8 Benign samples

Non-malignant (all benign, all non-neoplastic) (n=132)
Hashimoto Thyroiditis
Hashimoto Thyroiditis
Hashimoto Thyroiditis
Hashimoto Thyroiditis
Hashimoto Thyroiditis
Inflammation, chronic
Lymphocytic thyroiditis
No evidence of malignancy
No evidence of malignancy
No evidence of malignancy
No evidence of malignancy
No evidence of malignancy
No evidence of malignancy
No evidence of malignancy
No evidence of malignancy
No evidence of malignancy
No evidence of malignancy
No evidence of malignancy
No evidence of malignancy
No evidence of malignancy
No evidence of malignancy
No evidence of malignancy
Goitre, colloid
Goitre, colloid
Goitre, colloid
Goitre, colloid
Goitre
Goitre, colloid
Goitre, colloid
Goitre, colloid
Goitre, colloid
Goitre, colloid
Goitre, colloid
Goitre, colloid
Goitre, colloid
Goitre, colloid
Goitre, colloid
Goitre, colloid
Goitre, colloid
Goitre, colloid
Goitre
Goitre, colloid
Goitre
Goitre, adenomatous
Goitre
Goitre, adenomatous
Goitre, colloid
Goitre, colloid
Goitre, colloid
Goitre, colloid
Goitre, colloid
Goitre, adenomatous
Goitre, adenomatous

Graves
Graves
Graves
Graves
Graves
Hyperthyroidism
Hyperplasia, nodular
Hyperplasia, nodular
Hyperplasia, nodular
Hyperplasia, nodular
Hyperplasia, nodular
Hyperplasia, nodular
Hyperplasia
Hyperplasia, nodular
Hyperplasia, nodular
Hyperplasia, nodular
Hyperplasia, nodular
Hyperplasia, nodular
Hyperplasia, nodular
Hyperplasia
Hyperplasia, nodular
Hyperplasia + lymphocytic thyroiditis
Hyperplasia + lymphocytic thyroiditis
Hyperplasia, nodular + lymphocytic thyroiditis
Hyperplasia + lymphocytic thyroiditis
Hyperplasia, nodular
Hyperplasia
Hyperplasia, nodular
Hyperplasia, nodular
Hyperplasia, nodular
Hyperplasia, nodular
Hyperplasia, nodular
Hyperplasia
Hyperplasia
Hyperplasia
Hyperplasia, nodular
Hyperplasia, nodular
Hyperplasia, nodular
Hyperplasia
Hyperplasia
Hyperplasia
Hyperplasia
Hyperplasia, adenomatous
Hyperplasia, adenomatous
Hyperplasia, nodular
Hyperplasia
Hyperplasia, nodular
Hyperplasia, nodular
Hyperplasia, nodular
Hyperplasia, nodular
Hyperplasia, nodular
Adenoma
Adenoma
Adenoma
Adenoma, mixed cell

Adenoma
Hurthle cell adenoma
Hurthle cell adenoma
Hurthle cell adenoma
Follicular adenoma
Follicular adenoma
Follicular adenoma
Follicular adenoma
Follicular adenoma
Follicular adenoma
Follicular adenoma
Follicular adenoma
Follicular adenoma
Follicular adenoma
Follicular adenoma
Follicular adenoma
Follicular adenoma
Follicular adenoma
Follicular adenoma
Follicular adenoma
Follicular adenoma
Follicular adenoma
Follicular adenoma

Table 4.9 Non-malignant (all benign, all non-neoplastic) samples

Hurthle cell carcinoma (n=3)
Hurthle cell carcinoma
Hurthle cell carcinoma
Hurthle cell carcinoma

Table 4.10 Hurthle cell carcinoma samples

Follicular thyroid carcinoma (n=10)
Follicular thyroid carcinoma, Hurthle cell type
Follicular thyroid carcinoma, well differentiated
Follicular thyroid carcinoma
Follicular thyroid carcinoma, Hurthle cell type
Follicular thyroid carcinoma, Hurthle cell type
Follicular thyroid carcinoma
Follicular thyroid carcinoma
Follicular thyroid carcinoma
Follicular thyroid carcinoma
Follicular thyroid carcinoma

Table 4.11 Follicular thyroid carcinoma samples

Papillary thyroid carcinoma (not otherwise specified)
Papillary thyroid carcinoma, well differentiated
Papillary thyroid carcinoma
Papillary thyroid carcinoma
Papillary thyroid carcinoma
Papillary thyroid carcinoma
Papillary thyroid carcinoma
Papillary thyroid carcinoma
Papillary thyroid carcinoma
Papillary thyroid carcinoma
Papillary thyroid carcinoma
Papillary thyroid microcarcinoma
Papillary thyroid carcinoma, well differentiated
Papillary thyroid carcinoma, multifocal
Papillary thyroid carcinoma, multifocal
Papillary thyroid carcinoma, multifocal
Papillary thyroid carcinoma, multifocal
Papillary thyroid carcinoma, oxyphilic variant
Papillary thyroid carcinoma, trebecular
Papillary thyroid carcinoma
Papillary thyroid carcinoma
Papillary thyroid carcinoma
Papillary thyroid carcinoma
Papillary thyroid carcinoma
Papillary thyroid carcinoma
Papillary thyroid carcinoma
Papillary thyroid carcinoma
Papillary thyroid carcinoma
Papillary thyroid carcinoma
Papillary thyroid carcinoma
Papillary thyroid carcinoma
Papillary thyroid carcinoma
Papillary thyroid carcinoma

Table 4.12 Papillary thyroid carcinoma (NOS) samples

Papillary thyroid carcinoma follicular variant (n=14)
Papillary thyroid carcinoma, follicular variant
Papillary thyroid carcinoma, follicular variant
Papillary thyroid carcinoma, follicular variant
Papillary thyroid carcinoma, follicular variant
Papillary thyroid carcinoma, encapsulated follicular variant
Papillary thyroid carcinoma, follicular variant
Papillary thyroid carcinoma, follicular variant
Papillary thyroid carcinoma, follicular variant
Papillary thyroid carcinoma, follicular variant
Papillary thyroid carcinoma, follicular variant
Papillary thyroid carcinoma, follicular variant
Papillary thyroid carcinoma, follicular variant
Papillary thyroid carcinoma, follicular variant
Papillary thyroid carcinoma, follicular variant

Table 4.13 Papillary thyroid carcinoma follicular variant samples

Papillary thyroid carcinoma (all variants) (n=46)
Papillary thyroid carcinoma, well differentiated
Papillary thyroid carcinoma
Papillary thyroid carcinoma
Papillary thyroid carcinoma
Papillary thyroid carcinoma
Papillary thyroid carcinoma
Papillary thyroid carcinoma
Papillary thyroid carcinoma
Papillary thyroid carcinoma
Papillary thyroid carcinoma
Papillary thyroid microcarcinoma
Papillary thyroid carcinoma, well differentiated
Papillary thyroid carcinoma, multifocal
Papillary thyroid carcinoma, multifocal
Papillary thyroid carcinoma, multifocal
Papillary thyroid carcinoma, multifocal
Papillary thyroid carcinoma, oxyphilic variant
Papillary thyroid carcinoma, trebecular
Papillary thyroid carcinoma
Papillary thyroid carcinoma
Papillary thyroid carcinoma
Papillary thyroid carcinoma
Papillary thyroid carcinoma
Papillary thyroid carcinoma
Papillary thyroid carcinoma
Papillary thyroid carcinoma
Papillary thyroid carcinoma
Papillary thyroid carcinoma
Papillary thyroid carcinoma
Papillary thyroid carcinoma
Papillary thyroid carcinoma
Papillary thyroid carcinoma
Papillary thyroid carcinoma, follicular variant
Papillary thyroid carcinoma, follicular variant
Papillary thyroid carcinoma, follicular variant
Papillary thyroid carcinoma, follicular variant
Papillary thyroid carcinoma, encapsulated follicular variant
Papillary thyroid carcinoma, follicular variant
Papillary thyroid carcinoma, follicular variant
Papillary thyroid carcinoma, follicular variant
Papillary thyroid carcinoma, follicular variant
Papillary thyroid carcinoma, follicular variant
Papillary thyroid carcinoma, follicular variant
Papillary thyroid carcinoma, follicular variant
Papillary thyroid carcinoma, follicular variant
Papillary thyroid carcinoma, follicular variant

Table 4.14 Papillary thyroid carcinoma (all variants) samples

Anaplastic thyroid carcinoma (n=1)
Anaplastic thyroid carcinoma, giant cell type

Table 4.15 Anaplastic thyroid carcinoma sample

Medullary thyroid carcinoma (n=1)
Medullary thyroid carcinoma

Table 4.16 Medullary thyroid carcinoma sample

Neoplastic (n=90)
Adenoma
Adenoma
Adenoma
Adenoma, mixed cell
Adenoma
Hurthle cell adenoma
Hurthle cell adenoma
Hurthle cell adenoma
Follicular adenoma
Follicular adenoma
Follicular adenoma
Follicular adenoma
Follicular adenoma
Follicular adenoma
Follicular adenoma
Follicular adenoma
Follicular adenoma
Follicular adenoma
Follicular adenoma
Follicular adenoma
Follicular adenoma
Follicular adenoma
Follicular adenoma
Follicular adenoma
Follicular adenoma
Follicular adenoma
Follicular adenoma
Follicular adenoma
Hurthle cell carcinoma
Hurthle cell carcinoma
Hurthle cell carcinoma
Follicular thyroid carcinoma, Hurthle cell type
Follicular thyroid carcinoma, well differentiated
Follicular thyroid carcinoma
Follicular thyroid carcinoma, Hurthle cell type
Follicular thyroid carcinoma, Hurthle cell type
Follicular thyroid carcinoma
Follicular thyroid carcinoma
Follicular thyroid carcinoma
Follicular thyroid carcinoma
Follicular thyroid carcinoma

Papillary thyroid carcinoma, well differentiated
Papillary thyroid carcinoma
Papillary thyroid carcinoma
Papillary thyroid carcinoma
Papillary thyroid carcinoma
Papillary thyroid carcinoma
Papillary thyroid carcinoma
Papillary thyroid carcinoma
Papillary thyroid carcinoma
Papillary thyroid carcinoma
Papillary thyroid microcarcinoma
Papillary thyroid carcinoma, well differentiated
Papillary thyroid carcinoma, multifocal
Papillary thyroid carcinoma, multifocal
Papillary thyroid carcinoma, multifocal
Papillary thyroid carcinoma, multifocal
Papillary thyroid carcinoma, oxyphilic variant
Papillary thyroid carcinoma, trebecular
Papillary thyroid carcinoma
Papillary thyroid carcinoma
Papillary thyroid carcinoma
Papillary thyroid carcinoma
Papillary thyroid carcinoma
Papillary thyroid carcinoma
Papillary thyroid carcinoma
Papillary thyroid carcinoma
Papillary thyroid carcinoma
Papillary thyroid carcinoma
Papillary thyroid carcinoma
Papillary thyroid carcinoma
Papillary thyroid carcinoma
Papillary thyroid carcinoma
Well differentiated thyroiid tumour-unknown malignant potential
Papillary thyroid carcinoma, follicular variant
Papillary thyroid carcinoma, follicular variant
Papillary thyroid carcinoma, follicular variant
Papillary thyroid carcinoma, follicular variant
Papillary thyroid carcinoma, encapsulated follicular variant
Papillary thyroid carcinoma, follicular variant
Papillary thyroid carcinoma, follicular variant
Papillary thyroid carcinoma, follicular variant
Papillary thyroid carcinoma, follicular variant
Papillary thyroid carcinoma, follicular variant
Papillary thyroid carcinoma, follicular variant
Papillary thyroid carcinoma, follicular variant
Papillary thyroid carcinoma, follicular variant
Papillary thyroid carcinoma, follicular variant
Medullary thyroid carcinoma
Anaplastic thyroid carcinoma, giant cell type
Hurthle cell neoplasm

Table 4.17 Neoplastic samples

Malignant (n=61)
Hurthle cell carcinoma
Hurthle cell carcinoma
Hurthle cell carcinoma
Follicular thyroid carcinoma, Hurthle cell type
Follicular thyroid carcinoma, well differentiated
Follicular thyroid carcinoma
Follicular thyroid carcinoma, Hurthle cell type
Follicular thyroid carcinoma, Hurthle cell type
Follicular thyroid carcinoma
Follicular thyroid carcinoma
Follicular thyroid carcinoma
Follicular thyroid carcinoma
Follicular thyroid carcinoma
Papillary thyroid carcinoma, well differentiated
Papillary thyroid carcinoma
Papillary thyroid carcinoma
Papillary thyroid carcinoma
Papillary thyroid carcinoma
Papillary thyroid carcinoma
Papillary thyroid carcinoma
Papillary thyroid carcinoma
Papillary thyroid carcinoma
Papillary thyroid carcinoma
Papillary thyroid carcinoma
Papillary thyroid microcarcinoma
Papillary thyroid carcinoma, well differentiated
Papillary thyroid carcinoma, multifocal
Papillary thyroid carcinoma, multifocal
Papillary thyroid carcinoma, multifocal
Papillary thyroid carcinoma, multifocal
Papillary thyroid carcinoma, oxyphilic variant
Papillary thyroid carcinoma, trebecular
Papillary thyroid carcinoma
Papillary thyroid carcinoma
Papillary thyroid carcinoma
Papillary thyroid carcinoma
Papillary thyroid carcinoma
Papillary thyroid carcinoma
Papillary thyroid carcinoma
Papillary thyroid carcinoma
Papillary thyroid carcinoma
Papillary thyroid carcinoma
Papillary thyroid carcinoma
Papillary thyroid carcinoma
Papillary thyroid carcinoma
Papillary thyroid carcinoma
Papillary thyroid carcinoma, follicular variant
Papillary thyroid carcinoma, follicular variant
Papillary thyroid carcinoma, follicular variant
Papillary thyroid carcinoma, follicular variant
Papillary thyroid carcinoma, encapsulated follicular variant
Papillary thyroid carcinoma, follicular variant
Papillary thyroid carcinoma, follicular variant
Papillary thyroid carcinoma, follicular variant

Papillary thyroid carcinoma, follicular variant
Papillary thyroid carcinoma, follicular variant
Papillary thyroid carcinoma, follicular variant
Papillary thyroid carcinoma, follicular variant
Papillary thyroid carcinoma, follicular variant
Papillary thyroid carcinoma, follicular variant
Medullary thyroid carcinoma
Anaplastic thyroid carcinoma, giant cell type

Table 4.18 Malignant samples

4.4.2 Laser capture microdissection

7-µm thick sections were cut using a microtome (Microm HM 325, Medical Supply Co. Ltd, Ireland) from each paraffin block, mounted on uncharged slides, de-waxed and H&E stained (Tissue-Tek DRS 2000 Autostainer, Sakura, CA, USA). Pure populations of thyrocytes were obtained from each section by laser capture microdissection using the PixCell® II System (Acturus Engineering, Inc., CA, USA) (see section 2.6). Laser capture microdissection produces low yet accurate yields of RNA. Cells were captured according to a standard protocol: laser spot size = 30µm, pulse power = 40mW, pulse width = 1.5 ms, threshold voltage = 285 mV. The total number of pulses in each case was approximately 700 (range = 500-1200). After microdissection the Capsures® (Capsure® Macro LCM caps, LCM 0201, Techno-Path Ltd, Ireland) containing the homogenous cell populations were placed in a sterile microcentrifuge tube ready for RNA extraction.

4.4.3 RNA extraction and quantification

RNA was extracted using the Absolutely RNA® Formalin Fixed Paraffin Embedded Kit (Stratagene, CA, USA), using the protocol described in section 2.7. The tissue deparaffinization and dehydration step of the manufacturers protocol was removed as the sections had been deparaffinized during H&E staining. The manufacturers' protocol also recommended the use of two 10µm thick sections; however the quantity used in this experiment was sufficient (~150 cells in some cases). Purified RNA was eluted in 30µL volumes and the nanogram concentration per microlitre was established using a NanoDrop spectrophotometer (ND-1000, Labtech International, U.K) Yields in the range of 5ng/µL to 63ng/µL were achieved, to maintain equal quantities of RNA, 5ng/µL (or 0.125 µg in 25µL) of each sample was used.

4.4.4 cDNA archiving and Pre-Amp synthesis

The RNA was reverse transcribed to single-stranded cDNA using a High Capacity cDNA Archive Kit (Applied Biosytems, CA, USA) in 50 µL reactions as described in chapter 2, section 2.9. 25 µL of extracted total RNA (0.125 µg) from each sample was added to 25 µL of combined archiving reagents and incubated at 25°C for 10 minutes and 37°C for 2 hours (Perkin Elmer 9600 GeneAmp PCR system, Applied Biosystems, CA, USA).

Applied Biosystems TaqMan® Pre-Amp Master Mix Kit is intended for use with very small quantities of cDNA, and increases the quantity of cDNA for gene expression studies. Prior to running the pre-amplification reaction, the intended assays (containing primers and probes) were pooled together, as described in section 2.10.4.2 with 1X Tris-EDTA (TE) buffer in a 0.2X pooled assay mix. The pre-amplification reaction was performed in 50µL reactions for 10 minutes at 95°C, and 10 cycles of 15 seconds at 95°C and 4 minutes at 60°C (PE 9600 GeneAmp PCR system Applied Biosystems, CA, USA).

4.4.5 TaqMan® gene expression reaction

The eleven gene expression assays (including CDKN1B as the endogenous control) shown in table 4.19 were diluted 1:5 (20X to 4X) using 1X TE buffer. The pre-amplified products were diluted 1:5 using TE buffer. The gene expression reaction was performed in 20µL reactions containing 10µL of TaqMan® gene expression master mix w/UNG (2X), 5µL of diluted pre-amp product and 5µL of TaqMan® gene expression assay (4X). The following thermal cycling specifications were performed on the ABI Prism® 7000 sequence detection system (Applied Biosystems, CA, USA) 2 minutes at 50°C, 10 minutes at 95°C and 40 cycles each for 15 seconds at 95°C and 1 minute at 60°C.

Gene Symbol	Gene Name
HLA-DQB1	Major histocompatibility complex class II DQB1
HLA-DMA	Major histocompatibility complex class II DMA
MT1K	Metallothionein 1K
TGFB1	Transforming growth factor, beta 1
CSNK1G2	Casein kinase 1, gamma 2
KRAS2	v-Ki-ras2 Kirsten rat sarcoma viral oncogene homolog
MT1X	Metallothionein 1X
IRF3	Interferon regulatory factor 3
RAB23	RAB23, member RAS oncogene family
CD74	CD74 molecule, major histocompatibility complex, class II invariant chain
CDKN1B	Cyclin-dependent kinase inhibitor 1B

Table 4.19 Illustrates the panel of assays (including CDKN1B as the endogenous control) which were used to perform TaqMan® RT-PCR analysis

4.4.6 Analysis of relative gene expression data using the Comparative C_T method

Analysis of relative gene expression data was performed using the $2^{-\Delta\Delta C}{}_T$ method (Livak and Schmittgen, 2001) with cyclin dependent kinase inhibitor 1 B (CDKN1B) as the endogenous control/reference assay. Briefly, this algorithm presents data as a fold change in gene expression relative to a calibrator (follicular adenoma) and normalised to an endogenous reference gene, CDKN1B in this case. This method is described in more detail in section 2.10.2.

The threshold cycle (C_T) indicates the cycle number at which the amount of amplified target reaches a fixed threshold. The C_T data for all samples and target genes and the endogenous control (CDKN1B) were used to create ΔC_T values [ΔC_T = C_T(target gene)-C_T(CDKN1B)]. $\Delta\Delta C_T$ values were calculated by subtracting the calibrator (follicular adenoma) ΔC_T from the ΔC_T value of each target. Relative quantification (RQ) values are calculated by imputing $\Delta\Delta C_T$ values into the equation $2^{-\Delta\Delta C}{}_T$.

4.4.7 Statistical analysis

The distribution of the values in each group of samples was non-normal; therefore a non-parametric statistical test was required. As no more than two unpaired groups of values were being compared at a time, the Mann-Whitney U-test was chosen to determine statistical significance (Analyse-it® statistical software for Microsoft® Excel®).

4.5 Results

The following diagnostic categories of groups were formed from the cohort of 195 archival thyroid samples for comparative purposes.

Analysis Cohorts
Non-neoplastic (no thyroiditis, no hyperplasia) n=47
Non-neoplastic (no hyperplasia) n=54
Non-neoplastic (incl. hyperplasia + thyroiditis n=105
Thyroiditis n=7
Hashimoto Thyroiditis n=5
Hyperplasia n=51
Follicular adenoma n=19
Benign n=27
Non-malignant (all benign, all non-neoplastic) n=132
Hurthle cell carcinoma n=3
Follicular thyroid carcinoma n=10
Papillary thyroid carcinoma (NOS) n=32
Papillary thyroid carcinoma, follicular variant n=14
Papillary thyroid carcinoma, all variants n=46
Neoplastic n=90
Malignant n=61

Table 4.20 Demonstrates the analysis cohorts formed and the numbers included in each group for expression analysis of all 10 targets

The following table (table 4.21) illustrates the groups that were significantly ($p < 0.05$, Mann-Whitney U-test) discriminated at the gene expression level for RAB23, MT1K, MT1X, CSNK1G2, TGFB1, IRF3, CD74, HLA-DMA and HLA-DQB1. RAB23, MT1K, MT1X and CSNK1G2 were down-regulated in malignant and neoplastic groups in comparison to benign, hyperplastic, thyroiditis and non-neoplastic groups, while TGFB1, IRF3, CD74, HLA-DMA and HLA-DQB1 were all up-regulated in malignant and neoplastic groups in comparison to benign, hyperplastic, thyroiditis and non-neoplastic groups.

Analysis Cohorts	RAB23	MT1K	MT1X	CSNK1 G2	TGFβ1	IRF3	CD74	HLA-DMA	HLA-DQB1
Non-neoplastic (no hyperplasia, no thyroiditis) vs. Malignant	<0.0001	<0.0001	<0.0001				0.0035	<0.0001	0.0003
Non-neoplastic (no hyperplasia, no thyroiditis) vs. Neoplastic	<0.0001	<0.0001	<0.0001				0.00043	<0.0001	0.0009
Non-neoplastic (no hyperplasia, no thyroiditis) vs. Hyperplasia			0.0263						
Non-neoplastic (no hyperplasia, no thyroiditis) vs. Benign				0.0494				0.0086	
Non-neoplastic (no hyperplasia) vs. Malignant	<0.0001	<0.0001	<0.0001				0.0307	0.0022	0.0021
Non-neoplastic (no hyperplasia) vs. Neoplastic	<0.0001	<0.0001	<0.0001				0.0415	0.0022	0.0063
Non-neoplastic (no hyperplasia) vs. Benign				0.0324					
Non-neoplastic (incl. hyperplasia + thyroiditis) vs. Malignant	<0.0001	<0.0001	<0.0001				0.001	<0.0001	0.0001
Non-neoplastic (incl. hyperplasia + thyroiditis) vs. Neoplastic	<0.0001	<0.0001	<0.0001		0.0304		0.0007	<0.0001	0.0004
Non-neoplastic (incl. hyperplasia + thyroiditis) vs. Benign				0.0061	0.0366			0.0137	
Hyperplasia vs. Malignant	<0.0001	0.0002	<0.0001				0.0005	<0.0001	0.0004
Hyperplasia vs. Neoplastic	<0.0001	0.002	0.0116	0.0319	0.025		0.0003	<0.0001	0.0018
Benign vs. Malignant	0.0003	0.0316	<0.0001	0.0313					
Benign vs. Neoplastic	0.0074		0.001						
Non-malignant (all benign, all non-neoplastic) vs. Malignant	<0.0001	<0.0001	<0.0001				0.0033	0.0003	0.0002
Neoplastic vs. Malignant			0.0355						
Thyroiditis vs. PTC (all variants)		0.0405	0.0418		0.025	0.0273		0.0233	
Thyroiditis vs. PTC (NOS)		0.0338	0.0323		0.0404	0.0094		0.0088	
H.T vs. PTC (all variants)						0.0226	0.0514	0.046	
H.T vs. PTC (NOS)						0.01	0.0263		
FA vs. PTC (all variants)	<0.0001		<0.0001	0.0254					0.0027
FA vs. PTC (NOS)	<0.0001		<0.0001	0.0408					0.0057
FA vs. FVPTC	<0.0001		0.0022					0.023	0.0162
FA vs. FTC	0.0348								

Table 4.21 Displays the statistically significant p values (<0.05) for nine of the targets that were capable of discriminating between the different analysis cohorts
PTC = papillary thyroid carcinoma, NOS = not otherwise specified, FA = follicular adenoma, FVPTC = follicular variant papillary thyroid carcinoma, FTC= follicular thyroid carcinoma

4.5.1 Boxplots

The following graphs represent the $2^{-\Delta\Delta C}{}_T$ method or relative quantification (RQ) data graphically represented as box plots. RQ values have been transformed by $\log_{10}$ for graphical representation. A boxplot is a graph of the five number summary; the five number summary being a set of observations that consist of the smallest observation, the first quartile, the median, the third quartile, and the largest observation. The central box in the box plot spans the first and third quartile and represents 50% of the data, it is also known as the interquartile range (IQR). The line in the box marks the median while the lines that extend out from the box represent the smallest and largest observations. Outliers are points at a greater distance from the median than 1.5 or 3 times the IQR. Near outliers (1.5 x IQR) are represented here as + and far outliers (3 x IQR) are represented as *.

4.5.1.1 RAB23 boxplots

RAB23 is a member of the RAS superfamily of small GTPases that function in the regulation of vesicular trafficking. RAB23 was found to be down-regulated in all malignant and neoplastic cohorts when compared to benign, non-neoplastic and hyperplasia. Down-regulation of RAB23 was also seen in malignant follicular lesions compared to the benign follicular cohort.

RAB23

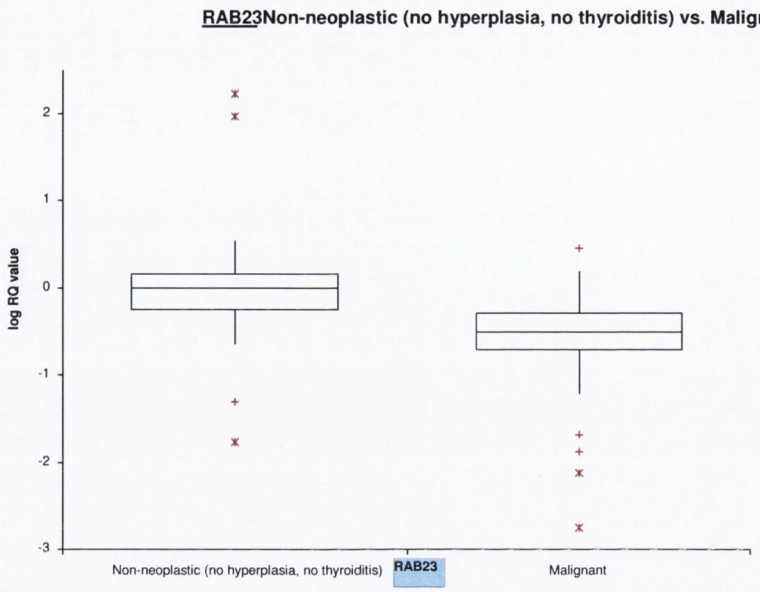

Figure 4.1 Displays down-regulation of RAB23 in the malignant cohort compared to the non-neoplastic thyroid group not including hyperplasia or thyroiditis, p value <0.0001

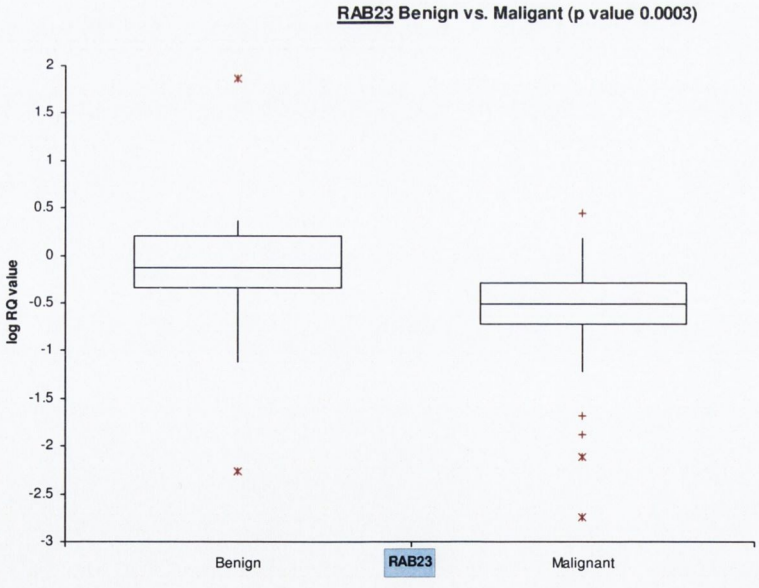

Figure 4.2 Represents down-regulation of RAB23 in the malignant group compared to benign, p value 0.0003

RAB23

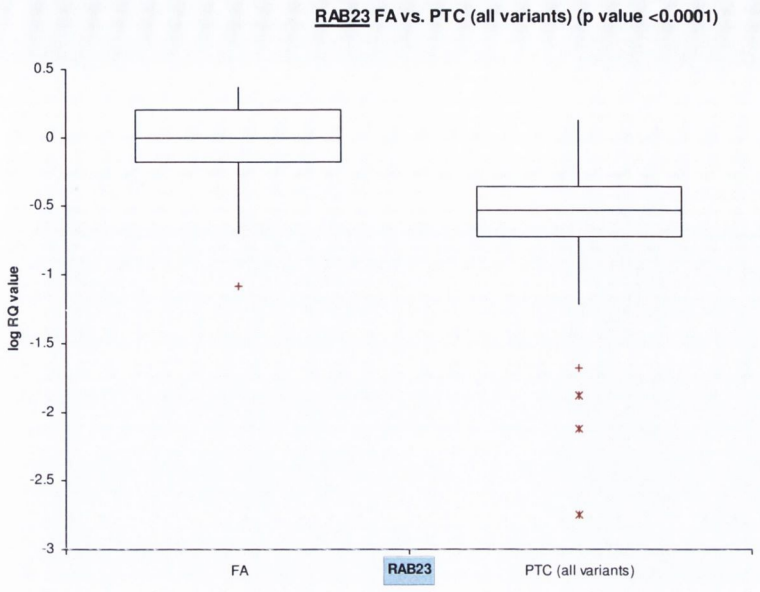

Figure 4.3 Demonstrates down-regulation of RAB23 in the malignant papillary thyroid carcinoma (PTC) group encompassing all variants compared to the benign follicular adenoma group, p value <0.0001

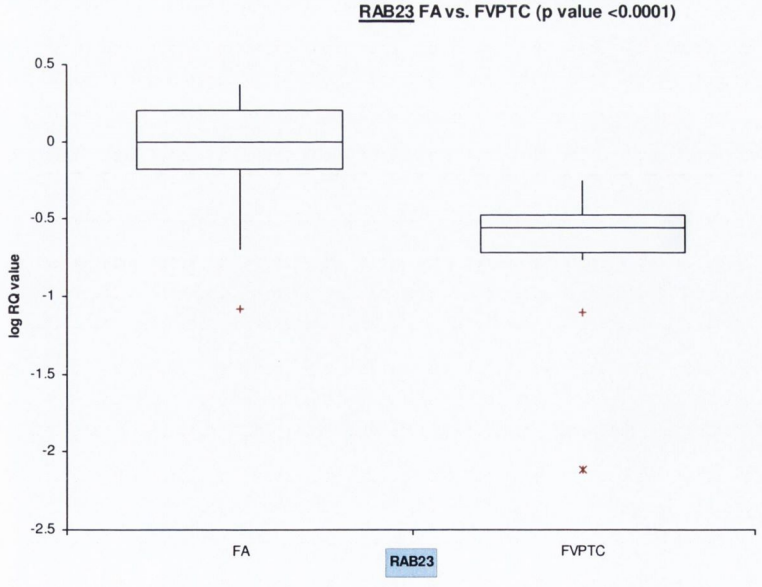

Figure 4.4 Demonstrates down-regulation of RAB23 in the malignant follicular variant papillary thyroid carcinoma (FVPTC) group compared to the benign follicular adenoma group, p value <0.0001

4.5.1.2 MT1K boxplots

MT1K is a member of the metallothionein family, which are a group of low-molecular weight, cystein-rich intracellular proteins. MT1K was down-regulated in all malignant and neoplastic cohorts compared to benign, non-neoplastic, hyperplasia and thyroiditis groups.

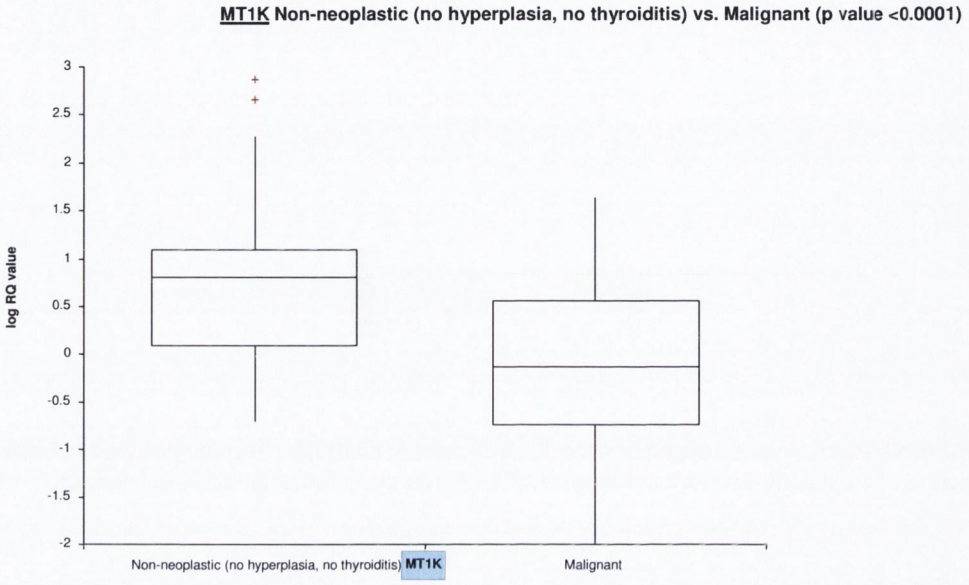

Figure 4.5 Illustrates down-regulation of MT1K in the malignant group versus the non-neoplastic (no hyperplasia, no thyroiditis) group, p value <0.0001

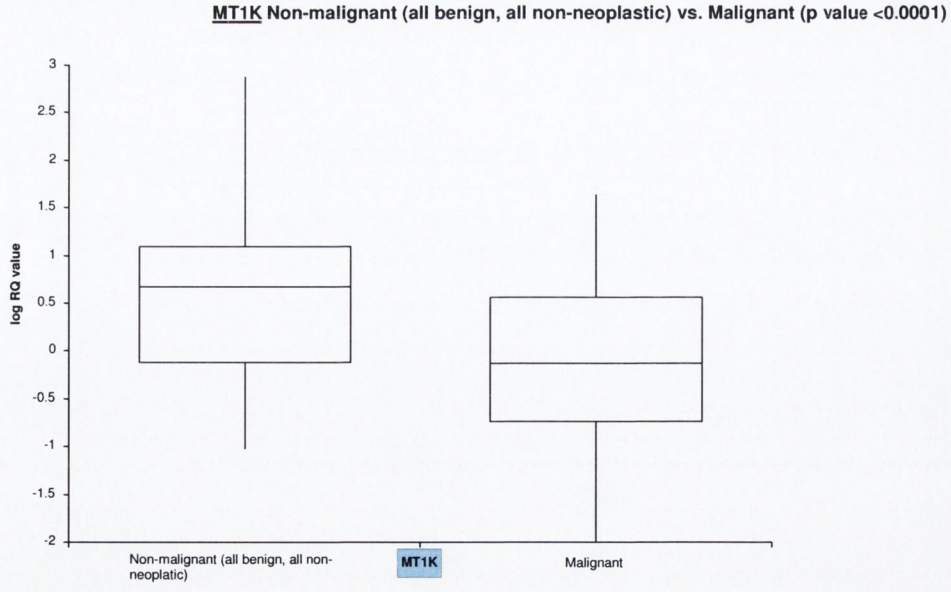

Figure 4.6 Demonstrates down-regulation of MT1K in the malignant group compared to the non-malignant group with encompasses all benign and all non-neoplastic (incl. hyperplasia and thyroiditis) samples, p value <0.0001

4.5.1.3 MT1X boxplots

MT1X is also a member of the metallothionein family and was also found to be down-regulated in all malignant and neoplastic groups when compared with non-neoplastic, benign, hyperplasia and thyroiditis cohorts, MT1X was also down-regulated in follicular variant papillary thyroid carcinoma compared to follicular adenoma.

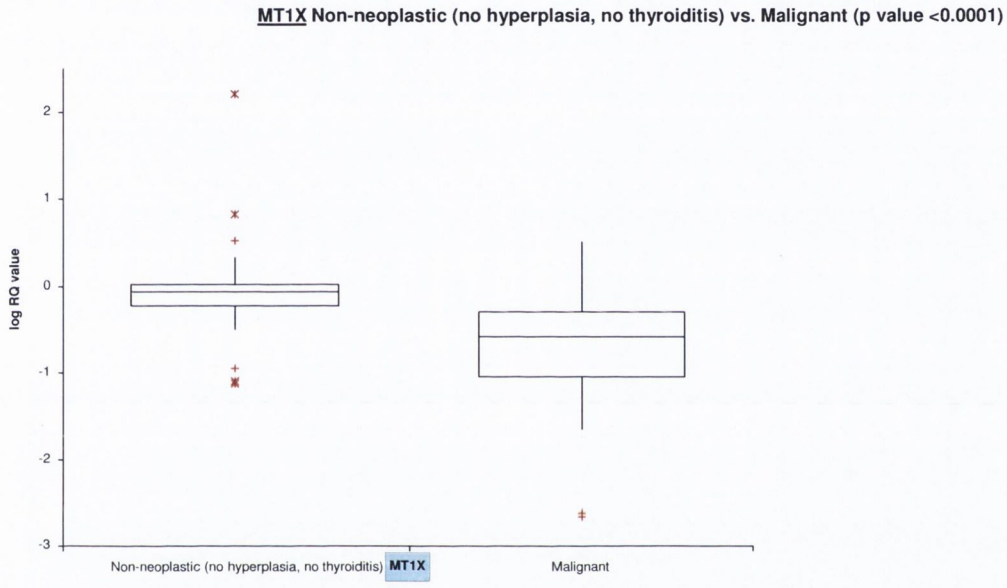

Figure 4.7 Displays the down-regulation of MT1X in the malignant group compared to the non-neoplastic group which does not include hyperplasia or thyroiditis, p value <0.0001

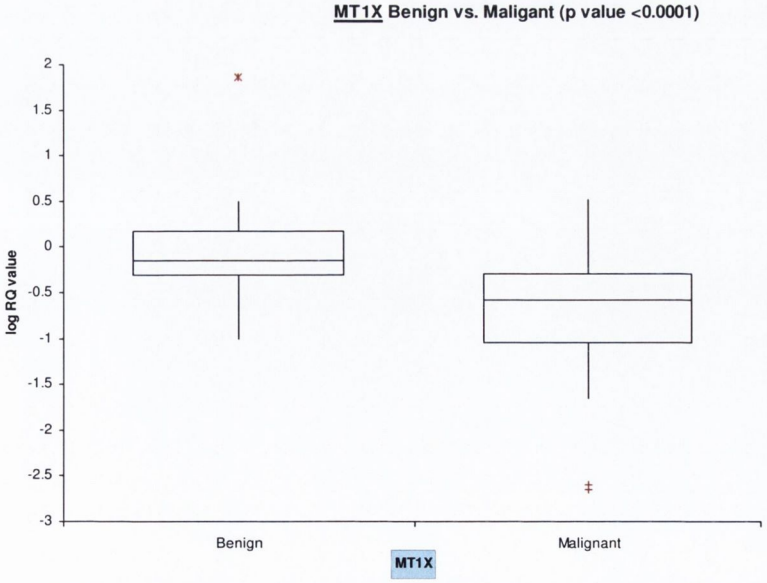

Figure 4.8 Displays the down-regulation of MT1X in the malignant cohort versus the benign cohort, p value <0.0001

MT1X

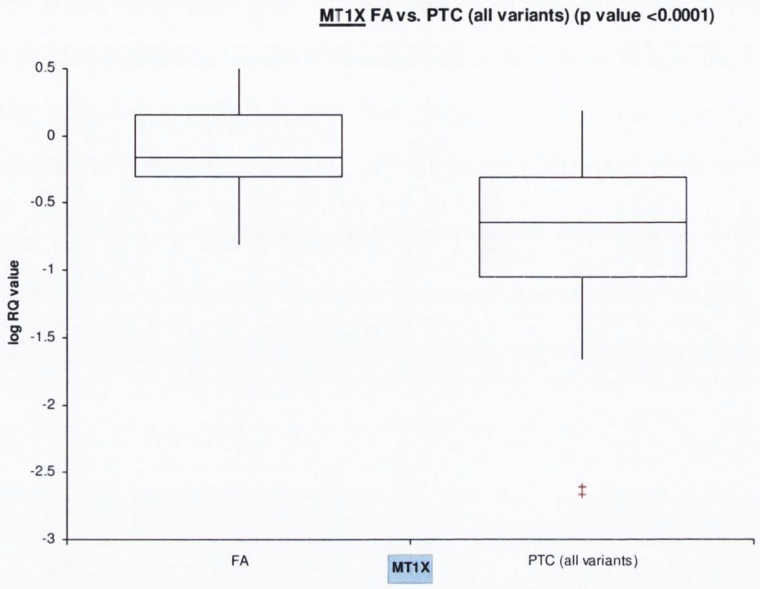

Figure 4.9 Illustrates how MT1X is down-regulated in the papillary thyroid carcinoma group, encompassing all variants of PTC versus the benign follicular adenoma (FA) cohort, p value <0.0001

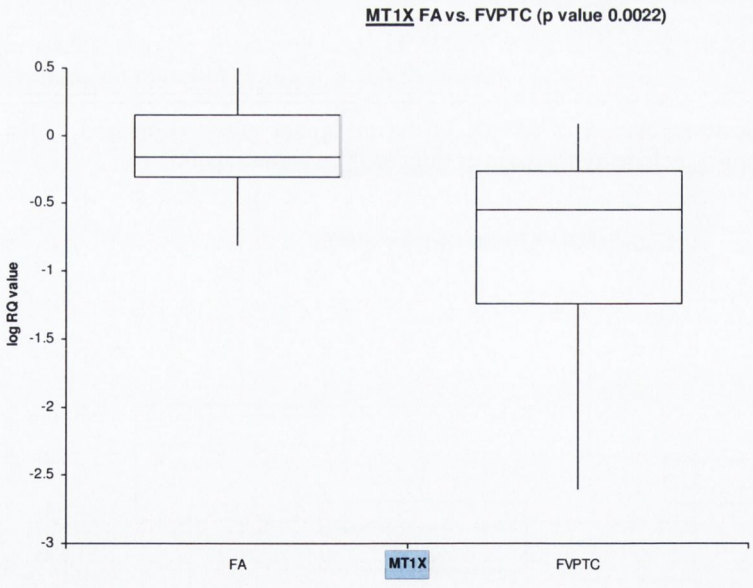

Figure 4.10 Demonstrates the down-regulation of the follicular variant of papillary thyroid carcinoma (FVPTC) versus the benign follicular adenoma group, p value 0.0022

4.5.1.4 CSNK1G2 boxplots

Caesin kinase I γ2 (CSNK1G2) is a serine/threonime protein kinase thought to be involved in insulin receptor and platelet-derived growth factor receptor signaling. As with the previous three targets, CSNK1G2 is down-regulated in malignant and neoplastic cohort compared to benign and hyperplasia.

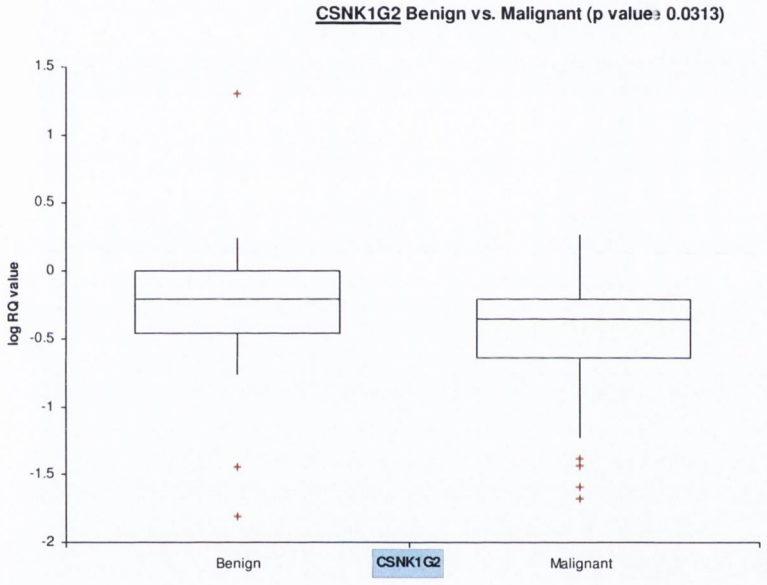

Figure 4.11 Demonstrates down-regulation of CSNK1G2 in the malignant cohort versus the benign cohort, p value 0.0313

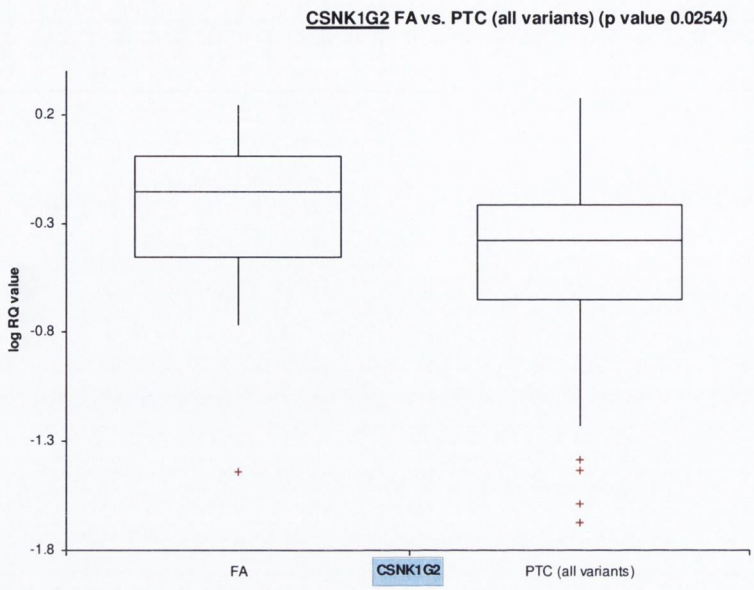

Figure 4.12 Displays the down-regulation of CSNK1G2 in the malignant papillary thyroid carcinoma group encompassing all variants of PTC versus the benign follicular adenoma (FA) group, p value 0.0254

4.5.1.5 TGFβ1 boxplots

Transforming growth factor beta 1 (TGFβ1) is a cytokine that regulates processes such as proliferation, differentiation and other functions in many cell types. Unlike the previous four targets TGFβ1 was up-regulated in neoplastic and PTC groups compared to non-neoplastic, benign and thyroiditis cohorts.

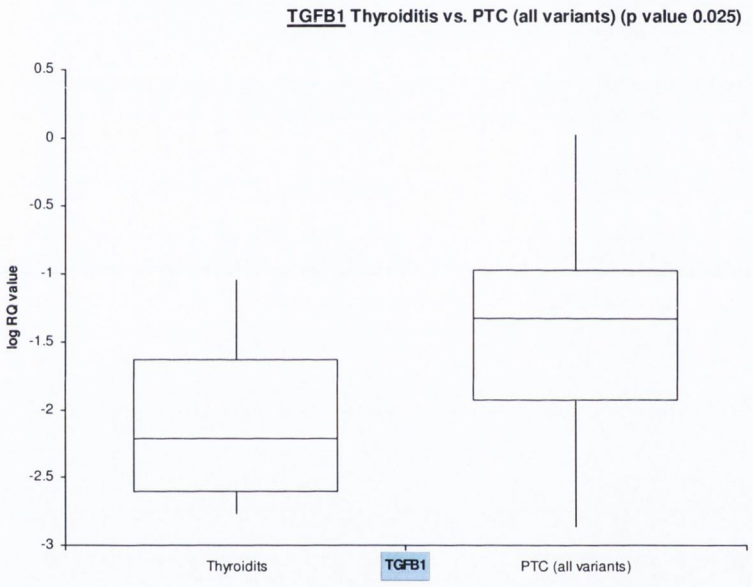

Figure 4.13 Illustrates the up-regulation of TGFβ1 in the malignant papillary thyroid carcinoma group encompassing all variants compared to the thyroiditis group, p value 0.025

4.5.1.6 IRF3 boxplots

Interferon regulatory factor 3 (IRF3) is a member of the interferon regulatory transcription factor family. IRF3 is up-regulated in the malignant papillary thyroid carcinoma groups compared to Hashimoto Thyroiditis and thyroiditis groups.

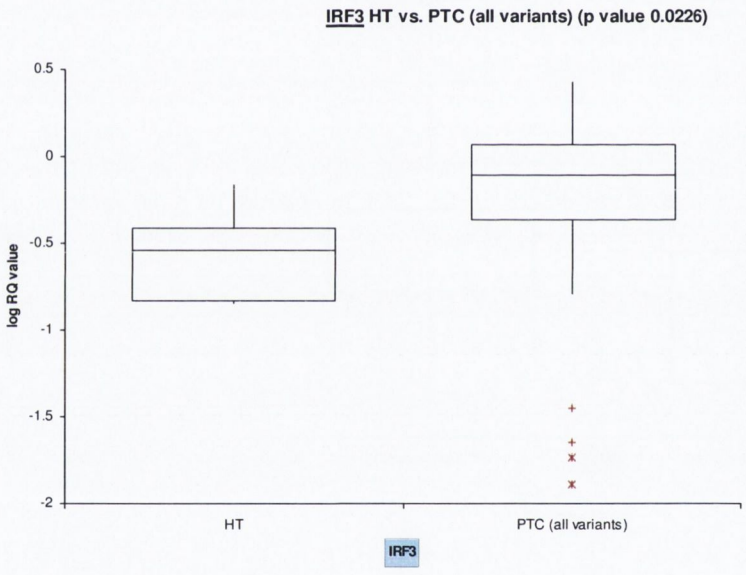

Figure 4.14 Illustrates the up-regulation of IRF3 in the malignant papillary thyroid carcinoma group (all variants) compared to Hashimoto Thyroiditis, p value 0.0226

4.5.1.7 CD74 boxplots

CD74 or the invariant chain (Ii) is a chaperone molecule that inhibits the binding of endogenous antigens to HLA class II. CD74 is up-regulated in the malignant and neoplastic cohorts versus non-neoplastic, hyperplasia and thyroiditis cohorts.

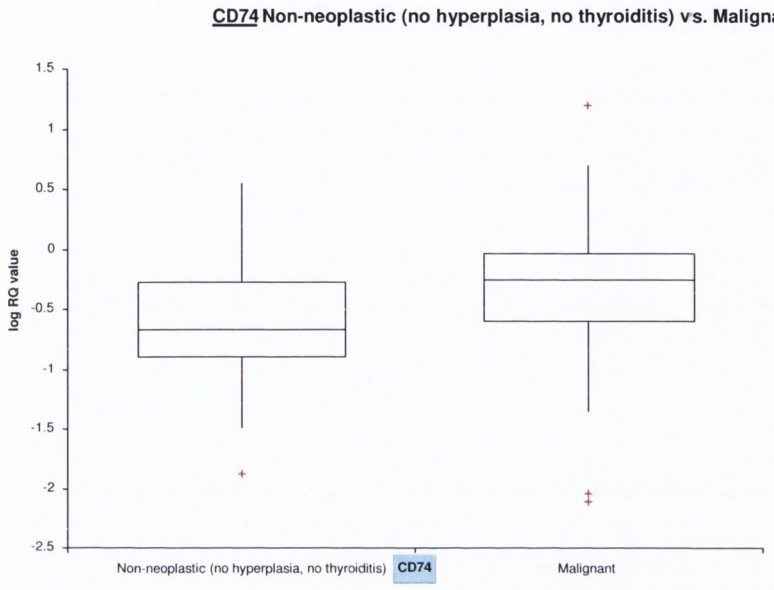

Figure 4.15 Displays the up-regulation of CD74 in the malignant cohort compared to the non-neoplastic (no hyperplasia, no thyroiditis) group, p value 0.0035

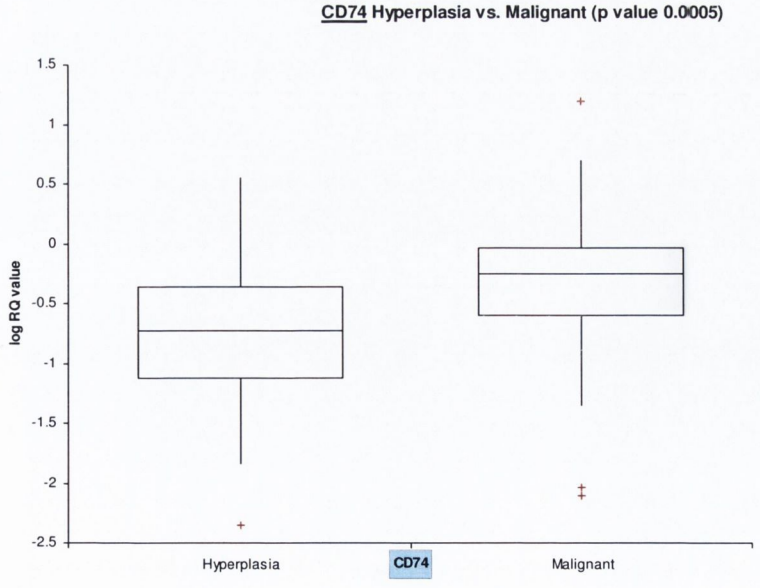

Figure 4.16 Illustrates up-regulation of the malignant cohort when compared to the hyperplastic cohort, p value 0.0005

4.5.1.8 HLA-DMA boxplots

HLA-DMA is a major histocompatibility complex (MHC) class II gene. As with CD74, HLA-DMA is up-regulated in the malignant and neoplastic groups versus non-neoplastic, hyperplasia and thyroiditis groups and in the follicular variant papillary thyroid carcinoma group when compared to follicular adenoma.

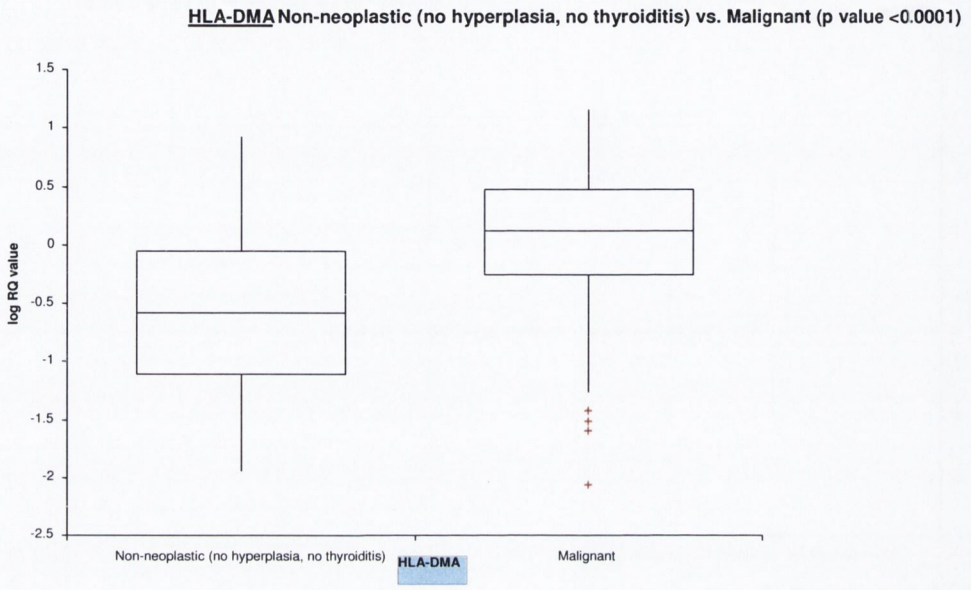

Figure 4.17 Illustrates the up-regulation of HLA-DMA in the malignant cohort versus non-neoplastic (no hyperplasia, no thyroiditis), p value <0.0001

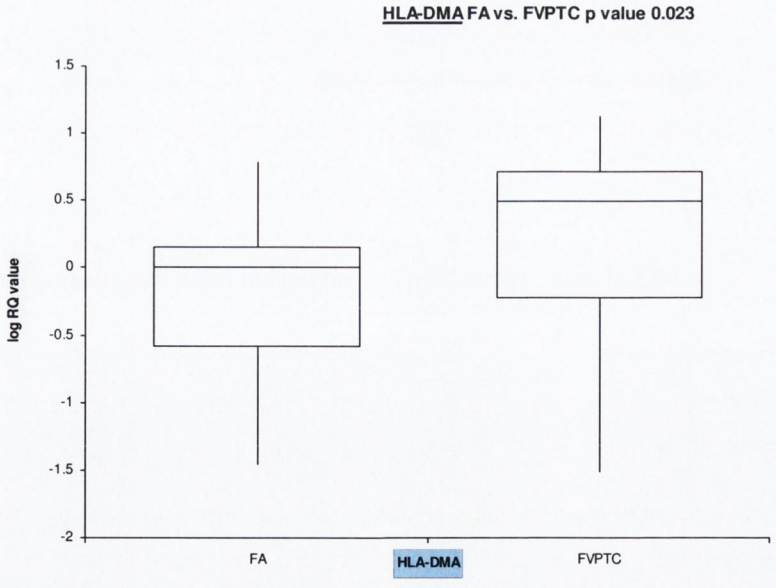

Figure 4.18 Demonstrates the up-regulation of HLA-DMA in the malignant follicular variant papillary thyroid carcinoma (FVPTC) group in comparison to the benign follicular adenoma (FA) group, p value 0.023

4.5.1.9 HLA-DQB1 boxplots

HLA-DQB1 is a member of the MHC class II genes and is also up-regulated in malignant and neoplastic groups compared to non-neoplastic, benign and hyperplasia cohorts.

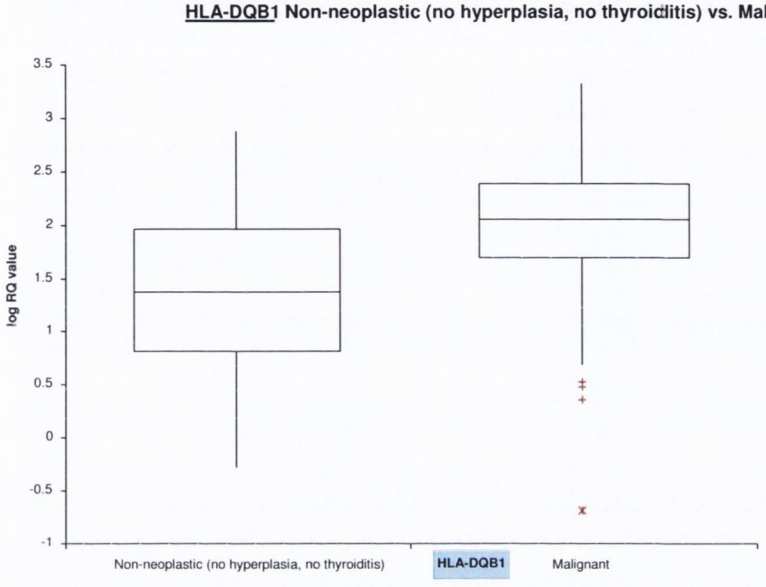

Figure 4.19 Illustrates the up-regulation of HLA-DQB1 in the malignant group versus the non-neoplastic (no hyperplasia, no thyroiditis) group, p value 0.0003

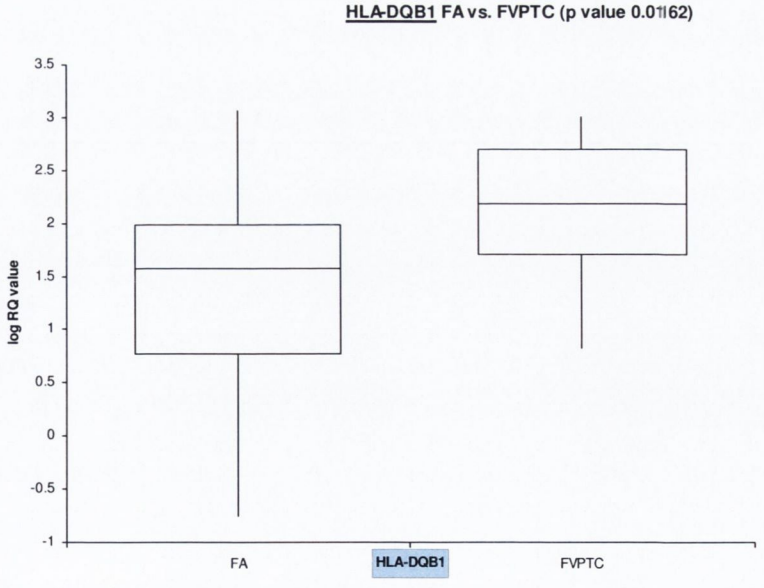

Figure 4.20 Illustrates the up-regulation of the malignant follicular variant papillary thyroid carcinoma (FVPTC) group compared to the benign follicular adenoma (FA) group, p value 0.0162

4.6 Discussion

4.6.1 Pre-amplification and endogenous control

The panel was applied to a series (n = 195) of formalin fixed paraffin embedded archival tissue samples using laser capture microdissection as a means to retrieve homogenous cell populations of thyroid epithelial cells. Although an accurate and precise technique, laser capture microdissection procures a small yield of RNA (yields in the range of 5ng/μL to 63ng/μL were achieved in this study). Relative quantitative analysis was performed to determine relative gene expression levels in each sample. To this end, equal quantities of RNA were used in each sample. Consequently only 5ng/μL (or 0.125μg in 25 μL) of RNA was available from each sample for use in each individual assay. In the past, gene expression studies using archival material have been limited to analysis of few targets (<4) in any given experiment (Kuramochi et al., 2006, Azuma et al., 2006, Chen and Ou, 2006, Vernooy et al., 2007). Limited quantities available from archival material become a greater issue when microdissection is introduced. While it is possible to repeat the preparation and microdissection using serial sections, this is time consuming and labour intensive, and requires pooling of extracts to achieve uniformity in analysis.

In this study we successfully performed TaqMan® RT-PCR analysis on a panel of eleven assays using a total of 0.125μg of input RNA for each of the one hundred and ninety five samples. This increased sensitivity was achieved using a novel pre-amplification technique (TaqMan® Pre-Amp Master Mix, Applied Biosysytems, CA, USA). The technique is intended for use with very small quantities of cDNA and facilitates multiplex pre-amplification up to 100-plex. Moreover, it generates unbiased amplicons of specific regions of the starting cDNA to be analyzed. In a separate study, (Li et al., 2008) our group has compared parallel extracts from fresh frozen paraffin embedded and snap frozen cell preparations using a normal thyroid cell line model applying the pre-amplification technique. The application of Pre-Amp lowered C_T values in snap frozen and fresh frozen paraffin embedded material when compared to snap frozen and formalin fixed paraffin embedded tissues that were not pre-amplified. This increased sensitivity was consistent and reproducible indicating that

pre-amplification does not distort relative expression levels rather it enhances sensitivity.

In selecting the endogenous control to be used as a normaliser in the study, two controls were initially proposed: glyceraldehyde-3-phosphate dehydrogenase (GAPDH) and cyclin dependent kinase inhibitor 1B (CDKN1B). Data correlating pre-amplified with unpre-amplified cDNA (Li et al., 2008) suggested that endogenous controls with an amplicon size similar to that of the assays to be utilized produced more reproducible expression data when parallel fresh and formalin fixed samples were analysed. The study compared amplicons over a range from 62 -122 base pairs (bp). In general, bias was introduced into the system when the amplicon size of the reference gene exceeded that of the target to be analysed. Given the commercially available GAPDH has an amplicon size of 122bp, it was decided to revert to CDKN1B (71bp) for calculation of relative expression, given its unchanging expression levels across samples tested.

4.6.2 Expression patterns

RAB23

Down-regulation of RAB23 was seen in all malignant and neoplastic cohorts compared to benign, non-neoplastic, and hyperplasia, also differentially expressed down-regulation of RAB23 in all follicular lesions compared to benign follicular adenoma was seen. RAB23 is a member of the RAS superfamily of small GTPases that function in the regulation of vesicular trafficking. It is the product of the gene mutated in the mouse open brain1 phenotype, which displays neural tube defects. It appears to antagonize sonic hedgehog (SHH)-mediated signalling during mouse development, presumably by regulating the intracellular trafficking of one or more of SHH's signalling components (Wang et al., 2006). The hedgehog signalling cascade is pivotal to embryonic development, and is involved in patterning a diverse range of vertebrate structures including the developing neural tube, lungs, skin, axial skeleton, teeth, hair and limbs, and also has a role in haematopoiesis (Wicking and McGlinn, 2001). In vertebrate neural systems, RAB23 acts as a negative regulator of hedgehog signalling (Evans et al., 2005, Eggenschwiler et al., 2001). Aberrant activation of this pathway in postnatal life has been associated with a range of cancers including lung,

prostate, colorectal and basal cell carcinomas of the skin (Daniel et al., 2006, Karhadkar et al., 2004, Akiyoshi et al., 2006, Athar et al., 2006). It is interesting to speculate that the absence of RAB23 and therefore the absence of a negative regulator of hedgehog signalling is implicated in the development of thyroid carcinoma.

Metallothioneins MT1K and MT1X

Metallothioneins (MTs) are a group of low molecular weight, cystein rich intracellular proteins, with at least ten functional isoforms in humans. Down-regulation of MT1K and MT1X was seen in all malignant and neoplastic groups compared to benign, non-neoplastic and hyperplastic. Both MT1K and MT1X were down-regulated in PTC versus thyroiditis while only MT1X showed differential expression between follicular lesions (FA vs. FVPTC). The expression and production of these proteins has been associated with protection against DNA damage, oxidative stress and apoptosis (Cherian et al., 2003). Work carried out in 2000 by Garett and co-workers (Garrett et al., 2000) confirmed down-regulation of MT1X in advanced prostate cancer. They used LCM and RT-PCR to demonstrate the loss of MT1X expression in prostate cancer samples in comparison to normal prostate tissue. MTs have also shown to be down-regulated in liver tumours (Deng et al., 1998, Cai et al., 1998) and colorectal adenocarcinomas (Ofner et al., 1994). To date, a number of microarray studies have show MT genes to be down-regulated in thyroid carcinoma (Huang et al., 2001, Barden et al., 2003, Finley et al., 2004). Huang and colleagues expanded on their initial microarray experiment by trying to identify novel tumour suppressor genes involved in thyroid tumourogenesis. They found that MT1G was down-regulated in PTC consequent to hypermethylation. In this study metallothioneins were observed to be under-expressed in all of the malignant cohorts. This finding fortifies their candidacy as tumor suppressor genes in the setting of thyroid neoplasia.

Casein kinase I γ2

Casein kinase I γ2 (CSNKIG2) was down-regulated in malignant and neoplastic groups compared to benign and hyperplasia. Casein kinase I represents a unique group of serine/threonine protein kinases that are ubiquitously expressed in eukaryotic organisms. Studies have shown that rat CSNKIG2 directly interacts with NCK adaptor protein (Lussier and Larose, 1997, Kitabayashi et al., 1997) and human CSNKIG2 has 94% homology with the rat homology (Kitabayashi et al., 1997). NCK is believed to act as an adaptor protein mediating signal transduction initiated by receptor tyrosine kinases, such as the insulin receptor, which has implications in the context of thyroid tumourogenesis as activation of the insulin receptor and other tyrosine kinase receptors are thought to play a role in thyroid cancer progression (Miyagi et al., 2004, Frittitta et al., 1999). It is feasible that CSNKIG2 is the isoform responsible for attenuating the insulin-mediated signalling pathway by modifying the receptor directly (Gross and Anderson, 1998). CSKNIG2 has also been shown to phosphorylate the ligand-activated platelet-derived growth factor receptor, a membrane protein-tyrosine kinase and result in its inactivation (Bioukar et al., 1999). Platelet-derived growth factor and the insulin receptor are essential for the regulation of cell growth and differentiation, factors which if were lost may result in cellular transformation. Marin and co-workers (Marin et al., 2003) showed that casein kinase I phosphotylates Ser-45 of β-catenin priming the subsequent phosphorylation by glycogen synthatase 3 that signals the degradation of β-catenin and prevents its function in triggering cell division in thyroid carcinoma. Furthermore, work by Garcia-Rostan et al (Garcia-Rostan et al., 2001, Garcia-Rostan et al., 1999) has correlated mutations of the casein kinase I target phosphorylation site in β-catenin with thyroid tumours.

Transforming growth factor beta 1 (TGFβ1)

TGFβ1 showed a differential pattern of gene regulation to the previous targets, it was up-regulated in neoplastic cohorts compared to non-neoplastic and hyperplasia, and was also up-regulated in PTC versus thyroiditis. TGFβ1 is initially secreted as a biologically latent complex that requires extracellular activation for receptor binding to occur and subsequent induction of gene expression through the transcription factors SMAD2 or SMAD3 complexed with SMAD4 (Wakefield and Roberts, 2002). Biological actions of TGFβ *in vitro* are very diverse. TGFβ appears to have tumour suppressive effects at early stages of cancer, while it appears to promote tumour progression in advanced carcinomas (Govinden and Bhoola, 2003, Glick, 2004, Prud'homme, 2007). TGFβ is a potent immunosuppressive cytokine; it is capable of counteracting and blocking production of IL-2, which is crucial for T cell proliferation, activation and expansion of cytotoxic T cells. TGFβ also inactivates natural killer and lymphokine-activated killer cells, enhances CD8 suppressor T cell formation and blocks immunoglobulin synthesis (Letterio and Roberts, 1998). Over-expression of TGFβ1 in neoplastic and malignant groups in this study may be due to its immunosuppressive effects aiding tumour growth and development.

Interferon regulatory factor 3 (IRF3)

IRF3 was up-regulated in the papillary thyroid carcinoma group when compared to the thyroiditis and Hashimoto Thyroiditis cohorts. IRF3 is a transcription factor that is activated in response to various environmental stresses such as viral infection and DNA-damaging agents. Korherr and colleagues (Korherr et al., 2006) used a genome wide phenotype screen to identify factors that induce proliferation of human umbilical vein endothelial cell (HUVEC), HUVEC proliferation being a recognized marker for factors that modulate vascularisation and angiogenesis. IRF3 was identified as a pro-angiogenic factor. IRF3 activates gene transcription of the CC chemokine CCL5 (RANTES) (Lin et al., 1999, Genin et al., 2000) which has been demonstrated to be produced by several tumours such as breast and melanoma (Azenshtein et al., 2002, Mrowietz et al., 1999, von Luettichau et al., 1996). CCL5s ability to promote tumourigenesis is thought to be due to monocyte recruitment within the tumour and

its ability to up-regulate matrix metalloproteases (Azenshtein et al., 2002). It is possible that the transcription factor IRF3 activates gene transcription of chemokines such as CCL5 which are capable of producing pro-tumourigenic affects in thyroid carcinoma.

Human leukocyte antigen (HLA) markers and associated genes (HLA-DMA, HLA-DQB1, CD74)

CD74 is a protein that regulates antigen presentation by HLA class II molecules by inhibiting their cytoplasmic form from binding to endogenously derived antigenic peptides (Ishigami et al., 2001). CD74 is then cleaved in an acidified endosome, leaving a short peptide fragment, CLIP, still bound to the MHC class II molecule. CD74 was up-regulated in malignant and neoplastic groups in comparison to benign, non-neoplastic, hyperplastic and Hashimoto Thyroiditis groups. It has been suggested that increased CD74 expression in tumour cells inhibits tumour antigen presentation by HLA-class II molecules, disrupting the HLA class II mediated immune stimulation by tumour cells (Clements et al., 1992, Ishigami et al., 2001, Jiang et al., 1999). This phenomenon could also occur in the setting of thyroid neoplasia as up-regulation of CD74 is seen in malignant and neoplastic groups.

As mentioned, CD74 is cleaved and leaves CLIP still bound to class II molecules. CLIP blocks the binding of endocytosed antigens that are degraded to peptides. HLA-DM binds to the class II: CLIP complex and catalyses the release of CLIP and the binding of other peptides to the empty MHC class II molecule. HLA-DM will continuously bind and rebind to peptide: class II complexes, removing weakly bound peptides and allowing other peptides to replace them, also known as "peptide editing" (Janeway, 2001). Expression of HLA-DMA was up-regulated in malignant and neoplastic groups in this study, it is interesting to speculate that over-production of HLA-DMA results in over-stimulation of this "peptide editing", resulting in the peptide: class II complex not being displayed for long enough on the surface of the antigen-presenting cell, and consequently the appropriate stimulation of CD4 cells does not occur and the tumour cell evades CD4 cell processing.

Up-regulated expression of HLA-DQB1 was also seen in the malignant and neoplastic cohorts. HLA-DQB1 binds and presents antigens on antigen presenting cells to CD4 T cells. A similar finding by Finn and colleagues (Finn et al., 2007) was observed where increased expression of class II MHC genes in follicular variant of papillary thyroid carcinoma was found. Hwang and colleagues (Hwang et al., 2004) have also demonstrated ret/PTC bearing papillary thyroid carcinoma cells that strongly express MHC class II (HLA-DRA) genes, although surrounding normal tissue did not. This observation suggests that over-expression of some MHC class II genes may represent a novel feature of malignant thyroid follicular epithelium, and may play a role in the evasion of the immune system.

4.6.3 Possible translational applications

Fine needle aspiration, histology and cytology are widely used in the initial diagnosis of thyroid malignancy. However they are impaired by limitations, such as the inability to definitively differentiate follicular adenomas from follicular carcinomas. Sangalli and co-workers (Sangalli et al., 2006) investigation into the efficacy of 5469 thyroid fine needle aspirations found a worryingly high false-negative rate of 6.2%, due to the failure to recognize follicular variant of papillary thyroid carcinoma. Inclusion of targets tested in this experiment into the routine testing protocol may provide useful adjunctive data in this setting. A number of groups have suggested molecular markers to assist in the diagnosis of papillary thyroid carcinoma from fine needle aspiration specimens (Cheung et al., 2001, Salvatore et al., 2004). Sapio and colleagues (Sapio et al., 2007) recently proposed detection of ret/PTC, TRK and BRAF (V600E) in fine needle aspiration specimens as a diagnostic adjunctive tool in the evaluation of thyroid nodules. They found that the discovery of oncogenes in fine needle aspiration specimens suspicious for malignancy guided the extent of surgical resection, changing the surgery from diagnostic to therapeutic in five cases. The application of these markers to the diagnosis of follicular lesions in thyroid carcinoma may hopefully provide another approach in the challenging diagnosis of these lesions.

4.7 Conclusions

In this experiment the aim was to validate the efficacy of a panel of markers identified through microarray analysis (Finn et al., 2007) by its application to a large series of archival benign and malignant thyroid lesions. Laser capture microdissection was employed to obtain homogenous populations of follicular epithelial cells. Any impediment due to low RNA yields from small cell numbers was surmounted using a novel pre-amplification technique that allowed interrogation of a large panel of targets in the study cohort. This study not only demonstrates the ability to draw on the substantial archive of formalin fixed paraffin embedded tissue available and to analyze samples with unbiased pre-amplification, but it also highlights nine gene targets that have robustly discriminated between sub-groups of thyroid lesions. There is scope for this panel to be further refined to include other gene targets proposed by microarray analysis. Future directions for this work may include further insight into the proposed tumor suppressor genes, in particular casein kinase I $\gamma 2$ as it appears to play a role in the activation of the insulin receptor and other tyrosine kinase receptors which are thought to be involved in thyroid cancer progression. Also further rationale is needed to explain the aberrant expression of the MHC II genes HLA-DMA and HLA-DQB1, as these could stand to represent a novel feature of malignant thyroid follicular epithelium.

Nonetheless, the study has established proof of principle that expression analysis may be reliably performed using a panel of markers in archival samples and this strategy may prove valuable as an adjunctive analytical tool in the diagnostic setting.

4.8 References:

Akiyoshi, T., Nakamura, M., Koga, K., Nakashima, H., Yao, T., Tsuneyoshi, M., Tanaka, M. & Katano, M. (2006) Gli1, downregulated in colorectal cancers, inhibits proliferation of colon cancer cells involving Wnt signalling activation. *Gut,* 55, 991-9.

Amrikachi, M., Ramzy, I., Rubenfeld, S. & Wheeler, T. M. (2001) Accuracy of fine-needle aspiration of thyroid. *Arch Pathol Lab Med,* 125, 484-8.

Athar, M., Tang, X., Lee, J. L., Kopelovich, L. & Kim, A. L. (2006) Hedgehog signalling in skin development and cancer. *Exp Dermatol,* 15, 667-77.

Azenshtein, E., Luboshits, G., Shina, S., Neumark, E., Shahbazian, D., Weil, M., Wigler, N., Keydar, I. & Ben-Baruch, A. (2002) The CC chemokine RANTES in breast carcinoma progression: regulation of expression and potential mechanisms of promalignant activity. *Cancer Res,* 62, 1093-102.

Azuma, M., Danenberg, K. D., Iqbal, S., El-Khoueiry, A., Zhang, W., Yang, D., Koizumi, W., Saigenji, K., Danenberg, P. V. & Lenz, H. J. (2006) Epidermal growth factor receptor and epidermal growth factor receptor variant III gene expression in metastatic colorectal cancer. *Clin Colorectal Cancer,* 6, 214-8.

Baloch, Z., and Va. Livolsi (2005) Pathology. *IN: The Thyroid A Fundamental and Clinical Text Braverman LE and Utiger RD.,* 9th Edition, 422-449.

Barden, C. B., Shister, K. W., Zhu, B., Guiter, G., Greenblatt, D. Y., Zeiger, M. A. & Fahey, T. J., 3rd (2003) Classification of follicular thyroid tumors by molecular signature: results of gene profiling. *Clin Cancer Res,* 9, 1792-800.

Bioukar, E. B., Marricco, N. C., Zuo, D. & Larose, L. (1999) Serine phosphorylation of the ligand-activated beta-platelet-derived growth factor receptor by casein kinase I-gamma2 inhibits the receptor's autophosphorylating activity. *J Biol Chem,* 274, 21457-63.

Cai, L., Wang, G. J., Xu, Z. L., Deng, D. X., Chakrabarti, S. & Cherian, M. G. (1998) Metallothionein and apoptosis in primary human hepatocellular carcinoma (HCC) from northern China. *Anticancer Res,* 18, 4667-72.

Chan, J., Hirokawa, M., Evan, H., Williams, E., Osamura, Y., Cady, B., Sobrinho-Simoes, M., Derwahl, M., Paschke, R., Belge, G., Oriola, J., Studer, H., Eng, C., Asa, S., Lloyd, R., Baloch, Z., Ghossein, R., Mazzaferri, E., Fagin, Ja (2004) *WHO classification of tumours: pathology and genetics of tumours of endocrine organs, Tumours of the thyroid and parathyroid: follicular adenoma. DELELLIS, R., LLOYD, R., HEITZ, P., ENG, C.* Lyon, IARC Press.

Chen, C. L. & Ou, D. L. (2006) Expression of syndecan-1 (CD138) in nasopharyngeal carcinoma is correlated with advanced stage and poor prognosis. *Hum Pathol,* 37, 1279-85.

Cherian, M. G., Jayasurya, A. & Bay, B. H. (2003) Metallothioneins in human tumors and potential roles in carcinogenesis. *Mutat Res,* 533, 201-9.

Cheung, C. C., Carydis, B., Ezzat, S., Bedard, Y. C. & Asa, S. L. (2001) Analysis of ret/PTC gene rearrangements refines the fine needle aspiration diagnosis of thyroid cancer. *J Clin Endocrinol Metab,* 86, 2187-90.

Clements, V. K., Baskar, S., Armstrong, T. D. & Ostrand-Rosenberg, S. (1992) Invariant chain alters the malignant phenotype of MHC class II+ tumor cells. *J Immunol,* 149, 2391-6.

Daniel, V. C., Peacock, C. D. & Watkins, D. N. (2006) Developmental signalling pathways in lung cancer. *Respirology,* 11, 234-40.

Deng, D. X., Chakrabarti, S., Waalkes, M. P. & Cherian, M. G. (1998) Metallothionein and apoptosis in primary human hepatocellular carcinoma and metastatic adenocarcinoma. *Histopathology,* 32, 340-7.

Eggenschwiler, J. T., Espinoza, E. & Anderson, K. V. (2001) Rab23 is an essential negative regulator of the mouse Sonic hedgehog signalling pathway. *Nature,* 412, 194-8.

Espina, V., Wulfkuhle, J. D., Calvert, V. S., Vanmeter, A., Zhou, W., Coukos, G., Geho, D. H., Petricoin, E. F., 3rd & Liotta, L. A. (2006) Laser-capture microdissection. *Nat Protoc,* 1, 586-603.

Eszlinger, M., Krohn, K., Hauptmann, S., Dralle, H., Giordano, T. J. & Paschke, R. (2008) Perspectives for improved and more accurate classification of thyroid epithelial tumors. *J Clin Endocrinol Metab.*

Evans, T. M., Simpson, F., Parton, R. G. & Wicking, C. (2005) Characterization of Rab23, a negative regulator of sonic hedgehog signaling. *Methods Enzymol,* 403, 759-77.

Faquin, W. C. (2008) The thyroid gland: recurring problems in histologic and cytologic evaluation. *Arch Pathol Lab Med,* 132, 622-32.

Finley, D. J., Arora, N., Zhu, B., Gallagher, L. & Fahey, T. J., 3rd (2004) Molecular profiling distinguishes papillary carcinoma from benign thyroid nodules. *J Clin Endocrinol Metab,* 89, 3214-23.

Finn, S. P., Smyth, P., Cahill, S., Streck, C., O'regan E, M., Flavin, R., Sherlock, J., Howells, D., Henfrey, R., Cullen, M., Toner, M., Timon, C., O'leary J, J. & Sheils, O. M. (2007) Expression microarray analysis of papillary thyroid carcinoma and benign thyroid tissue: emphasis on the follicular variant and potential markers of malignancy. *Virchows Arch,* 450, 249-60.

Frittitta, L., Sciacca, L., Catalfamo, R., Ippolito, A., Gangemi, P., Pezzino, V., Filetti, S. & Vigneri, R. (1999) Functional insulin receptors are overexpressed in thyroid tumors: is this an early event in thyroid tumorigenesis? *Cancer,* 85, 492-8.

Garcia-Rostan, G., Camp, R. L., Herrero, A., Carcangiu, M. L., Rimm, D. L. & Tallini, G. (2001) Beta-catenin dysregulation in thyroid neoplasms: down-regulation, aberrant nuclear expression, and CTNNB1 exon 3 mutations are markers for aggressive tumor phenotypes and poor prognosis. *Am J Pathol,* 158, 987-96.

Garcia-Rostan, G., Tallini, G., Herrero, A., D'aquila, T. G., Carcangiu, M. L. & Rimm, D. L. (1999) Frequent mutation and nuclear localization of beta-catenin in anaplastic thyroid carcinoma. *Cancer Res,* 59, 1811-5.

Garrett, S. H., Sens, M. A., Shukla, D., Flores, L., Somji, S., Todd, J. H. & Sens, D. A. (2000) Metallothionein isoform 1 and 2 gene expression in the human prostate: downregulation of MT-1X in advanced prostate cancer. *Prostate,* 43, 125-35.

Genin, P., Algarte, M., Roof, P., Lin, R. & Hiscott, J. (2000) Regulation of RANTES chemokine gene expression requires cooperativity between NF-kappa B and IFN-regulatory factor transcription factors. *J Immunol,* 164, 5352-61.

Glick, A. B. (2004) TGFbeta1, back to the future: revisiting its role as a transforming growth factor. *Cancer Biol Ther,* 3, 276-83.

Govinden, R. & Bhoola, K. D. (2003) Genealogy, expression, and cellular function of transforming growth factor-beta. *Pharmacol Ther,* 98, 257-65.

Gross, S. D. & Anderson, R. A. (1998) Casein kinase I: spatial organization and positioning of a multifunctional protein kinase family. *Cell Signal,* 10, 699-711.

Hall, T. L., Layfield, L. J., Philippe, A. & Rosenthal, D. L. (1989) Sources of diagnostic error in fine needle aspiration of the thyroid. *Cancer,* 63, 718-25.

Hawkins, F., Bellido, D., Bernal, C., Rigopoulou, D., Ruiz Valdepenas, M. P., Lazaro, E., Perez-Barrios, A. & De Agustin, P. (1987) Fine needle aspiration biopsy in the diagnosis of thyroid cancer and thyroid disease. *Cancer,* 59, 1206-9.

Huang, Y., Prasad, M., Lemon, W. J., Hampel, H., Wright, F. A., Kornacker, K., Livolsi, V., Frankel, W., Kloos, R. T., Eng, C., Pellegata, N. S. & De La Chapelle, A. (2001) Gene expression in papillary thyroid carcinoma reveals highly consistent profiles. *Proc Natl Acad Sci U S A,* 98, 15044-9.

Hwang, E. S., Kim, D. W., Hwang, J. H., Jung, H. S., Suh, J. M., Park, Y. J., Chung, H. K., Song, J. H., Park, K. C., Park, S. H., Yun, H. J., Kim, J. M. & Shong, M. (2004) Regulation of signal transducer and activator of transcription 1 (STAT1) and STAT1-dependent genes by RET/PTC (rearranged in transformation/papillary thyroid carcinoma) oncogenic tyrosine kinases. *Mol Endocrinol,* 18, 2672-84.

Ishigami, S., Natsugoe, S., Tokuda, K., Nakajo, A., Iwashige, H., Aridome, K., Hokita, S. & Aikou, T. (2001) Invariant chain expression in gastric cancer. *Cancer Lett,* 168, 87-91.

Janeway, C., Travers, P., Walport, M., Shlomchik (2001) *Immunobiology, The immune system in health and disease.* New York, NY, Garland Publishing.

Jiang, Z., Xu, M., Savas, L., Leclair, P. & Banner, B. F. (1999) Invariant chain expression in colon neoplasms. *Virchows Arch,* 435, 32-6.

Karhadkar, S. S., Bova, G. S., Abdallah, N., Dhara, S., Gardner, D., Maitra, A., Isaacs, J. T., Berman, D. M. & Beachy, P. A. (2004) Hedgehog signalling in prostate regeneration, neoplasia and metastasis. *Nature,* 431, 707-12.

Kitabayashi, A. N., Kusuda, J., Hirai, M. & Hashimoto, K. (1997) Cloning and chromosomal mapping of human casein kinase I gamma 2 (CSNK1G2). *Genomics,* 46, 133-7.

Korherr, C., Gille, H., Schafer, R., Koenig-Hoffmann, K., Dixelius, J., Egland, K. A., Pastan, I. & Brinkmann, U. (2006) Identification of proangiogenic genes and pathways by high-throughput functional genomics: TBK1 and the IRF3 pathway. *Proc Natl Acad Sci U S A,* 103, 4240-5.

Kuramochi, H., Hayashi, K., Uchida, K., Miyakura, S., Shimizu, D., Vallbohmer, D., Park, S., Danenberg, K. D., Takasaki, K. & Danenberg, P. V. (2006) Vascular endothelial growth factor messenger RNA expression level is preserved in liver metastases compared with corresponding primary colorectal cancer. *Clin Cancer Res,* 12, 29-33.

Letterio, J. J. & Roberts, A. B. (1998) Regulation of immune responses by TGF-beta. *Annu Rev Immunol,* 16, 137-61.

Li, J., Smyth, P., Cahill, S., Denning, K., Flavin, R., Aherne, S., Pirotta, M., Guenther, S. M., O'leary, J. J. & Sheils, O. (2008) Improved RNA quality and TaqMan Pre-amplification method (PreAmp) to enhance expression analysis from formalin fixed paraffin embedded (FFPE) materials. *BMC Biotechnol,* 8, 10.

Lin, R., Heylbroeck, C., Genin, P., Pitha, P. M. & Hiscott, J. (1999) Essential role of interferon regulatory factor 3 in direct activation of RANTES chemokine transcription. *Mol Cell Biol,* 19, 959-66.

Liu, J., Singh, B., Tallini, G., Carlson, D. L., Katabi, N., Shaha, A., Tuttle, R. M. & Ghossein, R. A. (2006) Follicular variant of papillary thyroid carcinoma: a clinicopathologic study of a problematic entity. *Cancer,* 107, 1255-64.

Livak, K. J. & Schmittgen, T. D. (2001) Analysis of relative gene expression data using real-time quantitative PCR and the 2(-Delta Delta C(T)) Method. *Methods,* 25, 402-8.

Lussier, G. & Larose, L. (1997) A casein kinase I activity is constitutively associated with Nck. *J Biol Chem,* 272, 2688-94.

Marin, O., Bustos, V. H., Cesaro, L., Meggio, F., Pagano, M. A., Antonelli, M., Allende, C. C., Pinna, L. A. & Allende, J. E. (2003) A noncanonical sequence phosphorylated by casein kinase 1 in beta-catenin may play a role in casein

kinase 1 targeting of important signaling proteins. *Proc Natl Acad Sci U S A,* 100, 10193-200.

McCall, A., Jarosz, H., Lawrence, A. M. & Paloyan, E. (1986) The incidence of thyroid carcinoma in solitary cold nodules and in multinodular goiters. *Surgery,* 100, 1128-32.

Miyagi, E., Braga-Basaria, M., Hardy, E., Vasko, V., Burman, K. D., Jhiang, S., Saji, M. & Ringel, M. D. (2004) Chronic expression of RET/PTC 3 enhances basal and insulin-stimulated PI3 kinase/AKT signaling and increases IRS-2 expression in FRTL-5 thyroid cells. *Mol Carcinog,* 41, 98-107.

Mrowietz, U., Schwenk, U., Maune, S., Bartels, J., Kupper, M., Fichtner, I., Schroder, J. M. & Schadendorf, D. (1999) The chemokine RANTES is secreted by human melanoma cells and is associated with enhanced tumour formation in nude mice. *Br J Cancer,* 79, 1025-31.

Nair, M., Kapila, K., Karak, A. K. & Verma, K. (2001) Papillary carcinoma of the thyroid and its variants: a cytohistological correlation. *Diagn Cytopathol,* 24, 167-73.

Ofner, D., Maier, H., Riedmann, B., Bammer, T., Rumer, A., Winde, G., Bocker, W., Jasani, B. & Schmid, K. W. (1994) Immunohistochemical metallothionein expression in colorectal adenocarcinoma: correlation with tumour stage and patient survival. *Virchows Arch,* 425, 491-7.

Prud'homme, G. J. (2007) Pathobiology of transforming growth factor beta in cancer, fibrosis and immunologic disease, and therapeutic considerations. *Lab Invest,* 87, 1077-91.

Ravetto, C., Colombo, L. & Dottorini, M. E. (2000) Usefulness of fine-needle aspiration in the diagnosis of thyroid carcinoma: a retrospective study in 37,895 patients. *Cancer,* 90, 357-63.

Rosai, J., Carcangiu, M., Delellis, R. (1992) *Tumors of the thyroid gland, Atlas of Tumor Pathology. ROSAI, J., SOBIN, LH.* Washington DC, Armed Forces Institute of Pathology

Salvatore, G., Giannini, R., Faviana, P., Caleo, A., Migliaccio, I., Fagin, J. A., Nikiforov, Y. E., Troncone, G., Palombini, L., Basolo, F. & Santoro, M. (2004) Analysis of BRAF point mutation and RET/PTC rearrangement refines the fine-needle aspiration diagnosis of papillary thyroid carcinoma. *J Clin Endocrinol Metab,* 89, 5175-80.

Sangalli, G., Serio, G., Zampatti, C., Bellotti, M. & Lomuscio, G. (2006) Fine needle aspiration cytology of the thyroid: a comparison of 5469 cytological and final histological diagnoses. *Cytopathology,* 17, 245-50.

Sapio, M. R., Posca, D., Raggioli, A., Guerra, A., Marotta, V., Deandrea, M., Motta, M., Limone, P. P., Troncone, G., Caleo, A., Rossi, G., Fenzi, G. & Vitale, M.

(2007) Detection of RET/PTC, TRK and BRAF mutations in preoperative diagnosis of thyroid nodules with indeterminate cytological findings. *Clin Endocrinol (Oxf),* 66, 678-83.

Schmid, K. W. & Farid, N. R. (2006) How to define follicular thyroid carcinoma? *Virchows Arch,* 448, 385-393.

Soderstrom, N. (1952) Puncture of goiters for aspiration biopsy. *Acta Med Scand,* 144, 237-44.

Vernooy, J. H., Moller, G. M., Van Suylen, R. J., Van Spijk, M. P., Cloots, R. H., Hoet, P. H., Pennings, H. J. & Wouters, E. F. (2007) Increased granzyme A expression in type II pneumocytes of patients with severe chronic obstructive pulmonary disease. *Am J Respir Crit Care Med,* 175, 464-72.

Von Luettichau, I., Nelson, P. J., Pattison, J. M., Van De Rijn, M., Huie, P., Warnke, R., Wiedermann, C. J., Stahl, R. A., Sibley, R. K. & Krensky, A. M. (1996) RANTES chemokine expression in diseased and normal human tissues. *Cytokine,* 8, 89-98.

Wakefield, L. M. & Roberts, A. B. (2002) TGF-beta signaling: positive and negative effects on tumorigenesis. *Curr Opin Genet Dev,* 12, 22-9.

Wang, Y., Ng, E. L. & Tang, B. L. (2006) Rab23: what exactly does it traffic? *Traffic,* 7, 746-50.

Wicking, C. & Mcglinn, E. (2001) The role of hedgehog signalling in tumorigenesis. *Cancer Lett,* 173, 1-7.

Chapter Five

A molecular expression signature distinguishing thyroid carcinoma lesions using pre-amplification Q-RT-PCR and immunohistochemistry

5.1 Summary

This chapter builds on themes introduced in the previous chapter where expression profiles distinguishing thyroid lesions were generated from microarray data using quantitative RT-PCR. In this chapter a more detailed molecular signature for thyroid malignancy is examined, again using targets chosen from microarray data, to interrogate its utility as a biomarker for thyroid malignancy. This molecular signature consists of a panel of targets (n=5) whose expression was examined in 205 archival thyroid samples at the gene and protein level of expression using pre-amplification Q-RT-PCR and immunohistochemistry.

Two hundred and five formalin fixed paraffin embedded (FFPE) thyroid samples were laser capture microdissected and a novel pre-amplification technique was used to facilitate gene expression analysis using TaqMan® Q-RT-PCR of a panel of 5 targets including MMP11, BAX, APOE, TOP2A and LYN plus endogenous control. A tissue microarray (TMA) was constructed using the same two hundred and five samples and immunohistochemical analysis was carried out for MMP11, BAX, APOE, TOP2A and LYN.

All five targets were found to significantly ($p < 0.05$) discriminate a range of benign from malignant thyroid disease states at mRNA and protein expression levels. Four out of the five targets were also shown to significantly differentiate, at the gene and protein level, corresponding groups of matched samples. This robust panel of molecular markers could prove extremely useful in assisting the classification and diagnosis of thyroid malignancy.

5.2 Introduction

In the previous chapter, a panel of ten targets were chosen from microarray data (Finn et al., 2007) to assess their utility as adjunctive markers in the diagnosis of thyroid malignancy. In this chapter the aim is to assess in more detail, the utility of another panel of targets, using immunohistochemistry as well as quantitative real time PCR.

As the previous chapter gave an introduction to the aspects of molecular biomarker discovery that are important in thyroid carcinoma, it is unnecessary to reiterate these topics in this chapter. However, an aspect that was not covered in the previous chapter, the use of tissue microarrays, will be discussed here.

5.2.1 Tissue microarrays

In 1986, Hector Battifora (Battifora, 1986) first introduced the so-called "sausage" or multi tumour tissue block, where 1 mm thick rods of tissue specimen were carefully wrapped in sheets of small intestine and this sausage of tissue was embedded into a paraffin block. Although this technique did allow simultaneous examination of multiple tissue specimens under identical conditions, the inability to satisfactorily identify individual tissue rods undid the cause (Radhakrishnan et al., 2008). It was Juha Kononen and colleagues in 1998 (Kononen et al., 1998) who described the technique in its current shape.

Tissue microarrays allow high-throughput molecular profiling of diseases by simultaneous analysis of hundreds of archival tissue specimens. It is a purely mechanical technique which involves taking tissue core samples from multiple "donor" blocks with subsequent precise insertion (arraying) into an empty "recipient" block-the TMA block (Gulmann, 2003). Commercially available (and homemade) tissue microarray devices principally consist of three key components: 1) a hollow needle (a 0.6mm needle in diameter was used here), which is used to produce holes in an empty paraffin block (the recipient block); 2) another hollow needle with a slightly thinner diameter to punch a tissue core from the donor tissue block and to release the

tissue core into the pre-made hole of the recipient block; and 3) a micromanipulated "XY" stage that moves the recipient block to the predefined coordinates (Simon and Sauter, 2003).

The preparation and design involved in making a TMA is time-consuming and may be considered as a project in itself. The most important prerequisite for TMA construction is a large collection of well characterised tissues. Most of the time and effort in TMA construction is spent in the search, organisation, pathological review and processing of the tissue specimens. Once all specimens have been selected that meet the histological requirements, the corresponding paraffin blocks are sorted in the order of appearance in the TMA. In parallel, a database is generated providing the array coordinates for each tissue sample.

A concern regarding TMA technology is whether the small size of the tissue samples (0.6 mm) can be representative of an entire tumour. Many published studies on TMAs have addressed the issue of heterogeneity and the concordance with whole sections (Nocito et al., 2001, Hoos et al., 2001, Engellau et al., 2001, Torhorst et al., 2001, Camp et al., 2000). Two to four 0.6 mm cores per case showed over 90% concordance with whole sections. As well as this, it has been noted that tumour heterogeneity is less of a concern if the focus of the study is expression profiles of tumour populations rather than individual cases, (Gulmann, 2003) as is the case here.

Finally some other advantages of note with regards to TMA technology are; standardisation - the use of TMAs provide uniform reaction conditions thereby reducing variability of incubation times, temperature, wash conditions and antigen retrieval. TMAs allow the economisation of reagents and labour, and speed up the analysis of results. Also, donor blocks may be cored without damaging them (due to the small size and number of cores taken) and returned to archives.

5.3 Aims

The aim of this chapter was to assess, in greater detail, the efficacy of a panel of markers chosen via microarray technology as adjuncts in the diagnosis of thyroid malignancy on a cohort (n=205) of archival thyroid samples. To this end, a novel pre-amplification technique was used to assist TaqMan® gene expression analysis, while a TMA was constructed for protein analysis using immunohistochemistry.

5.4 Materials and methods

5.4.1 Samples

Two hundred and five cases of formalin-fixed paraffin embedded thyroid samples were analysed in this chapter, this cohort includes the one hundred and ninety five cases that were utilised in chapter four plus an additional ten samples. All samples were accessioned from archives dating from 2000-2005 at St. James Hospital, Dublin. The study had the approval of the St. James Hospital and Adelaide and Meath Hospital research ethics committee. Haematoxylin and eosin (H&E) sections were reviewed by a histopathologist (S.F) and classified according to a recognized system (Rosai, 1992). Corresponding paraffin blocks were then collected from the archives of St. James Hospital. The tables overleaf list the two hundred and five samples grouped into their corresponding diagnostic categories. As in the previous chapter, the majority of the categories have an overlap of the two hundred and five samples. The non-neoplastic (incl. hyperplasia and thyroiditis) group (n=109) and the neoplastic group (n=96) constitute the overall cohort of two hundred and five samples.

The following tables (tables 5.1- 5.18) represent the grouping of samples into analysis cohorts. All samples emanate from the cohort of two hundred and five. Some samples are represented more than once in the different analysis groups.

Non-neoplastic (no thyroiditis, no hyperplasia) (n=47)
No evidence of malignancy
No evidence of malignancy
No evidence of malignancy
No evidence of malignancy
No evidence of malignancy
No evidence of malignancy
No evidence of malignancy
No evidence of malignancy
No evidence of malignancy
No evidence of malignancy
No evidence of malignancy
No evidence of malignancy
No evidence of malignancy
No evidence of malignancy
No evidence of malignancy
No evidence of malignancy
Goitre, colloid
Goitre, colloid
Goitre, colloid
Goitre, colloid
Goitre
Goitre, colloid
Goitre, colloid
Goitre, colloid
Goitre, colloid
Goitre, colloid
Goitre, colloid
Goitre, colloid
Goitre, colloid
Goitre, colloid
Goitre, colloid
Goitre, colloid
Goitre, colloid
Goitre, colloid
Goitre
Goitre, colloid
Goitre
Goitre, adenomatous
Goitre
Goitre, adenomatous
Goitre, colloid
Goitre, colloid
Goitre, colloid
Goitre, colloid

Goitre, colloid
Goitre, adenomatous
Goitre, adenomatous

Table 5.1 Non-neoplastic (no hyperplasia, no thyroiditis) samples

Non-neoplastic (no hyperplasia) (n=56)
Hashimoto Thyroiditis
Hashimoto Thyroiditis
Hashimoto Thyroiditis
Hashimoto Thyroiditis
Hashimoto Thyroiditis
Hashimoto Thyroiditis
Inflammation chronic
Lymphocytic thyroiditis
Lymphocytic infiltrate
No evidence of malignancy
No evidence of malignancy
No evidence of malignancy
No evidence of malignancy
No evidence of malignancy
No evidence of malignancy
No evidence of malignancy
No evidence of malignancy
No evidence of malignancy
No evidence of malignancy
No evidence of malignancy
No evidence of malignancy
No evidence of malignancy
No evidence of malignancy
No evidence of malignancy
No evidence of malignancy
Goitre, colloid
Goitre, colloid
Goitre, colloid
Goitre, colloid
Goitre
Goitre, colloid
Goitre, colloid
Goitre, colloid
Goitre, colloid
Goitre, colloid
Goitre, colloid
Goitre, colloid
Goitre, colloid
Goitre, colloid
Goitre, colloid
Goitre, colloid
Goitre, colloid
Goitre, colloid
Goitre
Goitre, colloid
Goitre

Goitre, adenomatous
Goitre
Goitre, adenomatous
Goitre, colloid
Goitre, colloid
Goitre, colloid
Goitre, colloid
Goitre, colloid
Goitre, adenomatous
Goitre, adenomatous

Table 5.2 Non-neoplastic (no hyperplasia) samples

Non-neoplastic (incl. hyperplasia and thyroiditis) (n=109)
Hashimoto Thyroiditis
Hashimoto Thyroiditis
Hashimoto Thyroiditis
Hashimoto Thyroiditis
Hashimoto Thyroiditis
Hashimoto Thyroiditis
Inflammation chronic
Lymphocytic thyroiditis
Lymphocytic infiltrate
No evidence of malignancy
No evidence of malignancy
No evidence of malignancy
No evidence of malignancy
No evidence of malignancy
No evidence of malignancy
No evidence of malignancy
No evidence of malignancy
No evidence of malignancy
No evidence of malignancy
No evidence of malignancy
No evidence of malignancy
No evidence of malignancy
No evidence of malignancy
No evidence of malignancy
No evidence of malignancy
No evidence of malignancy
Goitre, colloid
Goitre, colloid
Goitre, colloid
Goitre, colloid
Goitre
Goitre, colloid
Goitre, colloid
Goitre, colloid
Goitre, colloid
Goitre, colloid
Goitre, colloid
Goitre, colloid
Goitre, colloid
Goitre, colloid
Goitre, colloid

Goitre, colloid
Goitre, colloid
Goitre, colloid
Goitre, colloid
Goitre
Goitre, colloid
Goitre
Goitre, adenomatous
Goitre
Goitre, adenomatous
Goitre, colloid
Goitre, colloid
Goitre, colloid
Goitre, colloid
Goitre, colloid
Goitre, adenomatous
Goitre, adenomatous
Graves
Graves
Graves
Graves
Graves
Hyperthyroidism
Hyperplasia, nodular
Hyperplasia, nodular
Hyperplasia, nodular
Hyperplasia, nodular
Hyperplasia, nodular
Hyperplasia, nodular
Hyperplasia
Hyperplasia, nodular
Hyperplasia, nodular
Hyperplasia, nodular
Hyperplasia, nodular
Hyperplasia, nodular
Hyperplasia, nodular
Hyperplasia, nodular
Hyperplasia, nodular
Hyperplasia
Hyperplasia, nodular
Hyperplasia + lymphocytic thyroiditis
Hyperplasia + lymphocytic thyroiditis
Hyperplasia, nodular + lymphocytic thyroiditis
Hyperplasia + lymphocytic thyroiditis
Hyperplasia, nodular
Hyperplasia
Hyperplasia, nodular
Hyperplasia, nodular
Hyperplasia, nodular
Hyperplasia, nodular
Hyperplasia, nodular
Hyperplasia
Hyperplasia
Hyperplasia
Hyperplasia, nodular

Hyperplasia, nodular
Hyperplasia, nodular
Hyperplasia
Hyperplasia
Hyperplasia
Hyperplasia
Hyperplasia, adenomatous
Hyperplasia, adenomatous
Hyperplasia, nodular
Hyperplasia
Hyperplasia, nodular
Hyperplasia, nodular
Hyperplasia, nodular
Hyperplasia, nodular
Hyperplasia, nodular

Table 5.3 Non-neoplastic (incl. hyperplasia and thyroiditis) samples

Thyroiditis (n=9)
Hashimoto Thyroiditis
Hashimoto Thyroiditis
Hashimoto Thyroiditis
Hashimoto Thyroiditis
Hashimoto Thyroiditis
Hashimoto Thyroiditis
Inflammation chronic
Lymphocytic thyroiditis
Lymphocytic infiltrate

Table 5.4 Thyroiditis samples

Hashimoto Thyroiditis (n=6)
Hashimoto Thyroiditis
Hashimoto Thyroiditis
Hashimoto Thyroiditis
Hashimoto Thyroiditis
Hashimoto Thyroiditis
Hashimoto Thyroiditis

Table 5.5 Hashimoto Thyroiditis samples

Hyperplasia (n=53)
Graves
Graves
Graves
Graves
Graves
Hyperthyroidism
Hyperplasia, nodular
Hyperplasia, nodular
Hyperplasia, nodular
Hyperplasia, nodular
Hyperplasia, nodular
Hyperplasia, nodular
Hyperplasia, nodular
Hyperplasia, nodular
Hyperplasia
Hyperplasia, nodular
Hyperplasia, nodular
Hyperplasia, nodular
Hyperplasia, nodular
Hyperplasia, nodular
Hyperplasia, nodular
Hyperplasia
Hyperplasia, nodular
Hyperplasia + lymphocytic thyroiditis
Hyperplasia + lymphocytic thyroiditis
Hyperplasia, nodular + lymphocytic thyroiditis
Hyperplasia + lymphocytic thyroiditis
Hyperplasia, nodular
Hyperplasia
Hyperplasia, nodular
Hyperplasia, nodular
Hyperplasia, nodular
Hyperplasia, nodular
Hyperplasia, nodular
Hyperplasia
Hyperplasia
Hyperplasia
Hyperplasia, nodular
Hyperplasia, nodular
Hyperplasia, nodular
Hyperplasia
Hyperplasia
Hyperplasia
Hyperplasia
Hyperplasia, adenomatous
Hyperplasia, adenomatous
Hyperplasia, nodular
Hyperplasia
Hyperplasia, nodular
Hyperplasia, nodular
Hyperplasia, nodular
Hyperplasia, nodular
Hyperplasia, nodular

Table 5.6 Hyperplasia samples

Follicular adenoma (n=19)
Follicular adenoma
Follicular adenoma
Follicular adenoma
Follicular adenoma
Follicular adenoma
Follicular adenoma
Follicular adenoma
Follicular adenoma
Follicular adenoma
Follicular adenoma
Follicular adenoma
Follicular adenoma
Follicular adenoma
Follicular adenoma
Follicular adenoma
Follicular adenoma
Follicular adenoma
Follicular adenoma
Follicular adenoma

Table 5.7 Follicular adenoma samples

Benign (n=29)
Adenoma
Adenoma
Adenoma
Adenoma, mixed cell
Adenoma
Hurthle cell adenoma
Hurthle cell adenoma
Hurthle cell adenoma
Hurthle cell adenoma
Hurthle cell adenoma
Follicular adenoma
Follicular adenoma
Follicular adenoma
Follicular adenoma
Follicular adenoma
Follicular adenoma
Follicular adenoma
Follicular adenoma
Follicular adenoma
Follicular adenoma
Follicular adenoma
Follicular adenoma
Follicular adenoma
Follicular adenoma
Follicular adenoma
Follicular adenoma
Follicular adenoma
Follicular adenoma
Follicular adenoma

Table 5.8 Benign samples

Non-malignant (all benign, all non-neoplastic) (n=138)
Hashimoto Thyroiditis
Hashimoto Thyroiditis
Hashimoto Thyroiditis
Hashimoto Thyroiditis
Hashimoto Thyroiditis
Hashimoto Thyroiditis
Inflammation chronic
Lymphocytic thyroiditis
Lymphocytic infiltrate
No evidence of malignancy
No evidence of malignancy
No evidence of malignancy
No evidence of malignancy
No evidence of malignancy
No evidence of malignancy
No evidence of malignancy
No evidence of malignancy
No evidence of malignancy
No evidence of malignancy
No evidence of malignancy
No evidence of malignancy
No evidence of malignancy
No evidence of malignancy
No evidence of malignancy
No evidence of malignancy
No evidence of malignancy
Goitre, colloid
Goitre, colloid
Goitre, colloid
Goitre, colloid
Goitre
Goitre, colloid
Goitre, colloid
Goitre, colloid
Goitre, colloid
Goitre, colloid
Goitre, colloid
Goitre, colloid
Goitre, colloid
Goitre, colloid
Goitre, colloid
Goitre, colloid
Goitre, colloid
Goitre
Goitre, colloid
Goitre
Goitre, adenomatous
Goitre
Goitre, adenomatous
Goitre, colloid
Goitre, colloid
Goitre, colloid
Goitre, colloid
Goitre, colloid

Goitre, adenomatous
Goitre, adenomatous
Graves
Graves
Graves
Graves
Graves
Hyperthyroidism
Hyperplasia, nodular
Hyperplasia, nodular
Hyperplasia, nodular
Hyperplasia, nodular
Hyperplasia, nodular
Hyperplasia, nodular
Hyperplasia, nodular
Hyperplasia, nodular
Hyperplasia
Hyperplasia, nodular
Hyperplasia, nodular
Hyperplasia, nodular
Hyperplasia, nodular
Hyperplasia, nodular
Hyperplasia, nodular
Hyperplasia
Hyperplasia, nodular
Hyperplasia + lymphocytic thyroiditis
Hyperplasia + lymphocytic thyroiditis
Hyperplasia, nodular + lymphocytic thyroiditis
Hyperplasia + lymphocytic thyroiditis
Hyperplasia, nodular
Hyperplasia
Hyperplasia, nodular
Hyperplasia, nodular
Hyperplasia, nodular
Hyperplasia, nodular
Hyperplasia, nodular
Hyperplasia
Hyperplasia
Hyperplasia
Hyperplasia, nodular
Hyperplasia, nodular
Hyperplasia, nodular
Hyperplasia
Hyperplasia
Hyperplasia
Hyperplasia
Hyperplasia, adenomatous
Hyperplasia, adenomatous
Hyperplasia, nodular
Hyperplasia
Hyperplasia, nodular
Hyperplasia, nodular
Hyperplasia, nodular
Hyperplasia, nodular
Hyperplasia, nodular

Adenoma
Adenoma
Adenoma
Adenoma, mixed cell
Adenoma
Hurthle cell adenoma
Hurthle cell adenoma
Hurthle cell adenoma
Hurthle cell adenoma
Hurthle cell adenoma
Follicular adenoma
Follicular adenoma
Follicular adenoma
Follicular adenoma
Follicular adenoma
Follicular adenoma
Follicular adenoma
Follicular adenoma
Follicular adenoma
Follicular adenoma
Follicular adenoma
Follicular adenoma
Follicular adenoma
Follicular adenoma
Follicular adenoma
Follicular adenoma
Follicular adenoma
Follicular adenoma
Follicular adenoma

Table 5.9 Non-malignant (all benign, all non-neoplastic) samples

Hurthle cell carcinoma (n=3)
Hurthle cell carcinoma
Hurthle cell carcinoma
Hurthle cell carcinoma

Table 5.10 Hurthle cell carcinoma samples

Follicular thyroid carcinoma (n=10)
Follicular thyroid carcinoma, Hurthle cell type
Follicular thyroid carcinoma, well differentiated
Follicular thyroid carcinoma
Follicular thyroid carcinoma, Hurthle cell type
Follicular thyroid carcinoma, Hurthle cell type
Follicular thyroid carcinoma
Follicular thyroid carcinoma
Follicular thyroid carcinoma
Follicular thyroid carcinoma
Follicular thyroid carcinoma

Table 5.11 Follicular thyroid carcinoma samples

Papillary thyroid carcinoma (not otherwise specified)
Papillary thyroid carcinoma, well differentiated
Papillary thyroid carcinoma
Papillary thyroid carcinoma
Papillary thyroid carcinoma
Papillary thyroid carcinoma
Papillary thyroid carcinoma
Papillary thyroid carcinoma
Papillary thyroid carcinoma
Papillary thyroid carcinoma
Papillary thyroid carcinoma
Papillary thyroid carcinoma
Papillary thyroid carcinoma
Papillary thyroid microcarcinoma
Papillary thyroid microcarcinoma
Papillary thyroid carcinoma, well differentiated
Papillary thyroid carcinoma, multifocal
Papillary thyroid carcinoma, multifocal
Papillary thyroid carcinoma, multifocal
Papillary thyroid carcinoma, multifocal
Papillary thyroid carcinoma, oxyphilic variant
Papillary thyroid carcinoma, trebecular
Papillary thyroid carcinoma + lymphocytic thyroiditis, multifocal
Papillary thyroid carcinoma
Papillary thyroid carcinoma
Papillary thyroid carcinoma
Papillary thyroid carcinoma
Papillary thyroid carcinoma
Papillary thyroid carcinoma
Papillary thyroid carcinoma
Papillary thyroid carcinoma
Papillary thyroid carcinoma
Papillary thyroid carcinoma
Papillary thyroid carcinoma
Papillary thyroid carcinoma
Papillary thyroid carcinoma
Papillary thyroid carcinoma

Table 5.12 Papillary thyroid carcinoma (NOS) samples

Follicular variant papillary thyroid carcinoma (n=14)
Follicular variant papillary thyroid carcinoma
Follicular variant papillary thyroid carcinoma
Follicular variant papillary thyroid carcinoma
Follicular variant papillary thyroid carcinoma
Follicular variant papillary thyroid carcinoma, encapsulated
Follicular variant papillary thyroid carcinoma
Follicular variant papillary thyroid carcinoma
Follicular variant papillary thyroid carcinoma
Follicular variant papillary thyroid carcinoma
Follicular variant papillary thyroid carcinoma
Follicular variant papillary thyroid carcinoma
Follicular variant papillary thyroid carcinoma
Follicular variant papillary thyroid carcinoma
Follicular variant papillary thyroid carcinoma

Table 5.13 Papillary thyroid carcinoma follicular variant samples

Papillary thyroid carcinoma (all variants) (n=50)
Papillary thyroid carcinoma, well differentiated
Papillary thyroid carcinoma
Papillary thyroid carcinoma
Papillary thyroid carcinoma
Papillary thyroid carcinoma
Papillary thyroid carcinoma
Papillary thyroid carcinoma
Papillary thyroid carcinoma
Papillary thyroid carcinoma
Papillary thyroid carcinoma
Papillary thyroid carcinoma
Papillary thyroid carcinoma
Papillary thyroid microcarcinoma
Papillary thyroid microcarcinoma
Papillary thyroid carcinoma, well differentiated
Papillary thyroid carcinoma, multifocal
Papillary thyroid carcinoma, multifocal
Papillary thyroid carcinoma, multifocal
Papillary thyroid carcinoma, multifocal
Papillary thyroid carcinoma, oxyphilic variant
Papillary thyroid carcinoma, trebecular
Papillary thyroid carcinoma + lymphocytic thyroiditis, multifocal
Papillary thyroid carcinoma
Papillary thyroid carcinoma
Papillary thyroid carcinoma
Papillary thyroid carcinoma
Papillary thyroid carcinoma
Papillary thyroid carcinoma
Papillary thyroid carcinoma
Papillary thyroid carcinoma
Papillary thyroid carcinoma
Papillary thyroid carcinoma
Papillary thyroid carcinoma
Papillary thyroid carcinoma
Papillary thyroid carcinoma
Papillary thyroid carcinoma
Follicular variant papillary thyroid carcinoma
Follicular variant papillary thyroid carcinoma
Follicular variant papillary thyroid carcinoma
Follicular variant papillary thyroid carcinoma
Follicular variant papillary thyroid carcinoma, encapsulated
Follicular variant papillary thyroid carcinoma
Follicular variant papillary thyroid carcinoma
Follicular variant papillary thyroid carcinoma
Follicular variant papillary thyroid carcinoma
Follicular variant papillary thyroid carcinoma
Follicular variant papillary thyroid carcinoma
Follicular variant papillary thyroid carcinoma
Follicular variant papillary thyroid carcinoma
Follicular variant papillary thyroid carcinoma

Table 5.14 Papillary thyroid carcinoma (all variants) samples

Anaplastic thyroid carcinoma (n=1)
Anaplastic thyroid carcinoma, giant cell type

Table 5.15 Anaplastic thyroid carcinoma sample

Medullary thyroid carcinoma (n=1)
Medullary thyroid carcinoma

Table 5.16 Medullary thyroid carcinoma sample

Neoplastic (n=96)
Adenoma
Adenoma
Adenoma
Adenoma, mixed cell
Adenoma
Hurthle cell adenoma
Hurthle cell adenoma
Hurthle cell adenoma
Hurthle cell adenoma
Hurthle cell adenoma
Follicular adenoma
Follicular adenoma
Follicular adenoma
Follicular adenoma
Follicular adenoma
Follicular adenoma
Follicular adenoma
Follicular adenoma
Follicular adenoma
Follicular adenoma
Follicular adenoma
Follicular adenoma
Follicular adenoma
Follicular adenoma
Follicular adenoma
Follicular adenoma
Follicular adenoma
Follicular adenoma
Follicular adenoma
Follicular adenoma
Hurthle cell carcinoma
Hurthle cell carcinoma
Hurthle cell carcinoma
Follicular thyroid carcinoma, Hurthle cell type
Follicular thyroid carcinoma, well differentiated
Follicular thyroid carcinoma
Follicular thyroid carcinoma, Hurthle cell type
Follicular thyroid carcinoma, Hurthle cell type
Follicular thyroid carcinoma
Follicular thyroid carcinoma
Follicular thyroid carcinoma
Follicular thyroid carcinoma
Follicular thyroid carcinoma
Papillary thyroid carcinoma, well differentiated
Papillary thyroid carcinoma

Papillary thyroid carcinoma
Papillary thyroid carcinoma
Papillary thyroid carcinoma
Papillary thyroid carcinoma
Papillary thyroid carcinoma
Papillary thyroid carcinoma
Papillary thyroid carcinoma
Papillary thyroid carcinoma
Papillary thyroid carcinoma
Papillary thyroid carcinoma
Papillary thyroid microcarcinoma
Papillary thyroid microcarcinoma
Papillary thyroid carcinoma, well differentiated
Papillary thyroid carcinoma, multifocal
Papillary thyroid carcinoma, multifocal
Papillary thyroid carcinoma, multifocal
Papillary thyroid carcinoma, multifocal
Papillary thyroid carcinoma, oxyphilic variant
Papillary thyroid carcinoma, trebecular
Papillary thyroid carcinoma + lymphocytic thyroiditis, multifocal
Papillary thyroid carcinoma
Papillary thyroid carcinoma
Papillary thyroid carcinoma
Papillary thyroid carcinoma
Papillary thyroid carcinoma
Papillary thyroid carcinoma
Papillary thyroid carcinoma
Papillary thyroid carcinoma
Papillary thyroid carcinoma
Papillary thyroid carcinoma
Papillary thyroid carcinoma
Papillary thyroid carcinoma
Papillary thyroid carcinoma
Papillary thyroid carcinoma
Well differentiated thyroid tumour-unknown malignant potential
Papillary thyroid carcinoma, follicular variant
Papillary thyroid carcinoma, follicular variant
Papillary thyroid carcinoma, follicular variant
Papillary thyroid carcinoma, follicular variant
Papillary thyroid carcinoma, encapsulated follicular variant
Papillary thyroid carcinoma, follicular variant
Papillary thyroid carcinoma, follicular variant
Papillary thyroid carcinoma, follicular variant
Papillary thyroid carcinoma, follicular variant
Papillary thyroid carcinoma, follicular variant
Papillary thyroid carcinoma, follicular variant
Papillary thyroid carcinoma, follicular variant
Papillary thyroid carcinoma, follicular variant
Papillary thyroid carcinoma, follicular variant
Medullary thyroid carcinoma
Anaplastic thyroid carcinoma, giant cell type
Hurthle cell neoplasm

Table 5.17 Neoplastic samples

Malignant (n=65)
Hurthle cell carcinoma
Hurthle cell carcinoma
Hurthle cell carcinoma
Follicular thyroid carcinoma, Hurthle cell type
Follicular thyroid carcinoma, well differentiated
Follicular thyroid carcinoma
Follicular thyroid carcinoma, Hurthle cell type
Follicular thyroid carcinoma, Hurthle cell type
Follicular thyroid carcinoma
Follicular thyroid carcinoma
Follicular thyroid carcinoma
Follicular thyroid carcinoma
Follicular thyroid carcinoma
Papillary thyroid carcinoma, well differentiated
Papillary thyroid carcinoma
Papillary thyroid carcinoma
Papillary thyroid carcinoma
Papillary thyroid carcinoma
Papillary thyroid carcinoma
Papillary thyroid carcinoma
Papillary thyroid carcinoma
Papillary thyroid carcinoma
Papillary thyroid carcinoma
Papillary thyroid carcinoma
Papillary thyroid carcinoma
Papillary thyroid carcinoma
Papillary thyroid microcarcinoma
Papillary thyroid microcarcinoma
Papillary thyroid carcinoma, well differentiated
Papillary thyroid carcinoma, multifocal
Papillary thyroid carcinoma, multifocal
Papillary thyroid carcinoma, multifocal
Papillary thyroid carcinoma, multifocal
Papillary thyroid carcinoma, oxyphilic variant
Papillary thyroid carcinoma, trebecular
Papillary thyroid carcinoma + lymphocytic thyroiditis, multifocal
Papillary thyroid carcinoma
Papillary thyroid carcinoma
Papillary thyroid carcinoma
Papillary thyroid carcinoma
Papillary thyroid carcinoma
Papillary thyroid carcinoma
Papillary thyroid carcinoma
Papillary thyroid carcinoma
Papillary thyroid carcinoma
Papillary thyroid carcinoma
Papillary thyroid carcinoma
Papillary thyroid carcinoma
Papillary thyroid carcinoma
Papillary thyroid carcinoma
Papillary thyroid carcinoma, follicular variant
Papillary thyroid carcinoma, follicular variant
Papillary thyroid carcinoma, follicular variant
Papillary thyroid carcinoma, follicular variant

Papillary thyroid carcinoma, encapsulated follicular variant
Papillary thyroid carcinoma, follicular variant
Papillary thyroid carcinoma, follicular variant
Papillary thyroid carcinoma, follicular variant
Papillary thyroid carcinoma, follicular variant
Papillary thyroid carcinoma, follicular variant
Papillary thyroid carcinoma, follicular variant
Papillary thyroid carcinoma, follicular variant
Papillary thyroid carcinoma, follicular variant
Papillary thyroid carcinoma, follicular variant
Medullary thyroid carcinoma
Anaplastic thyroid carcinoma, giant cell type

Table 5.18 Malignant samples

5.4.2 Laser capture microdissection

7-μm thick sections were cut using a microtome (Microm HM 325, Medical Supply Co. Ltd, Ireland) from each paraffin block, mounted on uncharged slides, dewaxed and H&E stained (Tissue-Tek DRS 2000 Autostainer, Sakura, CA, USA). Pure populations of thyrocytes were obtained from each section by laser capture microdissection using the PixCell® II System (Acturus Engineering, Inc., CA, USA) (see section 2.6). After microdissection the Capsures® (Capsure® Macro LCM caps, LCM 0201, Techno-Path Ltd, Ireland) containing the homogenous cell populations were placed in a sterile microcentrifuge tube ready for RNA extraction.

5.4.3 RNA extraction and quantification

RNA was extracted using the Absolutely RNA® Formalin Fixed Paraffin Embedded Kit (Stratagene, CA, USA), using the protocol described in section 2.7. Purified RNA was eluted in 30μL volumes and the nanogram concentration per microlitre was established using a NanoDrop spectrophotometer (ND-1000, Labtech International, U.K) Yields in the range of 5ng/μL to 63ng/μL were achieved, to maintain equal quantities of RNA, 5ng/μL (or 0.125 μg in 25μL) of each sample was used.

5.4.4 cDNA archiving and Pre-Amp synthesis

The RNA was reverse transcribed to single-stranded cDNA using a High Capacity cDNA Archive Kit (Applied Biosytems, CA, USA) in 50 μL reactions as described in chapter 2.9.

Prior to running the pre-amplification reaction, the intended assays (containing primers and probes) were pooled together, as described in section 2.10.4.2 with 1X Tris-EDTA (TE) buffer in a 0.2X pooled assay mix. The pre-amplification reaction was performed in 50μL reactions as described in chapter 2, table 2.4.

5.4.5 TaqMan® gene expression reaction

The six gene expression assays (including CDKN1B as the endogenous control) shown in table 5.19 were diluted 1:5 (20X to 4X) using 1X TE buffer. The pre-amplified products were diluted 1:5 using TE buffer. The gene expression reaction was performed in 20µL reactions as described in chapter 2, table 2.5.

Gene Symbol	Gene Name
MMP11	Matrix metalloproteinase 11
BAX	Bcl2-associated X protein
APOE	Apolipoprotein E
TOP2A	Topoisomerase II alpha
LYN	V Yes- 1 Yamaguchi sarcoma viral related oncogene homolog
CDKN1B	Cyclin dependent kinase inhibitor 1B

Table 5.19 Illustrates the panel of assays (including CDKN1B as the endogenous control) which were used to perform TaqMan RT-PCR analysis

5.4.6 Tissue microarray construction and sectioning

The two hundred and five samples were arrayed into a tissue microarray (TMA) block as described in section 2.11.2. TMA technology is a powerful tool for high throughput large scale morphological in situ analysis of molecular targets, with the advantage of experimental uniformity. The two hundred and five samples were arrayed over four slides (approximately 51 cases in quadruplicate per slide). 4 μm sections were cut using a microtome and left to dry in an oven overnight at 50°C.

5.4.7 Immunohistochemistry

Analysis of protein expression of the five targets was carried out using immunohistochemistry on TMA sections encompassing the two hundred and five samples. The following antibodies were used: matrix metalloproteinase 11 (MMP11), Bcl2-associated X protein (BAX), apolipoprotein E (APOE), topoisomerase II alpha (TOP2A) (all Abcam, UK) and v-yes-1 yamaguchi sarcoma viral related oncogene homolog (LYN) (BD Biosciences, UK). Table 5.20 displays the species each antibody was raised in, clonality, the dilution and positive control used for each antibody. A polyclonal rabbit anti-mouse biotinylated secondary antibody was used at a dilution of 1 in 300 (Dako Cytomation, Denmark). The ABC method was employed, (see section 2.12.2), briefly, the TMA section is incubated with primary antibody raised against the antigen of interest, next a biotin-labeled secondary antibody is added which introduces biotins at the location of the primary antibody. The avidin: biotinylated enzyme complex (ABC) is added and binds to the biotinylated secondary antibody. Lastly, the antigen is localized by incubation with an enzyme substrate (DAB).

Primary Antibody	Species/Clonality	Dilution	Positive control
MMP11	Mouse/Monoclonal	Bought prediluted	Placenta
BAX	Mouse/Monoclonal	Bought prediluted	Breast
APOE	Mouse/Monoclonal	1 in 100	Brain
TOP2A	Mouse/Monoclonal	1 in 10	Tonsil
LYN	Mouse/Monoclonal	1 in 100	Tonsil

Table 5.20 Primary antibodies

5.4.8 Analysis of relative gene expression data using the Comparative C_T method

Analysis of relative gene expression data was performed using the $2^{-\Delta\Delta C}{}_T$ method (Livak and Schmittgen, 2001) with cyclin dependent kinase inhibitor 1 B (CDKN1B) as the endogenous control/reference assay. This algorithm presents data as fold change in gene expression relative to a calibrator (follicular adenoma) and normalised to an endogenous reference gene, CDKN1B in this case. This method is described in more detail in section 2.10.2.

5.4.9 Analysis of immunohistochemical scores

The evaluation of each targets expression in each sample was analyzed independently by two pathologists (R.F and S.F) using an immunohistochemical score (IHS). The IHS was calculated by combining an estimate of the percentage of immuoreactive cells (quantity score) with an estimate of the staining intensity (staining intensity score). The quantity score and intensity staining score were scored as follows, quantity score: no cells staining were scored as 0, 1-9% of cells stained positive scored as 1, 10-39% as 2, 40-69% as 3 and 70-100% as 4. Staining intensity was rated on a scale of 0-3, with 0 = negative, 1 = weak, 2 = moderate and 3 = strong. The raw data were converted to the IHS by adding the quantity and staining intensity scores, therefore the scores can range from 0-7. The immunohistochemistry scores for the four TMA cores representing one sample were averaged to give a final IHS for each sample.

5.4.10 Statistical analysis

As the distribution of samples in each group was non-normal, and no more than two unpaired groups of values were being compared at a time, the Mann-Whitney U-test was chosen to determine statistical significance for relative gene expression data and immunohistochemical scores (Analyse-it® statistical software for Microsoft® Excel®).

5.5 Results

The purpose of this chapter was to examine the expression of a cohort of targets at both the gene and protein level of expression on a panel of two hundred and five samples. To this end, any samples with results deemed unsuitable for inclusion in the final analysis of gene expression (inadequate C_T value) data and protein expression (due to loss of/inadequate TMA cores) data were removed resulting in parallel gene and protein expression data on 161 cases for MMP1, 178 cases for BAX, 175 cases for APOE, 179 cases for TOP2A and 180 cases for LYN.

The following diagnostic categories of groups were formed and used for analysis from the cohort of 161 samples for MMP11 (table 5.21), 178 samples for BAX (table 5.22), 175 samples for APOE (table 5.23), 179 samples for TOP2A (table 5.24) and 180 samples for LYN (table 5.25).

MMP11 Analysis cohorts n=161
Non-neoplastic (no thyroiditis, no hyperplasia) n=41
Non-neoplastic (no hyperplasia) n=47
Non-neoplastic (incl. hyperplasia + thyroiditis) n=92
Thyroiditis n=6
Hashimoto Thyroiditis n=4
Hyperplasia n=45
Follicular adenoma n=16
Benign n=22
Non-malignant (all benign, all non-neoplastic) n=114
Hurthle cell carcinoma n=1
Follicular thyroid carcinoma n=8
Papillary thyroid carcinoma (NOS) n=26
Papillary thyroid carcinoma, follicular variant n=8
Papillary thyroid carcinoma, all variants n=34
Neoplastic n=69
Malignant n=45

Table 5.21 Demonstrates the analysis cohorts formed and numbers included in each group for gene and protein analysis of MMP11. The majority of the groups have an overlap of the two hundred and five samples

BAX Analysis cohorts n=178
Non-neoplastic (no thyroiditis, no hyperplasia) n=42
Non-neoplastic (no hyperplasia) n=48
Non-neoplastic (incl. hyperplasia + thyroiditis) n=97
Thyroiditis n=6
Hashimoto Thyroiditis n=4
Hyperplasia n=49
Follicular adenoma n=19
Benign n=25
Non-malignant (all benign, all non-neoplastic) n=122
Hurthle cell carcinoma n=3
Follicular thyroid carcinoma n=10
Papillary thyroid carcinoma (NOS) n=27
Papillary thyroid carcinoma, follicular variant n=12
Papillary thyroid carcinoma, all variants n=39
Neoplastic n=81
Malignant n=54

Table 5.22 Demonstrates the analysis cohorts formed and numbers included in each group for gene and protein analysis of BAX. The majority of the groups have an overlap of the two hundred and five samples

APOE Analysis cohorts n=175
Non-neoplastic (no thyroiditis, no hyperplasia) n=42
Non-neoplastic (no hyperplasia) n=48
Non-neoplastic (incl. hyperplasia + thyroiditis) n=97
Thyroiditis n=6
Hashimoto Thyroiditis n=4
Hyperplasia n=49
Follicular adenoma n=18
Benign n=25
Non-malignant (all benign, all non-neoplastic) n=122
Hurthle cell carcinoma n=3
Follicular thyroid carcinoma n=9
Papillary thyroid carcinoma (NOS) n=26
Papillary thyroid carcinoma, follicular variant n=11
Papillary thyroid carcinoma, all variants n=37
Neoplastic n=78
Malignant n=51

Table 5.23 Demonstrates the analysis cohorts formed and numbers included in each group for gene and protein analysis of APOE. The majority of the groups have an overlap of the two hundred and five samples

TOP2A Analysis cohorts n=179
Non-neoplastic (no thyroiditis, no hyperplasia) n=46
Non-neoplastic (no hyperplasia) n=52
Non-neoplastic (incl. hyperplasia + thyroiditis) n=100
Thyroiditis n=6
Hashimoto Thyroiditis n=4
Hyperplasia n=48
Follicular adenoma n=19
Benign n=26
Non-malignant (all benign, all non-neoplastic) n=126
Hurthle cell carcinoma n=1
Follicular thyroid carcinoma n=9
Papillary thyroid carcinoma (NOS) n=28
Papillary thyroid carcinoma, follicular variant n=11
Papillary thyroid carcinoma, all variants n=39
Neoplastic n=79
Malignant n=51

Table 5.24 Demonstrates the analysis cohorts formed and numbers included in each group for gene and protein analysis of TOP2A. The majority of the groups have an overlap of the two hundred and five samples

LYN Analysis cohorts n=180
Non-neoplastic (no thyroiditis, no hyperplasia) n=46
Non-neoplastic (no hyperplasia) n=52
Non-neoplastic (incl. hyperplasia + thyroiditis) n=100
Thyroiditis n=6
Hashimoto Thyroiditis n=4
Hyperplasia n=48
Follicular adenoma n=19
Benign n=27
Non-malignant (all benign, all non-neoplastic) n=127
Hurthle cell carcinoma n=1
Follicular thyroid carcinoma n=10
Papillary thyroid carcinoma (NOS) n=29
Papillary thyroid carcinoma, follicular variant n=10
Papillary thyroid carcinoma, all variants n=39
Neoplastic n=80
Malignant n=51

Table 5.25 Demonstrates the analysis cohorts formed and numbers included in each group for gene and protein analysis of LYN. The majority of the groups have an overlap of the two hundred and five samples

5.5.1 Gene expression

The following table (table 5.26) illustrates the groups that were significantly ($p< 0.05$, Mann-Whitney U-test) discriminated at the gene expression level for MMP11, BAX, APOE, TOP2A and LYN. All targets were up-regulated in malignant and neoplastic groups in comparison to benign, hyperplastic, thyroiditis and non-neoplastic groups.

Analysis Cohorts For Gene Expression	MMP11	BAX	APOE	TOP2A	LYN
Non-neoplastic (no hyperplasia, no thyroiditis) vs. Malignant	0.0006	0.0004	<0.0001	0.0028	0.0055
Non-neoplastic (no hyperplasia, no thyroiditis) vs. Neoplastic	0.0142	0.0003	0.0005	0.0261	0.0052
Non-neoplastic (no hyperplasia, no thyroiditis) vs. Benign		0.0445			
Non-neoplastic (no hyperplasia) vs. Malignant	0.0123		<0.0001	0.0039	0.011
Non-neoplastic (no hyperplasia) vs. Neoplastic	0.0289	0.0004	0.0016	0.0374	0.0109
Non-neoplastic (no hyperplasia) vs. Hyperplasia					0.0216
Benign vs. Normal (no hyperplasia)		0.0004			
Non-neoplastic (incl. hyperplasia + thyroiditis) vs. Malignant	0.0003	<0.0001	<0.0001	0.0063	<0.0001
Non-neoplastic (incl. hyperplasia + thyroiditis) vs. Neoplastic	0.0004	<0.0001	<0.0001	0.0504	<0.0001
Non-neoplastic (incl. hyperplasia + thyroiditis) vs. Benign		0.045			0.0248
Hyperplasia vs. Malignant	0.0001	0.0014	<0.0001		<0.0001
Hyperplasia vs. Neoplastic	0.0002	0.0012	0.0003		<0.0001
Benign vs. Malignant			0.0009		
Non-malignant (all benign, all non-neoplastic) vs. Malignant	0.0006	0.0004	<0.0001		0.0009
FA vs. PTC (all variants)			0.0011	0.0222	
FA vs. PTC (NOS)			0.0016	0.0248	
FA vs. FVPTC			0.0246		
FA vs. FTC			0.035		

Table 5.26 Displays statistically significant p values (<0.05) for MMP11, BAX, APOE, TOP2A and LYN gene expression, which are capable of discriminating between the different analysis cohorts

5.5.1.1 Boxplots representing gene expression

The following boxplots represent a selection of comparative diagnostic groups illustrating the regulation of gene expression for APOE, TOP2A and LYN. All targets analysed were up-regulated in malignant and neoplastic groups when compared to benign, hyperplastic, thyroiditis and non-neoplastic groups.

5.5.1.1.1 APOE gene expression boxplots

Apolipoprotein E is an essential constituent of plasma lipoproteins and is responsible for lipid transport and metabolism.

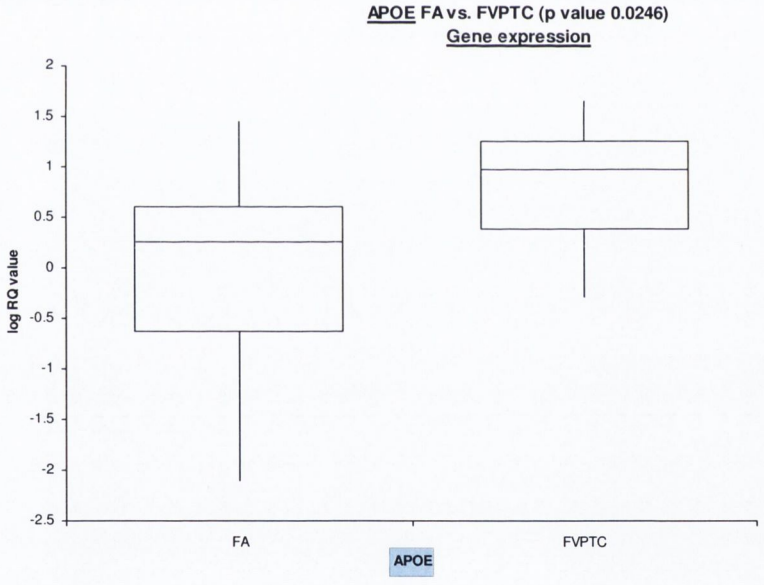

Figure 5.1 Displays up-regulated gene expression of APOE in the malignant follicular variant papillary thyroid carcinoma (FVPTC) group in comparison to the benign follicular adenoma group (FA), p value 0.0246

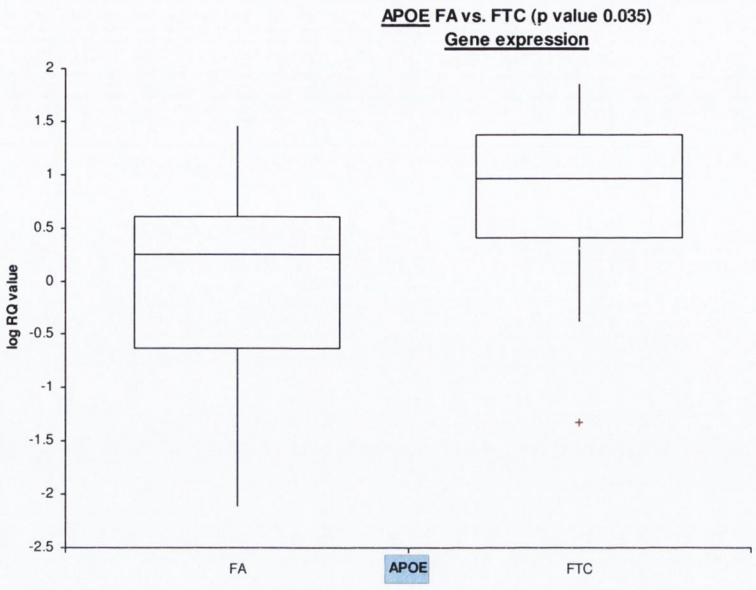

Figure 5.2 Illustrates the up-regulated gene expression of APOE in the malignant follicular thyroid carcinoma (FTC) cohort in comparison to the benign follicular adenoma group (FA), p value 0.035

5.5.1.1.2 TOP2A gene expression boxplots

Topoisomerase II alpha (TOP2A) is involved in the synthesis and transcription of DNA as well as chromosomal segregation during mitosis.

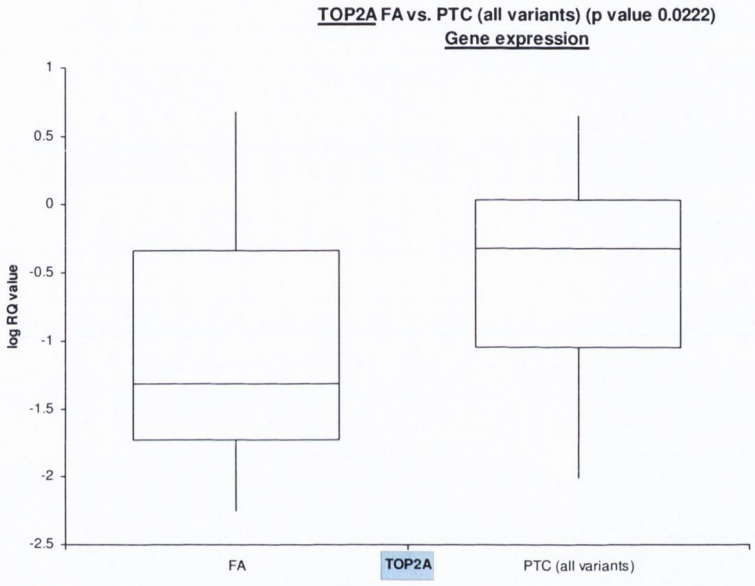

Figure 5.3 Demonstrates the up-regulated gene expression of TOP2A in the malignant papillary thyroid carcinoma group versus the benign follicular adenoma group, p value 0.0222

5.5.1.1.3 LYN gene expression boxplots

V-yes-1 yamaguchi sarcoma viral related oncogene homolog (LYN) is a tyrosine kinase that is involved in the regulation of cell signalling mechanisms.

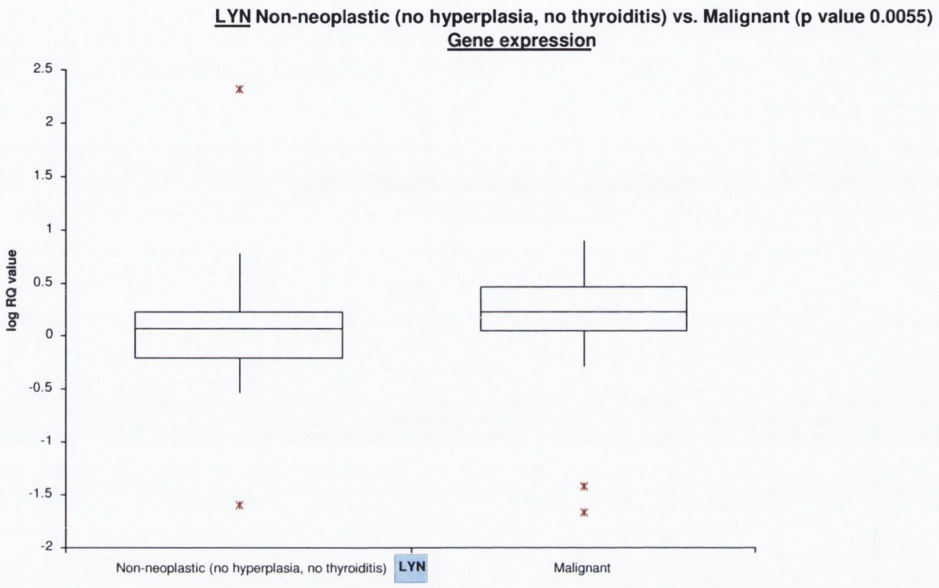

Figure 5.4 Displays the up-regulated gene expression of LYN in the malignant group versus the non-neoplastic group not including hyperplasia or thyroiditis, p value 0.0055

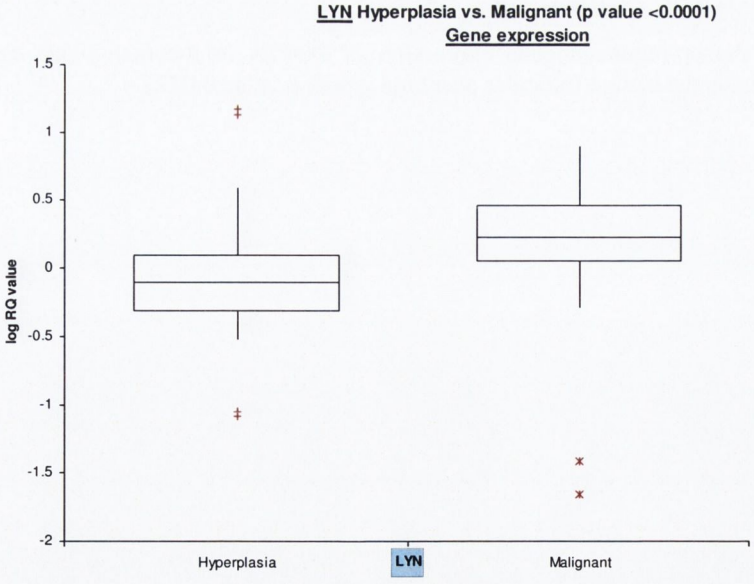

Figure 5.5 Represents the up-regulated gene expression of LYN in the malignant cohort versus the hyperplasia group, p value <0.0001

5.5.2 Protein expression

The following table (table 5.27) represents the groups that were significantly ($p < 0.05$) discriminated at the protein level of expression for MMP11, BAX, APOE, TOP2A and LYN. All targets were up-regulated in malignant and neoplastic cohorts when compared to benign, hyperplastic, thyroiditis and non-neoplastic groups.

Analysis Cohorts For Protein Expression	MMP11	BAX	APOE	TOP2A nuclear	TOP2A cytoplasmic	LYN membranous	LYN cytoplasmic
Non-neoplastic (no hyperplasia, no thyroiditis) vs. Malignant	0.0006	0.0011	0.0003	0.0047			
Non-neoplastic (no hyperplasia, no thyroiditis) vs. Neoplastic	0.0001	0.0039	0.0005	0.0058			
Non-neoplastic (no hyperplasia, no thyroiditis) vs. Benign	0.0054		0.0208				
Non-neoplastic (no hyperplasia, no thyroiditis) vs. Hyperplasia	0.0142						
Non-neoplastic (no hyperplasia) vs. Malignant	0.0029	0.008	0.0024	0.0015			
Non-neoplastic (no hyperplasia) vs. Neoplastic	0.0007	0.0243	0.0047	0.0018			
Benign vs. Normal (no hyperplasia)	0.0191			0.0482			
Non-neoplastic (incl. hyperplasia + thyroiditis) vs. Malignant	0.0057	0.0001	<0.0001	0.0011			
Non-neoplastic (incl. hyperplasia + thyroiditis) vs. Neoplastic	0.0009	0.0005	0.0001	0.0011			
Non-neoplastic (incl. hyperplasia + thyroiditis) vs. Benign	0.0289		0.0304				
Hyperplasia vs. Malignant		0.0002	0.0002	0.0249			
Hyperplasia vs. Neoplastic	0.0298	0.0007	0.0004	0.0342			
Benign vs. Malignant		0.0529					
Non-malignant (all benign, all non-neoplastic) vs. Malignant	0.0195	0.0002	0.0004	0.004			
Thyroiditis vs. PTC (variants)							0.0535
Thyroiditis vs. PTC (NOS)				0.025		<0.0001	
HT vs. PTC (all variants)		0.013			0.0269		0.0043
HT vs. PTC (NOS)		0.0157				<0.0001	0.0125
FA vs. PTC (NOS)						<0.0001	0.0482
FA vs. FVPTC			0.01			0.0036	
FA vs. FTC		0.0201			0.0075	<0.0001	0.0036
FVPTC vs. PTC (all variants)				0.047	0.039	0.0252	
FVPTC vs. PTC (NOS)				0.0122	0.011	0.0004	
FVPTC vs. FTC					0.0125		0.0503
FTC vs. PTC (all variants)					0.0054		0.0338
FTC vs. PTC (NOS)					0.0258	<0.0001	

Table 5.27 Displays significant p values for MMP11, BAX, APOE, TOP2A and LYN protein expression, which are capable of discriminating between the different analysis cohorts
PTC = papillary thyroid carcinoma, NOS = not otherwise specified, FA = follicular adenoma, FVPTC = follicular variant papillary thyroid carcinoma, FTC= follicular thyroid carcinom

5.5.2.1 Immunohistochemical images

5.5.2.1.1 MMP11

Matrix metalloproteinase 11 is an intracellularly activated member of the matrix metalloproteinase family, which are known to play roles in tumour development. MMP11 was up-regulated in malignant and neoplastic cohorts in comparison to non-neoplastic and benign.

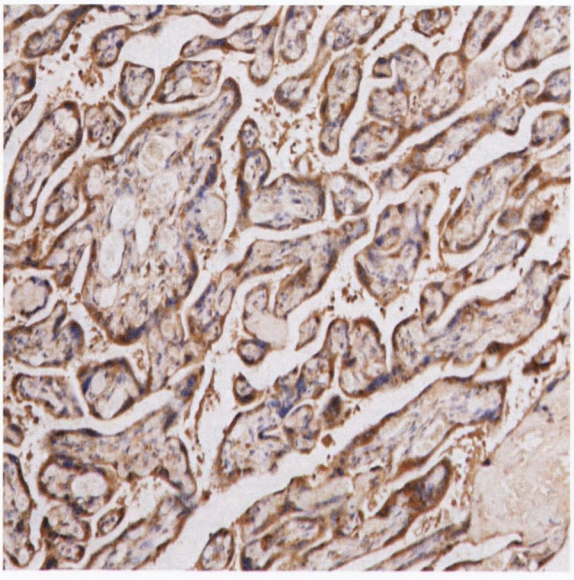

Figure 5.6 Strong cytoplasmic MMP11 staining in the control placental tissue (x40)

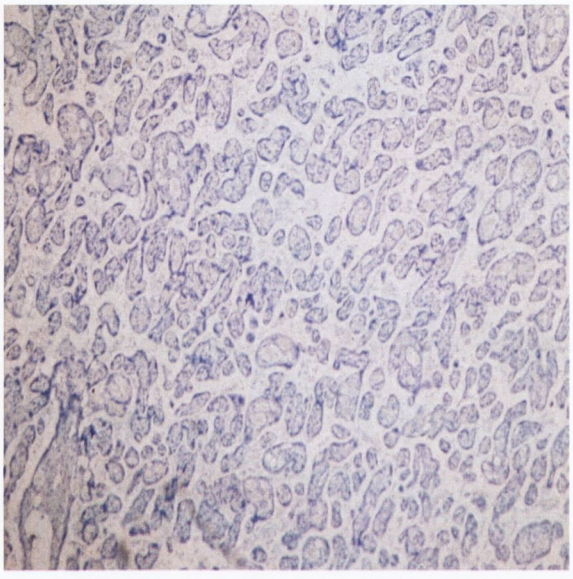

Figure 5.7 Negative MMP11 staining in the control placental tissue (x10)

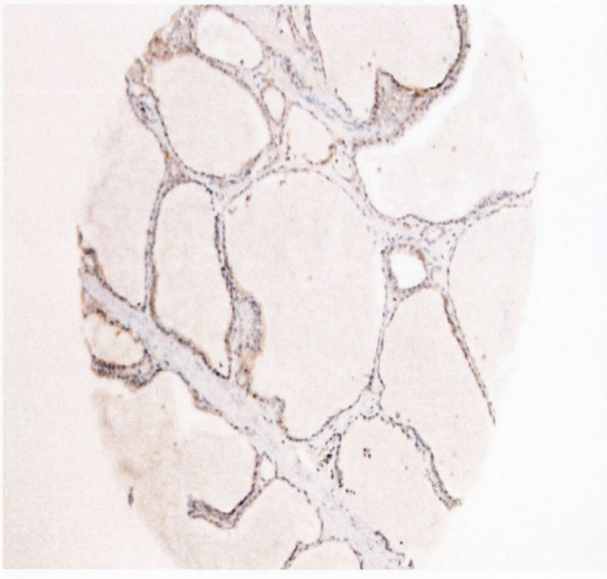

Figure 5.8 Weak cytoplasmic MMP11 staining in benign thyroid (goitre) (x10)

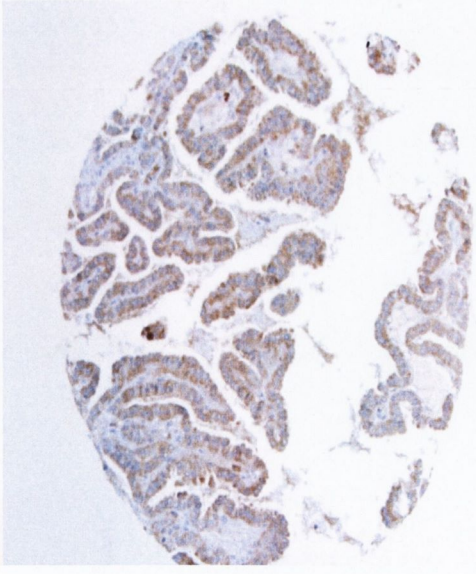

Figure 5.9 Strong cytoplasmic MMP11 staining in a malignant PTC (x10)

5.5.2.1.2 BAX

BAX is a member of the Bcl-2 family of proteins that interact to regulate cell survival and apoptosis, via the caspase cascade. BAX was up-regulated in malignant and neoplastic cohorts in comparison to non-neoplastic and benign.

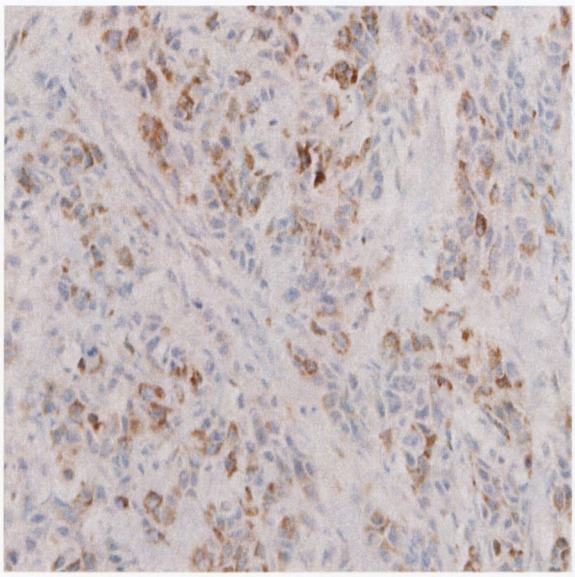

Figure 5.10 Cytoplasmic BAX expression in the control breast tissue (x20)

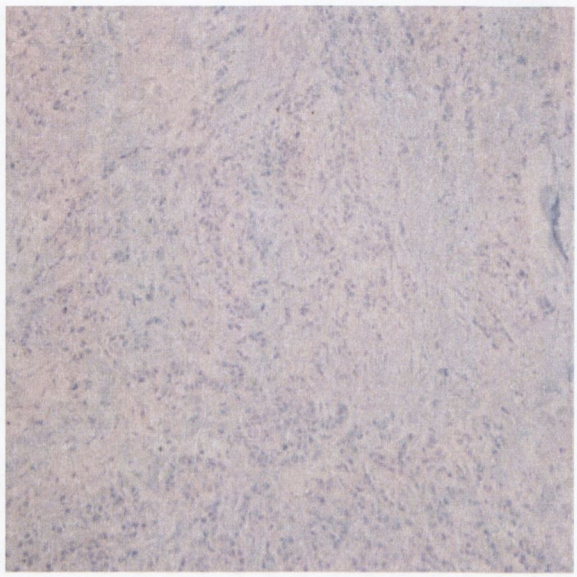

Figure 5.11 Negative BAX staining in the control breast tissue (x10)

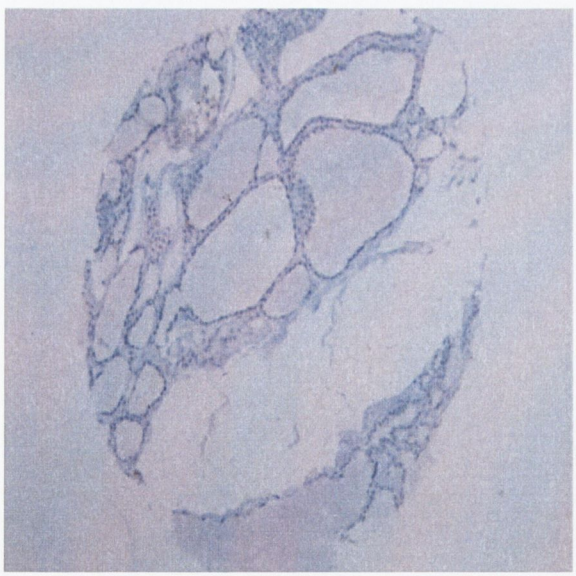

Figure 5.12 Negative BAX staining in a benign goitre (x10)

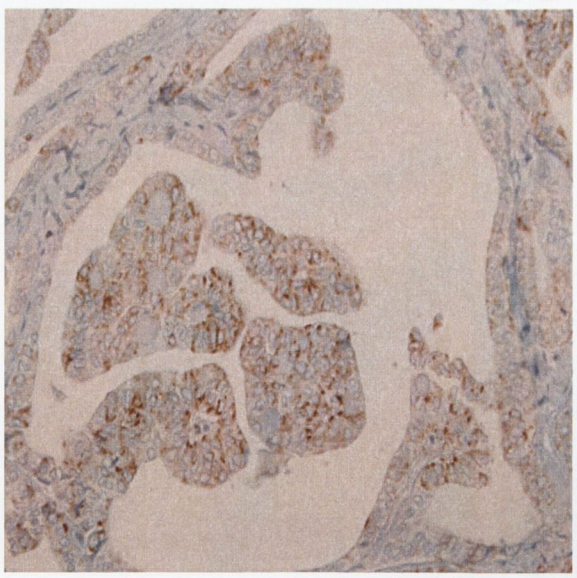

Figure 5.13 Positive cytoplasmic BAX expression in a malignant PTC (x20)

5.5.2.1.3 APOE

APOE is associated with lipid transport, metabolism and homeostasis. Its expression was up-regulated in malignant and neoplastic cohorts versus non-neoplastic and benign.

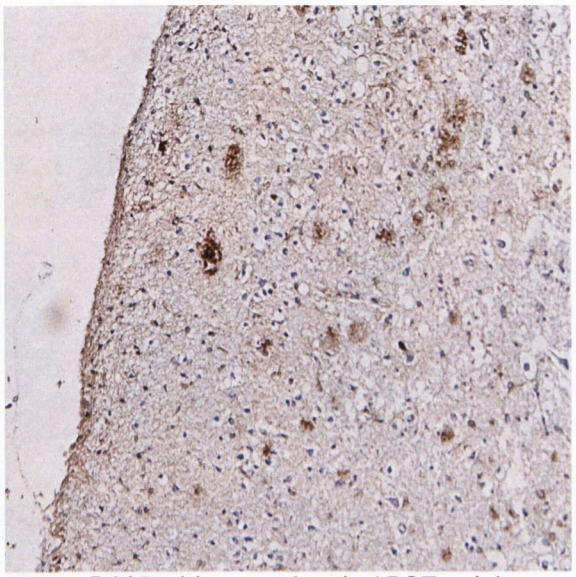

Figure 5.14 Positive cytoplasmic APOE staining in control brain tissue (x10)

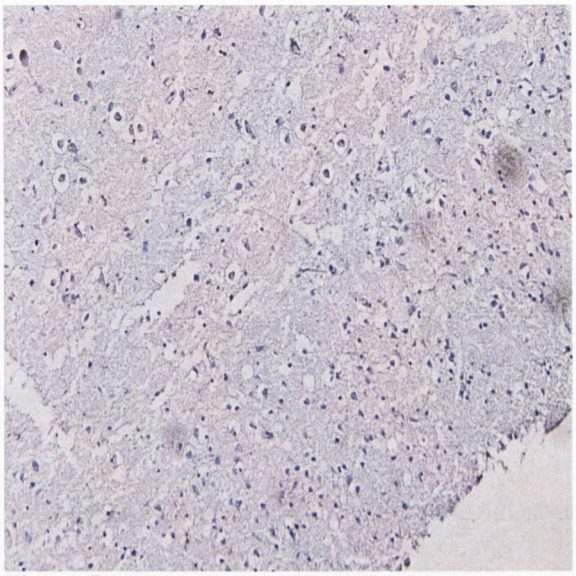

Figure 5.15 Negative APOE staining in control tissue (brain) (x10)

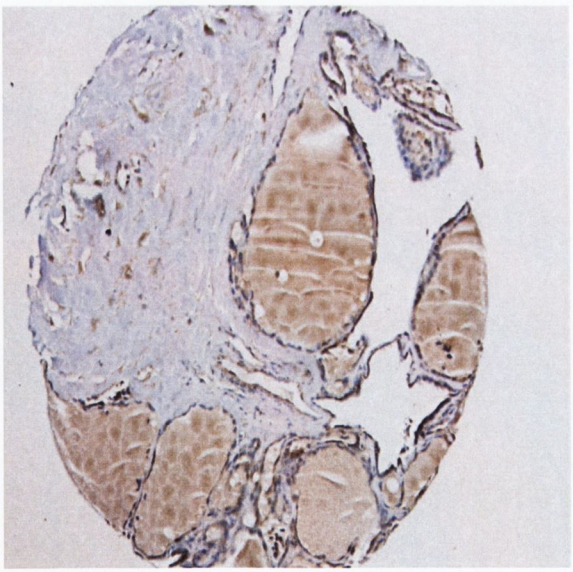

Figure 5.16 Weak cytoplasmic APOE staining in thyroid hyperplasia. 5.16 shows background colloid staining, however epithelial cells are negative (x10)

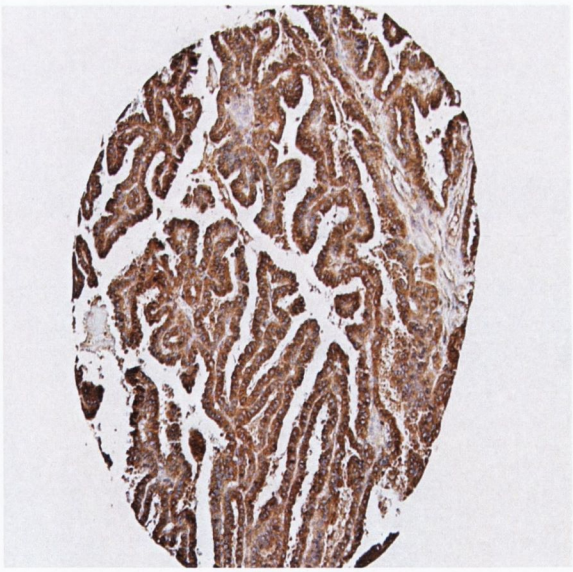

Figure 5.17 Strong cytoplasmic APOE staining in a malignant PTC (x10)

5.5.2.1.4 TOP2A

TOP2A is a DNA topoisomerase that plays a crucial role in the control of DNA topology. The TOP2A antibody is capable of nuclear and cytoplasmic staining, and its expression was up-regulated in malignant and neoplastic groups when compared to non-neoplastic and benign groups.

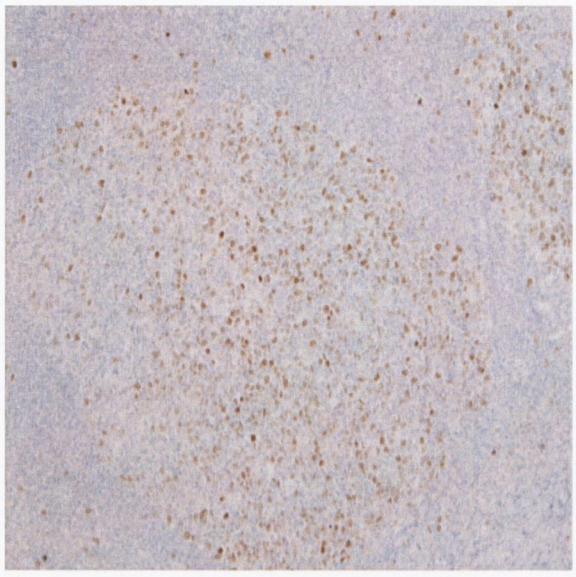

Figure 5.18 Nuclear TOP2A staining in the control tissue (tonsil) (x10)

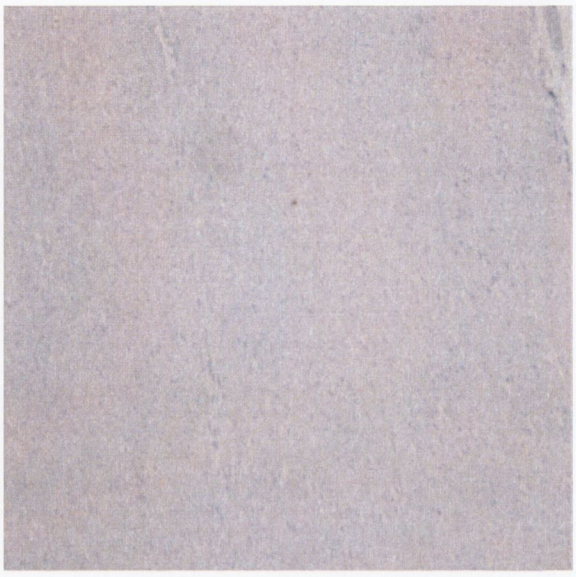

Figure 5.19 Negative TOP2A staining in the control tissue (tonsil) (x10)

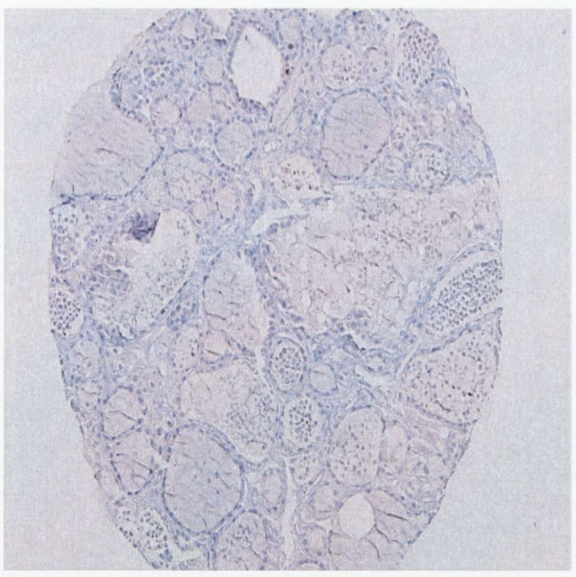

Figure 5.20 Negative TOP2A staining in thyroid hyperplastic tissue (x10)

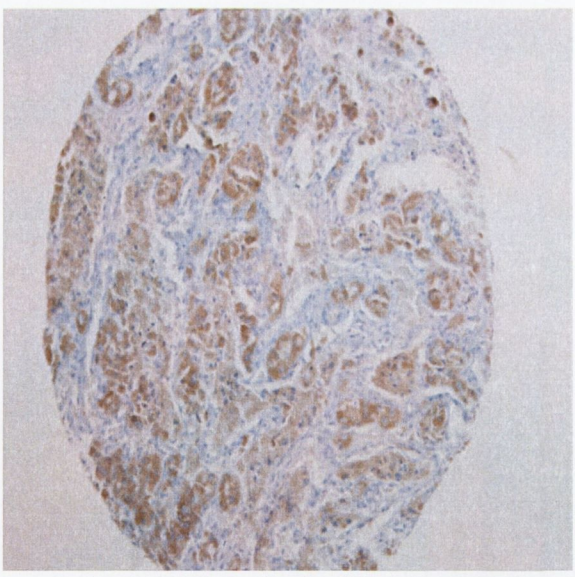

Figure 5.21 Strong cytoplasmic TOP2A staining in a malignant FTC (x10)

5.5.2.1.5 LYN

LYN is a member of the SRC family tyrosine kinases (SFK) which play an important role in the growth and metastasis of many types of human malignancies. The LYN antibody is capable of membranous and cytoplasmic staining. LYN expression was up-regulated in malignant follicular cohorts compared to benign follicular cohorts.

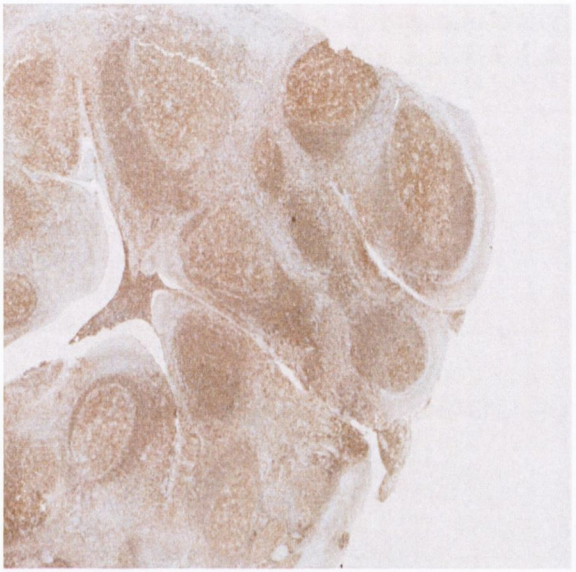

Figure 5.22 Strong cytoplasmic LYN staining in the control tissue (tonsil) (x10)

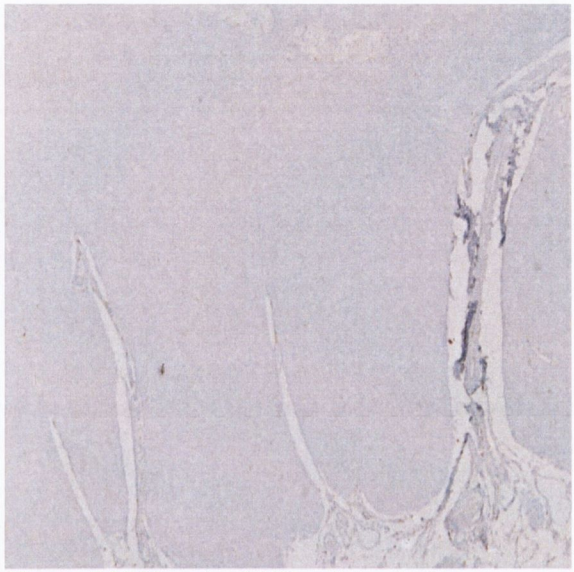

Figure 5.23 Negative LYN staining in the control tissue (tonsil) (x10)

Figure 5.24 Negative LYN staining in a benign goitre (x10)

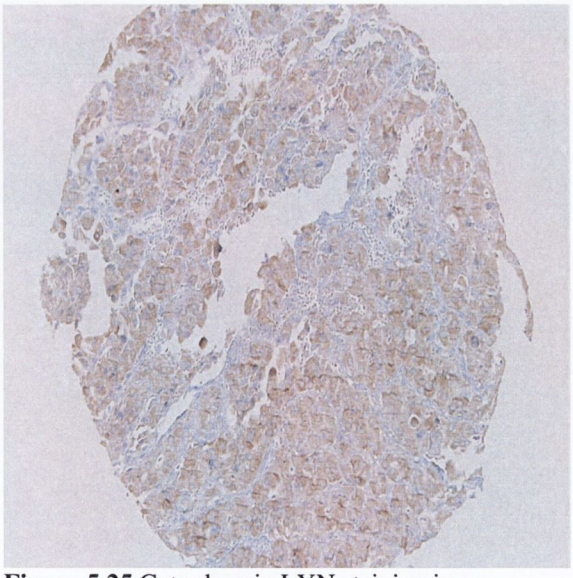

Figure 5.25 Cytoplasmic LYN staining in a malignant FTC (x10)

5.5.2.2 Boxplots representing protein expression

The following boxplots represent a selection of comparative diagnostic groups illustrating the regulation of protein expression for TOP2A (cytoplasmic stain) and LYN (cytoplasmic stain). All targets analysed were up-regulated in malignant and neoplastic groups versus benign, hyperplastic, thyroiditis and non-neoplastic cohorts.

5.5.2.2.1 TOP2A (cytoplasmic stain) protein expression boxplots

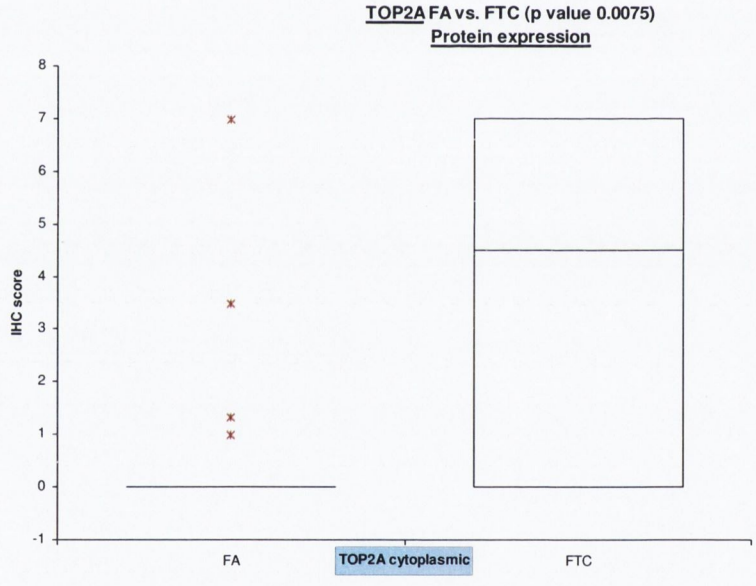

Figure 5.26 Illustrates the up-regulated expression of TOP2A in the malignant follicular thyroid carcinoma group versus the benign follicular adenoma (FA) group, p value 0.0075. The FA boxplot is illustrated as a simple line as all IHC scores were 0, apart from outliers. While the FTC boxplot is more drawn out than normal, it should be noted that the median is 4.5, compared to a median of 0 for FA, representing a substantial difference in expression

5.5.2.2.2 LYN (cytoplasmic stain) protein expression boxplots

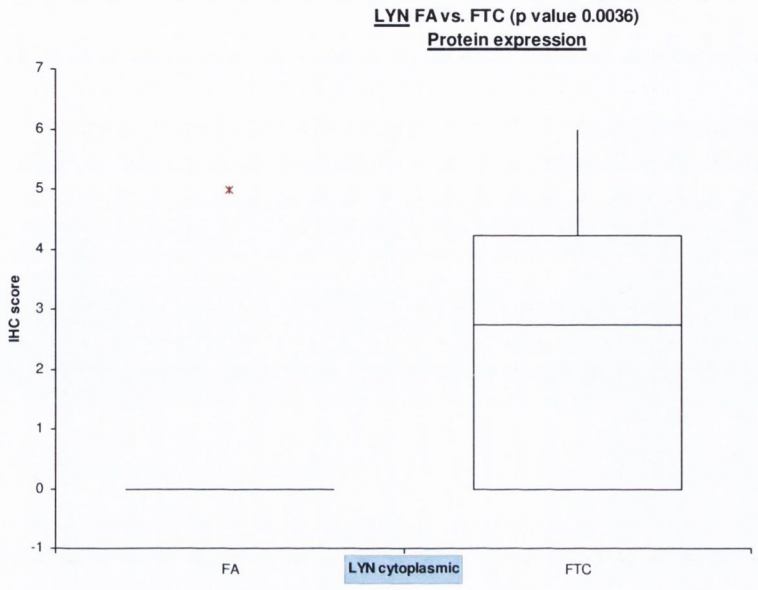

Figure 5.27 Illustrates the up-regulated expression of LYN in the malignant follicular thyroid carcinoma cohort versus the benign follicular adenoma (FA) group, p value 0.0036. Again, the FA boxplot is represented as a line due to the majority of IHC scores being 0

5.5.3 Corresponding gene and protein expression

Table 5.28 amalgamates the parallel significantly expressed results from the TaqMan® (table 5.26) and immunohistochemistry (table 5.27) data to display the categories that were expressed in matching samples at the gene and protein levels for MMP11, BAX, APOE and TOP2A (when compared to TOP2A nuclear immunohistochemical scores only).

Analysis Cohorts	MMP11 gene/protein p values	BAX gene/protein p values	APOE gene/protein p values	TOP2A (nuclear) gene/protein p values
Non-neoplastic (no hyperplasia, no thyroiditis) vs. Malignant	0.006/0.0006	0.0004/0.0011	<0.0001/0.0003	0.0028/0.0047
Non-neoplastic (no hyperplasia, no thyroiditis) vs. Neoplastic	0.0142/0.0001	0.0003/0.0039	0.0005/0.0005	0.0261/0.0058
Non-neoplastic (no hyperplasia) vs. Malignant	0.0123/0.0029	0.0004/0.008	<0.0001/0.0024	0.0039/0.0015
Non-neoplastic (no hyperplasia) vs. Neoplastic	0.0289/0.0007	0.0004/0.0243	0.0016/0.0047	0.0374/0.0018
Non-neoplastic (incl. hyperplasia + thyroiditis) vs. Malignant	0.0003/0.0057	<0.0001/0.0001	<0.0001/<0.0001	0.0063/0.0011
Non-neoplastic (incl. hyperplasia + thyroiditis) vs. Neoplastic	0.0004/0.0009	<0.0001/0.0005	<0.0001/0.0001	0.0504/0.0011
Hyperplasia vs. Malignant		0.0014/0.0002	<0.0001/0.0002	
Hyperplasia vs. Neoplastic	0.0002/0.0298	0.0012/0.0007	0.0003/0.0004	
Non-malignant (all benign, all non-neoplastic) vs. Malignant	0.0006/0.0195	0.0004/0.0002	<0.0001/0.0004	
FA vs. FVPTC			0.0246/0.01	

Table 5.28 Displays significant p values for gene and protein expression in parallel samples for MMP11, BAX, APOE and TOP2A

5.5.3.1 Boxplots representing corresponding gene and protein expression

The following boxplots represent some comparative diagnostic groups that illustrate the corresponding regulation of expression at the gene and protein level for MMP11, BAX, APOE and TOP2A.

5.5.3.1.1 MMP11 boxplots correlating gene and protein expression

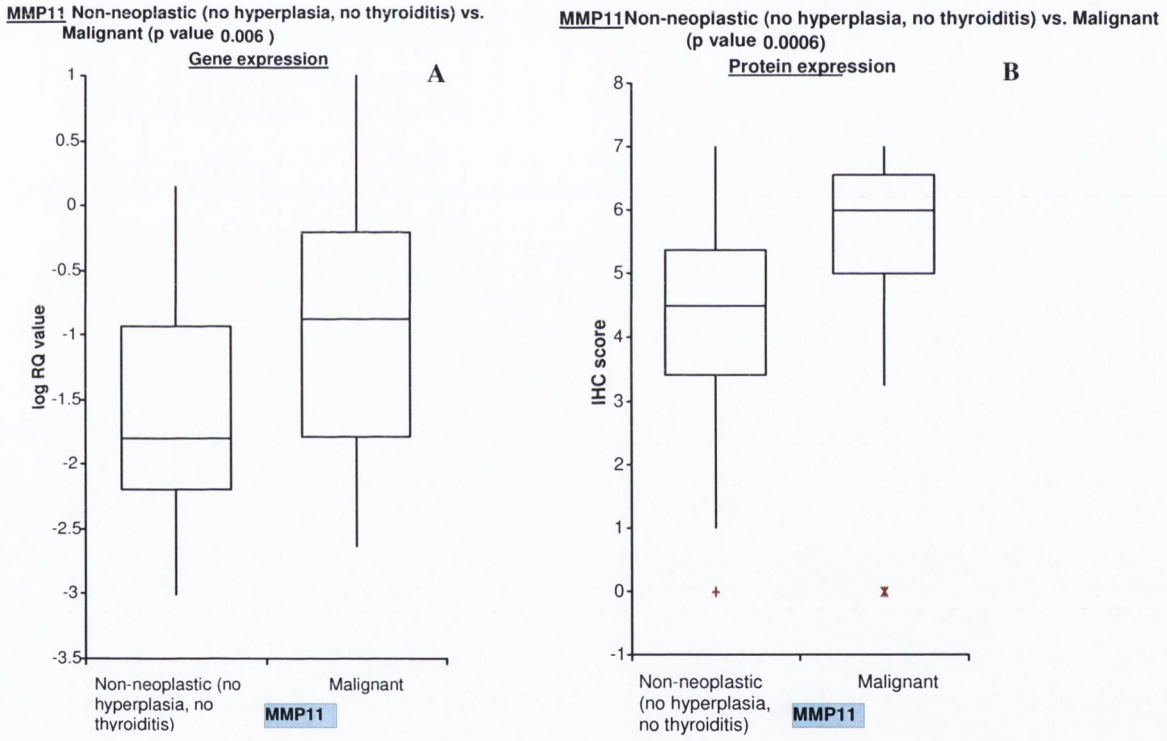

Figure 5.28 Illustrates the corresponding gene (a) and protein (b) up-regulation of MMP11 in the malignant gene cohort (a) and malignant protein cohort (b) in comparison to the non-neoplastic (no hyperplasia, no thyroiditis) gene and protein groups, p value for gene expression 0.006, p value for protein expression 0.0006

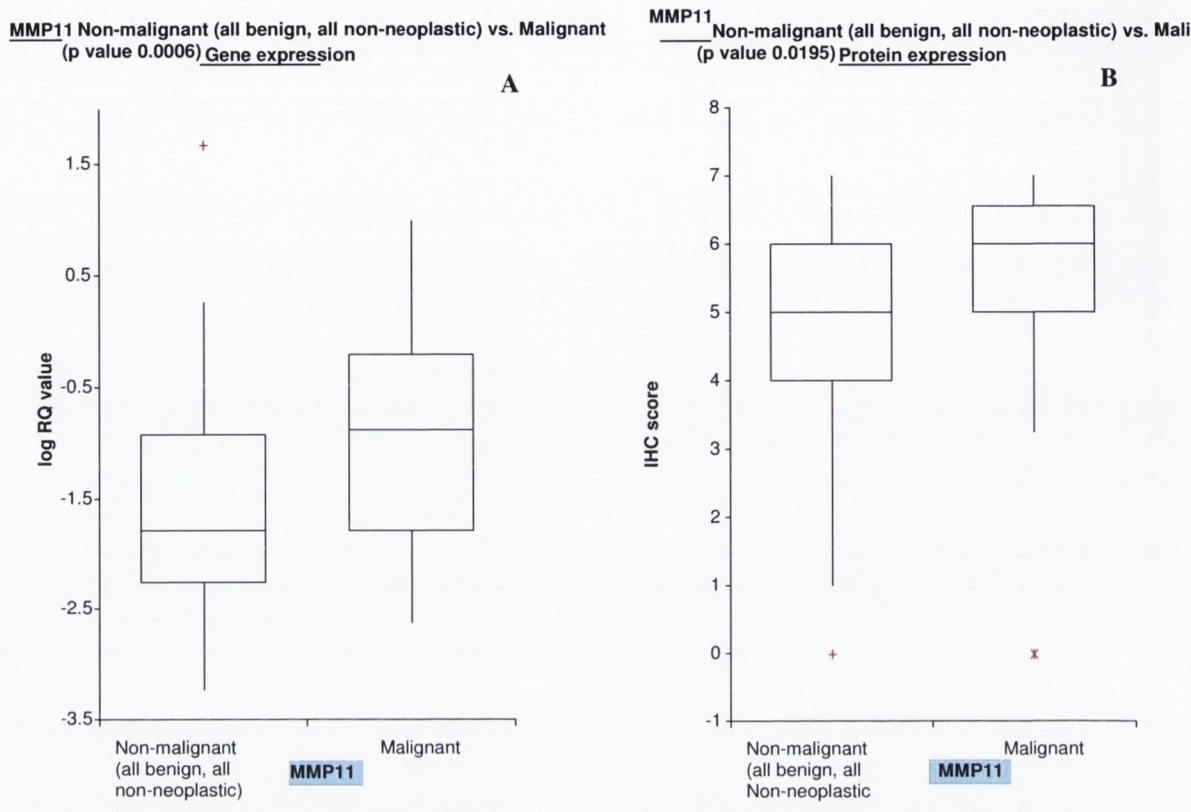

Figure 5.29 Illustrates the corresponding gene (a) and protein (b) up-regulation of MMP11, in the malignant gene cohort (a) and protein cohort (b) versus the non-malignant (all benign, all non-neoplastic) gene and protein cohorts, p value for gene expression 0.0006, p value for protein expression 0.0195

5.5.3.1.2 BAX boxplots representing corresponding gene and protein expression

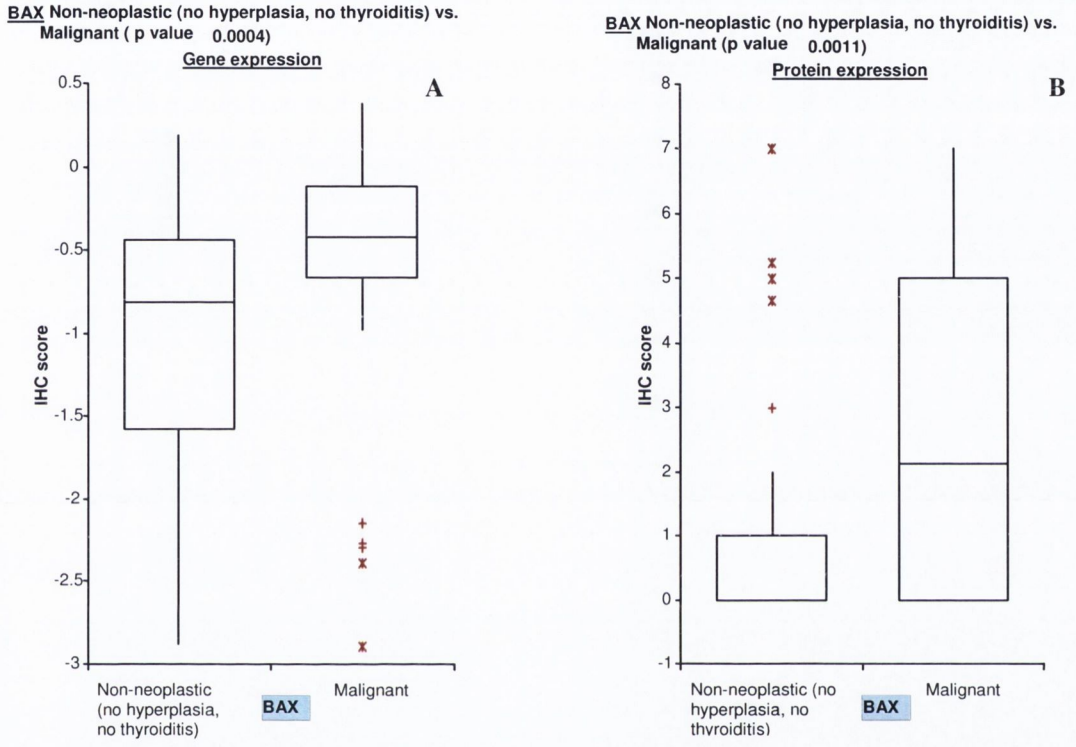

Figure 5.30 Illustrates the corresponding gene (a) and protein (b) up-regulation of BAX in the malignant versus non-neoplastic (no hyperplasia, no thyroiditis) cohorts for gene and protein expression, p value for gene expression 0.0004, p value for protein expression 0.0011. The non-neoplastic (no hyperplasia, no thyroiditis) boxplot representing protein expression (b) has its median line as the lower end of the box, at 0

5.5.3.1.3 APOE boxplots representing corresponding gene and protein expression

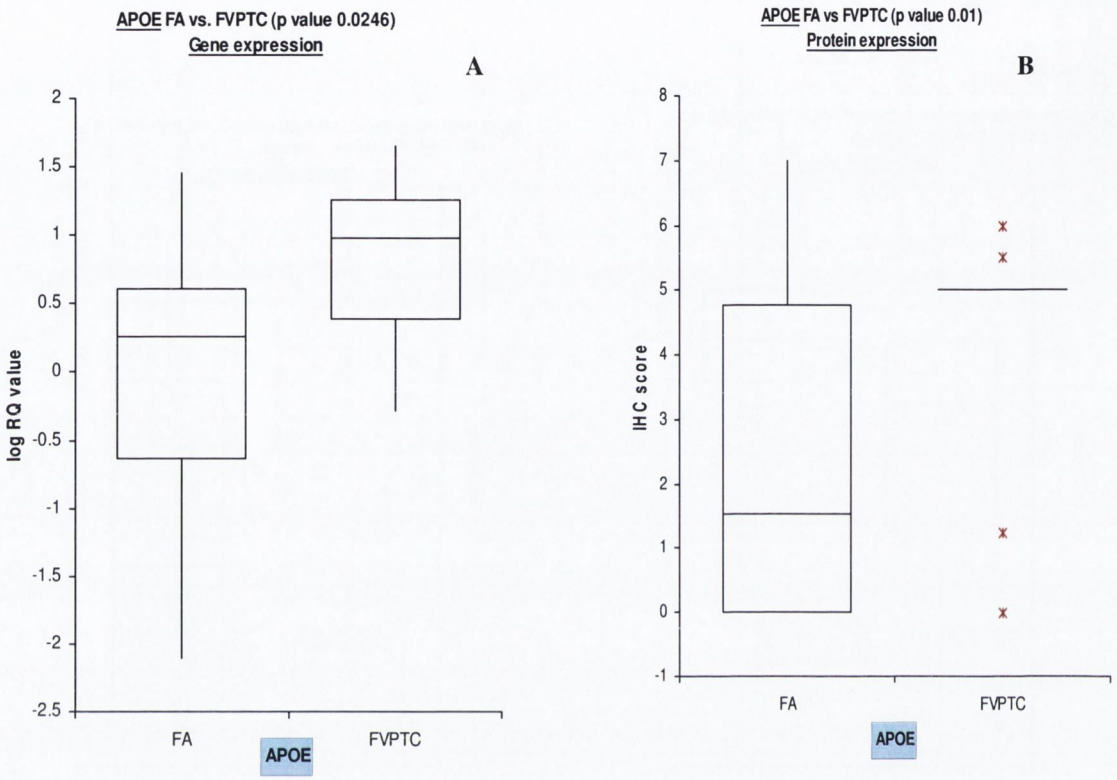

Figure 5.31 Represents the corresponding gene (a) and protein (b) up-regulation of APOE in the malignant follicular variant papillary thyroid carcinoma groups in comparison to the benign follicular adenoma groups for gene and protein expression, p value for gene expression 0.0246, p value for protein expression 0.01. The boxplot representing FVPTC protein expression (b) is one line as the median and majority of IHC scores were 5

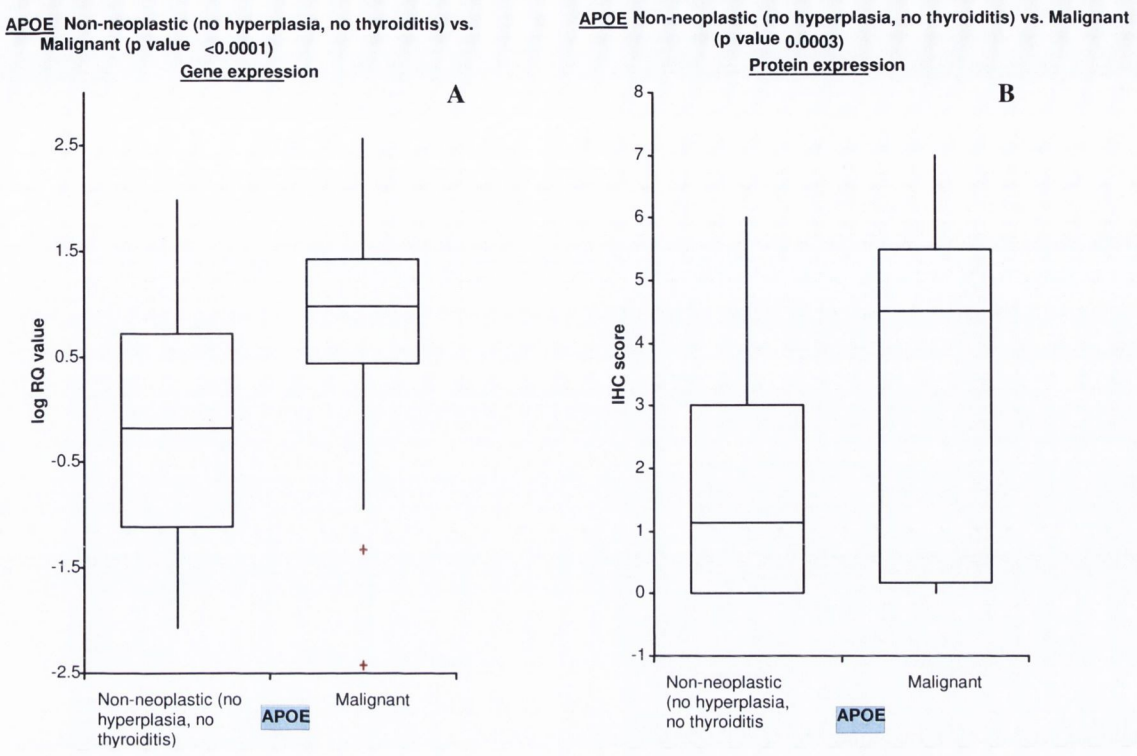

Figure 5.32 Illustrates the corresponding gene (a) and protein (b) up-regulation of APOE in the malignant cohorts compared to non-neoplastic (no hyperplasia, no thyroiditis) cohorts for gene and protein expression, p value for gene expression <0.0001, p value for protein expression 0.0003

5.5.3.1.4 TOP2A boxplots representing corresponding gene and protein expression

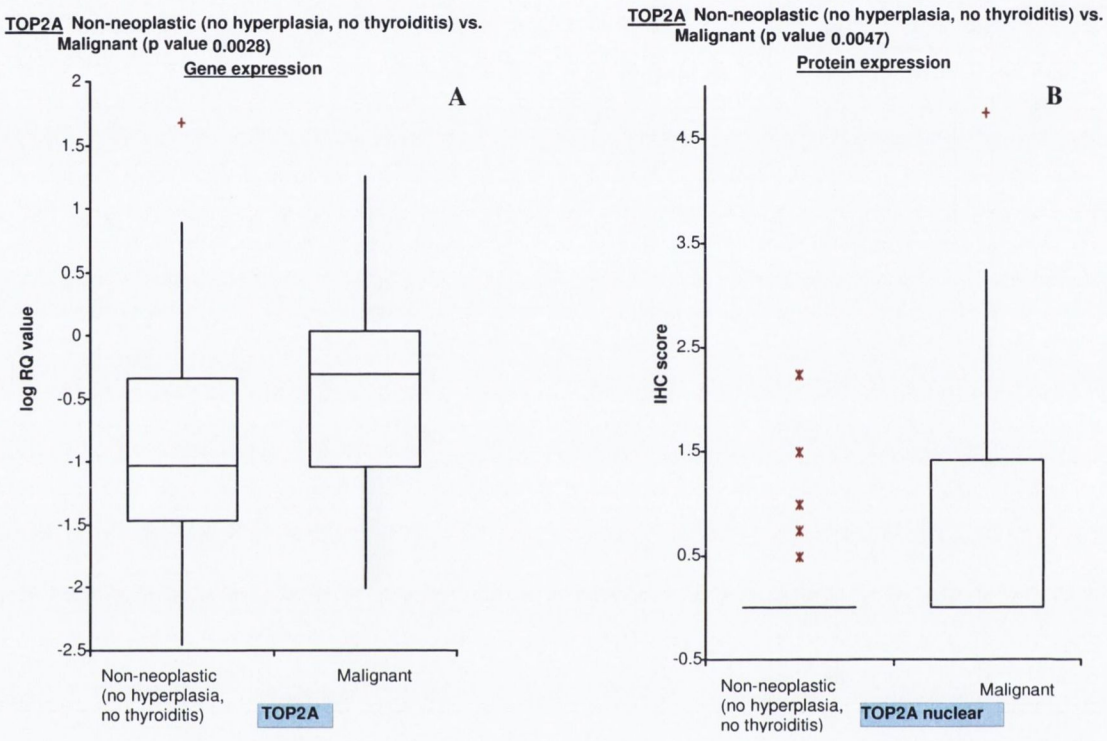

Figure 5.33 Displays corresponding up-regulated gene (a) and protein (nuclear stain) (b) expression of TOP2A in the malignant versus non-neoplastic (no hyperplasia, no thyroiditis) cohorts, p value for gene expression 0.0028, p value for protein expression 0.0047. The boxplot representing normal (no hyperplasia, no thyroiditis) protein expression (b) is again one line, illustrating that the median and the majority of IHC scores were 0

5.6 Discussion

5.6.1 Pre-amplification and endogenous control for gene expression analysis

As described in the previous chapter, the use of laser capture microdissection in archival samples leads to low yields of RNA, resulting in gene expression studies being limited to analysis of few targets (< 4 including endogenous control). As in the previous chapter, the amount of input RNA available for each of the two hundred and five samples was 0.125 μg leading to the application of a pre-amplification technique shown by our group to be unbiased and to enhance sensitivity of C_T values (Li et al., 2008). Cyclin dependent kinase inhibitor 1B (CDKN1B) was again used as the endogenous control due to its amplicon size in relation to the range of amplicon sizes of the panel of targets.

5.6.2 Expression patterns

MMP11

Matrix metalloproteinase 11 (MMP11) is a member of the matrix metalloproteinase family, which are a twenty five member family of zinc-dependent endopeptides that play a role in tumour development by promoting various events including the degradation of the extracellular matrix (Folgueras et al., 2004). Up-regulation of MMP11 was seen at the gene and protein level of expression in the malignant and neoplastic cohorts in comparison to non-neoplastic, hyperplastic and benign cohorts (tables 5.26 and 5.27). MMP11 was also over-expressed in matched samples in corresponding groups at the gene and protein level (table 5.28). In contrast to other MMPs, MMP11 (also known as stromelysin 3) is unable to degrade any major extracellular matrix component; it also has restricted substrate specificity (Duffy et al., 2000). In addition, unlike most other MMPs which are secreted as latent proteases and activated in the extracellular space, MMP11 is processed intracellularly by furin and secreted as a potentially active protease (Duffy et al., 2000).

MMP11 is up-regulated in many carcinomas and is confined to adjacent stromal areas in some tumours (Martinella-Catusse et al., 1999, Bolon et al., 1997, Basset et al., 1997, Boulay et al., 2001). However other studies examining nasopharyngeal carcinoma, cervical cancer, oral tumourigenesis, and papillary thyroid carcinoma (Sriuranpong et al., 2004, Vazquez-Ortiz et al., 2005, Ito et al., 2006, Soni et al., 2003) have shown MMP11 expression only in malignant cells. The MMP11 gene and protein expression seen in this experiment is restricted to malignant and neoplastic cells collected using laser capture microdissection. It has been proposed that MMP11 may help epithelial cells to circumvent homeostatic mechanisms and survive in an unusual and hostile environment, rendering them a selective growth advantage (Soni et al., 2003). In the setting of thyroid neoplasia, MMP11 may control proteinase activity or survival factor bioavailability (Matziari et al., 2007) to favour malignant cell survival. It is also interesting to speculate that in addition to proteinases and proteinase inhibitors, MMP11 may hydrolyze as yet uncharacterised specific substrates and act via other, as yet unknown mechanisms in thyroid malignancy.

BAX

BAX is a member of the BCL-2 family of proteins that interact to regulate cell survival and apoptosis. BAX was over-expressed at the gene and protein state in malignant and neoplastic versus non-neoplastic, thyroiditis, hyperplastic and benign cohorts (tables 5.26 and 5.27). BAX was also up-regulated in matched samples in corresponding diagnostic categories at the gene and protein level (table 5.28). In normal cells, cytoplasmic BAX is activated by cellular stress to aggregate on the membranes of the endoplasmic reticulum and mitochondria where it promotes the release of cytochrome c, (Murphy et al., 2008) which activates APAF-1, leading to the activation of the caspase cascade and execution of the cell. BAX gene and protein expression were up-regulated in a range of malignant and neoplastic groups compared to normal, thyroiditis hyperplasia and benign. This is an intriguing result as BAX is a pro-apoptotic protein, whose expression is commonly lost in carcinoma (Bargou et al., 1996, Sturm et al., 2001). However BAX expression in thyroid carcinoma has proven to be atypical, whereas many carcinomas display a lack of BAX expression, the paradoxical over-expression of pro-apoptotic BAX has been previously observed in thyroid carcinoma (Hermann et al., 2001, Murphy et al., 2008, Branet et al., 1996, Karlidag et al., 2007). Hermann and colleagues (Hermann et al., 2001) reported over-expression of BAX in malignant thyroid compared to normal and benign. They also examined expression and mutations of p53, a known transcriptional activator of BAX. They found that elevated BAX expression was associated with p53 over-expression; however no p53 mutations were detected in the carcinomas which led them to believe that the increased BAX expression may be the consequence of dysregulation of wild type p53.

In non-small-cell lung cancer, mutations in the loop-sheet motif of p53 are associated with BAX over-expression (Huang et al., 1999). Studies have also demonstrated that BAX along with other members of the BCL-2 family regulate not only apoptosis but also the cell cycle and cell proliferation. Over-expression of BAX has been correlated with accelerated entry into S phase, with decreased levels of cyclin dependent kinase inhibitor $p27^{Kip1}$ (Brady et al., 1996). In addition BAX has been shown to reverse the inhibitory effect of Bcl-2 on cell proliferation (Borner, 1996, O'Reilly et al., 1996),

although this is likely due to heterodimerization with BCL-2, as BAX alone does not accelerate cell proliferation (Borner, 1996).

It may be possible that the up-regulation of BAX seen in the malignant and neoplastic groups is due to dysregulation of either wild type or a mutated form of p53 or perhaps dimerization of BAX with other members of the BCL-2 family leading to increases in cell proliferation and resultant malignancy.

APOE

Apolipoprotein E (APOE), a 34kDa glycoprotein, is a major component of several classes of plasma lipoproteins and is capable of binding to a number of other molecules, including cell surface lipoprotein receptors and heparin sulphate proteoglycans (Ho et al., 2001). APOE was up-regulated in malignant and neoplastic versus non-neoplastic and hyperplastic groups, also in the follicular variant papillary thyroid carcinoma group (FVPTC) versus follicular adenoma (FA) at both expression levels (table 5.26 and 5.27). As with the previous two targets, APOE was up-regulated in matched samples in corresponding groups for gene and protein expression (table 5.28). APOE has long been associated with lipid transport, metabolism and homeostasis. However it is also involved in the pathophysiological processes of diseases unrelated to lipid homeostasis where specific isoforms are involved in Alzheimer's disease and immunoregulation suggesting that APOE plays a more general role than simply lipid transport (Chen et al., 2005). It has been proposed that APOE is involved in a number of signalling pathways (such as protein kinase based pathways) and resultant signal transduction pathways that may be involved in cancer development and progression. Over-expression of APOE has recently been found in a number of malignancies, such as ovarian, prostate, gastric and hepatocellular (Chen et al., 2005, Venanzoni et al., 2003, Oue et al., 2004, Yokoyama et al., 2006).

Chen and colleagues (Chen et al., 2005) reported that APOE is essential for proliferation and survival in ovarian cancer cells. Using siRNAs to knockdown APOE in an APOE expressing ovarian cancer cell line, they showed reduction of APOE

expression resulted in cell cycle arrest and apoptosis of tumour cells. They postulate that this may be due to APOEs enhancement of lipid transport (endocytosis) into tumour cells through binding to low density lipoprotein (LDL) receptor family members, which were expressed in their malignant ovarian cells. This binding of APOE to LDL receptor members results in activation of signal transduction pathways which activate downstream proliferative and anti-apoptotic signals. This may also be fallible in the setting of thyroid carcinoma as LDL receptor family members are present in thyroid carcinoma cell lines (Sid et al., 2006). Another possible explanation for the over-expression of APOE seen in malignant and neoplastic cohorts is that APOE is known to function as an antioxidant (Miyata and Smith, 1996) and due to oxidative stress in neoplastic and malignant thyroid tissues (Krohn et al., 2007); APOE may be over-expressed in these tissues.

TOP2A

Topoisomerase IIα (TOP2A) is a DNA topoisomerase, which are highly conserved essential nuclear enzymes that play a crucial role in the control of DNA topology. TOP2A was over-expressed in malignant and neoplastic groups in comparison to non-neoplastic and benign cohorts at the mRNA level (table 5.26). TOP2A nuclear staining was up-regulated in malignant and neoplastic groups versus non-neoplastic, hyperplastic and benign groups, while TOP2A cytoplasmic staining differentiated follicular lesions at the protein level of expression (table 5.27). Corresponding groups at the messenger and protein (nuclear only) state of expression showed up-regulation in malignant and neoplastic cohorts versus non-neoplastic in matched samples (table 5.28). Topoisomerases act by promoting transient DNA breakage in order to allow strand-passage events and DNA relaxation to occur before rejoining the broken DNA ends (Roca, 1995). TOP2A is involved in regulation of DNA topological structure, chromosome condensation and segregation, DNA recombination, transcription and cell cycle progression (Tretiakova et al., 2006).

TOP2A is a gene known to be amplified along with HER-2 in breast carcinoma (Jarvinen and Liu, 2003). It has also been shown to be over-expressed in a plethora of

cancers such as colon, melanoma, lung, prostate, gastric, bladder and leukaemia (Mu et al., 2000, Staley et al., 1999, Kobayashi et al., 2004, Kosari et al., 2008, Guerin et al., 2003, Simon et al., 2003, Varis et al., 2002). TOP2A is the molecular target for a large group of clinically relevant anticancer drugs termed topoII-inhibitors (Champoux, 2001). Expression of TOP2A is coupled to the cell cycle; reaching its peak in late S phase (Skotheim et al., 2003) Over-expression of TOP2A in thyroid malignancy may be involved in the cutting and religation of double stranded DNA and a resultant excessive amount of DNA replication, causing proliferation and tumourigenesis in thyroid cells.

LYN

LYN (v-yes-1 yamaguchi sarcoma viral related oncogene homolog) is a member of the SRC family tyrosine kinases (SFK) which play an important role in the growth and metastasis of many types of human malignancies. At the gene level of expression LYN was up-regulated in malignant and neoplastic cohorts versus non-neoplastic, hyperplastic and benign groups (table 5.26). At the protein level of expression, LYN showed differential membranous and cytoplasmic staining for follicular lesions (table 5.27). There were no corresponding groups of significant diagnostic comparisons for LYN expression. SRC family tyrosine kinases mediate signal transduction from several receptor tyrosine kinases, such as epidermal growth factor receptor, platelet-derived growth factor receptor, HER-2/NEU and fibroblast growth factor receptor, and are involved in the proliferation, adhesion, motility and invasion of the tumour cell (Guan et al., 2008). LYN was originally discovered in the context of haematopoietic cells, where it plays a role in the regulation of B-cell immune responses (Bolen et al., 1992). LYN over-expression has been found in haematological cancers (Roginskaya et al 1999) as well as solid tumours such as prostate, pancreatic and colon (Bates et al., 2001, Fu et al., 2006, Goldenberg-Furmanov et al., 2004).

A number of studies have shown that LYN stimulates cell proliferation and negatively regulates apoptosis (Daigle et al., 2002, Katagiri et al., 1996, Bates et al., 2001,

Grishin et al., 2001). LYN inhibition was shown to inhibit cell proliferation in prostate carcinoma (Goldenberg-Furmanov et al., 2004). Recently Stettner and colleagues demonstrated that LYN is necessary for platelet derived growth factor receptor (PDGFR) stimulated migration of cells in glioblastoma tumour cells. PDGFR is a receptor tyrosine kinase involved in multiple tumour processes (Ostman, 2004) and has been shown to be over-expressed in thyroid carcinoma (Broecker et al., 1998, Chen et al., 2006). In the setting of thyroid malignancy over-expression of LYN may result in excessive binding to PDGFR which may lead to excessive cell growth and proliferation via the MAPK signalling cascade. As mentioned, there was not any corresponding significant discrimination between groups at both the gene and protein expression level for LYN. Stettner and co-workers (Stettner et al., 2005) also found this phenomenon when comparing protein and message levels in glioblastoma samples; they found this phenomenon to be consistent with the complex regulation of cellular SRC family member activity that is not solely dependent on the level of SRC family member protein expressed. Cellular SRC activity is regulated by multiple mechanisms, which include the action of growth factor receptors and integrin receptors that activate cellular SRC. Moreover an elevated level of LYN protein could position more LYN molecules to become stimulated and to transmit signals that promote an invasive phenotype (Stettner et al., 2005). Therefore the complex nature of LYN activity may be attributable to the expression profiles seen.

5.7 Conclusions

This chapter was a follow on from the previous chapter, where the aim was to utilise the methods and knowledge gained from the application of pre-amplification to a large cohort of archival samples for gene expression analysis of a panel of targets to assess their utility as biomarkers of thyroid malignancy. With the knowledge that pre-amplification is a suitably applicable technique, it was decided to assess in more detail the utility of another potential panel of molecular markers capable of assisting in the diagnosis of thyroid malignancy. Consequently, we used pre-amplification and TaqMan® RT-PCR on a panel of five targets employing two hundred and five archival samples to assess gene expression. A tissue microarray was also constructed containing the two hundred and five samples and immunohistochemistry was used to analyse protein expression of the five targets. As in chapter four, this study not only demonstrates the ability to draw on the substantial archive of formalin fixed paraffin embedded tissue available, but it also produces five targets that can discriminate between sub groups of thyroid lesions. Moreover the study also highlights four targets capable of discriminating corresponding sub-groups of lesions at both the gene and protein level of expression in matching samples.

Further directions may include additional work involving the expression of LYN and its relation to the PDGFR, and also the aberrant expression of pro-apoptotic BAX. Nevertheless, this study has exhibited four targets that have proven their discriminatory abilities in matched samples at messenger and protein levels, leading to the conclusion that they could validly assist in the diagnosis of thyroid malignancy in the clinical setting.

5.8 References:

Bargou, R. C., Wagener, C., Bommert, K., Mapara, M. Y., Daniel, P. T., Arnold, W., Dietel, M., Guski, H., Feller, A., Royer, H. D. & Dorken, B. (1996) Overexpression of the death-promoting gene bax-alpha which is downregulated in breast cancer restores sensitivity to different apoptotic stimuli and reduces tumor growth in SCID mice. *J Clin Invest,* 97, 2651-9.

Basset, P., Bellocq, J. P., Lefebvre, O., Noel, A., Chenard, M. P., Wolf, C., Anglard, P. & Rio, M. C. (1997) Stromelysin-3: a paradigm for stroma-derived factors implicated in carcinoma progression. *Crit Rev Oncol Hematol,* 26, 43-53.

Bates, R. C., Edwards, N. S., Burns, G. F. & Fisher, D. E. (2001) A CD44 survival pathway triggers chemoresistance via lyn kinase and phosphoinositide 3-kinase/Akt in colon carcinoma cells. *Cancer Res,* 61, 5275-83.

Battifora, H. (1986) The multitumor (sausage) tissue block: novel method for immunohistochemical antibody testing. *Lab Invest,* 55, 244-8.

Bolen, J. B., Rowley, R. B., Spana, C. & Tsygankov, A. Y. (1992) The Src family of tyrosine protein kinases in hemopoietic signal transduction. *Faseb J,* 6, 3403-9.

Bolon, I., Devouassoux, M., Robert, C., Moro, D., Brambilla, C. & Brambilla, E. (1997) Expression of urokinase-type plasminogen activator, stromelysin 1, stromelysin 3, and matrilysin genes in lung carcinomas. *Am J Pathol,* 150, 1619-29.

Borner, C. (1996) Diminished cell proliferation associated with the death-protective activity of Bcl-2. *J Biol Chem,* 271, 12695-8.

Boulay, A., Masson, R., Chenard, M. P., El Fahime, M., Cassard, L., Bellocq, J. P., Sautes-Fridman, C., Basset, P. & Rio, M. C. (2001) High cancer cell death in syngeneic tumors developed in host mice deficient for the stromelysin-3 matrix metalloproteinase. *Cancer Res,* 61, 2189-93.

Brady, H. J., Gil-Gomez, G., Kirberg, J. & Berns, A. J. (1996) Bax alpha perturbs T cell development and affects cell cycle entry of T cells. *Embo J,* 15, 6991-7001.

Branet, F., Brousset, P., Krajewski, S., Schlaifer, D., Selves, J., Reed, J. C. & Caron, P. (1996) Expression of the cell death-inducing gene bax in carcinomas developed from the follicular cells of the thyroid gland. *J Clin Endocrinol Metab,* 81, 2726-30.

Broecker, M., Hammer, J. & Derwahl, M. (1998) Excessive activation of tyrosine kinases leads to inhibition of proliferation in a thyroid carcinoma cell line. *Life Sci,* 63, 2373-86.

Camp, R. L., Charette, L. A. & Rimm, D. L. (2000) Validation of tissue microarray technology in breast carcinoma. *Lab Invest,* 80, 1943-9.

Champoux, J. J. (2001) DNA topoisomerases: structure, function, and mechanism. *Annu Rev Biochem,* 70, 369-413.

Chen, K. T., Lin, J. D., Liou, M. J., Weng, H. F., Chang, C. A. & Chan, E. C. (2006) An aberrant autocrine activation of the platelet-derived growth factor alpha-receptor in follicular and papillary thyroid carcinoma cell lines. *Cancer Lett,* 231, 192-205.

Chen, Y. C., Pohl, G., Wang, T. L., Morin, P. J., Risberg, B., Kristensen, G. B., Yu, A., Davidson, B. & Shih Ie, M. (2005) Apolipoprotein E is required for cell proliferation and survival in ovarian cancer. *Cancer Res,* 65, 331-7.

Daigle, I., Yousefi, S., Colonna, M., Green, D. R. & Simon, H. U. (2002) Death receptors bind SHP-1 and block cytokine-induced anti-apoptotic signaling in neutrophils. *Nat Med,* 8, 61-7.

Duffy, M. J., Maguire, T. M., Hill, A., Mcdermott, E. & O'higgins, N. (2000) Metalloproteinases: role in breast carcinogenesis, invasion and metastasis. *Breast Cancer Res,* 2, 252-7.

Engellau, J., Akerman, M., Anderson, H., Domanski, H. A., Rambech, E., Alvegard, T. A. & Nilbert, M. (2001) Tissue microarray technique in soft tissue sarcoma: immunohistochemical Ki-67 expression in malignant fibrous histiocytoma. *Appl Immunohistochem Mol Morphol,* 9, 358-63.

Finn, S. P., Smyth, P., Cahill, S., Streck, C., O'regan, E. M., Flavin, R., Sherlock, J., Howells, D., Henfrey, R., Cullen, M., Toner, M., Timon, C., O'leary, J. J. & Sheils, O. M. (2007) Expression microarray analysis of papillary thyroid carcinoma and benign thyroid tissue: emphasis on the follicular variant and potential markers of malignancy. *Virchows Arch,* 450, 249-60.

Folgueras, A. R., Pendas, A. M., Sanchez, L. M. & Lopez-Otin, C. (2004) Matrix metalloproteinases in cancer: from new functions to improved inhibition strategies. *Int J Dev Biol,* 48, 411-24.

Fu, Y., Zagozdzon, R., Avraham, R. & Avraham, H. K. (2006) CHK negatively regulates Lyn kinase and suppresses pancreatic cancer cell invasion. *Int J Oncol,* 29, 1453-8.

Goldenberg-Furmanov, M., Stein, I., Pikarsky, E., Rubin, H., Kasem, S., Wygoda, M., Weinstein, I., Reuveni, H. & Ben-Sasson, S. A. (2004) Lyn is a target gene for prostate cancer: sequence-based inhibition induces regression of human tumor xenografts. *Cancer Res,* 64, 1058-66.

Grishin, A. V., Azhipa, O., Semenov, I. & Corey, S. J. (2001) Interaction between growth arrest-DNA damage protein 34 and Src kinase Lyn negatively regulates genotoxic apoptosis. *Proc Natl Acad Sci U S A,* 98, 10172-7.

Guan, H., Zhou, Z., Gallick, G. E., Jia, S. F., Morales, J., Sood, A. K., Corey, S. J. & Kleinerman, E. S. (2008) Targeting Lyn inhibits tumor growth and metastasis in Ewing's sarcoma. *Mol Cancer Ther,* 7, 1807-16.

Guerin, E., Entz-Werle, N., Eyer, D., Pencreac'h, E., Schneider, A., Falkenrodt, A., Uettwiller, F., Babin, A., Voegeli, A. C., Lessard, M., Gaub, M. P., Lutz, P. & Oudet, P. (2003) Modification of topoisomerase genes copy number in newly diagnosed childhood acute lymphoblastic leukemia. *Leukemia,* 17, 532-40.

Gulmann, C., O' Grady, A. (2003) Tissue microarrays: an overview. *Current Diag Path,* 9, 149-154.

Hermann, S., Sturm, I., Mrozek, A., Klosterhalfen, B., Hauptmann, S., Dorken, B. & Daniel, P. T. (2001) Bax expression in benign and malignant thyroid tumours: dysregulation of wild-type P53 is associated with a high Bax and P21 expression in thyroid carcinoma. *Int J Cancer,* 92, 805-11.

Ho, Y. Y., Deckelbaum, R. J., Chen, Y., Vogel, T. & Talmage, D. A. (2001) Apolipoprotein E inhibits serum-stimulated cell proliferation and enhances serum-independent cell proliferation. *J Biol Chem,* 276, 43455-62.

Hoos, A., Urist, M. J., Stojadinovic, A., Mastorides, S., Dudas, M. E., Leung, D. H., Kuo, D., Brennan, M. F., Lewis, J. J. & Cordon-Cardo, C. (2001) Validation of tissue microarrays for immunohistochemical profiling of cancer specimens using the example of human fibroblastic tumors. *Am J Pathol,* 158, 1245-51.

Huang, C., Kohno, N., Inufusa, H., Kodama, K., Taki, T. & Miyake, M. (1999) Overexpression of bax associated with mutations in the loop-sheet-helix motif of p53. *Am J Pathol,* 155, 955-65.

Ito, Y., Yoshida, H., Kakudo, K., Nakamura, Y., Kuma, K. & Miyauchi, A. (2006) Inverse relationships between the expression of MMP-7 and MMP-11 and predictors of poor prognosis of papillary thyroid carcinoma. *Pathology,* 38, 421-5.

Jarvinen, T. A. & Liu, E. T. (2003) Topoisomerase IIalpha gene (TOP2A) amplification and deletion in cancer--more common than anticipated. *Cytopathology,* 14, 309-13.

Karlidag, T., Cobanoglu, B., Keles, E., Alpay, H. C., Ozercan, I., Kaygusuz, I., Yalcin, S. & Sakallioglu, O. (2007) Expression of Bax, p53, and p27/kip in patients with papillary thyroid carcinoma with or without cervical nodal metastasis. *Am J Otolaryngol,* 28, 31-6.

Katagiri, K., Yokoyama, K. K., Yamamoto, T., Omura, S., Irie, S. & Katagiri, T. (1996) Lyn and Fgr protein-tyrosine kinases prevent apoptosis during retinoic acid-induced granulocytic differentiation of HL-60 cells. *J Biol Chem,* 271, 11557-62.

Kobayashi, K., Nishioka, M., Kohno, T., Nakamoto, M., Maeshima, A., Aoyagi, K., Sasaki, H., Takenoshita, S., Sugimura, H. & Yokota, J. (2004) Identification

of genes whose expression is upregulated in lung adenocarcinoma cells in comparison with type II alveolar cells and bronchiolar epithelial cells in vivo. *Oncogene,* 23, 3089-96.

Kononen, J., Bubendorf, L., Kallioniemi, A., Barlund, M., Schraml, P., Leighton, S., Torhorst, J., Mihatsch, M. J., Sauter, G. & Kallioniemi, O. P. (1998) Tissue microarrays for high-throughput molecular profiling of tumor specimens. *Nat Med,* 4, 844-7.

Kosari, F., Munz, J. M., Savci-Heijink, C. D., Spiro, C., Klee, E. W., Kube, D. M., Tillmans, L., Slezak, J., Karnes, R. J., Cheville, J. C. & Vasmatzis, G. (2008) Identification of prognostic biomarkers for prostate cancer. *Clin Cancer Res,* 14, 1734-43.

Krohn, K., Maier, J. & Paschke, R. (2007) Mechanisms of disease: hydrogen peroxide, DNA damage and mutagenesis in the development of thyroid tumors. *Nat Clin Pract Endocrinol Metab,* 3, 713-20.

Li, J., Smyth, P., Cahill, S., Denning, K., Flavin, R., Aherne, S., Pirotta, M., Guenther, S. M., O'leary, J. J. & Sheils, O. (2008) Improved RNA quality and TaqMan Pre-amplification method (PreAmp) to enhance expression analysis from formalin fixed paraffin embedded (FFPE) materials. *BMC Biotechnol,* 8, 10.

Livak, K. J. & Schmittgen, T. D. (2001) Analysis of relative gene expression data using real-time quantitative PCR and the 2(-Delta Delta C(T)) Method. *Methods,* 25, 402-8.

Martinella-Catusse, C., Nawrocki, B., Gilles, C., Birembaut, P. & Polette, M. (1999) Matrix-metalloproteinases in bronchopulmonary carcinomas. *Histol Histopathol,* 14, 839-43.

Matziari, M., Dive, V. & Yiotakis, A. (2007) Matrix metalloproteinase 11 (MMP-11; stromelysin-3) and synthetic inhibitors. *Med Res Rev,* 27, 528-52.

Miyata, M. & Smith, J. D. (1996) Apolipoprotein E allele-specific antioxidant activity and effects on cytotoxicity by oxidative insults and beta-amyloid peptides. *Nat Genet,* 14, 55-61.

Mu, X. C., Tran, T. A., Ross, J. S. & Carlson, J. A. (2000) Topoisomerase II-alpha expression in melanocytic nevi and malignant melanoma. *J Cutan Pathol,* 27, 242-8.

Murphy, K. M., Chen, F. & Clark, D. P. (2008) Identification of immunohistochemical biomarkers for papillary thyroid carcinoma using gene expression profiling. *Hum Pathol,* 39, 420-6.

Nocito, A., Bubendorf, L., Tinner, E. M., Suess, K., Wagner, U., Forster, T., Kononen, J., Fijan, A., Bruderer, J., Schmid, U., Ackermann, D., Maurer, R., Alund, G., Knonagel, H., Rist, M., Anabitarte, M., Hering, F., Hardmeier, T., Schoenenberger, A. J., Flury, R., Jager, P., Fehr, J. L., Schraml, P., Moch, H., Mihatsch, M. J., Gasser, T. & Sauter, G. (2001) Microarrays of bladder cancer

tissue are highly representative of proliferation index and histological grade. *J Pathol,* 194, 349-57.

O'reilly, L. A., Huang, D. C. & Strasser, A. (1996) The cell death inhibitor Bcl-2 and its homologues influence control of cell cycle entry. *Embo J,* 15, 6979-90.

Ostman, A. (2004) PDGF receptors-mediators of autocrine tumor growth and regulators of tumor vasculature and stroma. *Cytokine Growth Factor Rev,* 15, 275-86.

Oue, N., Hamai, Y., Mitani, Y., Matsumura, S., Oshimo, Y., Aung, P. P., Kuraoka, K., Nakayama, H. & Yasui, W. (2004) Gene expression profile of gastric carcinoma: identification of genes and tags potentially involved in invasion, metastasis, and carcinogenesis by serial analysis of gene expression. *Cancer Res,* 64, 2397-405.

Radhakrishnan, R., Solomon, M., Satyamoorthy, K., Martin, L. E. & Lingen, M. W. (2008) Tissue microarray - a high-throughput molecular analysis in head and neck cancer. *J Oral Pathol Med,* 37, 166-76.

Roca, J. (1995) The mechanisms of DNA topoisomerases. *Trends Biochem Sci,* 20, 156-60.

Rosai, J., Carcargiu, M., Delellis, R. (1992) *Tumours of the thyroid gland, Atlas of tumour pathology. ROSAI, J., SOBIN, LH.* Washington DC, Armed forces institute of pathology.

Sid, B., Dedieu, S., Delorme, N., Sartelet, H., Rath, G. M., Bellon, G. & Martiny, L. (2006) Human thyroid carcinoma cell invasion is controlled by the low density lipoprotein receptor-related protein-mediated clearance of urokinase plasminogen activator. *Int J Biochem Cell Biol,* 38, 1729-40.

Simon, R., Atefy, R., Wagner, U., Forster, T., Fijan, A., Bruderer, J., Wilber, K., Mihatsch, M. J., Gasser, T. & Sauter, G. (2003) HER-2 and TOP2A coamplification in urinary bladder cancer. *Int J Cancer,* 107, 764-72.

Simon, R. & Sauter, G. (2003) Tissue microarray (TMA) applications: implications for molecular medicine. *Expert Rev Mol Med,* 5, 1-12.

Skotheim, R. I., Kallioniemi, A., Bjerkhagen, B., Mertens, F., Brekke, H. R., Monni, O., Mousses, S., Mandahl, N., Soeter, G., Nesland, J. M., Smeland, S., Kallioniemi, O. P. & Lothe, R. A. (2003) Topoisomerase-II alpha is upregulated in malignant peripheral nerve sheath tumors and associated with clinical outcome. *J Clin Oncol,* 21, 4586-91.

Soni, S., Mathur, M., Shukla, N. K., Deo, S. V. & Ralhan, R. (2003) Stromelysin-3 expression is an early event in human oral tumorigenesis. *Int J Cancer,* 107, 309-16.

Sriuranpong, V., Mutirangura, A., Gillespie, J. W., Patel, V., Amornphimoltham, P., Molinolo, A. A., Kerekhanjanarong, V., Supanakorn, S., Supiyaphun, P.,

Rangdaeng, S., Voravud, N. & Gutkind, J. S. (2004) Global gene expression profile of nasopharyngeal carcinoma by laser capture microdissection and complementary DNA microarrays. *Clin Cancer Res,* 10, 4944-58.

Staley, B. E., Samowitz, W. S., Bronstein, I. B. & Holden, J. A. (1999) Expression of DNA topoisomerase I and DNA topoisomerase II-alpha in carcinoma of the colon. *Mod Pathol,* 12, 356-61.

Stettner, M. R., Wang, W., Nabors, L. B., Bharara, S., Flynn, D. C., Grammer, J. R., Gillespie, G. Y. & Gladson, C. L. (2005) Lyn kinase activity is the predominant cellular SRC kinase activity in glioblastoma tumor cells. *Cancer Res,* 65, 5535-43.

Sturm, I., Petrowsky, H., Volz, R., Lorenz, M., Radetzki, S., Hillebrand, T., Wolff, G., Hauptmann, S., Dorken, B. & Daniel, P. T. (2001) Analysis of p53/BAX/p16(ink4a/CDKN2) in esophageal squamous cell carcinoma: high BAX and p16(ink4a/CDKN2) identifies patients with good prognosis. *J Clin Oncol,* 19, 2272-81.

Torhorst, J., Bucher, C., Kononen, J., Haas, P., Zuber, M., Kochli, O. R., Mross, F., Dieterich, H., Moch, H., Mihatsch, M., Kallioniemi, O. P. & Sauter, G. (2001) Tissue microarrays for rapid linking of molecular changes to clinical endpoints. *Am J Pathol,* 159, 2249-56.

Tretiakova, M., Turkyilmaz, M., Grushko, T., Kocherginsky, M., Rubin, C., Teh, B. & Yang, X. J. (2006) Topoisomerase IIalpha in Wilms' tumour: gene alterations and immunoexpression. *J Clin Pathol,* 59, 1272-7.

Varis, A., Wolf, M., Monni, O., Vakkari, M. L., Kokkola, A., Moskaluk, C., Frierson, H., Jr., Powell, S. M., Knuutila, S., Kallioniemi, A. & El-Rifai, W. (2002) Targets of gene amplification and overexpression at 17q in gastric cancer. *Cancer Res,* 62, 2625-9.

Vazquez-Ortiz, G., Pina-Sanchez, P., Vazquez, K., Duenas, A., Taja, L., Mendoza, P., Garcia, J. A. & Salcedo, M. (2005) Overexpression of cathepsin F, matrix metalloproteinases 11 and 12 in cervical cancer. *BMC Cancer,* 5, 68.

Venanzoni, M. C., Giunta, S., Muraro, G. B., Storari, L., Crescini, C., Mazzucchelli, R., Montironi, R. & Seth, A. (2003) Apolipoprotein E expression in localized prostate cancers. *Int J Oncol,* 22, 779-86.

Yokoyama, Y., Kuramitsu, Y., Takashima, M., Iizuka, N., Terai, S., Oka, M., Nakamura, K., Okita, K. & Sakaida, I. (2006) Protein level of apolipoprotein E increased in human hepatocellular carcinoma. *Int J Oncol,* 28, 625-31.

Chapter Six

MicroRNA let-7a is down-regulated in thyroid malignancy

6.1 Summary

MicroRNAs (miRNAs) are a recently discovered class of small (~22nt); non-coding RNAs that negatively regulate their target messenger RNA (mRNA), and are believed to be involved in cancer development. The previous chapter established four targets that can adequately discriminate benign from malignant thyroid disease states at messenger RNA and protein expression levels. Of these four targets, MMP11 and APOE, which were over-expressed in malignant tissues, were found to be targets of microRNA let-7a using miRNA target prediction databases. Expression analysis of let-7a in a cohort of archival thyroid lesions would not only add to the expression signature that is being established for thyroid malignancy, and assess its usefulness as a marker of thyroid malignancy but it will also give more insight into the role of this miRNA in thyroid cancer.

A cohort of one hundred and four formalin fixed paraffin embedded thyroid tissues arrayed into a tissue microarray were analysed for expression of let-7a using a novel *in situ* (ISH) hybridisation technique for miRNA expression in archival samples.

Expression of let-7a was significantly ($p < 0.05$) down-regulated in all malignant and neoplastic groups. This miRNA has proven useful in discriminating benign from malignant thyroid disease and lends further knowledge to the expression signature of thyroid disease being established. It also lends further evidence to the role of let-7a as a tumour suppressor miRNA in cancer, potentially by negatively regulating MMP11 and APOE.

6.2 Introduction

During both developmental and adult life transcriptional regulators, DNA and chromatin modifiers play crucial roles to ensure that proper gene expression patterns are established and maintained in any given cell type. However, the control of gene expression also occurs at the RNA level. This includes alternative splicing, messenger RNA (mRNA) stability, and translational control, all of which appear to enhance the diversity and flexibility of gene expression regulation. Recent findings in molecular biology have shown that the participation of small regulatory non-coding RNA is required for cellular diversity in a developing and adult organism. These molecules, called microRNAs (miRNAs), act as sequence specific post-transcriptional regulators in the expression of other RNA transcripts (Fazi and Nervi, 2008).

MiRNAs are non-coding single-strand RNAs of approximately 20-23 nucleotides (nt) in length in their mature forms, that are individually encoded by their own set of genes. Genes for miRNAs are an integral component of the cells' genetic programme, many of them also being evolutionarily conserved (Ambros, 2004, Bartel, 2004). MiRNAs function as guide molecules in post-transcriptional gene silencing by base pairing with target mRNAs, which leads to mRNA cleavage or translational repression. During the past eight years, the number of miRNAs has rapidly increased, and today there are 154 miRNAs in *Caenohabditis elegans* (*C. elegans*), 152 in *Drosophila*, 472 in mouse and 678 in humans (miRBase version 11.0) (Griffiths-Jones et al., 2006) which are differentially expressed depending on the cell type and developmental stage. Bioinformatics analysis suggests that up to thirty percent of human genes may be regulated by miRNAs (Lewis et al., 2005). MiRNAs and their targets seem to form complex regulatory networks. For example, a single miRNA can bind to and regulate many different mRNA targets and, conversely, several different miRNAs can bind to and cooperatively control a single mRNA target (Kim, 2005). Therefore it is unsurprising that miRNAs have been shown to play key roles in diverse regulatory pathways.

6.2.1 MiRNA discovery

The discovery of these very short non-coding RNAs as regulators of gene activity began fifteen years ago when researchers studying larval development in the nematode worm *C. elegans* discovered a gene, lin-4, that encoded short RNA transcripts able to inhibit translation of the mRNA of a different gene, lin-14, by binding to its 3′ untranslated region (UTR) (Lee et al., 1993). This form of post-transcriptional gene silencing by a small regulatory RNA was initially regarded as a rare phenomenon, specific for nematodes. Several years later another small regulatory RNA, let-7 was identified as an additional regulator of developmental timing in *C. elegans*. Its expression pattern was found to be conserved in a wide variety of animals suggesting a more general role for small RNAs in gene regulation. Nevertheless the broad significance of these findings was not fully appreciated until hundreds of similar small RNAs were identified in *C. elegans*, *Drosophila* and mammals by molecular cloning and bioinformatics analysis in early 2001 and as a result of this, miRNAs have captured the attention of scientists in various fields.

6.2.2 MiRNA location

The distribution of miRNA genes within genomes is not random. More than half of known mammalian miRNA genes are within introns of host genes (Fazi and Nervi, 2008). Approximately forty percent of human miRNA genes are in genomic clusters, where miRNAs are found in close proximity to one another and are believed to be transcribed as polycistronic primary transcripts and subsequently cleaved into multiple miRNAs. Finally, miRNA genes are frequently located at fragile sites and genomic regions involved in cancers (Wienholds and Plasterk, 2005).

6.2.3 MiRNA biogenesis

Initial processing

The mammalian miRNA biogenesis pathway can be divided into multiple steps. Initially, miRNA genes are transcribed (generally) by RNA polymerase II into long primary miRNAs (pri-miRNAs) (Lee et al., 2004) which may be several kilobases long bearing hairpin-shaped structures. The processing of the pri-miRNA occurs in the nucleus, in a stepwise fashion, through activity of a double stranded specific endonuclease RNase III (ds-RNAseIII), Drosha. Drosha and its partner, the double stranded RNA binding domain protein DGCR8, form a microprocessor complex which cleaves the pri-miRNA near the hairpin base and releases an ~70-90 nt pre-miRNA hairpin shaped stem-loop precursor (Lee et al., 2003).

Export from the nucleus

pre-miRNAs are exported from the nucleus by Exportin-5 in the presence of Ran-GTP as cofactor. Exportin-5 interacts with the pre-miRNA "mini-helix motif" (consisting of an ~14nt stem and a short overhang), which also stabilises the pre-miRNA structure (Yi et al., 2003).

Processing into the mature form

Following export from the nucleus, the pre-miRNA is processed in the cytoplasm by the ds-RNaseIII Dicer into an ~22nt miRNA:miRNA duplex with 2nt overhanging its 3′ end (Hutvagner et al., 2001). Dicer interacts with the dsRNA-binding protein TRBP, which likely bridges the initiator and effector steps of miRNA action. Next, miRNA duplexes are unwound, which starts at the duplex end with the lowest thermodynamic stability. The miRNA strand that has it 5′ terminus at this end is the future mature miRNA (Wienholds and Plasterk, 2005). The mature miRNAs are incorporated into effector complexes that are known as miRISC (miRNA-containing RNA-induced silencing complex) (Kim, 2005). The cleavage products (~22nt miRNA duplexes) do not persist for long. Usually, one strand of this short lived duplex disappears, whereas the other strand remains as a mature miRNA.

Target recognition and down-regulation

When assembled into the miRISC complex, the mature miRNA sequence targets its complementary mRNA and negatively regulates gene expression by causing either translational inhibition or target mRNA cleavage. The choice is made based on the degree of complementarity between the miRNA and the target gene in combination with an Argonaute family protein (Wienholds and Plasterk, 2005). miRNAs recognise their target mRNAs mainly through a limited base-pairing interaction between the 5′ end "seed" region (2-8nt from the 5′ end) and the complementary sequences present in the 3′-UTRs of phylogenetically conserved target mRNAs (Bartel, 2004). Near perfect complementarity results in cleavage and as few animal miRNAs have enough complementarities to mRNA to allow cleavage (slicing), this method of repression is less common. The majority of animal miRNAs imprecisely match their targets, thereby causing target mRNA destabilisation through "non-slicer" mechanisms, including de-adenylation and other forms of translational repression (e.g. decapping). When targeted for silencing by miRNAs, mRNAs can be concentrated, sequestered from translational machinery, degraded or stored for subsequent use in large macroscopic cytoplasmic foci, named processing bodies (P bodies). The P bodies contain a wide range of enzymes involved in RNA turnover, including de-capping enzymes, de-adenylases and exonucleases (Fazi and Nervi, 2008). Figure 6.1 displays a graphic overview of the process.

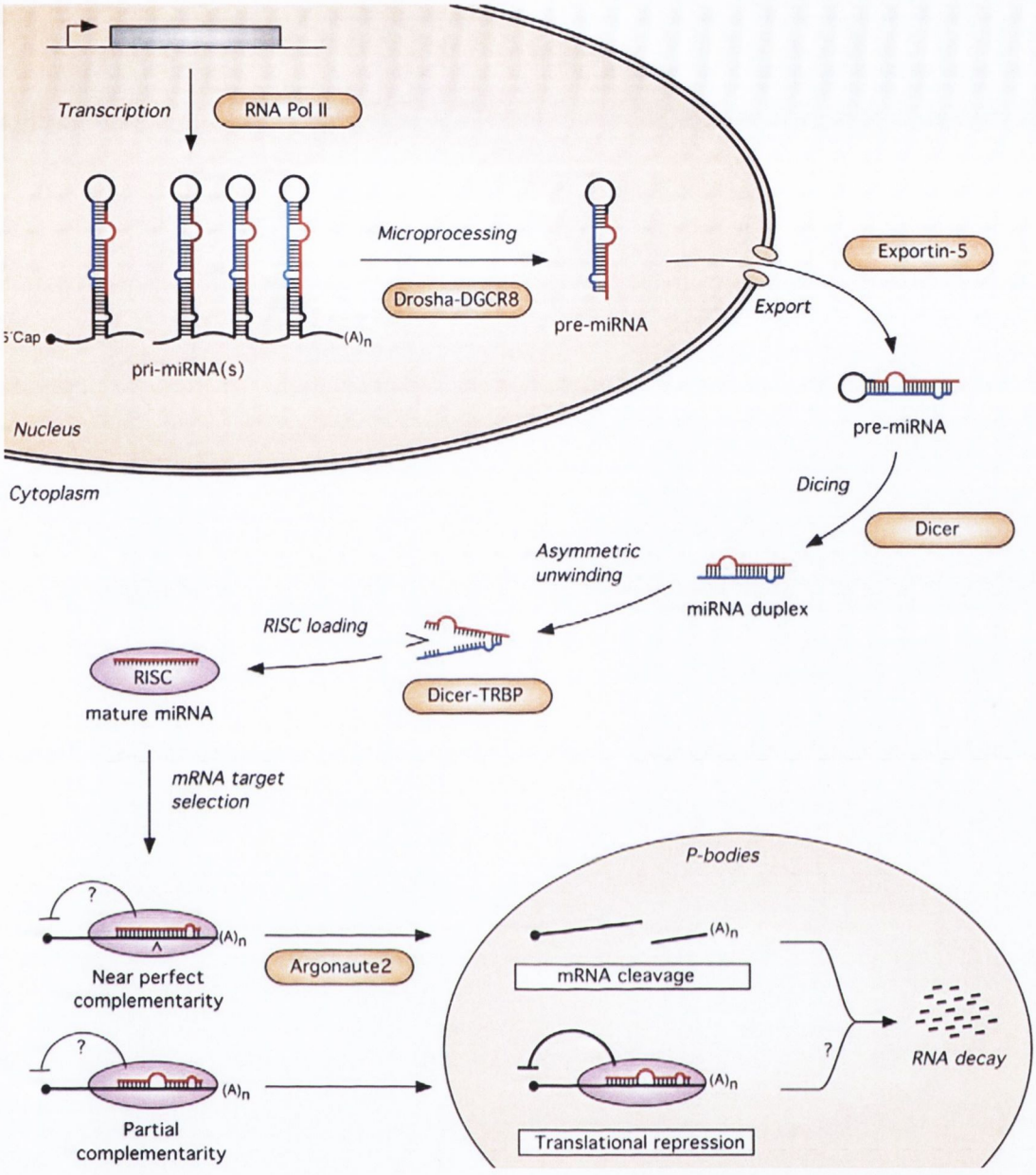

Figure 6.1 The miRNA biogenesis pathway and mechanism in mammals, see text above for details (Wienholds and Plasterk, 2005)

6.2.4 MiRNA roles and functions

MiRNAs have diverse biological functions. Cloning and measurement of miRNAs from various human tissues has proceeded quickly. We now have an overview of the sites of expression of many miRNAs. About one-third of miRNAs show substantial tissue specificity, while the others may vary in expression level but are not particularly tissue or cell type specific, at least at the resolution of currently available data (Boyd, 2008). Studies on regulatory roles of miRNAs in a variety of organisms suggest that they have critical roles in central biological processes and are regulators in development, cell proliferation, cell differentiation, stress resistance, metabolism and apoptosis. As mentioned previously, it is believed that miRNAs may be responsible for regulating approximately thirty percent of the human genome (Lewis et al., 2005). Comprising one percent of all expressed human genes, this makes miRNAs one of the largest classes of gene regulator (Bartel, 2004). The following are some examples of the functional and regulatory roles that miRNAs play in biological systems.

Embryonic development

The essential role of miRNA activity regulation during tissue development is supported by the consequences of the targeted inactivation of Dicer. In mice, the elimination of Dicer activity causes embryo death before gastrulation (Bernstein et al., 2003). Dicer inactivation in mammalian limb, myogenic compartments, lung and skin results in severe morphological defects (Harfe et al., 2005, O'Rourke et al., 2007, Andl et al., 2006, Harris et al., 2006). miRNA-21 (miR-21) is capable of suppressing embryonic stem cell self renewal by affecting the expression of the earliest expressed set of genes that play essential roles in early development, Oct4, Sox2 and Nanog (Singh et al., 2008).

Skeletal and cardiac muscle

Members of the miR-1, miR-133 families and miR-206 have recently been described in key regulatory circuitries controlling: 1) skeletal muscle cell proliferation and differentiation; 2) many aspects of cardiac biology, ranging from organogenesis in the embryo to hypertrophy in adulthood (Chen et al., 2006, Liu et al., 2007, Rao et al., 2006).

Nervous system

miR-9, miR-124 and miR-128 are among the miRNAs most highly and specifically expressed in the mammalian brain (Cao et al., 2006, Lagos-Quintana et al., 2002). Deletion of the well conserved miR-9 in fruit flies causes duplication of sensory neurons and sensory organs in development (Li et al., 2006).

Haematopoiesis

Normal haematopoiesis is guided by miRNA mediated gene regulation. Down-regulation of miR-221 and miR-222 is required for erythropoietic differentiation (Felli et al., 2005). Ectopic expression of miR-181 increases the fraction of B-lymphoid cells, whereas increased miR-223 levels re-programme granulocyte differentiation (Chen et al., 2004, Fazi et al., 2005).

The role of miRNAs in cancer will be considered in the discussion.

6.2.5 MiRNA registry and target databases/prediction

Based on targets proven to be good discriminators of benign from malignant thyroid disease in the previous chapter, and the recent explosion of interest in the role and function of miRNAs, it was decided to locate a miRNA related to some of these targets using computational approaches and analyse its expression in thyroid malignancy.

miRBase is the primary online database and repository for published miRNA sequences and annotation. The resource has three main aims, fulfilled by three distinct sections: 1) to co-ordinate a stable and sustainable nomenclature for all miRNA genes in all organisms (miRBase registry). 2) To provide all published miRNA sequences and annotation in an online database for easy searching and bulk downloads (miRBase sequences) and 3) to generate and distribute updated miRNA target predictions (miRBase targets). miRBase deals with miRNAs identified by two broad methodologies: by homology with a previously described miRNA, and by experimental validation. Novel miRNAs should be experimentally validated by cloning, sequencing, or evidence of expression of the mature miRNA product. Criteria for the identification of miRNAs have been published (Ambros et al., 2003), these guidelines remain relevant, but are subject to continued discussion and consideration.

Currently there are 678 (miRBase version 11.0) confirmed miRNAs in humans (Griffiths-Jones et al., 2006), although there may be many more. As previously mentioned, miRNAs have multiple targets. However, very few have been experimentally confirmed. The absence of a high-throughput experimental technique for miRNA target identification provided the motivation for the development of computational target prediction programmes. Several computational approaches have been implemented for miRNA gene prediction using methods based on sequence conservation and/or structural similarity. These databases also allow input of mRNA targets to obtain their associated miRNAs which is how the databases were used in this chapter. Approximately fifteen computational programmes have been developed and published since the first programme in late 2003 (Megraw et al., 2007).

The databases use algorithms for predicting miRNA associations, the main approaches look for sequence complementarity and/or for favourable miRNA-target duplex thermodynamics. The following are databases that were used to predict potential miRNAs from the targets uncovered in the previous chapter.

miRanda

miRanda identifies potential binding sites by looking for high-complementarity regions on the 3′ UTRs. The resulting binding sites are then evaluated thermodynamically using the Vienna RNA folding package (Wuchty et al., 1999).

TargetScanS

This method requires perfect complementarity to the seed region of a miRNA and then extends these regions to unravel complementarity outside the region. This aims at filtering a lot of false positives from the beginning of the prediction process. It also tests for thermodynamic stability using the Vienna RNA folding package.

PicTar

PicTar uses a group of orthologous 3′ UTRs from multiple species as input data sets and then uses an algorithm to scan the alignments of 3′ UTRs of those with seed matches to miRNAs. Alignments are filtered according to thermodynamic stability and each predicted target is scored using a Hidden Markov Model maximum likelihood fit approach.

miRGen

miRGen computes and stores miRNA targets according to combinations of widely used prediction programmes (including the above programmes). miRGen allows users to chose from: 1) predicted targets from the union of first and second generation mammalian target prediction programmes (PicTar, TargerScanS, miRanda, DIANA-microT) (DIANA-microT programme uses a thirty eight nucleotide window progressively moved across a 3′ UTR sequence). 2) Predicted targets from the intersection of second generation mammalian programmes (PicTar, TargetScanS, miRanda), 3) predicted targets from the optimal intersection of programmes (PicTar,

TargetScanS) and 4) experimentally supported targets from TarBase (Megraw et al., 2007).

Of the five targets (MMP11, BAX, APOE, TOP2A and LYN) shown to have discriminatory powers in the previous chapter, MMP11 and APOE were found to be targets of let-7a, a miRNA previously shown to be down-regulated in cancer (Johnson et al., 2005, Takamizawa et al., 2004). MMP11 was found to be a target of let-7a via an optimal intersection of PicTar and TargetScanS using miRGen, while APOE was found to be a target of let-7a using the miRBase targets database miRanda.

6.2.6 *In situ* hybridisation analysis of miRNA expression using locked nucleic acid (LNA) probes

In situ hybridization (ISH) analysis of nucleic acids was first described in 1969 (Gall and Pardue, 1969, John et al., 1969). ISH represents a unique method in which molecular biological and histochemical techniques are combined to study expression levels in tissue sections, cytological preparations and whole mounts. The method involves the specific annealing of a labelled nucleic acid probe to complementary sequences in fixed tissue or cells which is followed by visualization of the hybridized probe (Jin and Lloyd, 1997).

ISH techniques have thus far been associated with hybridization to RNA or DNA sequences; however, presented here are methods for *in situ* analysis of miRNA expression levels in formalin fixed paraffin embedded (FFPE) material.

Due to their small size and sometimes low expression level, detection of miRNA by ISH has been technically demanding. However with the advent of locked nucleic acid (LNA) probes, specific hybridization to miRNAs is now possible. LNA is a new class of bicyclic high-affinity RNA analogs in which the furnose ring of the ribose sugar is chemically locked in an RNA-mimicking conformation by the introduction of an O2′, C4′-methylene bridge, resulting in unprecedented hybridization affinity towards complementary DNA and RNA molecules (Vester and Wengel, 2004). Each incorporated LNA monomer (approximately 30% of the sequence) increases the melting temperature (T_m) of a DNA/RNA hybrid by 2-10 °C. The increased thermal stability of the LNA-DNA/RNA duplex makes it possible to make probes as short as ~20nt with high melting temperatures (>70 °C), providing the basis for high stringency required for *in situ* hybridizations (Obernosterer et al., 2007).

6.3 Aims

The aim of this chapter was to firstly assess the utility of the microRNA (miRNA) target prediction databases in selecting a miRNA target from mRNA targets used in the previous chapter. Using these databases and a review of the literature, it was decided that expression of let-7a would be analysed in a cohort of archival thyroid lesions using a novel *in situ* hybridisation method for miRNA analysis in paraffin embedded material to determine its utility as a marker of thyroid malignancy, and also to get further insight into its role in thyroid cancer.

6.4 Materials and methods

6.4.1 Samples

One hundred and four cases of formalin fixed paraffin embedded thyroid samples were analysed in this chapter, this cohort is a subset of the samples used in the previous two chapters. These cases were accessioned from archives dating from 2000 - 2005 at St. James Hospital, Dublin. The study had the approval of the St. James Hospital and Adelaide and Meath Hospital research ethics committee. Haematoxylin and eosin (H&E) sections were reviewed by a histopathologist (S.F) and classified according to a recognized system (Rosai et al., 1992). Corresponding paraffin blocks were then collected from the archives of St. James Hospital. The tables overleaf list the one hundred and four samples grouped into their diagnostic categories. As in the previous chapters, many of the groups have an overlap of the one hundred and five samples. The non-neoplastic (incl. hyperplasia) group (n=55) and the neoplastic group (n=49) constitute the overall cohort of one hundred and four samples.

The following tables (tables 6.1- 6.12) represent the grouping of samples into analysis cohorts. All samples emanate from the cohort of one hundred and four. Some samples are represented more than once in the different analysis groups.

Non-neoplastic (no hyperplasia (n=29)
No evidence of malignancy
No evidence of malignancy
No evidence of malignancy
No evidence of malignancy
No evidence of malignancy
No evidence of malignancy
Goitre, colloid
Goitre, colloid
Goitre, colloid
Goitre, colloid
Goitre, colloid
Goitre, colloid
Goitre, colloid
Goitre, colloid
Goitre, colloid
Goitre, colloid
Goitre, colloid
Goitre, colloid
Goitre, colloid
Goitre, colloid
Goitre, colloid
Goitre
Goitre
Goitre
Goitre
Goitre, adenomatous
Goitre, adenomatous
Goitre, adenomatous
Goitre, adenomatous

Table 6.1 Non-neoplastic (no hyperplasia) samples

Non-neoplastic (incl. hyperplasia) (n=55)
No evidence of malignancy
No evidence of malignancy
No evidence of malignancy
No evidence of malignancy
No evidence of malignancy
No evidence of malignancy
Goitre, colloid
Goitre, colloid
Goitre, colloid
Goitre, colloid
Goitre, colloid
Goitre, colloid
Goitre, colloid
Goitre, colloid
Goitre, colloid
Goitre, colloid
Goitre, colloid
Goitre, colloid
Goitre, colloid
Goitre, colloid
Goitre, colloid
Goitre
Goitre
Goitre
Goitre
Goitre, adenomatous
Goitre, adenomatous
Goitre, adenomatous
Goitre, adenomatous
Hyperplasia, nodular
Hyperplasia, nodular
Hyperplasia, nodular
Hyperplasia, nodular
Hyperplasia, nodular
Hyperplasia, nodular
Hyperplasia, nodular
Hyperplasia
Hyperplasia
Hyperplasia
Hyperplasia
Hyperplasia
Hyperplasia
Hyperplasia
Hyperplasia
Hyperplasia
Hyperplasia
Hyperplasia
Hyperplasia
Hyperplasia
Hyperplasia

Hyperplasia
Hyperplasia
Hyperplasia
Hyperplasia
Hyperplasia
Hyperplasia

Table 6.2 Non-neoplastic (incl. hyperplasia)

Hyperplasia (n=26)
Hyperplasia, nodular
Hyperplasia, nodular
Hyperplasia, nodular
Hyperplasia, nodular
Hyperplasia, nodular
Hyperplasia, nodular
Hyperplasia, nodular
Hyperplasia
Hyperplasia
Hyperplasia
Hyperplasia
Hyperplasia
Hyperplasia
Hyperplasia
Hyperplasia
Hyperplasia
Hyperplasia
Hyperplasia
Hyperplasia
Hyperplasia
Hyperplasia
Hyperplasia
Hyperplasia
Hyperplasia
Hyperplasia
Hyperplasia
Hyperplasia

Table 6.3 Hyperplasia samples

Follicular adenoma (n=8)
Follicular adenoma
Follicular adenoma
Follicular adenoma
Follicular adenoma
Follicular adenoma
Follicular adenoma
Follicular adenoma
Follicular adenoma

Table 6.4 Follicular adenoma samples

Benign (n=13)
Follicular adenoma
Follicular adenoma
Follicular adenoma
Follicular adenoma
Follicular adenoma
Follicular adenoma
Follicular adenoma
Follicular adenoma
Adenoma
Adenoma
Adenoma
Adenoma
Adenoma, mixed cell type

Table 6.5 Benign samples

Non-malignant (all benign, all non-neoplastic) (n=68)
No evidence of malignancy
No evidence of malignancy
No evidence of malignancy
No evidence of malignancy
No evidence of malignancy
No evidence of malignancy
Goitre, colloid
Goitre, colloid
Goitre, colloid
Goitre, colloid
Goitre, colloid
Goitre, colloid
Goitre, colloid
Goitre, colloid
Goitre, colloid
Goitre, colloid
Goitre, colloid
Goitre, colloid
Goitre, colloid
Goitre, colloid

Goitre, colloid
Goitre
Goitre
Goitre
Goitre
Goitre, adenomatous
Goitre, adenomatous
Goitre, adenomatous
Goitre, adenomatous
Hyperplasia, nodular
Hyperplasia, nodular
Hyperplasia, nodular
Hyperplasia, nodular
Hyperplasia, nodular
Hyperplasia, nodular
Hyperplasia, nodular
Hyperplasia
Hyperplasia
Hyperplasia
Hyperplasia
Hyperplasia
Hyperplasia
Hyperplasia
Hyperplasia
Hyperplasia
Hyperplasia
Hyperplasia
Hyperplasia
Hyperplasia
Hyperplasia
Hyperplasia
Hyperplasia
Hyperplasia
Hyperplasia
Hyperplasia
Follicular adenoma
Follicular adenoma
Follicular adenoma
Follicular adenoma
Follicular adenoma
Follicular adenoma
Follicular adenoma
Follicular adenoma
Adenoma
Adenoma
Adenoma
Adenoma
Adenoma, mixed cell type

Table 6.6 Non-malignant (all benign, all non-neoplastic) samples

Follicular thyroid carcinoma (n=8)
Follicular thyroid carcinoma
Follicular thyroid carcinoma
Follicular thyroid carcinoma
Follicular thyroid carcinoma
Follicular thyroid carcinoma
Follicular thyroid carcinoma
Follicular thyroid carcinoma, well differentiated
Follicular thyroid carcinoma, Hurthle cell type

Table 6.7 Follicular thyroid carcinoma samples

Papillary thyroid carcinoma (NOS) (n=25)
Papillary thyroid carcinoma
Papillary thyroid carcinoma
Papillary thyroid carcinoma

Neoplastic (n=49)
Follicular adenoma
Follicular adenoma
Follicular adenoma
Follicular adenoma
Follicular adenoma
Follicular adenoma
Follicular adenoma
Follicular adenoma
Adenoma
Adenoma
Adenoma
Adenoma
Adenoma, mixed cell type
Papillary thyroid carcinoma
Papillary thyroid carcinoma
Papillary thyroid carcinoma
Papillary thyroid carcinoma
Papillary thyroid carcinoma
Papillary thyroid carcinoma
Papillary thyroid carcinoma
Papillary thyroid carcinoma
Papillary thyroid carcinoma
Papillary thyroid carcinoma
Papillary thyroid carcinoma
Papillary thyroid carcinoma
Papillary thyroid carcinoma
Papillary thyroid carcinoma
Papillary thyroid carcinoma
Papillary thyroid carcinoma
Papillary thyroid carcinoma
Papillary thyroid carcinoma
Papillary thyroid carcinoma
Papillary thyroid carcinoma
Papillary thyroid carcinoma
Papillary thyroid carcinoma
Papillary thyroid carcinoma
Papillary thyroid carcinoma
Papillary thyroid carcinoma
Papillary thyroid carcinoma
Papillary thyroid carcinoma, trebecular
Follicular thyroid carcinoma
Follicular thyroid carcinoma
Follicular thyroid carcinoma
Follicular thyroid carcinoma
Follicular thyroid carcinoma
Follicular thyroid carcinoma
Follicular thyroid carcinoma, well differentiated
Follicular thyroid carcinoma, Hurthle cell type
Anaplastic thyroid carcinoma, giant cell type
Medullary thyroid carcinoma
Well differentiated tumour-unknown malignant potential

Table 6.11 Neoplastic samples

Malignant (n=35)
Papillary thyroid carcinoma
Papillary thyroid carcinoma
Papillary thyroid carcinoma
Papillary thyroid carcinoma
Papillary thyroid carcinoma
Papillary thyroid carcinoma
Papillary thyroid carcinoma
Papillary thyroid carcinoma
Papillary thyroid carcinoma
Papillary thyroid carcinoma
Papillary thyroid carcinoma
Papillary thyroid carcinoma
Papillary thyroid carcinoma
Papillary thyroid carcinoma
Papillary thyroid carcinoma
Papillary thyroid carcinoma
Papillary thyroid carcinoma
Papillary thyroid carcinoma
Papillary thyroid carcinoma
Papillary thyroid carcinoma
Papillary thyroid carcinoma
Papillary thyroid carcinoma
Papillary thyroid carcinoma
Papillary thyroid carcinoma
Papillary thyroid carcinoma
Papillary thyroid carcinoma
Papillary thyroid carcinoma, trebecular
Follicular thyroid carcinoma
Follicular thyroid carcinoma
Follicular thyroid carcinoma
Follicular thyroid carcinoma
Follicular thyroid carcinoma
Follicular thyroid carcinoma
Follicular thyroid carcinoma, well differentiated
Follicular thyroid carcinoma, Hurthle cell type
Anaplastic thyroid carcinoma, giant cell type
Medullary thyroid carcinoma

Table 6.12 Malignant samples

6.4.2 Tissue microarray construction and sectioning

The one hundred and four samples were arrayed into a tissue microarray block as described in section 2.11.2. Tissue microarrays (TMAs) allow high-throughput molecular profiling of disease by simultaneous analysis of multiple cores of archival tissue specimens. The one hundred and four samples were arrayed over two slides (52 cases per slide). Two rather than four TMA slides were analysed due to sample availability.

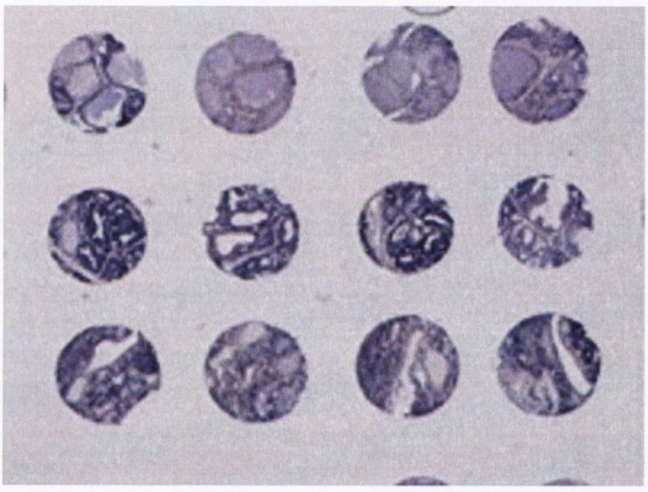

Figure 6.2 Global overview of a TMA slide stained for let-7a (x2)

6.4.3 MicroRNA expression analysis using *in situ* hybridisation

Expression of the let-7a miRNA was analysed in one hundred and four archival thyroid samples, arrayed over two TMA slides, using a novel *in situ* hybridisation (ISH) detection method for miRNA expression in paraffin embedded material. Briefly, TMA sections are deparaffinised and proteinase K is used to digest protein and remove nucleases. Hybridization of LNA modified probes to target miRNA sequences is carried out. Immuodetection of the 3′ DIG-labelled probes is carried out using anti-DIG-AP, fab fragments. Visualisation of the miRNA in the tissue section is done using a NBT-BCIP colorimetric reaction which detects the alkaline phosphate which is labelled to the miRNA via DIG (see section 2.13.2. for detailed protocol). U6 was used as a positive control and a scrambled probe was used as the negative control. Let-7a expression in breast was used as an internal positive control. U6 should not be thought of as a typical positive control as the presence or absence of this can only tell the efficacy of the experimental condition (i.e. if all conditions, bar probe concentration and stringency conditions, are optimised successfully). An internal positive control also needs to be used, which is a tissue known to be positive for the target miRNA detection probe. Therefore, normal breast tissue was used as it is known to express let-7a (Sempere et al., 2007).

Table 6.13 displays the probes analysed, their sequence (with LNA enhancement) and their melting temperature (T_m).

miRNA probe	**Sequence** (enhanced with LNA) 5′-3′	T_m (° C)
let-7a	aactatacaacctactacctca	70
U6	cacgaatttgcgtgtcatcctt	75
Scrambled-miR	ttcacaatgcgttatcggatgt	74

Table 6.13 The sequence and melting temperatures of the miRNA probes used

6.4.4 Analysis of *in situ* hybridisation scores

The evaluation of let-7a miRNA expression in each sample was evaluated independently by two histopathologists (R.F and C.B) using an *in situ* hybridisation (ISH) score. The ISH score was calculated by combining an estimate of the percentage of positively staining cells (quantity score) with an estimate of the staining intensity (intensity score). The quantity and intensity score were scored as follows, quantity score: no cells staining were scored as 0, <30% of cells staining positive were scored as 1 and >30% of cells staining positive were scored as 2. Staining intensity was rated on a scale of 0-2, with 0 = negative, 1= weak and 2 = strong. Quantity and intensity scores were added to achieve an *in situ* hybridisation score, therefore scores can range from 0-4. The ISH scores for each of the four cores representing one sample were averaged to give one final ISH score for each sample.

6.4.5 Statistical analysis

As in the previous two chapters, the distribution in each group of samples was non-normal or non-parametric, and no more than two unpaired groups of values were being compared at a time. Therefore the Mann-Whitney U-test was used to determine statistical significance for *in situ* hybridisation scores (Analyse-it® statistical software for Microsoft® Excel®).

6.5 Results

Four samples had to be removed from the analysis due to loss of TMA core tissue, these included one follicular adenoma sample and three papillary thyroid carcinoma samples, leaving a final cohort of one hundred samples to be analysed for miRNA expression of let-7a. The following diagnostic categories of groups (table 6.14) were formed from the cohort of one hundred archival samples for comparative purposes.

Analysis Cohorts
Non-neoplastic (no hyperplasia) n=29
Non-neoplastic (incl. hyperplasia) n=55
Hyperplasia n=26
Follicular adenoma n=7
Benign n=12
Non-malignant (all benign, all non-neoplastic) n=67
Follicular thyroid carcinoma n=8
Papillary thyroid carcinoma (not otherwise specified) n=22
Neoplastic n=45
Malignant n=32

Table 6.14 Demonstrates the analysis cohorts formed and numbers included in each group for miRNA analysis of let-7a

The following table (table 6.15) illustrates the groups that let-7a significantly ($p < 0.05$, Mann-Whitney U-test) discriminated between, and their corresponding p values. Let-7a was down-regulated in all malignant and neoplastic groups in comparison to benign and non-neoplastic groups.

Analysis Cohorts	Let-7a
Non-neoplastic (no hyperplasia) vs. Malignant	0.0002
Non-neoplastic (no hyperplasia) vs. Neoplastic	0.0037
Hyperplasia vs. Non-neoplastic (no hyperplasia)	0.0066
Non-neoplastic (incl. hyperplasia) vs. Malignant	0.0025
Non-neoplastic (incl. hyperplasia) vs. Neoplastic	0.0538
Benign vs. Malignant	0.0015
Benign vs. Neoplastic	0.0154
Non-malignant (all benign, all non-neoplastic) vs. Malignant	0.0006
FA vs. FTC	0.0037
PTC (NOS) vs. FTC	0.0169

Table 6.15 Displays significant p values for let-7a expression that are capable of discriminating between different analysis cohorts

6.5.1 *In situ* hybridisation images

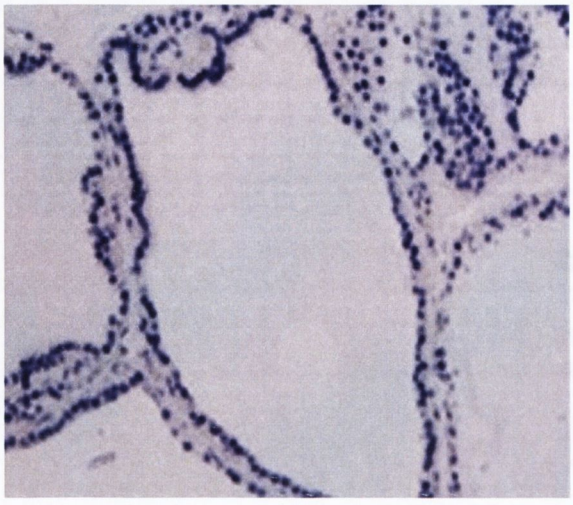

Figure 6.3 Illustrates nuclear staining of the miRNA positive control U6 in thyroid follicular cells (x20)

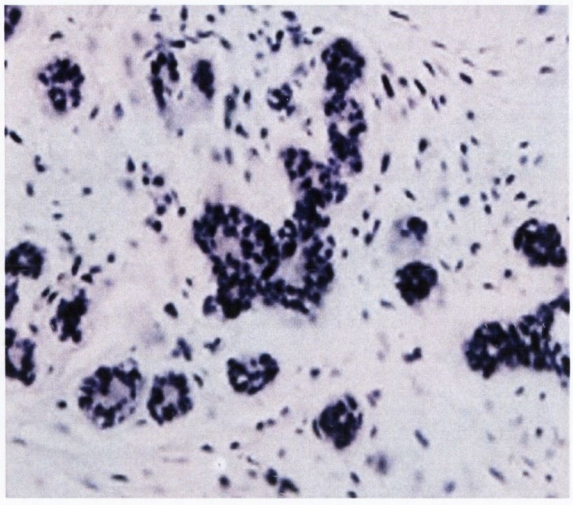

Figure 6.4 Illustrates nuclear staining of the positive control U6 in another tissue type- breast (breast lobule) (x20)

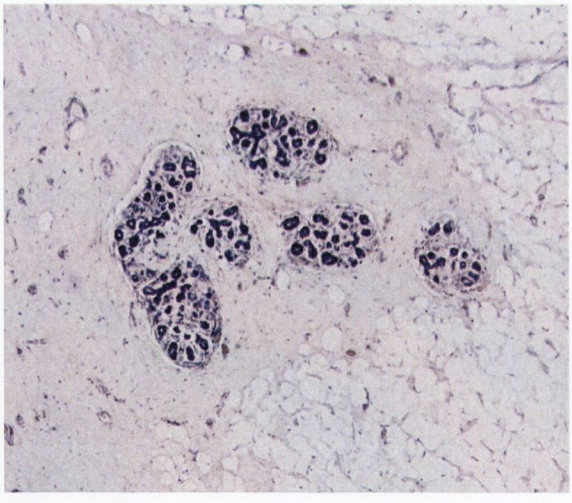

Figure 6.5 Demonstrates cytoplasmic staining of let-7a in breast tissue (breast lobule) , which was used as an internal positive control (x40)

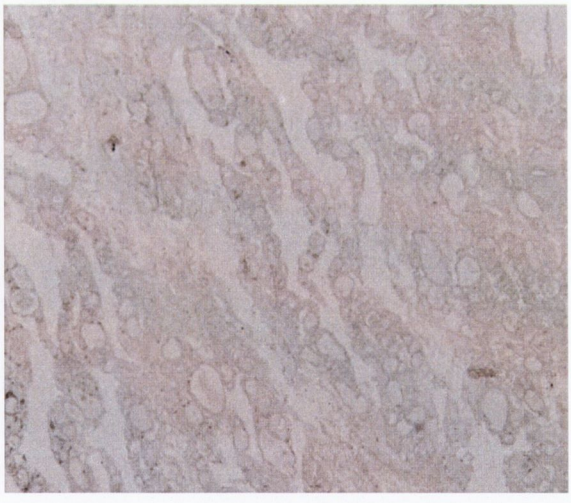

Figure 6.6 Illustrates negative scrambled probe staining in thyroid follicular cells (x20)

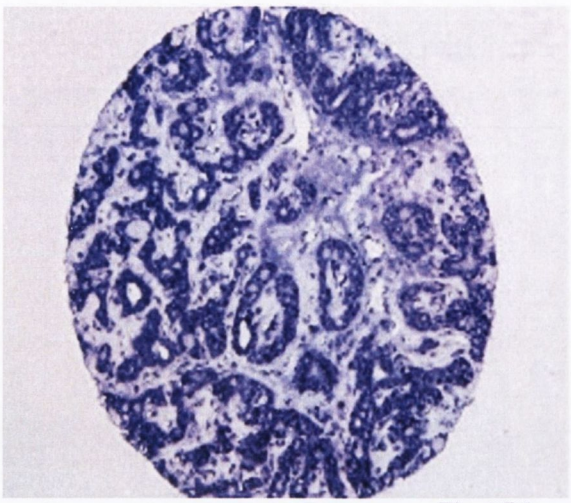

Fig. 6.7.1

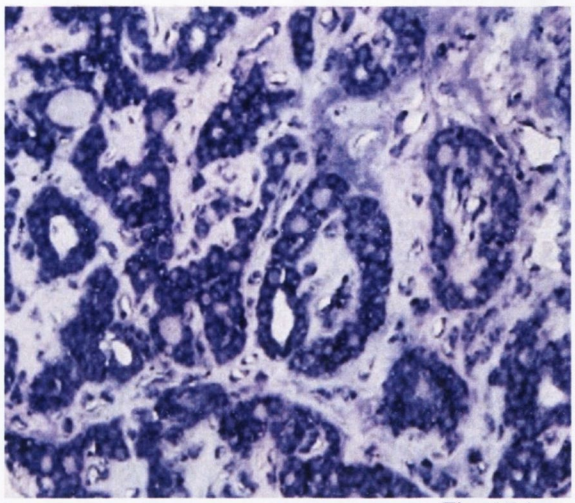

Fig. 6.7.2

Figure 6.7.1 and **6.7.2** demonstrate strong cytoplasmic staining of let-7a in a benign follicular adenoma, **6.7.1** demonstrates staining at x10 while **6.7.2** demonstrates staining at x20 resolution

Figure 6.8 Negative let-7a staining in a malignant follicular thyroid carcinoma at x20 resolution

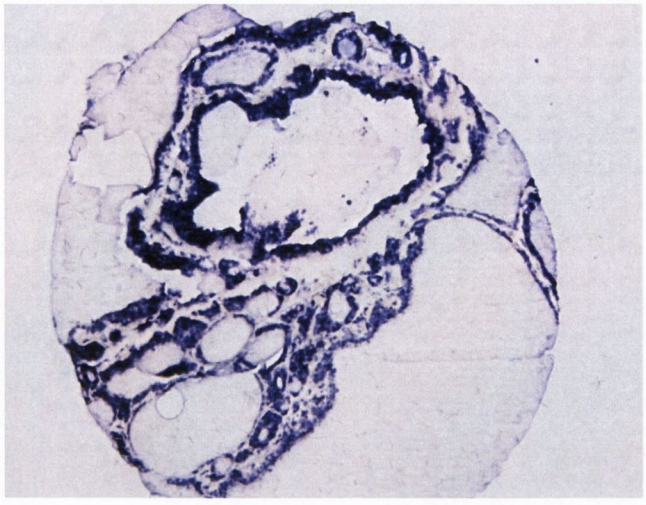

Figure 6.9 Strong cytoplasmic staining for let-7a in a normal thyroid tissue, goitre (x10)

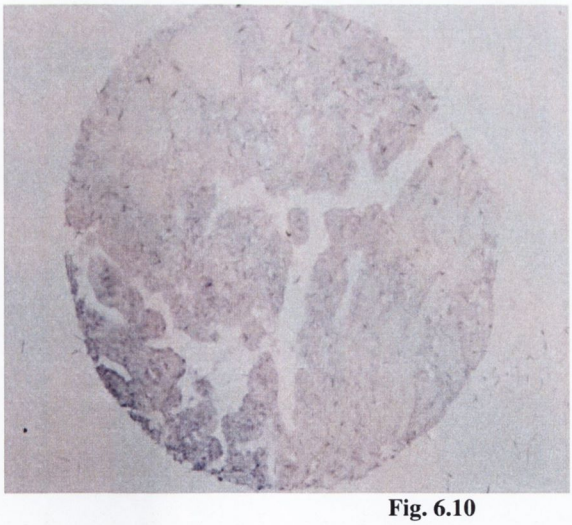

Fig. 6.10

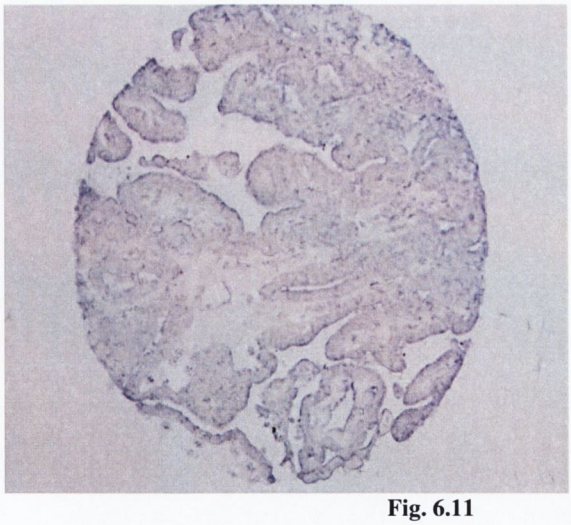

Fig. 6.11

Figure 6.10 Displays absent staining of let-7a in a malignant papillary thyroid carcinoma core at x10 resolution, while **figure 6.11** displays weak staining in another malignant papillary thyroid carcinoma core at x10

6.5.2 Let-7a expression boxplots

The following boxplots illustrate the regulation of let-7a expression among the different diagnostic categories.

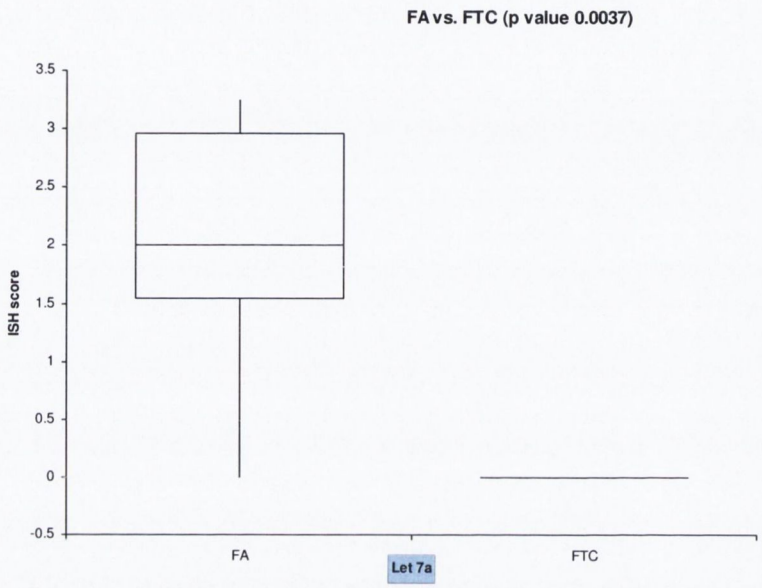

Figure 6.12 Displays up-regulation of let-7a in the benign follicular adenoma (FA) group compared to the malignant follicular thyroid carcinoma group (FTC), p value 0.0037. The boxplot for the FTC cohort is displayed as one line as ISH scores and therefore the median were all 0

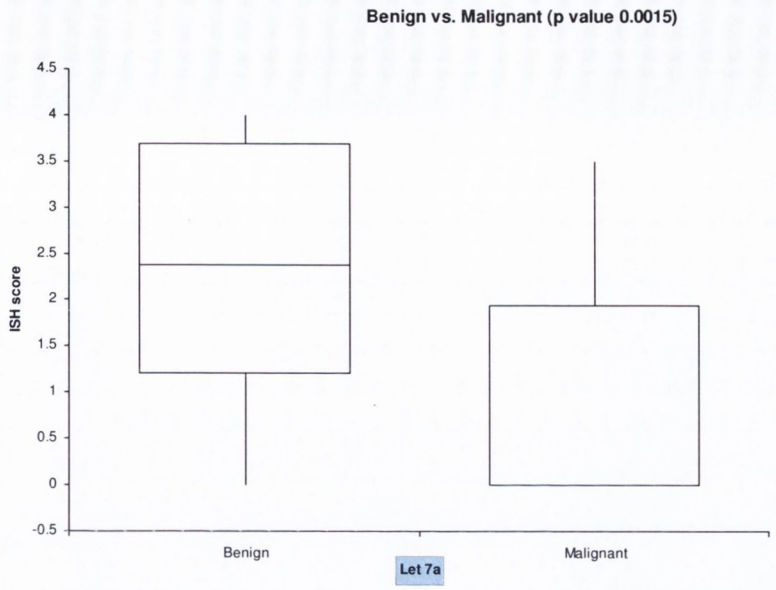

Figure 6.13 Displays the up-regulation of let-7a in the benign versus the malignant cohort, p value 0.0015. The median for the malignant cohort is at the lower end of the boxplot at 0

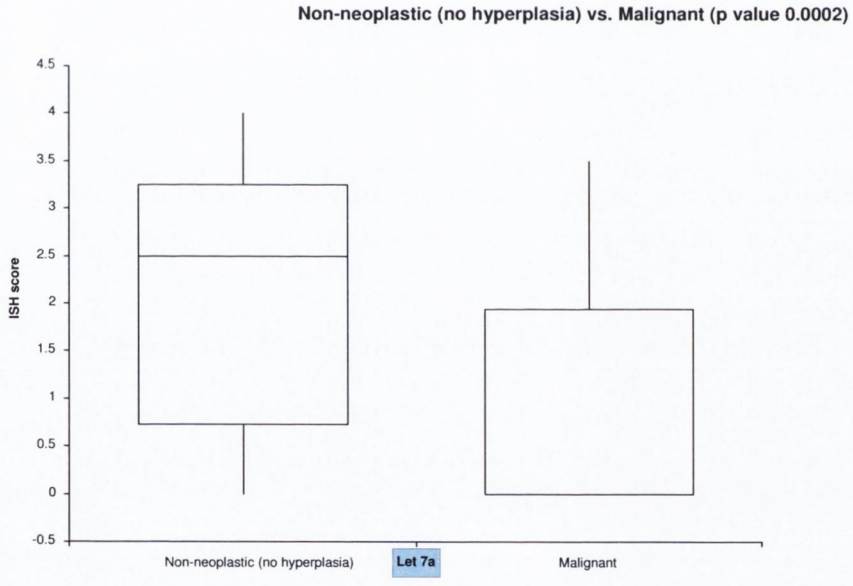

Figure 6.14 Demonstrates the over-expression of let-7a in the non-neoplastic, not including hyperplasia group, versus the malignant group, p value 0.0002. Again the median for the malignant group is 0

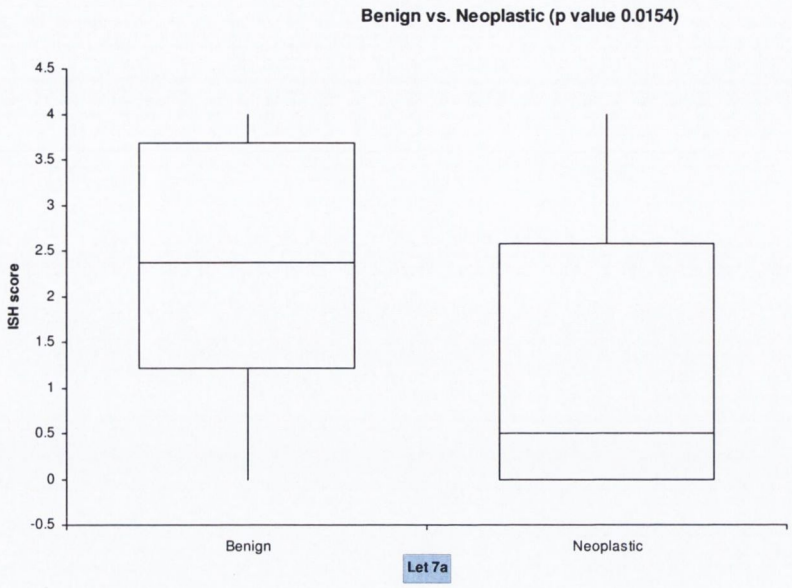

Figure 6.15 Illustrates the over-expression of let-7a in the benign cohort compared to the neoplastic cohort, p value 0.0154

6.6 Discussion

6.6.1 MiRNA analysis using in situ hybridisation in archival material

MicroRNAs (miRNAs) were first reported in mammalian systems in 2001. Since then, 6396 miRNAs (miRBase release 11.0) have been identified in vertebrates, invertebrates and plants. However the function of most miRNAs is still poorly characterised.

The challenges of studying miRNAs are two-fold. First, the short nature (~22nt) of miRNA sequences makes it difficult for traditional DNA-based analysis tools to achieve the required target sensitivity. Second, closely related miRNA family members differ by as little as one nucleotide, emphasising the need for high sensitivity and single base-pair mismatch discrimination. The use of locked nucleic acid (LNA) technology significantly increases both affinity and specificity of the probe for its miRNA target, thereby addressing both of the research challenges above. LNA detection probes bind to their target with high affinity and enable specific and sensitive detection of miRNAs. *In situ* hybridisation (ISH) detection of miRNAs is possible in whole mounts, thin sections, single cells, frozen samples and in formalin-fixed, paraffin embedded (FFPE) tissue sections. The use of LNA enhanced miRNA detection probes for ISH is a new technique. Kloosterman and colleagues (Kloosterman et al., 2006) were the first group in early 2006 to publish work on zebrafish embryos using these probes for ISH detection. Since then there has been many publications using LNA enhanced probes, however, all have been in whole mounts and frozen samples. Only two papers have published work on ISH miRNA detection in FFPE material, in brain and breast (Nelson et al., 2006, Sempere et al., 2007). The use of FFPE material requires additional optimisation and retrieval steps to unlock the formalin fixing between proteins and DNA/RNA. The successful analysis of miRNA let-7a in a panel of archival thyroid lesions demonstrates the first example of this novel technique in FFPE thyroid tissue.

6.6.2 MiRNAs and cancer

The first clue that miRNAs play a role in cancer pathogenesis came from studies in model systems where it was demonstrated that specific miRNAs contribute to the regulation of cellular differentiation, proliferation and apoptosis. Consistent with a role in controlling these processes, numerous studies have now documented widespread dysregulation of these molecules in diverse cancers (Kent and Mendell, 2006).

6.6.3 MiRNAs as tumour suppressors and oncogenes

Recent evidence has shown that miRNA mutations or mis-expression correlate with various human cancers and indicates that miRNAs can function as tumour suppressors and oncogenes (Esquela-Kerscher and Slack, 2006). Hypothetically, a miRNA that is down-regulated in cancer and targets an oncogene might act as a tumour suppressor, whereas an up-regulated miRNA that targets a tumour suppressor or a gene important for differentiation might act as an oncogene. See figure 6.16 for a graphic overview.

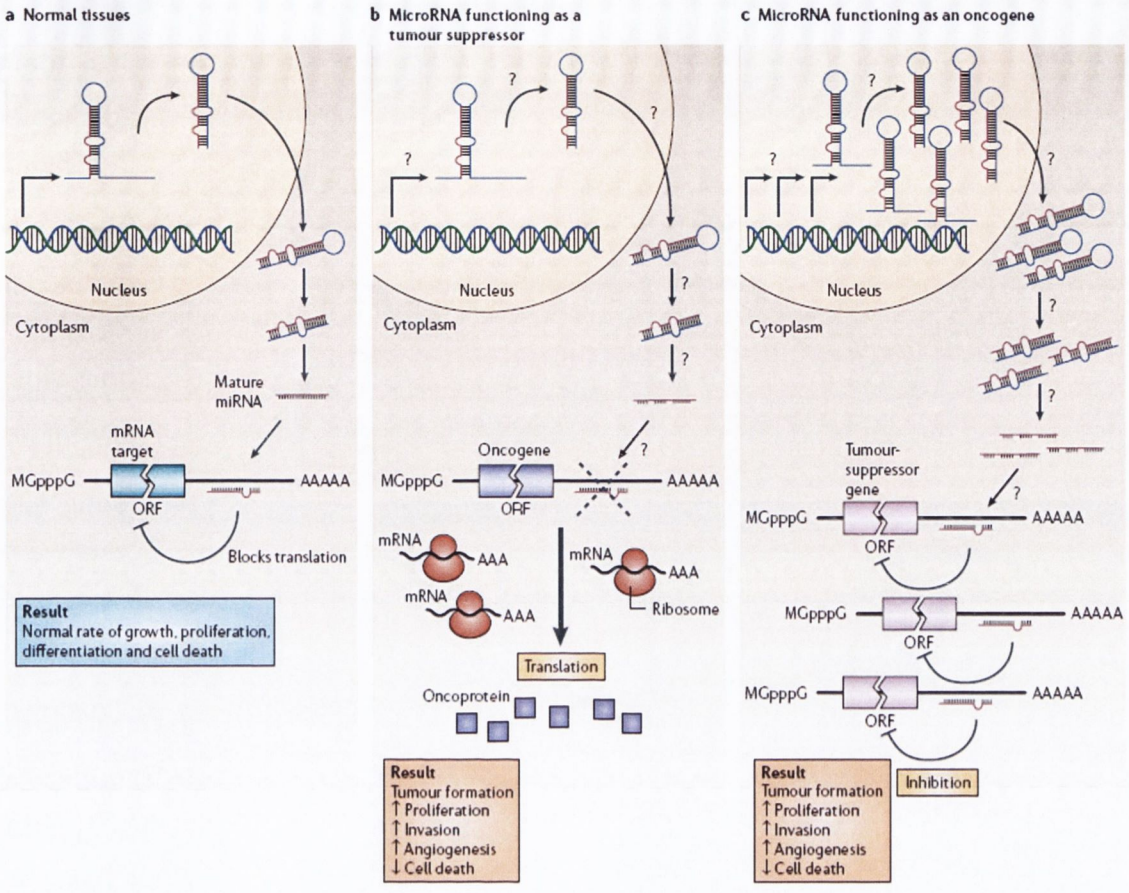

Figure 6.16 Illustrates how miRNAs can function as tumour suppressors and oncogenes

a) In normal tissues miRNAs exert their effect by targeting mRNAs which results in the repression of gene expression through a block in protein translation or mRNA stability.

b) The reduction of a miRNA that functions as a tumour suppressor leads to tumour formation. A reduction in mature miRNA levels can occur because of defects at any stage of the miRNA biogenesis process. This is shown by the question marks. This leads to inappropriate expression of the miRNA target oncogene.

c) The over-expression of a miRNA that acts as an oncogene would also result in tumour formation. Increased amounts of miRNA might be produced at inappropriate times or in the wrong tissue and would eliminate the expression of a miRNA-target tumour suppressor gene. Increased expression might occur because of amplification of the miRNA, increased efficiency in miRNA processing or increased stability of the miRNA. These are all again indicated by question marks (Esquela-Kerscher and Slack, 2006)

miR-15a and miR-16-1

The first indication that miRNAs could function as tumour suppressors came from a study by Calin and colleagues (Calin et al., 2002) that showed that patients diagnosed with B-cell chronic lymphocytic leukaemia (CLL) often have deletions or down-regulation of two clustered miRNA genes, miR-15a and miR-16-1. These two miRNAs are located in a commonly deleted area in CLL and a study by Cimmino and co-workers (Cimmino et al., 2005) showed that these two miRNAs both act as tumour suppressors by negatively-regulating B-cell CLL/lymphoma 2 (BCL2), an anti-apoptotic gene frequently up-regulated in CLL. Therefore the down-regulation of miR-15a and miR-16-1 results in increased expression of BCL2, promoting anti-apoptotic effects.

miR-143 and miR-145

The tumour suppressor roles of miR-143 and miR-145 have been shown via down-regulation of these miRNAs in colorectal and breast tumours (Iorio et al., 2005, Michael et al., 2003). Interestingly, the hairpin precursor transcripts of these miRNAs were detected in similar quantities in normal and tumour colorectal tissues, indicating that the processing of miR-143 and miR-145 might be disrupted in these cancer samples (Michael et al., 2003).

The miR-17 cluster

Recent evidence implicates a cluster of six miRNAs (miR-17-5p, miR-18a, miR-19a, miR-20a, miR-19b-1, and miR-92) as a potent oncogene. This cluster is frequently amplified in B cell lymphomas and over-expression of the cluster prevents apoptosis and accelerates the formation of c-myc-induced B-cell lymphomas in mouse models (He et al., 2005). Interestingly, c-myc itself also up-regulates the expression of miRNAs from the miR-17 cluster and the cell cycle promoter E2F1, as a target for some of these miRNAs, resulting in a tightly controlled proliferative signal (O'Donnell et al., 2005).

6.6.4 Let-7a expression in archival thyroid malignancy

Let-7a was chosen as a potential target of MMP11 and APOE using the computational databases for miRNA targets as described in section 6.2.5. and a review of the literature. Previous studies (Johnson et al., 2005, Takamizawa et al., 2004) have found let-7 to act as a tumour suppressor, where in its normal state let-7 would exert its effects by targeting mRNAs which may have oncogenic capabilities, resulting in the repression of tumour promoting gene expression. Therefore the reduction of a tumour suppressor miRNA such as let-7 would result in inappropriate expression of let-7 target mRNAs and tumour formation. Expression of MMP11 and APOE was up-regulated in all malignant and neoplastic thyroid cohorts compared to normal, hyperplastic and benign at the mRNA and protein level. *In situ* expression analysis of let-7a in a cohort of one hundred archival thyroid samples found let-7a to be down-regulated in all malignant and neoplastic groups compared to non-neoplastic and benign. Therefore let-7a may act as a tumour suppressor gene in thyroid carcinoma, where its expression is lost in malignancy, resulting in a lack of control and regulation of genes such as MMP11 and APOE. This then results in their over-expression in thyroid malignancy as we have seen in the previous chapter. Let-7a expression was found in the cytoplasm of cells. This was an expected result as the LNA incorporated miRNA probes that were used to analyse let-7a expression were complementary to the mature form of let-7a which is processed in the cytoplasm of the cell. The positive control U6 displayed nuclear rather than cytoplasmic expression as it detects human U6 small nuclear RNA.

Let-7 (lethal-7) was originally discovered in the nematode *C.elegans*, where it functions as a regulator of the transition from undifferentiated, proliferating stem cells to differentiated, quiescent cells through coordinated regulation of several target genes (Bussing et al., 2008). The let-7 family is conserved in invertebrates and vertebrates, including humans where the let-7 family consists of 12 genes encoding for nine distinct miRNAs (let-7a to let-7 i) (Torrisani et al., 2007). Let-7a is the mature miRNA whose sequence is identical across animal species from *C.elegans* to humans. By contrast, the other family members share the seed sequence but differ in the remaining nucleotides to varying extents. The sequence similarity has been a

challenge for assigning physiological functions to individual family members. However, it has been proposed that this to some degree may resemble the situation in a cell, where functional assays have thus far failed to determine any functional differences between the family members (Bussing et al., 2008).

Let-7 has been shown to control cell proliferation. Loss of let-7 activity in *C.elegans* and *Drosophila* leads to cell over-proliferation (Caygill and Johnston, 2008, Reinhart et al., 2000). Johnson and colleagues (Johnson et al., 2007) demonstrated that let-7 directly regulates key cell cycle proto-oncogenes such as RAS, CDC25a, CDK6 and cyclin D, thus controlling cell proliferation by reducing flux through the pathways promoting the G_1 to S transition. Therefore in cells with let-7 deletions or poor let-7 expression, many of these genes would be up-regulated, which is likely to stimulate cell cycle and cell division.

Let-7a's most detailed achievement as a tumour suppressor miRNA to date has been in lung carcinoma. The first piece of direct evidence for a role of let-7 in cancer came from the observation that let-7 was reduced in a significant number of lung cancer tissues and cell lines (Johnson et al., 2005, Takamizawa et al., 2004). Forced over-expression of let-7a and let-7f in one of the lung cancer cell lines resulted in an inhibition of cell proliferation (Takamizawa et al., 2004). Takamizawa and colleagues also found that let-7 levels were more powerful predictors of patient survival than age, tumour histology and smoking history, the only factor that more significantly impacted survival was disease state. In addition, Johnson and colleagues demonstrated that let-7 is a potent and direct regulator of RAS expression in cultured human cells and that there is a reciprocal expression of RAS protein and let-7 in lung, with low let-7 and high RAS in tumours but high let-7 and low RAS in adjacent normal tissue. RAS mutations are frequently found in human tumours (Malumbres and Barbacid, 2003), resulting in activation of many signalling pathways. The RAS oncogene is also widely associated with follicular thyroid carcinomas (Vasko et al., 2003). It has been shown in this experiment that let-7a expression is completely absent from follicular thyroid carcinomas (FTC) (figure 6.8) and also that its expression is absent in comparison to benign follicular adenomas (figure 6.12). In addition, expression of let-7a in FTCs was significantly down-regulated in comparison to papillary thyroid

carcinomas (not otherwise specified). It has already been shown that let-7 acts as a tumour suppressor in regulating RAS expression. This suggests that the absence of let-7 expression in FTCs may lead to RAS activated tumourigenesis in thyroid malignancy.

Reduced expression of let-7 has been found in a range of other cancers, such as breast, gastric, colon and melanoma (Sempere et al., 2007, Yu et al., 2007, Akao et al., 2006, Zhang et al., 2007, Muller and Bosserhoff, 2008).

What are the causes of abnormal miRNA expression in cancer? Calin and Croce (Calin and Croce, 2006) offer three explanations:

1) The location of miRNAs at cancer-associated genomic regions

More than half of the known human miRNAs reside in particular genomic regions that are prone to alteration in cancer cells. Such regions include minimal regions of loss of heterozygosity (LOH), which are thought to harbour tumour suppressor genes, minimal regions of amplification, which might contain oncogenes, common breakpoint regions in or near possible oncogenes or tumour suppressor genes and fragile sites.

2) Epigenetic regulation of miRNA expression

DNA hypomethylation, CpG island hypermethylation and histone-modification losses all represent epigenetic markers of malignant transformation; therefore these effects have also been investigated in miRNAs. Scott and co-workers reported a rapid alteration of miRNA levels in breast carcinoma cells in response to treatment with a hydroxamic acid histone deacetylase inhibitor LAQ824 (Scott et al., 2006). Furthermore, miRNA analysis revealed a decreased expression of the let-7 family upon LAQ824 treatment. More recently, Brueckner and colleagues demonstrated that let-7a3 is heavily methylated in normal lung samples while the tumourous let-7a3 gene remains unmethylated (Brueckner et al., 2007).

3) Abnormalities in miRNA processing genes and proteins

The protein machinery that is involved in the biogenesis of miRNAs is complex. Theoretically, alterations in these proteins should have dramatic effects on miRNA expression. It was shown that a failure of the Drosha processing step could explain the down-regulation of miRNA observed in primary tumours (Thomson et al., 2006).

Furthermore in a study of patients with non-small cell lung cancer, Karube and co-workers found that expression levels of Dicer, but not Drosha were reduced in a fraction of lung cancers (Karube et al., 2005).

6.7 Conclusions

Gene and protein expression signatures, as we have seen in the previous two chapters, are capable of differentiating disease and disease-free states in thyroid malignancy, these signatures may prove valuable in assisting diagnosis of thyroid malignancy. These signatures are simply a representation of a biological state, in the form of a pattern of gene and protein expression that is unique to the disease state. With the recent explosion of interest in the expression, role and functions of miRNAs, it is unsurprising that their expression in disease states is now also being assessed for utility in aiding diagnosis of malignancy. Recently a miRNA classifier comprising 217 miRNAs was developed to evaluate tumours of unknown origin (Lu et al., 2005, Ramaswamy et al., 2001). The miRNA-based classifier established the correct diagnosis of samples with greater accuracy (12 of 17 correct) than an mRNA classifier (1 of 17 correct). Interestingly profiling ~200 miRNAs had a better predictive power for diagnosis than profiling ~15,000 mRNAs. It has been demonstrated that the mRNA and protein targets in this thesis are robust and functional; therefore the combination of those targets plus a miRNA target would only strengthen the signature.

The potential for using miRNAs in cancer therapy is also being explored. Two groups recently used a mouse model with a gain of function KRAS mutation, which can be activated in the lung to cause tumour formation. Esquela-Kerscher and colleagues (Esquela-Kerscher et al., 2008) expressed let-7a ectopically in the lung using an adenovirus system, resulting in significant reduction of tumour formation. Kumar and colleagues (Kumar et al., 2008) infected their mouse model with a let-7g containing lentivirus, resulting in significant reduction of tumour number and tumour area. However, as in any approach involving use of therapeutic RNAs, safe and efficient delivery to the target tissue remains a major obstacle.

With the current interest in miRNA expression and function in cancer, this chapter set out to assess the utility of miRNAs in discriminating thyroid lesions. The miRNA to be analysed was chosen using targets from the previous chapter and miRNA target prediction databases, as well as a review of the literature. A novel ISH method for miRNA analysis in archival material was used, illustrating the ability to detect these tiny RNAs in the large banks of paraffin embedded material available. This chapter demonstrates the capabilities of let-7a as a marker for thyroid malignancy. As well as this, it lends further support to the role of let-7a as a tumour suppressor miRNA, and may well negatively regulate genes such as MMP11 and APOE in thyroid malignancy, although this needs to be verified using functional knock-down work. Nonetheless, the finding that let-7a can function as a proficient molecular marker for thyroid disease adds to the portfolio of the expression signature that was established in previous chapters, and certifies the signatures ability further in supporting and aiding the diagnosis of thyroid malignancy.

6.8 References:

Akao, Y., Nakagawa, Y. & Naoe, T. (2006) let-7 microRNA functions as a potential growth suppressor in human colon cancer cells. *Biol Pharm Bull,* 29, 903-6.

Ambros, V. (2004) The functions of animal microRNAs. *Nature,* 431, 350-5.

Ambros, V., Bartel, B., Bartel, D. P., Burge, C. B., Carrington, J. C., Chen, X., Dreyfuss, G., Eddy, S. R., Griffiths-Jones, S., Marshall, M., Matzke, M., Ruvkun, G. & Tuschl, T. (2003) A uniform system for microRNA annotation. *Rna,* 9, 277-9.

Andl, T., Murchison, E. P., Liu, F., Zhang, Y., Yunta-Gonzalez, M., Tobias, J. W., Andl, C. D., Seykora, J. T., Hannon, G. J. & Millar, S. E. (2006) The miRNA-processing enzyme dicer is essential for the morphogenesis and maintenance of hair follicles. *Curr Biol,* 16, 1041-9.

Bartel, D. P. (2004) MicroRNAs: genomics, biogenesis, mechanism, and function. *Cell,* 116, 281-97.

Bernstein, E., Kim, S. Y., Carmell, M. A., Murchison, E. P., Alcorn, H., Li, M. Z., Mills, A. A., Elledge, S. J., Anderson, K. V. & Hannon, G. J. (2003) Dicer is essential for mouse development. *Nat Genet,* 35, 215-7.

Boyd, S. D. (2008) Everything you wanted to know about small RNA but were afraid to ask. *Lab Invest,* 88, 569-78.

Brueckner, B., Stresemann, C., Kuner, R., Mund, C., Musch, T., Meister, M., Sultmann, H. & Lyko, F. (2007) The human let-7a-3 locus contains an epigenetically regulated microRNA gene with oncogenic function. *Cancer Res,* 67, 1419-23.

Bussing, I., Slack, F. J. & Grosshans, H. (2008) let-7 microRNAs in development, stem cells and cancer. *Trends Mol Med.*

Calin, G. A. & Croce, C. M. (2006) MicroRNA signatures in human cancers. *Nat Rev Cancer,* 6, 857-66.

Calin, G. A., Dumitru, C. D., Shimizu, M., Bichi, R., Zupo, S., Noch, E., Aldler, H., Rattan, S., Keating, M., Rai, K., Rassenti, L., Kipps, T., Negrini, M., Bullrich, F. & Croce, C. M. (2002) Frequent deletions and down-regulation of micro-RNA genes miR15 and miR16 at 13q14 in chronic lymphocytic leukemia. *Proc Natl Acad Sci U S A,* 99, 15524-9.

Cao, X., Yeo, G., Muotri, A. R., Kuwabara, T. & Gage, F. H. (2006) Noncoding RNAs in the mammalian central nervous system. *Annu Rev Neurosci,* 29, 77-103.

Caygill, E. E. & Johnston, L. A. (2008) Temporal regulation of metamorphic processes in Drosophila by the let-7 and miR-125 heterochronic microRNAs. *Curr Biol,* 18, 943-50.

Chen, C. Z., Li, L., Lodish, H. F. & Bartel, D. P. (2004) MicroRNAs modulate hematopoietic lineage differentiation. *Science,* 303, 83-6.

Chen, J. F., Mandel, E. M., Thomson, J. M., Wu, Q., Callis, T. E., Hammond, S. M., Conlon, F. L. & Wang, D. Z. (2006) The role of microRNA-1 and microRNA-133 in skeletal muscle proliferation and differentiation. *Nat Genet,* 38, 228-33.

Cimmino, A., Calin, G. A., Fabbri, M., Iorio, M. V., Ferracin, M., Shimizu, M., Wojcik, S. E., Aqeilan, R. I., Zupo, S., Dono, M., Rassenti, L., Alder, H., Volinia, S., Liu, C. G., Kipps, T. J., Negrini, M. & Croce, C. M. (2005) miR-15 and miR-16 induce apoptosis by targeting BCL2. *Proc Natl Acad Sci U S A,* 102, 13944-9.

Esquela-Kerscher, A. & Slack, F. J. (2006) Oncomirs - microRNAs with a role in cancer. *Nat Rev Cancer,* 6, 259-69.

Esquela-Kerscher, A., Trang, P., Wiggins, J. F., Patrawala, L., Cheng, A., Ford, L., Weidhaas, J. B., Brown, D., Bader, A. G. & Slack, F. J. (2008) The let-7 microRNA reduces tumor growth in mouse models of lung cancer. *Cell Cycle,* 7, 759-64.

Fazi, F. & Nervi, C. (2008) MicroRNA: basic mechanisms and transcriptional regulatory networks for cell fate determination. *Cardiovasc Res,* 79, 553-61.

Fazi, F., Rosa, A., Fatica, A., Gelmetti, V., De Marchis, M. L., Nervi, C. & Bozzoni, I. (2005) A minicircuitry comprised of microRNA-223 and transcription factors NFI-A and C/EBPalpha regulates human granulopoiesis. *Cell,* 123, 819-31.

Felli, N., Fontana, L., Pelosi, E., Botta, R., Bonci, D., Facchiano, F., Liuzzi, F., Lulli, V., Morsilli, O., Santoro, S., Valtieri, M., Calin, G. A., Liu, C. G., Sorrentino, A., Croce, C. M. & Peschle, C. (2005) MicroRNAs 221 and 222 inhibit normal erythropoiesis and erythroleukemic cell growth via kit receptor down-modulation. *Proc Natl Acad Sci U S A,* 102, 18081-6.

Gall, J. G. & Pardue, M. L. (1969) Formation and detection of RNA-DNA hybrid molecules in cytological preparations. *Proc Natl Acad Sci U S A,* 63, 378-83.

Griffiths-Jones, S., Grocock, R. J., Van Dongen, S., Bateman, A. & Enright, A. J. (2006) miRBase: microRNA sequences, targets and gene nomenclature. *Nucleic Acids Res,* 34, D140-4.

Harfe, B. D., Mcmanus, M. T., Mansfield, J. H., Hornstein, E. & Tabin, C. J. (2005) The RNaseIII enzyme Dicer is required for morphogenesis but not patterning of the vertebrate limb. *Proc Natl Acad Sci U S A,* 102, 10898-903.

Harris, K. S., Zhang, Z., Mcmanus, M. T., Harfe, B. D. & Sun, X. (2006) Dicer function is essential for lung epithelium morphogenesis. *Proc Natl Acad Sci U S A,* 103, 2208-13.

He, L., Thomson, J. M., Hemann, M. T., Hernando-Monge, E., Mu, D., Goodson, S., Powers, S., Cordon-Cardo, C., Lowe, S. W., Hannon, G. J. & Hammond, S. M. (2005) A microRNA polycistron as a potential human oncogene. *Nature,* 435, 828-33.

Hutvagner, G., Mclachlan, J., Pasquinelli, A. E., Balint, E., Tuschl, T. & Zamore, P. D. (2001) A cellular function for the RNA-interference enzyme Dicer in the maturation of the let-7 small temporal RNA. *Science,* 293, 834-8.

Iorio, M. V., Ferracin, M., Liu, C. G., Veronese, A., Spizzo, R., Sabbioni, S., Magri, E., Pedriali, M., Fabbri, M., Campiglio, M., Menard, S., Palazzo, J. P., Rosenberg, A., Musiani, P., Volinia, S., Nenci, I., Calin, G. A., Querzoli, P., Negrini, M. & Croce, C. M. (2005) MicroRNA gene expression deregulation in human breast cancer. *Cancer Res,* 65, 7065-70.

Jin, L. & Lloyd, R. V. (1997) In situ hybridization: methods and applications. *J Clin Lab Anal,* 11, 2-9.

John, H. A., Birnstiel, M. L. & Jones, K. W. (1969) RNA-DNA hybrids at the cytological level. *Nature,* 223, 582-7.

Johnson, C. D., Esquela-Kerscher, A., Stefani, G., Byrom, M., Kelnar, K., Ovcharenko, D., Wilson, M., Wang, X., Shelton, J., Shingara, J., Chin, L., Brown, D. & Slack, F. J. (2007) The let-7 microRNA represses cell proliferation pathways in human cells. *Cancer Res,* 67, 7713-22.

Johnson, S. M., Grosshans, H., Shingara, J., Byrom, M., Jarvis, R., Cheng, A., Labourier, E., Reinert, K. L., Brown, D. & Slack, F. J. (2005) RAS is regulated by the let-7 microRNA family. *Cell,* 120, 635-47.

Karube, Y., Tanaka, H., Osada, H., Tomida, S., Tatematsu, Y., Yanagisawa, K., Yatabe, Y., Takamizawa, J., Miyoshi, S., Mitsudomi, T. & Takahashi, T. (2005) Reduced expression of Dicer associated with poor prognosis in lung cancer patients. *Cancer Sci,* 96, 111-5.

Kent, O. A. & Mendell, J. T. (2006) A small piece in the cancer puzzle: microRNAs as tumor suppressors and oncogenes. *Oncogene,* 25, 6188-96.

Kim, V. N. (2005) MicroRNA biogenesis: coordinated cropping and dicing. *Nat Rev Mol Cell Biol,* 6, 376-85.

Kloosterman, W. P., Wienholds, E., De Bruijn, E., Kauppinen, S. & Plasterk, R. H. (2006) In situ detection of miRNAs in animal embryos using LNA-modified oligonucleotide probes. *Nat Methods,* 3, 27-9.

Kumar, M. S., Erkeland, S. J., Pester, R. E., Chen, C. Y., Ebert, M. S., Sharp, P. A. & Jacks, T. (2008) Suppression of non-small cell lung tumor development by the let-7 microRNA family. *Proc Natl Acad Sci U S A,* 105, 3903-8.

Lagos-Quintana, M., Rauhut, R., Yalcin, A., Meyer, J., Lendeckel, W. & Tuschl, T. (2002) Identification of tissue-specific microRNAs from mouse. *Curr Biol,* 12, 735-9.

Lee, R. C., Feinbaum, R. L. & Ambros, V. (1993) The C. elegans heterochronic gene lin-4 encodes small RNAs with antisense complementarity to lin-14. *Cell,* 75, 843-54.

Lee, Y., Ahn, C., Han, J., Choi, H., Kim, J., Yim, J., Lee, J., Provost, P., Radmark, O., Kim, S. & Kim, V. N. (2003) The nuclear RNase III Drosha initiates microRNA processing. *Nature,* 425, 415-9.

Lee, Y., Kim, M., Han, J., Yeom, K. H., Lee, S., Baek, S. H. & Kim, V. N. (2004) MicroRNA genes are transcribed by RNA polymerase II. *Embo J,* 23, 4051-60.

Lewis, B. P., Burge, C. B. & Bartel, D. P. (2005) Conserved seed pairing, often flanked by adenosines, indicates that thousands of human genes are microRNA targets. *Cell,* 120, 15-20.

Li, Y., Wang, F., Lee, J. A. & Gao, F. B. (2006) MicroRNA-9a ensures the precise specification of sensory organ precursors in Drosophila. *Genes Dev,* 20, 2793-805.

Liu, N., Williams, A. H., Kim, Y., Mcanally, J., Bezprozvannaya, S., Sutherland, L. B., Richardson, J. A., Bassel-Duby, R. & Olson, E. N. (2007) An intragenic MEF2-dependent enhancer directs muscle-specific expression of microRNAs 1 and 133. *Proc Natl Acad Sci U S A,* 104, 20844-9.

Lu, J., Getz, G., Miska, E. A., Alvarez-Saavedra, E., Lamb, J., Peck, D., Sweet-Cordero, A., Ebert, B. L., Mak, R. H., Ferrando, A. A., Downing, J. R., Jacks, T., Horvitz, H. R. & Golub, T. R. (2005) MicroRNA expression profiles classify human cancers. *Nature,* 435, 834-8.

Malumbres, M. & Barbacid, M. (2003) RAS oncogenes: the first 30 years. *Nat Rev Cancer,* 3, 459-65.

Megraw, M., Sethupathy, P., Corda, B. & Hatzigeorgiou, A. G. (2007) miRGen: a database for the study of animal microRNA genomic organization and function. *Nucleic Acids Res,* 35, D149-55.

Michael, M. Z., Sm, O. C., Van Holst Pellekaan, N. G., Young, G. P. & James, R. J. (2003) Reduced accumulation of specific microRNAs in colorectal neoplasia. *Mol Cancer Res,* 1, 882-91.

Muller, D. W. & Bosserhoff, A. K. (2008) Integrin beta(3) expression is regulated by let-7a miRNA in malignant melanoma. *Oncogene.*

Nelson, P. T., Baldwin, D. A., Kloosterman, W. P., Kauppinen, S., Plasterk, R. H. & Mourelatos, Z. (2006) RAKE and LNA-ISH reveal microRNA expression and localization in archival human brain. *Rna,* 12**,** 187-91.

O'Donnell, K. A., Wentzel, E. A., Zeller, K. I., Dang, C. V. & Mendell, J. T. (2005) c-Myc-regulated microRNAs modulate E2F1 expression. *Nature,* 435**,** 839-43.

O'Rourke, J. R., Georges, S. A., Seay, H. R., Tapscott, S. J., Mcmanus, M. T., Goldhamer, D. J., Swanson, M. S. & Harfe, B. D. (2007) Essential role for Dicer during skeletal muscle development. *Dev Biol,* 311**,** 359-68.

Obernosterer, G., Martinez, J. & Alenius, M. (2007) Locked nucleic acid-based in situ detection of microRNAs in mouse tissue sections. *Nat Protoc,* 2**,** 1508-14.

Ramaswamy, S., Tamayo, P., Rifkin, R., Mukherjee, S., Yeang, C. H., Angelo, M., Ladd, C., Reich, M., Latulippe, E., Mesirov, J. P., Poggio, T., Gerald, W., Loda, M., Lander, E. S. & Golub, T. R. (2001) Multiclass cancer diagnosis using tumor gene expression signatures. *Proc Natl Acad Sci U S A,* 98**,** 15149-54.

Rao, P. K., Kumar, R. M., Farkhondeh, M., Baskerville, S. & Lodish, H. F. (2006) Myogenic factors that regulate expression of muscle-specific microRNAs. *Proc Natl Acad Sci U S A,* 103**,** 8721-6.

Reinhart, B. J., Slack, F. J., Basson, M., Pasquinelli, A. E., Bettinger, J. C., Rougvie, A. E., Horvitz, H. R. & Ruvkun, G. (2000) The 21-nucleotide let-7 RNA regulates developmental timing in Caenorhabditis elegans. *Nature,* 403**,** 901-6.

Rosai, J., Carcangio, M. & Delellis, R. (1992) *Tumours of the thyroid gland, Atlas of tumour pathology. ROSAI, J. & SOBIN, L.* Washington DC, Armed forces institute of pathology.

Sempere, L. F., Christensen, M., Silahtaroglu, A., Bak, M., Heath, C. V., Schwartz, G., Wells, W., Kauppinen, S. & Cole, C. N. (2007) Altered MicroRNA expression confined to specific epithelial cell subpopulations in breast cancer. *Cancer Res,* 67**,** 11612-20.

Singh, S. K., Kagalwala, M. N., Parker-Thornburg, J., Adams, H. & Majumder, S. (2008) REST maintains self-renewal and pluripotency of embryonic stem cells. *Nature,* 453**,** 223-7.

Takamizawa, J., Konishi, H., Yanagisawa, K., Tomida, S., Osada, H., Endoh, H., Harano, T., Yatabe, Y., Nagino, M., Nimura, Y., Mitsudomi, T. & Takahashi, T. (2004) Reduced expression of the let-7 microRNAs in human lung cancers in association with shortened postoperative survival. *Cancer Res,* 64**,** 3753-6.

Thomson, J. M., Newman, M., Parker, J. S., Morin-Kensicki, E. M., Wright, T. & Hammond, S. M. (2006) Extensive post-transcriptional regulation of microRNAs and its implications for cancer. *Genes Dev,* 20**,** 2202-7.

Torrisani, J., Parmentier, L., Buscail, L. & Cordelier, P. (2007) Enjoy the Silence: The Story of let-7 MicroRNA and Cancer. *Curr Genomics,* 8, 229-33.

Vasko, V., Ferrand, M., Di Cristofaro, J., Carayon, P., Henry, J. F. & De Micco, C. (2003) Specific pattern of RAS oncogene mutations in follicular thyroid tumors. *J Clin Endocrinol Metab,* 88, 2745-52.

Vester, B. & Wengel, J. (2004) LNA (locked nucleic acid): high-affinity targeting of complementary RNA and DNA. *Biochemistry,* 43, 13233-41.

Wienholds, E. & Plasterk, R. H. (2005) MicroRNA function in animal development. *FEBS Lett,* 579, 5911-22.

Wuchty, S., Fontana, W., Hofacker, I. L. & Schuster, P. (1999) Complete suboptimal folding of RNA and the stability of secondary structures. *Biopolymers,* 49, 145-65.

Yi, R., Qin, Y., Macara, I. G. & Cullen, B. R. (2003) Exportin-5 mediates the nuclear export of pre-microRNAs and short hairpin RNAs. *Genes Dev,* 17, 3011-6.

Yu, F., Yao, H., Zhu, P., Zhang, X., Pan, Q., Gong, C., Huang, Y., Hu, X., Su, F., Lieberman, J. & Song, E. (2007) let-7 regulates self renewal and tumorigenicity of breast cancer cells. *Cell,* 131, 1109-23.

Zhang, H. H., Wang, X. J., Li, G. X., Yang, E. & Yang, N. M. (2007) Detection of let-7a microRNA by real-time PCR in gastric carcinoma. *World J Gastroenterol,* 13, 2883-8.

Chapter Seven

General discussion, future work and conclusions

7.1 Background

This thesis examined a series of potential biomarkers of disease biology and progression in thyroid neoplastic and inflammatory disease. The molecular pathogenesis of thyroid carcinoma is poorly characterised with only a few chromosomal or genetic abnormalities being described. The assessment was carried out using techniques including TaqMan® low density arrays, TaqMan® RT-PCR, immunohistochemistry and *in situ* hybridisation analysis of microRNA (miRNA) expression.

7.2 Review of the results

This thesis has examined transcriptomic, protein and miRNA targets as potential markers of disease throughout. At the start of this thesis TaqMan® low density arrays were used to highlight a global overview of how the ret/PTC-1 oncogene affects the immunoprofile of thyroid follicular cells. In chapter three the immune response elicited by a normal and endogenously expressing ret/PTC-1 thyroid cell line after a time course of co-culture with Hashimoto Thyroiditis (H.T.) and normal lymphocytic supernatant was investigated; this work was published in Molecular Cancer in 2008 (Denning et al., 2008). This study was carried out firstly to get an overview of the immune related gene expression that occurs when a normal thyroid cell line model receives an inflammatory infiltrate, this inflammatory infiltrate being in the form of co-culture with activated lymphocytic supernatant from a H.T. and normal donor. Secondly, the study introduced the ret/PTC-1 oncogene into the model, using a cell line that endogenously expresses the oncogene; it too was subjected to this inflammatory infiltrate. The aim of the second part of the study was to ascertain whether activation of the oncogene would affect the immunoprofile of the thyroid cells upon co-culture with activated lymphocytic supernatants.

When the normal cell line model was exposed to H.T. supernatant, virtually all immune targets in the low density array were up-regulated when compared to exposure to control supernatant. This was unsurprising as the typical autoimmune

(A.I.) response involves a plethora of cytokines, chemokines and immune regulators. Within this global up-regulation of genes certain groups of targets showed the potential to be involved in the tissue destruction seen in H.T. Those included granzyme B and Fas ligand, two mediators of cytotoxic cell death. Granzyme B triggers caspase activation indirectly by activating Bid which results in the leakage of pro-apoptotic mediators such as cytochrome c into the cytosol. Cytochrome c then forms a complex with Apaf-1 and caspase 9. Caspase 9 activates caspase 3, the major effector caspase, resulting in apoptosis. It is likely that this process occurs in H.T. leading to apoptosis of thyroid follicular cells. Granzyme B is commonly found in the synovium of the A.I condition rheumatoid arthritis (R.A.), where it has been demonstrated as a useful prognostic marker in early R.A (Goldbach-Mansky et al., 2005). Perhaps granzyme B holds potential as an early marker for H.T.

Fas ligand (FasL) induces apoptosis by binding Fas, which binds to FADD and caspase 8, which triggers the downstream caspase cascade. As mentioned, until recently expression of FasL was thought to be exclusive to "immune privileged" sites in the body such as the cornea, brain and placenta where constitutive expression of FasL is thought to control the entry of Fas expressing lymphoid cells. Immune privilege is thought to be an evolutionary adaptation to protect vital structures from the potentially damaging effects of an inflammatory immune response. Inflammation in the brain or eye could lead to loss of organ function, while immune responses directed against a fetus could lead to loss of the fetus. Many groups have found FasL expression in thyrocytes (Giordano et al., 1997, Mitsiades et al., 1998, Stassi et al., 1999), leading some to suggest that the thyroid may act as an immune privileged site. However, it is unlikely that the thyroid enjoys such an immune-privileged status as it is a frequent target of autoimmune damage. The expression of Fas in the normal cell line model was negligible (RQ value <10), suggesting that perhaps only low levels of Fas are needed for Fas/FasL induced apoptosis, or that Fas is only induced under certain biological conditions with appropriate cytokine stimulation.

Another interesting group of over-expressed targets in the normal cell line model were the T cell receptor (TCR) and T cell signaling molecules. Again it is quite plausible to find a role for these targets in H.T. pathogenesis, via over-stimulation of T cell

activation and signaling resulting in an overt immune response, and thyrocyte damage.

The role that the ret/PTC-1 oncogene plays in H.T. has yet to be characterised. ret/PTC-1 is an oncogene frequently found in papillary thyroid carcinoma (PTC), and until recently it was thought to be exclusively found in PTC (Sheils et al., 2000, Wirtschafter et al., 1997). Therefore to further evaluate the expression and role of this oncogene, the co-culture conditions were reapplied to another cell line which harbours ret/PTC-1. While the RET negative cell line was found to up-regulate a discreet group of five immune targets involved in apoptosis and T cell signaling (granzyme B, CD3, CD25, CD152 and CD45), the RET positive cell line, upon lymphocytic exposure, down-regulated these same targets, in comparison to control supernatant.

This was an interesting finding, ret/PTC-1 has previously been found in benign thyroid conditions such as H.T. (Sheils et al., 2000, Wirtschafter et al., 1997), therefore it is interesting to speculate that ret/PTC-1 may occur in the absence of malignancy, and when it does, it may lessen the pre-existing immune response by down-regulating immune targets such as granzyme B, CD3, CD25, CD152 and CD45. This may assist, along with additional genetic changes, in the development of PTC, a carcinoma that the ret/PTC-1 oncogene is well known to be implicated in. This theory is strengthened by the fact that H.T. and PTC are frequently found to co-exist, with evidence of PTC being found in 15-28% of cases of H.T. (Di Pasquale et al., 2001, Prasad et al., 2004, Singh et al., 1999). Lymphocytic thyroiditis and PTC are also frequently found together (Mechler et al., 2001, Tamimi, 2002). Therefore H.T. may possibly be classed as a "pre-malignant" state; this title may only be suitable for H.T. cases that are ret/PTC-1 positive. Histologically diagnosed H.T. sections could be tested for the presence of the oncogene; this could be done with a simple RT-PCR assay. H.T. RET positive lesions could be monitored closely for the development of PTC. This situation gives rise to an exciting prospect; if H.T. is indeed a pre-malignant state, monitoring some RET positive cases closely may give insight into the elusive mechanism of RET derived tumour development and formation. The question remains, what causes the RET chimera in H.T? Could the immune response somehow activate the oncogene, or is there some, as yet unknown mechanism of silencing that

keeps the oncogene from signaling until the immune response has been established. Further work is needed to elucidate this possible mode of activation.

TaqMan® LDAs were used in chapter three to get a global overview of the immunogenic targets that may be involved in H.T. pathogenesis. As a result of this, five targets (granzyme B, CD3, CD25, CD152 and CD45) were found to show differential expression patterns depending on the presence or absence of the ret/PTC oncogene. Therefore future work carrying on from this study could involve examining the expression of these five targets using single gene expression assays rather that immunoprofiling LDAs on a larger cohort of patients to further clarify the role that they play in H.T. pathogenesis and potential PTC development. Further understanding of the role that they may play in disease pathogenesis could ultimately lead to therapeutic advances in PTC, although it should be noted that therapeutic regulation of these five targets would have to be fully understood and tightly regulated as all five targets are important immunoregulatory elements.

Chapters four and five used a cohort of on average two hundred formalin fixed paraffin embedded (FFPE) thyroid tissue samples to analyse the efficacy of two panels of gene and protein expression markers for their utility in assisting the diagnosis of thyroid malignancy. A paper on the ability of the targets in chapter four to differentiate follicular thyroid lesions was published in Modern Pathology in July 2007 (Denning et al., 2007). The tissue samples and methods employed in chapter four and five are noteworthy. Formaldehyde was first use to fix tissues in the 1890s, and unlike alcohol fixatives, it produced only slight shrinkage and distortion of tissues (Medeiros et al., 2007). Today, formaldehyde as ten percent neutral-buffered formalin is still the most common fixative used in histopathology labs. Obviously a compelling need exists for the development of techniques that facilitate and accelerate the discovery of novel biomarkers with diagnostic and even therapeutic potential. The development and the subsequent transition between discovery and validation phases of biomarker experimentation are reliant on access to large numbers of consistently collected and banked biological samples. The several million FFPE tissue samples worldwide offer an extensive resource of normal and disease tissue for retrospective and prospective screening for disease biomarkers (Nirmalan et al., 2008). While the discovery phase (microarray analysis) (Finn et al., 2007) of this work used whole

genome analysis that produced significantly expressed targets, the validation phase (the gene and protein analysis) still needed to analyse expression of a substantial number of targets (5-11 assays). With regards to gene expression, this had not previously been carried out using FFPE material and laser capture microdissection. The use of TaqMan® pre-amplification allowed unbiased amplification of target mRNA and the subsequent analysis of >10 gene expression targets. In this thesis it has shown that the vast archives of FFPE material available to researchers can be used effectively in the validation stages of biomarker discovery.

The biomarkers examined in chapter four and five have proven that they are capable of discriminating benign from malignant thyroid disease; however these markers could also be possible therapeutic targets. The biomarkers up-regulated in malignant cohorts in chapter four (TGFβ1, IRF3, CD74, HLA-DMA and HLA-DQB1) and all markers in chapter five (as they were all over-expressed in malignancy) could be targeted with nucleic acid inhibitors of gene expression such as small interfering RNAs (siRNAs) or antisense oligonucleotides to silence their gene expression and therefore obstruct there oncogenic effect. RNA interference is an evolutionary conserved process of gene silencing initiated by a short interfering RNA (siRNA) that has become a powerful tool for studying and silencing gene function by reverse genetics (Jia et al., 2007). Antisense oligonucleotides can hybridise to a target mRNA and induce specific degradation as RNA/DNA hybrids are substrates of RnaseH (Ramon et al., 2008). Gene silencing using siRNAs has been achieved for MMP11 and APOE by other groups in gastric and ovarian cancer (Chen et al., 2005, Deng et al., 2005), leading to siRNA treated cells exhibiting significantly decreased growth ability. Thus, the potential therapeutic ability of these markers could be tested in thyroid carcinoma cell lines (after confirming the targets are present in the cell line using RT-PCR) by knocking down the targets shown to be up-regulated in malignancy using siRNAs or antisense oligonucleotides, their transfection and silencing could be proven using RT-PCR and western blotting. With regards to the therapeutic ability of these nucleic acid inhibitors for patients in the clinical setting, several clinical trials are underway for antisense oligonucleotides and siRNAs (Coppelli and Grandis, 2005, de Fougerolles et al., 2007). However despite abundant promise, a number of hurdles remain for oligonucleotide-based therapies, the most important issue remains to be the effective delivery of antisense or siRNA

oligonucleotides to their respective sites of action. However, many animal studies and virtually all of the clinical studies thus far have used "free" antisense or siRNA compounds (without a delivery agent), thereby demonstrating that oligonucleotides can function in this form (Juliano et al., 2008), holding future promise for the use of these technologies in combating thyroid malignancy.

The cohort of FFPE samples used in chapters four and five (and the subset of these samples used in chapter six) were grouped into diagnostic categories for comparative purposes. There were three classes of non-neoplastic categories, the first being "non-neoplastic (no thyroiditis, no hyperplasia) which comprised only the archetypal normal thyroid tissues - no evidence of malignancy and goitre, the second category being "non-neoplastic (no hyperplasia)" which comprised the typically normal tissues plus thyroiditis and lastly the "non-neoplastic (incl. hyperplasia and thyroiditis) which contained the typically normal samples plus hyperplasia and thyroiditis. The reason for these groupings was to assess whether the inclusion or exclusion of groups such as thyroiditis and hyperplasia, which are not normal, benign or malignant, would have any influence on expression profiles.

It was found that whether hyperplasia and thyroiditis are included or not in the typically normal category when compared to malignancy or neoplasia, the discriminatory power of the comparison (see tables 4.21, 5.26, 5.27, 5.28 and 6.15) remained unchanged at a molecular level. Therefore, molecularly, all of these non-neoplastic categories (typically normal, thyroiditis and hyperplasia) can be considered "normal" when compared to neoplasia and malignancy.

However if one compares the three non-neoplastic classes (typically normal, thyroiditis and hyperplasia) against each other, an interesting phenomenon occurs. When comparing "non-neoplastic (no hyperplasia but incl. thyroiditis)" versus hyperplasia, there is no statistically significant difference found for any of the targets analysed in chapter four, five or six (data not shown on tables 4.21, 5.26, 5.27, 5.28 and 6.15 as there was no statistical significance found). This suggests that molecularly there is no difference (in any of the targets analysed) between the non-neoplastic (no hyperplasia but incl. thyroiditis) and hyperplasia groups. However, when the thyroiditis group is taken out of the non-neoplastic group (therefore it is now "non-

neoplastic (no thyroiditis, no hyperplasia)"), this group is now statistically significantly discriminated from the hyperplastic group for MT1X gene expression (table 4.21) and MMP11 protein expression (table 5.27). Therefore, one can hypothesize from this that removing the thyroiditis cohort and leaving the group as purely normal samples, the group contains "a more normal cohort" of tissues and a statistical difference (for MT1X and MMP11 expression) can be then seen between it and hyperplasia. One could take from this that inclusion of thyroiditis, molecularly, makes the group "less normal".

Hyperplasia is a physiological response of follicular epithelium to hormonal changes that result in disturbances in the feedback mechanism of thyrotropin-releasing hormone and thyroid stimulating hormone. Some of the histological changes that can be observed in hyperplasia can sometimes lead to an incorrect diagnosis of malignancy due to the spectrum of morphological changes that they are able to assume. Perez-Montiel and Suster's study in 2008 (Perez-Montiel and Suster, 2008) found that in 300 hyperplasia cases, florid papillary hyperplasia of follicular epithelium was observed in thirteen percent of cases, in several instances closely resembling the papillary structures of PTC, such as "Orphan-Annie" nuclei, nuclear grooves and pseudoinclusions. Cytologic atypia was observed in seven percent of cases and mitoses were observed in six percent of cases. Their study confirmed that thyroid hyperplasia can sometimes display features that may be confused for a malignant or neoplastic process. In this thesis many targets showed a significant discriminatory ability when comparing hyperplasia and malignancy, therefore these markers may also aid in diagnosis. Hyperplasia versus malignancy was frequently found to be discriminated by many of the targets analysed. This discrimination was found more frequently than the benign versus malignant discrimination (see tables 4.21, 5.26, 5.27, 5.28 and 6.15). This may be related to the fact that benign is on the neoplastic continuum, whereas hyperplasia is not, therefore it maybe expected that benign samples would be more similar to malignancy. In addition, many of the markers were more commonly seen to discriminate the non-malignant group (which included, all three non-neoplastic groups and benign) compared to malignancy than the benign versus malignancy groups. This may be due to the fact that by including all non-neoplastic samples with benign in the non-malignant category, the group is

having more non-neoplastic samples added in and the cohort is essentially being "normalised".

In conclusion, when the two hundred archival thyroid tissue samples were divided up into the range of diagnostic categories shown in tables 4.21, 5.26, 5.27, 5.28 and 6.15, it was observed that all non-neoplastic categories are significantly different from malignancy, however comparing the different classes of non-neoplastic among each other finds that thyroiditis lessens the "normality" of the typically normal tissues leading one to believe that, molecularly, thyroiditis is not a normal tissue. This hypothesis would lend favour to what was discussed in chapter four and the beginning of this general discussion where the theory of H.T. being a pre-malignant state was discussed.

Chapter five saw the expansion of biomarker expression analysis by using immunohistochemistry to assess protein expression as well as gene expression, on matching FFPE thyroid tissue samples. The five markers in this chapter all demonstrated up-regulated gene and protein expression in malignant cohorts. In general it would be expected that biomarkers that are over-expressed are more likely to have utility than markers that are under-expressed.

A tissue microarray (TMA) was constructed and used in chapter five and six for immunohistochemisty analysis and *in situ* miRNA expression analysis. While collecting, assessing and organising archival material for TMA construction is a time-consuming process, the finished product is a valuable and useful one, the greatest advantage being the high throughput of samples that is possible with use of a TMA section. In addition, the construction of TMA blocks for a cohort of samples (e.g. the four TMA blocks that were constructed encompassing two hundred and five thyroid samples for this thesis) can be used in subsequent or additional projects over a number of years. Most TMA blocks produce approximately two hundred sections, depending on core tissue depth consistency. TMAs consisting of control tissues could be used in the clinical laboratory setting to aid immunohistochemical diagnosis of specimens.

A common concern that arises when discussing TMAs is the ability of a TMA core to represent a traditional "large" tissue section, although this issue has been examined by many and the general consensus is that sufficient numbers of cores (4) are capable of

representing traditional sections (Hoos et al., 2001, Nocito et al., 2001, Engellau et al., 2001, Torhorst et al., 2001, Camp et al., 2000).

Let-7a expression was found to be down-regulated in all malignant and neoplastic cohorts compared to normal and benign cohorts. Let-7a was also found to be completely absent from all follicular thyroid carcinomas when compared to benign follicular adenoma. It has been shown by others that let-7a acts as a tumour suppressor in regulating oncogenic RAS expression (Johnson et al., 2005) and that the RAS oncogene is frequently found in follicular carcinomas (Malumbres and Barbacid, 2003). An interesting next step carrying on from this project would be to examine the gene and protein expression of RAS to assess expression levels in malignant and benign follicular lesions. One would expect expression of RAS to be up-regulated in malignant follicular lesions. If this is the case, future work could involve over-expressing let-7a in thyroid follicular carcinoma cell lines to see if this results in retarding cell growth of follicular carcinoma cells.

As discussed above, not only could the biomarkers analysed in this thesis aid in the diagnosis of malignancy, they may also hold therapeutic potential by silencing their expression using nucleic acid inhibitors. The same could be said for let-7a where disruption of its expression could also offer a potential novel target for treatment. Artificial over-expression of miRNAs that normally function as tumour suppressors, such as those that are encoded by the let-7 family, could be used to treat malignancies such as thyroid cancer. Transient expression systems that use viral or liposomal delivery might be useful approaches for administering large quantities of miRNAs. These techniques would involve expressing the pre-miRNA hairpin and flanking sequence promoters, to stimulate the endogenous miRNA machinery to direct proper miRNA processing and gene-targeted repression (Esquela-Kerscher and Slack, 2006). Oncomir miRNAs could also be inactivated in tumour cells by administering synthetic antisense oligonucleotides anti-miRNA oligonucleotides (AMOs) or antagomirs (AMOs conjugated with cholesterol). A word of caution should be raised about unwanted effects given the multiplicity of miRNA targets. This is an important concern when the goal is restoration of the loss of miRNA expression, especially as many miRNAs promote cell proliferation. Tightly controlled expression of the

miRNA and precise and specific delivery to the target cell will be key factors for successful therapy.

The first and only clinical trial using miRNAs as a therapeutic tool began in May 2008 (Santaris Pharma) using a LNA-based antisense molecule against miR-122 for the treatment of Hepatitis C. Hopefully further understanding of the complete roles that miRNAs play in cancer and additional advances in the methods employed to deliver them will result in more clinical trials involving these novel RNAs as therapeutic agents.

7.3 Conclusions

The expression signatures produced in this thesis robustly discriminated lesions in thyroid malignancy at three levels of transcriptional expression, namely gene, protein and miRNA. Ultimately these gene and regulatory profiles may assist in the fundamental goal of translational research/medicine: bringing this expression signature from bench to bedside where it can aid and assist patient diagnosis of thyroid malignancy.

7.4 References:

Camp, R. L., Charette, L. A. & Rimm, D. L. (2000) Validation of tissue microarray technology in breast carcinoma. *Lab Invest,* 80, 1943-9.

Chen, Y. C., Pohl, G., Wang, T. L., Morin, P. J., Risberg, B., Kristensen, G. B., Yu, A., Davidson, B. & Shih Ie, M. (2005) Apolipoprotein E is required for cell proliferation and survival in ovarian cancer. *Cancer Res,* 65, 331-7.

Coppelli, F. M. & Grandis, J. R. (2005) Oligonucleotides as anticancer agents: from the benchside to the clinic and beyond. *Curr Pharm Des,* 11, 2825-40.

De Fougerolles, A., Vornlocher, H. P., Maraganore, J. & Lieberman, J. (2007) Interfering with disease: a progress report on siRNA-based therapeutics. *Nat Rev Drug Discov,* 6, 443-53.

Deng, H., Guo, R. F., Li, W. M., Zhao, M. & Lu, Y. Y. (2005) Matrix metalloproteinase 11 depletion inhibits cell proliferation in gastric cancer cells. *Biochem Biophys Res Commun,* 326, 274-81.

Denning, K., Smyth, P., Cahill, S., Li, J., Flavin, R., Aherne, S., Jj, O. L. & Sheils, O. (2008) ret/PTC-1 expression alters the immunoprofile of thyroid follicular cells. *Mol Cancer,* 7, 44.

Denning, K. M., Smyth, P. C., Cahill, S. F., Finn, S. P., Conlon, E., Li, J., Flavin, R. J., Aherne, S. T., Guenther, S. M., Ferlinz, A., O'leary, J. J. & Sheils, O. M. (2007) A molecular expression signature distinguishing follicular lesions in thyroid carcinoma using preamplification RT-PCR in archival samples. *Mod Pathol,* 20, 1095-102.

Di Pasquale, M., Rothstein, J. L. & Palazzo, J. P. (2001) Pathologic features of Hashimoto's-associated papillary thyroid carcinomas. *Hum Pathol,* 32, 24-30.

Engellau, J., Akerman, M., Anderson, H., Domanski, H. A., Rambech, E., Alvegard, T. A. & Nilbert, M. (2001) Tissue microarray technique in soft tissue sarcoma: immunohistochemical Ki-67 expression in malignant fibrous histiocytoma. *Appl Immunohistochem Mol Morphol,* 9, 358-63.

Esquela-Kerscher, A. & Slack, F. J. (2006) Oncomirs - microRNAs with a role in cancer. *Nat Rev Cancer,* 6, 259-69.

Finn, S. P., Smyth, P., Cahill, S., Streck, C., O'regan, E. M., Flavin, R., Sherlock, J., Howells, D., Henfrey, R., Cullen, M., Toner, M., Timon, C., O'leary, J. J. & Sheils, O. M. (2007) Expression microarray analysis of papillary thyroid carcinoma and benign thyroid tissue: emphasis on the follicular variant and potential markers of malignancy. *Virchows Arch,* 450, 249-60.

Giordano, C., Stassi, G., De Maria, R., Todaro, M., Richiusa, P., Papoff, G., Ruberti, G., Bagnasco, M., Testi, R. & Galluzzo, A. (1997) Potential involvement of Fas and its ligand in the pathogenesis of Hashimoto's thyroiditis. *Science,* 275, 960-3.